

DIVISION OF VIROLOGY, FACULTY OF HEALTH SCIENCES

**UNIVERSITY OF THE
FREE STATE
UNIVERSITEIT VAN DIE
VRYSTAAT
YUNIVESITHI YA
FREISTATA**



Immunogenicity of Sindbis based replicons for Crimean-Congo hemorrhagic fever virus.

Thomas Tipih

Thesis submitted in fulfillment of the requirements for the degree Ph.D. Medical Virology in the Division of Virology, Faculty of Health Sciences, University of the Free State, Bloemfontein

Promotor: Prof Felicity Burt, Division of Virology, Faculty of Health Sciences, University of the Free State, Bloemfontein

February 2019

Contents

Declaration	viii
Acknowledgments	ix
List of tables	x
List of figures	xi
Abbreviations.....	xvi
Presentations and publications	xix
Abstract	xx
Chapter 1	1
Literature Review	1
1.1 History of Crimean-Congo Hemorrhagic Fever	1
1.2 The virus.....	2
1.2.1 Classification	2
1.2.2 Virion Structure and Genomic Organization	3
1.2.3 Replication Cycle	3
1.3 Genetic diversity	4
1.4 Epidemiology	5
1.4.1 Geographic distribution.....	5
1.4.2 Life cycle of the tick and transmission pathway of CCHFV	7
1.5 Signs and symptoms.....	10
1.6 CCHF animal models	11
1.7 Pathogenesis	11
1.8 Laboratory diagnosis.....	13
1.8.1 Viral Isolation.....	14

1.8.2 Serological Assays.....	14
1.8.3 Molecular Techniques	15
1.9 Treatment	16
1.9.1 Supportive Therapy.....	16
1.9.2 Ribavirin.....	17
1.9.3 Specific immunoglobulin	17
1.9.4 Monoclonal Antibodies	17
1.10 Vaccines.....	18
1.10.1 Bulgarian Vaccine	18
1.10.2 Nucleic acid vaccines	18
1.10.2.1 History.....	18
1.10.2.2 Construction of DNA vaccines	19
1.10.2.3 Mechanism of action.....	19
1.10.2.4 Advantages	19
1.10.2.5 Disadvantages	20
1.10.2.6 Strategies for enhancing immunogenicity.....	20
1.10.2.7 Replicon vaccines	20
1.10.3 CCHF Vaccine development	22
1.10.3.1 Nucleoproteins.....	22
1.10.3.2 Glycoproteins.....	22
1.10.3.3 Inactivated Vaccines.....	22
1.10.3.4 CCHF vaccine candidates	23
1.10.3.4.1 Viral vectors	23
1.10.3.4.2 DNA vaccines.....	23
1.10.3.4.3 Plant-based vaccines	24
1.11 Problem Statement	24

1.12 Aim.....	25
1.13 Objectives	25
CHAPTER 2	27
Preparation and expression of constructs expressing the glycoprotein and the nucleoprotein of different CCHFV strains.....	27
2.1 Introduction.....	27
2.2 Aim	29
2.3 Methods and Materials	29
2.3.1 Primer design	29
2.3.2 cDNA Synthesis.....	30
2.3.3 Phusion High fidelity DNA PCR	30
2.3.4 PCR product confirmation and purification.....	31
2.3.5 Concentration of DNA	31
2.3.6 Cloning CCHF-31M, CCHF-52M, CCHF-31S and CCHF-52S into the intermediate vector pMini T	32
2.3.7 Transformation of JM109 Cells with pMiniTCCHF-31M, pMiniTCCHF-52M, pMiniTCCHF-31S and pMiniTCCHF-52S.....	33
2.3.8 Plasmid purification	34
2.3.9 DNA sequencing of CCHF-31M, CCHF-52M, CCHF-31S and CCHF-52S in pMini T	34
2.3.10 Restriction enzyme digestion of pMiniTCCHF-31M, pMiniTCCHF-52M, pMiniTCCHF-31S and pMiniTCCHF-52S.....	35
2.3.11 Gel Purification	35
2.3.12 Restriction enzyme digestion of pSinGFP and pSin-DLR-CCHF	36
2.3.13 Dephosphorylating the linearized replicon from pSin-DLR-CCHF	38
2.3.14 Construction of vaccine candidates.....	39
2.3.15 Transformation of JM109 cells.....	39
2.3.16 Plasmid purification	40

2.3.17 Vaccine constructs confirmation	40
2.3.18 DNA Sequencing of CCHF genes in Sindbis replicon vector.....	40
2.3.19 Next-generation sequencing of vaccine constructs and data analysis.....	41
2.3.20 Plasmid DNA purification for transfection experiments	41
2.3.21 Transfection experiments.....	42
2.3.21.1 Cell maintenance.....	42
2.3.21.2 Transfection of HEK-293 cells.....	42
2.3.21.3 Transfection of BHK-21 cells	42
2.3.21.4 Optimizing transfection reactions	43
2.3.21.5 Cell preparation for electroporation	44
2.3.21.6 Electroporation procedure	44
2.3.21.7 Optimizing electroporation.....	45
2.3.21.8 Indirect Immunofluorescence assay	45
2.3.21.9 Confirming glycoproteins and nucleoprotein expression using CCHF serum	46
2.3.21.10 Sodium dodecyl sulfate polyacrylamide gel (SDS-PAGE) analysis.....	46
2.3.21.11 Immunoblot analysis	47
2.3.21.11.1 Immunoblot using anti-His ₆ antibody.....	47
2.3.21.11.2 Immunoblot using CCHF serum	48
2.4 Results	49
2.4.1 PCR Amplification of CCHF-31S, CCHF-52S, CCHF-31M and CCHF-52M	49
2.4.2 Cloning CCHF-31S and CCHF-52S into pMiniT	51
2.4.3 Cloning CCHF-31M and CCHF-52M into pMiniT	53
2.4.4 Sub-cloning CCHF-31S, CCHF-52S, CCHF-31M and CCHF-52M genes into pSin replicon vector.....	54
2.4.5 DNA Sequencing of CCHF-31S, CCHF-31M, CCHF-52S and CCHF-52M genes in Sindbis replicon vector	56
2.4.6 Next-generation sequencing of vaccine constructs	58

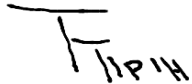
2.4.7 Optimization of transfection with Lipofectamine reagent.....	58
2.4.8 Optimization of electroporation experiments	59
2.4.9 Indirect Immunofluorescent Assays	60
2.4.10 Western Blot analysis of CCHFV NP and GP	65
2.5 Discussion	66
CHAPTER 3	70
Self-replication rates and induction of apoptosis in cells transfected <i>in vitro</i> with DNA launched replicons expressing the glycoprotein and the nucleoprotein of different CCHFV strains.	70
3.1 Introduction.....	70
3.2 Aim	72
3.3 Methods and Materials	72
3.3.1 Primer design	72
3.3.2 Vaccine constructs preparation for transfection.....	73
3.3.3 Cell maintenance	73
3.3.4 Cell preparation and electroporation	74
3.3.5 Cell harvesting.....	74
3.3.6 RNA extraction from transfected cells	74
3.3.7 Development of two-step quantitative RT-PCR	75
3.3.7.1 Preparation of DNA controls for development of RT-qPCR.....	75
3.3.7.2 cDNA synthesis.....	76
3.3.7.3 Quantitative real-time PCR assays.....	76
3.3.11 Induction of apoptosis.....	77
3.3.12 Statistical analysis.....	78
Pairwise comparisons between groups were assessed with the Kruskal-Wallis test. Statistical significance was set at $p < 0.05$. Analyses were performed with the SAS software Version 9.3.	78
3.4 Results	79

3.4.1 DNase treatment and plasmid DNA contamination check (Post DNase treatment)	79
3.4.2 Standard curve for two-step RT-qPCR	80
3.4.3 Vaccine constructs self-replication	81
3.4.4 Apoptosis induction	87
3.5 Discussion	91
CHAPTER 4	93
Immunogenicity of DNA-launched Sindbis replicons expressing the glycoprotein and the nucleoprotein of different CCHFV strains	93
4.1 Introduction	93
4.2 Aim	95
4.3 Methods and Materials	95
4.3.1 Plasmid DNA purification and confirmation for immunogenicity studies	95
4.3.2 Animal immunizations	96
4.3.3 Determination of cellular immune responses	99
4.3.4 Determination of humoral immune responses	101
4.3.5 Statistical analysis	101
4.4 Results	102
4.4.1 Humoral immune responses	102
4.4.2 Cellular immune responses	106
4.5 Discussion	111
CHAPTER 5	113
Further Discussion and concluding remarks	113
References	123
Appendices	144
Appendix A: Letters of ethics approval Ethical approval for the use of human serum from CCHF survivors in research studies.	144

Appendix B: Laboratory experimental work ethics approval	145
Appendix C: Animal Ethics clearance and Section 20 permit	147
Appendix D: Next-generation sequencing data.....	151
Appendix E: Apoptosis ELISA raw data post electroporation	156
Appendix F: ELISA raw data mouse experiment 1	157
Appendix G: ELISA raw data mouse experiment 2	167
Appendix H: Composition of buffers, media and solutions	176

Declaration

"I, Thomas Tipih, declare that the Doctoral's Degree research thesis that I herewith submit for the Doctoral's Degree qualification Medical Virology at the University of the Free State is my independent work, and that I have not previously submitted it for a qualification at another institution of higher education."

A handwritten signature in black ink, appearing to read 'T. Tipih'.

Thomas Tipih

Acknowledgments

I wish to extend my heartfelt gratitude to the following,

My distinguished supervisor Prof Felicity Jane Burt for introducing me to the world of arboviruses and mentorship throughout the research. My scientific knowledge has grown tremendously since I joined your research group.

The Division of Virology, National Health Laboratory Service and the University of the Free State for providing the facilities to complete the laboratory work.

The National Health Laboratory Service Research Trust grant for funding the research project.

Polio Research Foundation, South African Chairs initiative National Research Foundation, University of the Free State School of Medicine, Dr. Edward Tiffy Scholarship for financial assistance.

The team at the University of the Free State Animal Unit, Seb Lamprecht, Riaan van Zyl and Poifo Mokgathe for assistance with animal inoculations, feeding, monitoring, bleeding and harvesting of splenocytes.

Prof Gina Joubert for assisting with statistical analysis.

Armand Bester for analysis of sequence data generated from Next-generation sequencing.

Natalie Viljoen for the planning of the research experiments throughout the study.

My wife Blessings for the moral support and my daughter Myrna for keeping company late into the night as I was writing the thesis.

My parents for their love, unfailing support and encouragement to strive for excellence.

The Lord Jesus Christ my sustainer and role model, “in whom are hidden all the treasures of wisdom and knowledge” Colossians 2: 3.

List of tables

Chapter 2

Table 2. 1: Primer nucleotide sequences designed to amplify the CCHFV nucleoprotein open reading frame. <i>Not</i> I and <i>Cla</i> I restriction sites were added to the forward and reverse sequences respectively. <i>Not</i> I site Histidine tag stop codon <i>Cla</i> I site Start codon.....	30
Table 2. 2: Ligation reaction mixture for cloning CCHF-31S and CCHF-52S into pMiniT.....	32
Table 2. 3: Ligation reaction mixture for cloning CCHF-31M and CCHF-52M into pMiniT	32
Table 2. 4: Primers used for sequencing CCHF genes in pMiniT. Cloning primer sequence and primer position attachment on pMiniT vector.....	34
Table 2. 5: Reaction composition mixture for ligating CCHF-31S and CCHF-52S into pSin vector	39
Table 2. 6: Reaction composition mixture for ligating CCHF-31M and CCHF-52M into pSin vector	39
Table 2. 7: Primers used for CCHF gene sequencing in Sindbis replicon vector	41
Table 2. 8: Optimisation parameters of DNA plasmids in BHK-21 and HEK-293 cells.....	43
Table 2. 9: Electroporation parameters investigated for optimizing transfection experiments.....	45
Table 2. 10: 12% and 4% resolving gel components using 30% Bis-acrylamide (Sigma-Aldrich, Missouri, USA)	47
Table 2. 11: Percentage transfection efficiency rate in BHK-21 and HEK-293 cells after transfections with the Lipofectamine 3000 reagent.....	59
Table 2. 12: Percentage transfection efficiency rate in BHK-21 and HEK-293 cells after electroporation.....	61

Chapter 3

Table 3. 1: Nucleotide sequences for primers and probes	73
Table 3. 2: RT-qPCR viral load results following transfection of pSinCCHF-52S and pSinCCHF-31S in BHK-21 cells.	82
Table 3. 3: RT-qPCR viral load results following transfection of pSinCCHF-52M in BHK-21 cells. Samples were analyzed in duplicate.....	83
Table 3. 4: Calculated enrichment factors after electroporation of BHK-21 cells.....	88

Chapter 4

Table 4. 1: Restriction enzyme digestion for confirmation of vaccine constructs.....	96
Table 4. 2: Route of administration, dose and amount of dosages for different plasmids	96
Table 4. 3: Route of administration, dose and amount of dosages for different plasmids	98
Table 4. 4: Analysis of CCHFV IgG antibody in mice serum after immunization with Sindbis replicons expressing CCHFV glycoprotein and nucleoprotein using an indirect immunofluorescent assay	103
Table 4. 5: Analysis of CCHFV IgG antibody in mice serum after immunization with Sindbis replicons expressing CCHFV glycoprotein and nucleoprotein using an indirect immunofluorescent assay	104

List of figures

Chapter 1

Figure 1. 1: Geographic distribution of Crimean-Congo hemorrhagic fever. The map highlights annual global occurrence of CCHF, countries with documented viral and serological evidence of CCHFV and the regions with known presence of the the principal vector, *Hyalomma* ticks. Figure created by the World Health Organization, (https://www.who.int/emergencies/diseases/crimean-congo-haemorrhagic-fever/Global_CCHFRisk_2017.jpg?ua=1 .7

Figure 1. 2: Cycle of transmission of CCHFV. CCHFV infects competent vectors following a blood meal. Infected female ticks lay eggs which hatch and develop into larvae. The larvae feed on small mammals and molt. The nymph attaches to small vertebrates for a blood meal. After dropping off the host, the nymphs molt into adults. Adult ticks feed on large herbivores. Human infections follow bites by infected ticks, contact with infected animal fluids or human to human transmission. (Image by Prof FJ Burt, unpublished)

Chapter 2

Figure 2. 1: Vector map for pMiniT drawn using SnapGene software version 2.2.2. The cloning analysis primers indicated are used for sequencing ligated nucleotide sequences. The vector allows cloning of blunt ended as well as PCR products with A overhangs. The vector has a pUC19 origin of replication, a Shine-Dalgarno sequence ribosome binding site, a toxic minigene, an IS10 tnpA gene encoding the transposase and ampicillin gene giving resistance to ampicillin, carbenicillin and associated antibiotics.....

Figure 2. 2: Vector map for pSin-DLR-CCHF drawn using SnapGene software version 2.2.2. The replicons contain human cytomegalovirus (hCMV) immediate-early promoter/enhancer element, consisting of a strong constitutive promoter and an enhancer element, essential for eukaryotic expression, a bacterial origin of replication, a bovine growth hormone (BGH) eukaryotic transcription terminator sequence and the NeoR/KanR selectable marker sequence. The genome of Sindbis virus nonstructural proteins constitute the plasmid backbone while the structural genes have been replaced with genes encoding for the glycoprotein precursor of CCHFV strain IbAr 10200. The cloning site is flanked by *Not*I restriction sites.....

Figure 2. 3: Vector map for pSinGFP drawn using SnapGene software version 2.2.2 The replicons contain human cytomegalovirus (hCMV) immediate-early promoter/enhancer element, consisting of a strong constitutive promoter and an enhancer element, essential for eukaryotic expression, a bacterial origin of replication, a bovine growth hormone (BGH) eukaryotic transcription terminator sequence and the NeoR/KanR selectable marker sequence. The genome of Sindbis virus nonstructural proteins constitute the plasmid backbone while the structural genes of the have been replaced with genes encoding for the GFP. The cloning site is flanked by <i>Not</i> I restriction sites.....	38
Figure 2. 4: Agarose gel electrophoretic analysis of CCHF NP (left) and GP (right) PCR products. Left, Lane 1: Molecular marker SM 1173, Lane 2: CCHF-31S, Lane 3: CCHF-52S. Right, Lane 1: Molecular marker SM 1173, Lane 2: CCHF-31M, Lane 3: CCHF-52M.....	49
Figure 2. 5: Agarose gel electrophoretic analysis of CCHF NP purified PCR products. CCHF-31S (Left) and CCHF-52S (Right). Lane 1: Molecular marker SM 1173, Lane 2: Purified PCR amplicon.....	50
Figure 2. 6: Agarose gel electrophoretic analysis of CCHF GP purified PCR products. Lane 1: Molecular marker SM 1173, Lane 2: Purified CCHF-31M PCR amplicon. Lane 3: Purified CCHF-52M PCR amplicon.....	51
Figure 2. 7: Representative CCHF-52S sequences showing the <i>Cla</i> I restriction site overlapped with the <i>dam</i> methylation site. CCHF-52S sequences, Stop codon, <i>Cla</i> I enzyme site, <i>dam</i> methylation site, pMiniT vector. F and R denote the forward and reverse pMiniT sequencing primers. Sample 11 was cloned in a reverse orientation while the rest cloned in a forward orientation resulting in the GATC sequence which is a <i>dam</i> methylation site.....	52
Figure 2. 8: Agarose gel electrophoretic analysis of pMiniTCCHF-31S and pMiniTCCHF-52S double digestion using <i>Not</i> I-HF and <i>Cla</i> I. Lane 1: Molecular marker SM 1173. Lane 2: pMiniTCCHF-31S double restriction digestion with <i>Not</i> I-HF and <i>Cla</i> I. Lane 3: Undigested plasmid pMiniTCCHF-31S Lane 4: pMiniTCCHF-52S double digestion restriction digestion with <i>Cla</i> I and <i>Not</i> I-HF. Lane 5: Undigested pMiniTCCHF-52S plasmid.....	53
Figure 2. 9: Agarose gel electrophoretic analysis of pSinCCHF-31M and pSinCCHF-52M restriction digestion using <i>Not</i> I-HF restriction enzyme. Lane 1: Molecular marker SM 1173. Lane 2: pSinCCHF-31M restriction digestion with <i>Not</i> I-HF. Lane 3: Undigested plasmid pSinCCHF-31M Lane 4: pSinCCHF-52M digestion restriction digestion with <i>Not</i> I-HF. Lane 5: Undigested pSinCCHF-52M plasmid.....	54
Figure 2. 10: Agarose gel PCR confirmation of pSinCCHF-31S and pSinCCHF-52S. Lane 1: Molecular marker SM 1173. Lanes 2-3 CCHF-31S, Lanes 4-5 CCHF-52S PCR products.....	55
Figure 2. 11: Agarose gel analysis for PCR confirmation of CCHF-52M alignment in the replicon vector. Lane 1: Molecular marker SM 1173. Lanes 2-6: CCHFV GP PCR products. Lanes 3 and 5 show PCR products from plasmids with the insert in the correct orientation and of the expected size while lanes 2, 4 and 6 show PCR products from plasmids without the required insert sizes or correct orientation. Bands observed in lanes 2,4 and 6 could have resulted from non-specific PCR amplification in plasmids with inserts in the reverse orientation or plasmids with the correct orientation but with inserts smaller than the expected size of 5000 bp.	56
Figure 2. 12: Agarose gel analysis for PCR confirmation of CCHF-31M alignment in the replicon vector. Lane 1: Molecular marker SM 1173. Lanes 2-6: CCHFV PCR products. Lanes 2, 3 and 5 show PCR products from plasmids with the insert in the correct orientation and of the expected size while lanes 4 and 6 show PCR products from plasmids without the required insert sizes or correct orientation. Bands observed in lanes 4 and 6 could have resulted	

from non-specific PCR amplification in plasmids with inserts in the reverse orientation or plasmids with the correct orientation but with inserts smaller than the expected size of 5000 bp.57

Figure 2. 13: DNA sequencing chromatogram for CCHFV-52S obtained after Sanger sequencing58

Figure 2. 14: Confirmation of CCHFV nucleoprotein and glycoprotein expression in BHK-21 cells using commercial mouse anti-His₆ antibody. (A): BHK-21 cells transfected with replicon pSinCCHF-31S. (B): BHK-21 cells transfected with replicon pSinCCHF-52S. (C): BHK-21 cells transfected with replicon pSinCCHF-52M (D): untransfected BHK-21 cells62

Figure 2. 15: Confirmation of CCHFV nucleoprotein and glycoprotein expression in HEK-293 cells using commercial mouse anti-His₆ antibody. (A): HEK-293 cells transfected with replicon pSinCCHF-31S. (B): HEK-293 cells transfected with replicon pSinCCHF-52S. (C): HEK-293 cells transfected with replicon pSinCCHF-52M (D): untransfected HEK-293 cells63

Figure 2. 16: Confirmation of CCHFV glycoprotein and nucleoprotein expression in BHK-21 cells using anti-CCHF IgG human serum. (A): BHK-21 cells transfected with replicon pSinCCHFV-52M. (B): BHK-21 cells transfected with replicon pSinCCHFV-31S. (C): BHK-21 cells transfected with replicon pSinCCHFV-52M. (D): untransfected BHK-21 cells64

Figure 2. 17: Confirmation of CCHFV glycoprotein and nucleoprotein expression in HEK-293 cells using anti-CCHF IgG human serum. (A): HEK-293 cells transfected with replicon pSinCCHFV-52M. (B): HEK-293 cells transfected with replicon pSinCCHFV-31S. (C): HEK-293 cells transfected with replicon pSinCCHFV-52M. (D): untransfected BHK-21 cells.65

Figure 2. 18: Western blot analysis of CCHFV NP. From left to right; Lane 1: MagicMark XP Western Protein Standard, lane 2 CCHF-52S , Lane 3 CCHF-31S, Lane 4 mock electroporated cells66

Chapter 3

Figure 3. 1: Post DNase treatment of RNA samples. Plasmid DNA contamination check of extracted RNA from transfected cells. CCHF-31S RNA (A), CCHF-52S RNA (B) and CCHF-52M RNA (C) Lane 1: Molecular marker SM 1173. Lane 2: RNA at 4 hours. Lane 3: RNA at 8 hours. Lane 4: RNA at 12 hours. Lane 5: RNA at 24 hours. Lane 6: RNA at 48 hours. Lane 7: Positive control79

Figure 3. 2: Standard curve for quantifying CCHF-31S and CCHF-52S genes generated using log concentration of CCHF-52S standards plotted against the crossing points.....80

Figure 3. 3: Standard curve for quantifying CCHF-52M genes generated using log concentration of CCHF-52M standards plotted against the crossing points.81

Figure 3. 4: Amplification curves for CCHFV RNA. (A) CCHF-31S (B), CCHF-52S (C) and CCHF-52M RNA. CCHFV RNA collected at various time points was converted to cDNA using SuperScript™ III reverse transcriptase enzyme and amplified using the qPCR.....84

Figure 3. 5: Replication kinetics of CCHF NP total RNA expression in BHK-21 cells electroporated with pSinCCHF-31S and pSinCCHF-52S over 48 hours. (A) pSinCCHF-31S (B) and pSinCCHF-52S85

Figure 3. 6: Replication kinetics of CCHF GP total RNA expression in BHK-21 cells electroporated with pSinCCHF-52M over 48 hours.86

Figure 3. 7: Vaccine constructs apoptosis induction in BHK-21 cells transfected with pSinCCHF-31S and pSinCCHF-52S. To assess release of mono and oligonucleosomes in cells undergoing apoptosis following electroporation with (A) pSinCCHF-31S, (B) pSinCCHF-52S as well as control plasmid pSinGFP and electroporation in the absence of DNA (electroporation control) was analyzed using the ELISA technique. All values represent an average of two readings.89

Figure 3. 8: Vaccine constructs apoptosis induction in BHK-21 cells transfected with pSinCCHF-52M. To assess the release of mono and oligonucleosomes in cells undergoing apoptosis following electroporation with pSinCCHF-52M as well as control plasmid pSinGFP and electroporation in the absence of DNA (electroporation control) was analyzed using the ELISA technique. All values represent an average of two readings.90

Chapter 4

Figure 4. 1: Allocation of mice into different groups. A total of 15 mice were used in the experiment. Mice were randomly assigned to the control group and test groups. Three mice were used per group.....97

Figure 4. 2: Allocation of mice into various groups. A total of 18 mice were used in the experiment. Mice were randomly assigned to the control group and test groups. Three mice were used per group. Vaccine constructs administered to mice in control group 1 and test groups 3, 4 and 6 were co-immunized with adjuvant poly(I:C). Group 2 animals received vaccine construct pSinCCHF-52M in the absence of poly(I:C). Mice in test groups 5 and 6 were administered with the two constructs pSinCCHF-52S and pSinCCHF-52M.99

Figure 4. 3: Anti-CCHFV NP IgG total endpoint antibody titer. Mice (NIH; N=3/group) were immunized three times intramuscularly with prepared vaccine constructs expressing CCHFV glycoprotein and nucleoprotein. Serum total endpoint anti-CCHFV NP IgG were analyzed using an indirect immunofluorescent assay. Data is expressed as the mean for three mice and the standard error of the mean. **pSinCCHF-52S + pSinCCHF-52M105

Figure 4. 4: Anti-CCHFV NP IgG isotypes endpoint titer. Mice (NIH; N=3/group) were immunized three times intramuscularly with prepared vaccine constructs expressing CCHFV glycoprotein and nucleoprotein. Serum anti-CCHFV NP IgG subtypes were analyzed using an indirect immunofluorescent assay. Data is expressed as the mean for three mice and the standard error of the mean. **pSinCCHF-52S + pSinCCHF-52M106

Figure 4. 5: Cytokine secretion levels after splenocyte stimulation with a CCHFV antigen. Mice (NIH; N=3/group) were immunized three times intramuscularly with prepared vaccine constructs expressing CCHFV glycoprotein and nucleoprotein. Harvested splenocytes were stimulated with a CCHF antigen and levels of secreted interleukins in supernatants were analyzed using ELISA. Data is expressed as the mean for three mice and the standard error of the mean. (A) IL-2, (B) IFN- γ , (C) TNF- α , (D) IL-6, (E) IL-10. *p < 0.05108

Figure 4. 6: Cytokine profiling by ELISA from splenocytes harvested from NIH mice (N=3/group) after immunization with pSinCCHF-52S and pSinCCHF-52M independently or combined in the presence or absence of adjuvant

poly(I:C). (A) IL-2, (B) IFN- γ , (C) TNF- α , (D) IL-6, (E) IL-10, (F) IL-4. Data is expressed as the mean for three mice and the standard error of the mean. **pSinCCHF-52S + pSinCCHF-52M. * p < 0.05110

Abbreviations

ATCC	American Type Culture Collection
APS	ammonium persulfate
Amp	ampicillin
APCs	antigen presenting cells
ABTS	2,2'-azinobis-(3-ethylbenzothiazoline-6-sulfonate)
BHK	baby hamster kidney
BLAST	Basic Local Alignment Search Tool
BSL4	biosafety level 4
BGH	bovine growth hormone
CFR	case fatality rate
CAR	cloning analysis reverse primer
CAF	cloning analysis forward primer
cDNA	complementary deoxyribonucleic acid
CCHFV	Crimean Congo hemorrhagic fever virus
DC	dendritic cell
DNA	deoxyribonucleic acid
DREP	DNA launched replicon
DIC	disseminated intravascular coagulation
DTT	dithiothreitol
dsRNA	double-stranded RNA
DMEM	Dulbecco's Modified Eagle Medium
EEEV	eastern equine encephalitis virus
EEEV C	eastern equine encephalitis virus capsid protein
EEEV E3	eastern equine encephalitis virus signal peptide
EEEV 6K	eastern equine encephalitis virus signal peptide
EC	endothelial cell
EDTA	ethylenediaminetetraacetic acid
ELISA	enzyme-linked immunosorbent assay
FBS	fetal bovine serum
GP	glycoprotein
GFP	green fluorescence protein
HF	high fidelity
HMW	high molecular weight
HIS	histidine
HRPO	horseradish peroxidase
hCMV-IE	human cytomegalovirus immediate early promoter
HEK	human embryonic kidney
HCL	hydrochloric acid
H ₂ SO ₄	sulphuric acid
Gn & Gc	CCHFV surface glycoproteins
IFA	immunofluorescent assay
IFNAR ^{-/-}	interferon alpha/beta receptor-deficient

ICAM-1	intercellular Adhesion Molecule 1
IFN- β	interferon beta
IFN- γ	interferon alpha
IL	interleukin
KanR	kanamycin resistance
LB	Luria-Bertani
MHC	major histocompatibility complex
MDA-5	melanoma differentiation-associated protein 5
mRNA	messenger ribonucleic acid
mg	milligram
ml	milliliter
mAb	monoclonal antibody
ng	nanogram
NIH	National Institute of Health
NeoR	neomycin resistance
NEB	New England Biolabs
NP	nucleoprotein
ORF	open reading frame
PBS	phosphate buffered saline
Poly (I:C)	polyinosinic-polycytidylic acid
PVDF	polyvinylidene fluoride
Poly ICLC	carboxymethylcellulose, polyinosinic-polycytidylic acid
qPCR	quantitative polymerase chain reaction
RT-PCR	reverse transcriptase polymerase chain reaction
RIG-1	retinoic acid-inducible gene 1
RNA	ribonucleic acid
STAT-1	signal transducer and activator of transcription
SDS-PAGE	sodium dodecyl sulfate-polyacrylamide gel electrophoresis
SOC	Super Optimal broth with Catabolite repression
SPU	Special Pathogens Unit
TEMED	N,N,N',N'-Tetramethylethylenediamine
TBS	tris-buffered saline
TBST	tris-buffered saline with Tween 20
TMB	3,3',5,5'-tetramethylbenzidine
Th	T helper
TLR	toll-like receptors
TAE	tris acetic ethylenediaminetetraacetic acid
TAT	turnaround time
TNF- α	tumor necrosis factor alpha
μ l	microliter
μ g	microgram
UK	United Kingdom
USA	United States of America

USSR-----Union of Soviet Socialist Republics
VCAM-1-----vascular cell adhesion molecule 1
VEEV-----Venezuelan equine encephalitis virus
V-----voltage
WHO-----World Health Organization
x g -----gravitational force

Presentations and publications

Oral presentations

Tipih T & Burt FJ. Immunogenicity of Sindbis based replicons for Crimean-Congo hemorrhagic fever virus. Faculty of Health Sciences Forum 2018, University of the Free State 30-31 August 2018.

Tipih T & Burt FJ. Immunogenicity of Sindbis based replicons for Crimean-Congo hemorrhagic fever virus. University of the Free State postgraduate academic conference 24 October 2018.

Tipih T & Burt FJ. Immunogenicity of Sindbis based replicons for Crimean-Congo hemorrhagic fever virus. Free State Department of Health Research day. 8-9 November 2018, University of the Free State.

Proposed publications

Tipih T & Burt FJ. Preparation and expression of Sindbis based constructs expressing the glycoprotein and the nucleoprotein of different CCHFV strains. (In preparation)

Tipih T & Burt FJ. Self-replication rates and induction of apoptosis in cells transfected *in vitro* with DNA launched replicons expressing the glycoprotein and the nucleoprotein of different CCHFV strains. (In preparation)

Tipih T & Burt FJ. Immunogenicity of DNA-launched Sindbis replicons expressing the glycoprotein and the nucleoprotein of different CCHFV strains. (In preparation)

Awards

2016: Dr Edward (tiffy) King scholarship

2018: Runner-up, Faculty of Health Sciences Forum 2018- Junior Laboratory Paper. Tipih T & Burt FJ. Immunogenicity of Sindbis based replicons for Crimean-Congo hemorrhagic fever virus. Faculty of Health Sciences Forum 2018, University of the Free State 25-26 August 2018.

2018: Joint Winner Ph.D. category: University of the Free State postgraduate academic conference. Tipih T & Burt FJ. Immunogenicity of Sindbis based replicons for Crimean-Congo hemorrhagic fever virus 24 October 2018.

2018: Runner up: Free State Department of Health Research day- Second best oral presentation in the emerging scientist category. 8-9 November 2018, University of the Free State.

Abstract

Introduction and Aim: Crimean-Congo hemorrhagic fever virus (CCHFV) infrequently causes hemorrhagic fever in humans with a case fatality rate of 30%. Currently, there is neither an internationally approved antiviral drug nor vaccine against the virus. In a move aimed at averting future epidemics, the World Health Organization has added the virus to the list of priority infectious organisms.

The aim of the study was to investigate mechanisms of immunogenicity of Sindbis replicons encoding CCHFV glycoproteins and nucleoproteins for future development of an efficacious vaccine.

Methodology: Genes encoding the complete open reading frames of the CCHFV nucleoprotein and glycoprotein precursor proteins of South African strains were amplified by the reverse transcription polymerase chain reaction technique and cloned into a Sindbis virus replicon vector. Sanger sequencing and next-generation sequencing were carried out to confirm gene sequences. Nucleoprotein and glycoprotein expression were demonstrated by transfecting baby hamster kidney cells and human embryonic kidney cells. Vaccine construct self-replication rates were assessed by transfecting BHK-21 cells and assaying for CCHFV RNA using gene-specific primers. Apoptosis induction in transfected BHK-21 cells was determined by measuring the enrichment of nucleosomes in the cytoplasm using an ELISA. Groups of three NIH mice were immunized with 100 µg of vaccine constructs three times intramuscularly three weeks apart with plasmid constructs pSinCCHF-31S, pSinCCHF-52S and pSinCCHF-52M. To augment cytokine responses the adjuvant poly (I:C) was co-inoculated with pSinCCHF-52S and pSinCCHF-52M separately. In addition, the constructs pSinCCHF-52M and pSinCCHF-52S were co-immunised with and without poly(I:C) to induce a response against both proteins simultaneously. Two weeks after receiving the third dose mice were sacrificed and blood was collected for determination of humoral immune responses while harvested splenocytes were stimulated with a CCHFV antigen for cytokine responses.

Results: Two vaccine constructs (pSinCCHF-31S and pSinCCHF-52S) expressing CCHFV nucleoprotein and a construct (pSinCCHF-52M) expressing CCHFV glycoprotein were prepared. Recombinant protein expression was demonstrated by immunofluorescence assays targeting the histidine tag fused to the CCHFV proteins. Further confirmation of protein expression was performed by immunofluorescence assays using serum from CCHF survivors. All prepared vaccine constructs transcribed CCHFV RNA, as demonstrated by detection of protein using immunofluorescent antibody assays, and induced apoptosis in transfected cells. Immunized mice responded with the production of high titers of CCHFV IgG NP specific antibodies and higher levels of IgG2a in comparison to IgG1 responses were observed in responders suggesting a predominant Th1 antibody response. CCHFV IgG GP specific antibodies were not induced in vaccinated mice. Vaccine construct pSinCCHF-52S resulted in higher secretion of IL-2, ($p = 0.0495$) IFN- γ ($p = 0.0369$) and TNF- α ($p = 0.0495$) relative to immunisation with pSinGFP. An enhanced secretion of IFN- γ and IL-2 ($p = 0.0463$) was observed from splenocytes from mice co-immunised with pSinCCHF-

52S and pSinCCHF-52M while vaccinating with pSinCCHF-52M increased IL-2 secretion ($p = 0.0463$). Co-administration of pSinCCHF-52M and pSinCCHF-52S constructs augmented IFN- γ ($p = 0.0463$) secretion. Co-inoculation of vaccine constructs with adjuvant poly (I:C) did not enhance cytokine secretion.

Conclusion: The study demonstrated the expression of CCHFV nucleoproteins and glycoproteins by a Sindbis virus vector in mammalian cells. Vaccination of mice with construct pSinCCHF-52S induced type 1 immunity. Immunoglobulin G subtyping demonstrated IgG2a/IgG1 >1 as well as significantly higher IL-2, IFN- γ and TNF- α . Immunisation with pSinCCHF-31S and pSinCCHF-52M did not elicit specific antibody production and cytokines responses were weak. Further studies in CCHFV susceptible animals are necessary to determine whether the immune responses generated by vaccinating with pSinCCHF-52S are protective. However, this study shows the utility of Sindbis replicons in vaccine development against CCHFV.

Chapter 1

Literature Review

1.1 History of Crimean-Congo Hemorrhagic Fever

The first description of Crimean-Congo hemorrhagic fever (CCHF) as an entity came about in 1944 after military personnel in the Crimean peninsula were infected and the disease was given the name Crimean hemorrhagic fever (CHF). Upon investigating the outbreak, the researchers observed a high proportion of tick bites in farmers working on land that had not been cultivated during the German occupation, in the course of World War II, and the increase in population of hares and other wild mammal hosts for *Hyalomma* ticks (Bente et al. 2013). A viral cause was suggested upon the realization that CHF patients had in their blood filterable agents which trigger a febrile syndrome when used as pyrogenic therapy. Co-administration of antibiotics and filtered suspensions from *Hyalomma marginatum* ticks in volunteers prompted a mild CHF course again pointing to a viral cause and ticks as sources of infection (Chumakov 1974). After the 1944 outbreak in the Crimean peninsula, several outbreaks of related diseases with high mortalities were reported in Central Asia, some parts of the Soviet Union and Bulgaria (Hoogstraal 1979). Limited knowledge on the nature of the causative agent, reagents for serological, diagnostic, experimental, and epidemiological survey purposes meant there wasn't a solid base to formulate the prevention and control measures (Hoogstraal 1979). In the meanwhile, Dr Courtois used new born mice to isolate the Congo virus strain V3011 from a blood sample of a 13 year old boy presenting with fever in the Belgian Congo in 1956 (Simpson et al. 1967, Williams et al. 1967). A month later, Dr Courtois contracted an infection apparently from handling the V3011 and from his blood sample was isolated the Congo virus strain V3010 strain (Hoogstraal 1979). Between 1958 and 1965, ten Congo virus strains were recovered from blood samples of febrile patients in Entebbe, Uganda (Simpson et al. 1967, Williams et al. 1967). Using newborn white mouse inoculation technique for viral isolation and study, the Drozdov strain was isolated from a febrile patient presenting with CHF by the name of Drozdov in 1967 in the Soviet Union (Butenko et al. 1968, Chumakov et al. 1968). The Drozdov strain was extensively used in experimental studies paving the way for the production of reagents for serological surveys and typing of new isolates discovered in different regions of the world. Researchers found that causative agents of this tick-borne hemorrhagic fever from different regions were antigenically indistinguishable (Chumakov et al. 1970). During further characterisation studies of the Drozdov strain by Casals in 1968 at the Yale Arbovirus Research Unit, it was discovered that the virus causing CHF in the Crimean peninsula was antigenically alike to the Congo virus strains (Hoogstraal 1979) isolated from humans from the Congo and Uganda (Casals 1969, Simpson et al. 1967) and *Hyalomma* ticks collected from Pakistan (Begum et al. 1970). This finding broadened the geographical range of the CHF agent to Pakistan and Africa. A new name linking the two locations was coined thus disease name and virus, initially to CHF-Congo virus (Casals 1970) and then to Crimean-Congo hemorrhagic fever (virus) (Hoogstraal 1979).

CCHF was first recognized in South Africa in 1981 after a fatal infection in a teenage boy. CCHFV was confirmed as the cause of death after viral isolation from the patient's blood sample. It was initially thought then, that the virus had been recently introduced in South Africa by migratory birds (Gear et al. 1982). However, investigations in the aftermath of the first case led to CCHFV isolation from *Hyalomma marginatum rufipes* and *Halomma truncatum* ticks from the nature reserve where the teenager contracted the infection while antibodies were detected in humans (6.75% n=74), wild vertebrates (30.7% n=26) sheep (27.4% n=270) and cattle (64.1% n=170) from the reserve and surrounding farms (Swanepoel et al 1983). Sera from hares originating from across South Africa also tested positive for CCHFV antibodies (Swanepoel et al 1983). These findings led to an antibody survey in cattle in South Africa. A high prevalence of CCHFV antibodies was found in cattle from the interior but prevalence was low along the southern coast where some species of the *Hyalomma* ticks are absent (Swanepoel et al 1987). In addition from February 1981 to January 1986, 29 cases were diagnosed in various locations in South Africa (Swanepoel et al 1987). Since 1981, sporadic CCHF cases have been reported averaging five a year despite high seroprevalence rates in wild and domesticated animals. Although most cases are unrelated in origin, there are four instances of nosocomial and laboratory transmissions reported in the 1980s and 2006 (van Eeden et al. 1985a, Richards 2015). In 1996, 17 cases of CCHF were reported amongst workers at an ostrich abattoir (Swanepoel et al. 1998). Since the first reported case in 1981, cases have been reported infrequently with an average of five a year (Msimang et al. 2013). These cases tend to be strewn across the year although there is a slight association with the seasonal activity of the principal vectors (*Hyalomma* ticks) (Burt et al. 2007). Human disease is more common in adult males who are the majority in the livestock industry. Notwithstanding that the cases had been reported all over the country, the majority of cases have been from the dry farming provinces of the Free State and the Northern Cape (Richard et al. 2015). Currently, there is no evidence to suggest that the pathogenicity of South African strains is different from those isolated in other parts of the globe.

1.2 The virus

1.2.1 Classification

CCHFV is a member of the *Nairoviridae* family and the *Orthonairovirus* genus. The *Orthonairovirus* genus is divided into 12 species within which are more than 35 viruses (Adams et al. 2017, Kuhn et al. 2016). The *Orthonairovirus* genus is further divided into nine serogroups (Walker et al. 2015). CCHF and Nairobi sheep disease are the only known serogroups to have public health and veterinary importance. CCHFV and Hazara virus belongs to the former while the latter comprises of Nairobi sheep disease and Dugbe viruses (Whitehouse 2004). Initially CCHFV was classified in the family *Bunyaviridae*, genus *Nairovirus* but the taxonomy was updated in 2017 and this was meant to bring order in the old *Bunyaviridae* family (now *Bunyavirales*) which had grown too extensive. Classification of bunyaviruses was initially based on serological assays owing to the unavailability of genomic sequence information of

the bunyaviruses (Plyusnin et al. 2011), thus many viruses could not be classified. The advent of next-generation sequencing and advancements in bioinformatic tools such as whole genome assembly allows classification of previously uncharacterised bunyaviruses and categorization of novel bunyavirus clades (Kuhn et al. 2016).

1.2.2 Virion Structure and Genomic Organization

CCHF virions are spherical with an approximate diameter of 100 nm. The virus particle has an envelope, a lipid bilayer membrane derived from the host cell. Glycoprotein spikes protrude through the envelope. The genome is made up of three single-stranded RNA segments of negative polarity (Mariott and Nuttall 1992). The three RNA segments are designated small (S), medium (M) and large (L) denoting their relative nucleotide length. Each segment has a coding region sandwiched by non-coding regions at the 5' and 3' termini (Walter and Barr 2011). The base sequence at the termini of each segment exhibits complementarity, and this allows base pairing thus the segments form a pseudo-circular structure (Elliott et al. 1991). The S, M and L segments encode the nucleocapsid (N) protein and the non-structural S protein (NSs); glycoprotein precursor which is proteolytically cleaved to form mature envelope glycoproteins (Gn and Gc) as well as nonstructural proteins GP160/85, GP38 and non-structural M protein (NS_M,) and the viral polymerase (L protein) respectively. These segments are each encapsidated by the N protein forming ribonucleocapsids, and each ribonucleocapsid is associated with the L protein. Each of these ribonucleocapsids must be packaged in a mature virion though equal numbers are not always found. The NP encapsidates viral RNA and complementary RNA (Zivcec et al. 2016) while the NSs demonstrates apoptotic activity in transfected cells (Barnwal et al 2016). The Gn–Gc heterodimer mediates viral assembly, budding of newly formed virus particle and attachment to new target cells (Walter and Barr 2011). The function of non-structural proteins and NS_M is yet to be described. The L protein functions in viral mRNA transcription and translation (Walter and Barr 2011) and interferon response suppression through the deubiquitinating and deISGylating activities of the N-terminal ovarian tumor (OTU) domain (Scholte et al. 2017).

1.2.3 Replication Cycle

CCHFV attaches to host cell receptors through Gn-Gc glycoproteins. The receptor(s) the virus uses remains to be characterized. Entry into the host cell is believed to be by clathrin-dependent endocytosis (Simon et al. 2009). Viral entry is followed by membrane fusion releasing viral ribonucleocapsids and RNA-dependent RNA polymerase into the host cytoplasm. Viral entry has also been demonstrated to be a pH-dependent process (Simon et al. 2009) with low pH promoting a productive infection (Gonzalez-Scarano et al. 1984). Apart from that, successful viral entry also relies on host-cell microtubule through which they are transported to transcription and replication sites.

Viral replication occurs in the cytoplasm, and it begins when enough N protein has been synthesized (Bergeron et al. 2010). Viral polymerase transcribes the mRNA and complementary RNA from viral RNA. Viral proteins are

synthesized from mRNA, and complementary RNA is copied into new viral RNA. Viral polymerase and viral RNA complex with the N protein and are transported to the Golgi complex where they associate with Gn-Gc glycoproteins. Virions exit the host cell by fusing with its plasma membrane (Bente et al. 2013). Transcription is independent of host cell microtubule while replication, assembly, and exiting are dependent on host cell-microtubule (Simon et al. 2009).

1.3 Genetic diversity

The advent of nucleic acid sequence analysis unmasked genetically highly divergent strains. Although the strains are genetically different, they are not antigenically different. CCHF isolates thus belong to a single serogroup. The CCHFV genome segments exhibit substantial nucleotide variation: 20% (S), 22% (L) and 31% (M) segments and amino acid variation for N, Gn-Gc, and L proteins of 8, 27 and 10% respectively. This contrasts with other arboviruses which often show low levels of genome diversity (Deyde et al. 2006). The virus has been grouped into six to eight phylogenetic clades based on S segment sequence analysis (Bente et al. 2013), (Deyde et al. 2006) and these clades correlate to the geographic origin: Clade I constitute strains from West Africa, Democratic Republic of Congo (DRC) strains are in clade II, strains from South Africa, Nigeria and Mauritania are in clade III, Clade IV comprises strains from Asia and the Middle East, European strains are in clade V and the AP92 strain is in clade VI (Deyde et al. 2006). The varied number of clades has nothing to do with the phylogenetic trees themselves but the contentious interpretation of very similar branches (Bente et al. 2013). M segment sequence analysis has led to the identification of six clades (Papa et al. 2005, Morikawa et al. 2002). There is evidence of significant viral genetic diversity within each phylogenetic clade (Anagnostou and Papa 2009). As CCHFV varies within several geographical regions, strains with closely related sequences in different continents suggest virus dispersion. There exist local topotypes in Turkey (Ozkaya et al. 2010), and there are several variants of the virus within endemic areas (Aradaib et al. 2011, Ozkaya et al. 2010).

Factors responsible for the present diversity of CCHFV are genetic drift, environmental factors driving the formation of discrete genetic lineages, increased travel of livestock between continents and genetic reassortment and recombination (Bente et al. 2013). The error-prone RNA-dependent RNA polymerase introduces genome sequence changes ensuring that the virus adapts to different ticks and vertebrate hosts (Bente et al. 2013). The CCHFV M segment exhibits the greatest sequence diversity of the three segments-31% nucleotide and 27% amino acid divergence. The observed diversity in Gn and Gc glycoproteins could be a result of immune selection or the need to attach effectively to cell-surface receptors of different tick and vertebrate hosts (Deyde et al. 2006). However, this diversity at the nucleotide level is not accompanied by a corresponding greater antigenic diversity, as CCHFV form a single antigenic group (Foulke et al. 1981).

CCHFV circulates in multiple areas, not in a single homogenous geographic region. Adjustment of CCHFV to region-specific hosts that have been shaped by factors like climate and vegetation leads to the formation of discrete genetic lineages or clades (Bente et al. 2013). The existence of CCHFV with closely related sequences in different geographical locations indicates long-distance viral transfer. This transfer could have been brought by migration of birds carrying infected ticks or international trade in livestock. The latter could have seen the migration of viraemic animals or infection free animals but harboring infected ticks (Deyde et al. 2006).

Genetic diversity is also driven by reassortment and recombination. Co-infection of vertebrates or ticks by two virus strains increases the potential of genetic reassortment because of the tri-segmented nature of CCHFV genome. Reassortment is however more likely in ticks than vertebrates because infections are brief in the latter while they may last a lifetime in ticks. Reported incongruencies in S, M and L sequence data have provided the basis of genetic reassortment in CCHFV and is most common in the M segments. Reassortment has the potential to generate novel strains with modified transmission potential in ticks and vertebrates as well as increased or reduced disease severity in humans. There are however not many studies that have researched the effect reassortment has on virulence. The only available South African study in medical literature reported high mortality from reassortment (Burt et al. 2009). Reassortment can be both advantageous and deleterious to pathogen evolution. Since it can confer properties for increased transmission and virulence, interactions among genes are distorted. Such distortions have the potential to complicate the rate and progress of pathogen adaptation (Sanjuan et al. 2004). Although genetic recombination is rare among CCHFV, just like other negative-stranded RNA viruses, and has been reported only in the S segment (Deyde et al. 2006), its contribution to the high genetic diversity of CCHFV should however not be underestimated.

1.4 Epidemiology

1.4.1 Geographic distribution

The geographical distribution of CCHFV is quite extensive as shown in Figure 1.1. CCHFV has the most expansive geographic distribution of the entire tick-borne viruses. The virus is endemic in some countries in sub-Saharan Africa, the Balkans, the Middle East, South East Europe, and Western Asia. On the African continent, CCHF cases have been reported in the DRC, Kenya, Mauritania, Namibia, South Africa, Senegal, Sudan and Uganda (Dunster et al. 2002, Saluzzo et al. 1985, Gear et al. 1982, Nabeth et al. 2004, Aradaib et al. 2010, Simpson et al. 1967) while serological evidence of CCHFV circulation has been demonstrated in Cameroon, Egypt, Mali, Madagascar, Nigeria, Tanzania, Tunisia and Zimbabwe (Sadeuh-Mba et al. 2018, Hoogstraal 1979, Maiga et al. 2017, Mathiot et al. 1989, Hoogstraal 1979, Bukbuk et al. 2016, Wasfi et al. 2016, Shepherd et al. 1987). In the Middle East, CCHF cases have been reported in Iran, Iraq, Saudi Arabia, Oman and United Arab Emirates (Chinikar et al. 2005, Tantawi et al. 1980, El Azazy et al. 1997, Khan et al. 1996, Mohamed Al Dabal et al. 1997). Countries in south East Europe with reported CCHF cases include Albania, Bulgaria, Greece, Kosovo, Turkey, and Russia (Papa et al. 2001, Papa et al. 2004,

Maltezou et al. 2009, Drosten et al. 2002b, Karti et al. 2004, Onishchenko 2001). While in the Asian continent, CCHF cases have been reported in Pakistan, China and India (Burney et al. 1980, Yen et al 1985, Bajpai and Nadkar 2011). European countries in which human cases are yet to be reported but with evidence of serological CCHFV circulation include Portugal, Hungary and Romania (Filipe et al. 1985, Németh et al. 2013, Ceianu et al. 2012)

CCHFV emerged in Turkey in 2002, and almost 900 new cases are reported annually with a case fatality rate (CFR) of around 5% (Leblebicioglu et al. 2016). In the Russian Federation, the virus resurfaced in 1999 after almost three decades without cases, and 2388 human cases were reported between 1948 & 2012. Iran reported its first case in 1999 and the period from 2000-2014 has seen 1017 cases with 14.7% CFR. Some of the countries to have reported outbreaks from 1981-2014 are Albania, Greece, India, Kosovo, Sudan, Mauritania, Afghanistan, and South Africa. The CFR reported in these countries range from 3.1% to as high as 25.6% (Papa et al. 2015). Bulgaria has however reported a decline in cases. Though some countries are yet to report cases, viral circulation in ticks, wild and domesticated animals has been demonstrated. Seroepidemiological surveys in humans and animals have also provided evidence of viral circulation in the form of CCHFV specific antibodies (Bente et al. 2013). Climate change and increased migration of animals between continents can broaden the geographic range of CCHFV. The first autochthonous human case in Western Europe was reported in Spain in 2016 following the discovery of ticks infected with CCHFV in 2010 (Estrada-Pena et al. 2012, Garcia Rada 2016). There is however a documented imported case in France from Senegal (Jauréguiberry et al. 2005). As CCHFV continues to expand its geographical range, more human cases are being reported. However, increased incidence of cases could be due to increased awareness or diagnostic capacity. CCHFV is a notifiable pathogen both to the World Health Organization (WHO) and the World Organization for Animal Health because of its potential zoonotic risk. Nevertheless, CCHF occurs sporadically even in countries where it is considered endemic (Keshtkar-Jahromia et al. 2011).

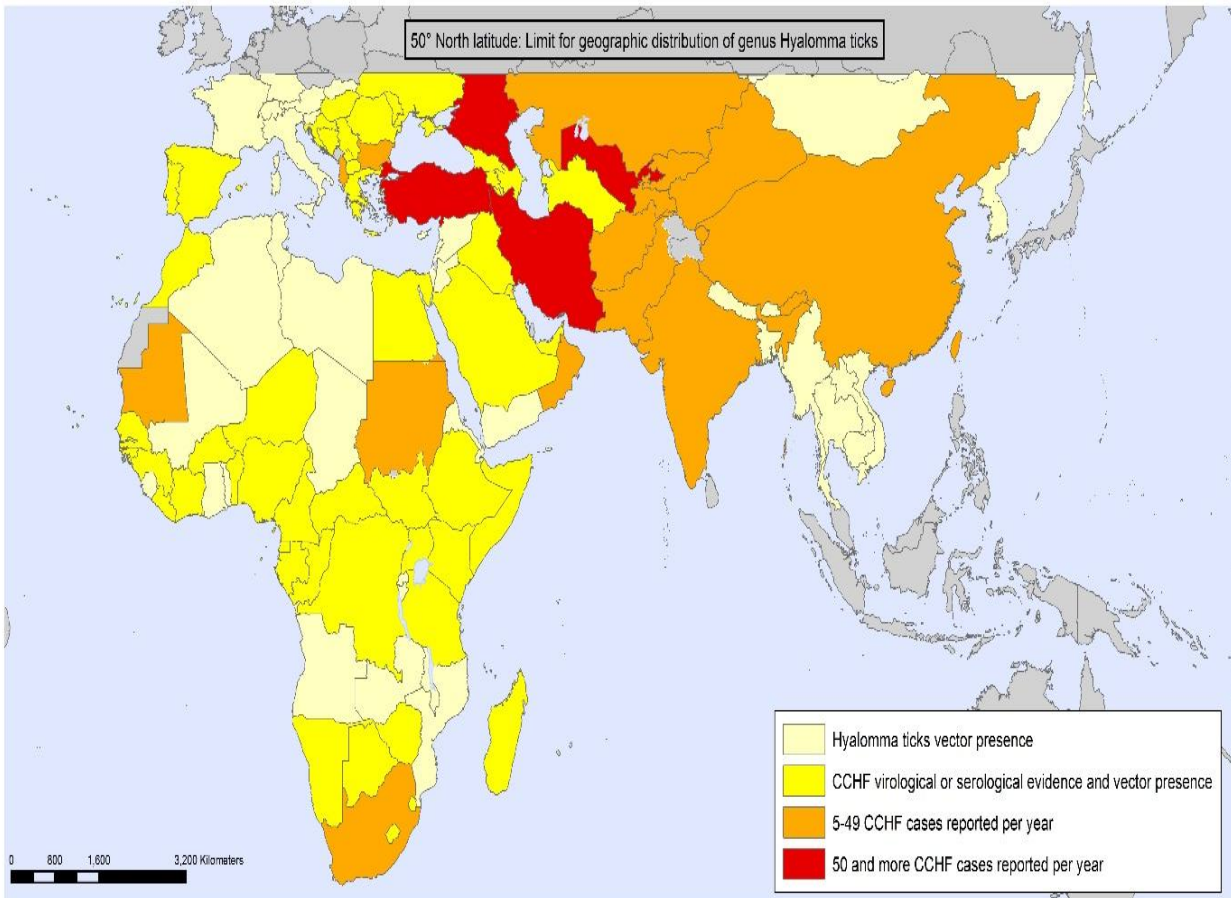


Figure 1. 1:Geographic distribution of Crimean-Congo hemorrhagic fever. The map highlights annual global occurrence of CCHF, countries with documented viral and serological evidence of CCHFV and the regions with known presence of the the principal vector, *Hyalomma* ticks. Figure created by the World Health Organization, (https://www.who.int/emergencies/diseases/crimean-congo-haemorrhagic-fever/Global_CCHF_Risk_2017.jpg?ua=1

Date accessed, 23 April 2019).

1.4.2 Life cycle of the tick and transmission pathway of CCHFV

A number of domestic and wild animals are susceptible to CCHFV as witnessed either by viral isolation or demonstration of specific antibodies. These vertebrates could be important for CCHFV maintenance and transmission since vector ticks feed on them. Birds, however, appear to resist infection (except ostriches and West African ground feeding birds) even though they can carry virus-infected ticks (Whitehouse 2004). However, they may act as catalysts for viral transfer between regions (Ergonul 2012).

Cycle of transmission of CCHFV

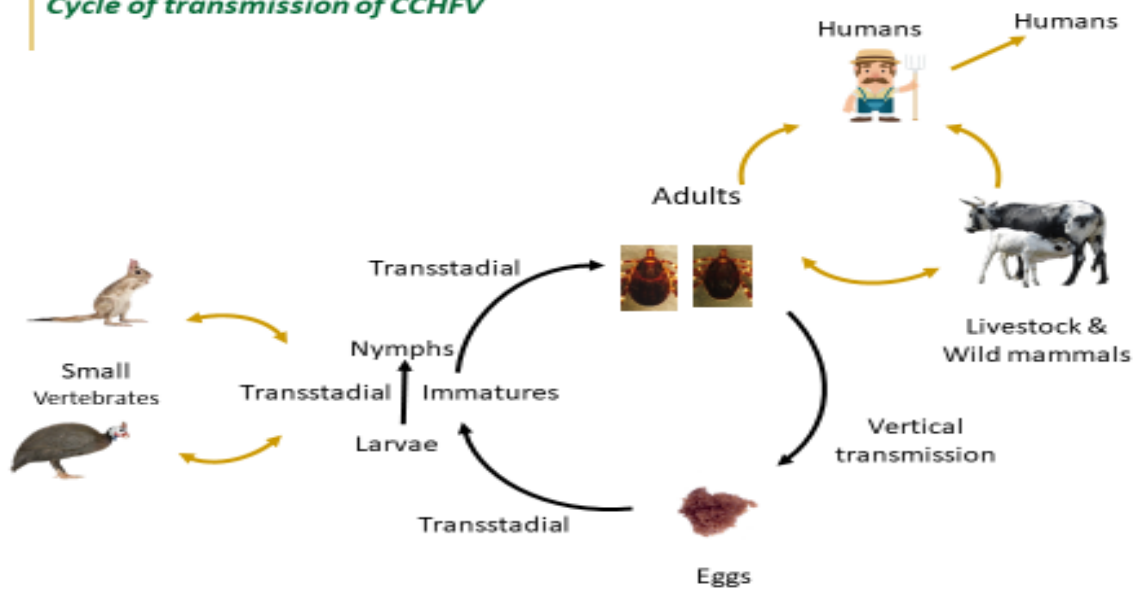


Figure 1. 2: Cycle of transmission of CCHFV. CCHFV infects competent vectors following a blood meal. Infected female ticks lay eggs which hatch and develop into larvae. The larvae feed on small mammals and molt. The nymph attaches to small vertebrates for a blood meal. After dropping off the host, the nymphs molt into adults. Adult ticks feed on large herbivores. Human infections follow bites by infected ticks, contact with infected animal fluids or human to human transmission. (Image by Prof FJ Burt, unpublished)

CCHFV circulates in an enzootic tick–vertebrate–tick cycle with human beings serving as accidental hosts. Cycle of transmission for of CCHFV is described in Figure 1.2. Two families of ticks are recognized, *Argasidae* possessing a soft body and *Ixodidae* or hard ticks (Black and Piesman 1994). CCHFV persistence has only been demonstrated in ixodid ticks while ticks from the *Argasidae* family could not support viral persistence in experimental studies (Durden et al. 1993). Ixodid ticks have three developmental stages: larvae, nymphs, and adults. Development from one stage to another requires nutrients obtained through a blood meal from vertebrates. CCHFV infection is maintained in the three tick stages larva, nymph and adult (trans-stadial) (Appannanavar and Mishra 2011). The larva and nymph feed on small mammals transmitting the virus to the host and the small vertebrate animal function as viral amplification hosts (Charrel et al. 2004). Uninfected ticks acquire infection upon feeding viraemic animals. Horizontal transmission (from ticks to mammals) occurs predominantly in the course of the spring and summer months (Bente et al. 2013). The tick midgut lining supports CCHFV replication which is followed by viral dissemination around tick body organs, notably the reproductive organs and the salivary glands (Dickson and Turell 1992). After nymphs molt into adults, the adult ticks feed on large herbivores, and this is the time for mating which takes place while attached to the large vertebrates. Subsequently, the females lay eggs in a suitable environment. Infection invades the ovaries resulting in

infection of eggs thus infection passes from the mother to the offspring (transovarial). Female ticks lay thousands of eggs which if are infected can sustain a large population of infected ticks (Nuttall et al. 2004). Viral transmission from an infected tick to a healthy tick transmission has been demonstrated to occur through co-feeding in the absence of viraemia (Labuda et al. 1996). This non-viraemic transmission is mediated by pharmacologically active substances in tick saliva (Nuttall et al. 2004).

Even though CCHFV is found in over 30 species of hard ticks, the *Hyalomma* species are considered to play a significant role in viral epidemiology. To this end, it has been discovered that CCHFV is commonly found in regions with the *Hyalomma* species (Watts et al. 1989). Viral isolation, replication and tissue tropism has been demonstrated ruling out the possibility that these ticks serve in mechanical transmission of CCHFV but are indeed primary vectors (Dickson and Turell 1992). CCHFV has also been detected in other genera of ticks such as *Rhipicephalus* and *Dermacentor* (Yesilbag et al. 2013, Gargili et al. 2011) but the role played by these tick species in viral transmission and maintenance is not yet clear.

People at risk of contracting CCHF are those who reside in endemic areas especially those occupationally exposed to infected humans or animals. This group includes health care workers, livestock breeders and abattoir workers. There seems to be no association between gender and acquisition of the virus (Ergonul 2012). Human infections are a result of bites from infected ticks, crushing infected ticks with bare hands, percutaneous or permucosal exposure to infected human and animal tissue, blood, excreta or secreta (Ergonul and Whitehouse 2007) and drinking raw milk from infected animals (Swanepoel 1985).

Hemorrhages act as an essential vehicle of viral spread thus nosocomial transmission is common. Higher mortality rates in nosocomial transmissions compared to tick bites could be a consequence higher viral load in the former (Shayan et al. 2015). There are reports of hospital outbreaks following procedures such as exploratory surgery on undiagnosed patients (Whitehouse 2004). An internet search of articles published in PubMed in 2007 by a group of researchers yielded nine nosocomial outbreaks (Vorou et al. 2007). In a nosocomial outbreak at a hospital in Pakistan in January 1976, 10 out of 12 medical personnel who cared a CCHF patient contracted the virus. Two of them died while eight recovered after severe illness (Burney et al. 1976). In another nosocomial outbreak at a hospital in South Africa, 33% of health care professionals developed CCHF via unintentional needle pricks when caring for CCHF patients. Another 8.7% health care professionals contracted infection after they had been exposed to the patient's blood (van de Wal et al. 1985). One other group, particularly at risk, are laboratory workers who handle viral material and cases have been reported in Africa (Simpson et al. 1967).

1.5 Signs and symptoms

Findings from serological surveys show that CCHFV does infect several wild and domestic animals (Spengler et al. 2016) even though severe disease outcome has only been reported in humans and newborn mice. Animals clear infection without overt signs of illness. There are four phases of disease: incubation, pre-hemorrhagic, hemorrhagic and convalescence. The clinical spectrum of CCHF varies from asymptomatic or mild to severe disease and death (Bodur et al. 2012). The incubation period ranges from 1-9 days depending on the route of transmission and amount of inoculum. It is shortest in infections resulting from tick bites, fairly long from those resulting from livestock contact and longest in nosocomial infections (Vorou et al. 2007). It is believed that different hosts modulate CCHFV virulence by inducing viral phenotypic changes (Gonzalez et al. 1995). Not only does the route of entry affect the incubation period but disease severity as well. Nosocomial infections have higher mortality than tick bite infections and this has been attributed to a high level of viremia in the former (Akinci et al. 2013).

After the incubation period comes the pre-hemorrhagic phase for which the symptoms are non-specific. These include abrupt fever (39-41°C), headache, chills, photophobia, back and abdominal pains. Some people lose appetite while others feel nauseous with a propensity towards vomiting and diarrhea (Whitehouse 2004). Still, others experience neuropsychiatric changes such as mood swings, confusion and aggression which can be accompanied by episodes of violent behavior (Swanepoel et al. 1989).

Hemorrhagic manifestations develop in severe cases 3-6 days after onset of disease and these ranges from small to large areas of bleeding into tissues. Bleeding is usually from the gastrointestinal tract, nose, urinary system and cerebrum in severe cases (Swanepoel et al. 1987). Enlarged heart and spleen occur in 30% of patients. Main laboratory features are leucopenia, thrombocytopenia, elevated liver enzymes and abnormal coagulation indices (Hatipoglu et al. 2010). Fibrin split products are indicative of disseminated intravascular coagulation (DIC) while elevated serum creatinine and urea point to renal insufficiency. Hemorrhage, hypovolemic shock and multiorgan failure lead to death (Ergonul 2012). The mortality rate is estimated at 30%. Higher case fatality rates (CFR) have been reported in some outbreaks and it could be that mild cases are not being diagnosed thus they are left out in the calculation of CFR. However, differences in the quality of medical care, timing of instituting treatment interventions and differences in viral virulence could be responsible for the different CFRs reported.

For those who survive, convalescence begins on average 15-20 days after onset of symptoms. There is weakness, weak pulse, bad eyesight, poor appetite and hair loss (Hoogstraal 1979). These sequelae may last for more than a year but are rarely permanent and infection is not known to relapse.

1.6 CCHF animal models

Coming up with an animal model in which the CCHF disease pattern closely resembled human CCHF disease has been a challenge until recently (Dowall et al. 2017). Infant mice though receptive to CCHFV cannot be a fitting animal model because of the immature immune system while adult mice like a number of non-human vertebrates do not show symptoms. Thus, appropriate animal models for investigating CCHF disease course in humans have therefore not been available until recently when studies with mice deficient in the interferon system demonstrated development of symptoms similar to humans after inoculation with CCHFV. The earliest models were mice lacking type 1 interferons (IFNAR^{-/-}) (Berezky et al. 2010) and all the three types of interferons (STAT^{-/-}) (Bente et al. 2010) then a mouse model in which type 1 interferons are temporarily suppressed (IS) has also demonstrated susceptibility to CCHF infection (Garrison et al. 2017). These innate immune deficient mice are highly responsive to infection, death occurring within five days of infection. Animals exhibit elevated levels of pro-inflammatory cytokines, elevated hepatic enzymes, leukopenia and thrombocytopenia prior death; features which are common in human infections (Zivcec et al. 2013, Berezky et al. 2010, Bente et al. 2010). However, immune responses in these animal models are limited due to the deficiencies in the interferon system and death which occurs before development of antibody responses (Hawman and Feldman 2018). An additional model including humanized mice has also been reported (Spengler et al., 2017). Strain-specific virulence was observed with the humanised mice model (Hawman and Feldman 2018), death occurring within 2-3 weeks after inoculation with a CCHFV Turkish strain while infecting mice with an Oman strain did not result in mortality (Spengler et al. 2017). Significantly, neuropathology was described in mice infected with the Turkish strain raising possibilities that the humanized mice model can be used to investigate CCHFV associated neuropathogenesis (Spengler et al. 2017). An animal model in higher mammals (*Cynomolgus macaque*) was reported in 2018 (Haddock et al. 2018). This latest model will be more valuable for the development of therapies against CCHFV since the *Cynomolgus* macaques are immunocompetent, unlike earlier models.

1.7 Pathogenesis

There is paucity of knowledge regarding the pathogenesis of CCHF. WHO classifies CCHF into Risk group IV and as such pathogens in this group require highly specialized facilities for their handling. The requirement for Biosafety Level 4 (BSL-4) conditions and absence of suitable animal models (until recently) limits studies on CCHFV. Apart from that infections are usually sporadic and occur in limited resource areas where complete autopsies are rarely performed. Available knowledge is thus mainly from the body's response to infection and studies on liver biopsies of patients (Whitehouse 2004) and newborn mice (Keshtkar-Jahromia 2011). Newborn mice do not serve as the best of disease models since many pathogens can establish an infection. Moreover, disease course in mice does not closely resemble human disease. Interferon- α/β deficient and STAT^{-/-} mice are however promising animal models (Bente et al. 2010) even though they are not immunocompetent.

Following CCHFV entry into the host, it replicates in dendritic cells (DC) and tissue macrophages from which the virus disseminates to regional lymph nodes where the virus is transmitted to the liver, spleen and lymph nodes via lymph and blood monocytes (Ergonul 2012). The brain is involved but at a later stage in the infection (Bente et al. 2010).

The endothelium could be the main target of CCHF as evidenced by hemorrhage, increased vascular permeability and the presence of viral antigens in endothelial cells (EC) (Burt et al. 1997). There is upregulation of soluble adhesion molecules, ICAM-1 and VCAM-1 in CCHF patients and fatal cases. These molecules can be used as markers of endothelial activation, indicators of vascular damage and disease severity (Ozturk et al. 2010). Secretion of proinflammatory cytokines interleukin (IL)-1, IL-6, IL-8, IL-10 and tumor necrosis factor- α is enhanced by CCHFV infection of ECs, DCs and macrophages. These cytokines are chief in the progression of CCHF as such high levels of these cytokines are implicated as prognostic factors showing disease severity in CCHF patients (Bente et al. 2010, Saksida et al. 2010). Excessive release of these cytokines is known to damage the endothelium resulting in increased vascular permeability, vasodilation, multiple organ failure and shock (Connolly-Anderson 2010).

The innate immune system constitutes the first line of defense against viruses. Observations that CCHFV do result in severe disease in mice lacking interferon signaling and not in mice with the intact immune systems is evidence of the role played by the innate immune systems in restricting CCHFV pathogenesis (Hawman and Feldman 2018). Innate immune sensor retinoic acid-inducible gene-I (RIG-1) recognizes CCHFV RNA in the cytoplasm stimulating type 1 interferon response (Spengler et al. 2015). The presence of other innate immune sensors for CCHFV cannot be ruled out (Hawman and Feldman 2018). Studies in humans have demonstrated correlation between polymorphism in Toll-like receptors (TLR) 7, 8, 9 and 10 and clinical course of CCHF disease in Turkey (Arslan et al. 2015, Engin et al. 2010, Kızıldağ et al. 2018). Apart from TLRs, studies in CCHF patients suggest that polymorphism in nuclear factor (NF)- κ B is a predictor of CCHF disease course (Arslan and Engin 2012). It however remains to be established whether occurrence of these polymorphisms correlate with disease severity and outcome with strains from different geographical regions (Hawman and Feldman 2018).

Pathogen invasion elicits host defence mechanisms such as addition of ubiquitin to proteins for proteosomal degradation and non-degradative ubiquitination (Davies and Gack 2015) and induction of interferon stimulated genes (ISG) by interferons to inhibit viral replication and immune modulation (Perng 2018). One of the ISGs upregulated to modulate innate antiviral responses is ISG15 (Perng 2018). The CCHFV OTU domain prevents conjugation of ubiquitin to proteins and has de-ISGylation activity (Scholte et al. 2017, James et al. 2011). In vitro studies have demonstrated inferior growth kinetics of recombinant CCHFV strains with deficient de-ubiquitinase and de-ISGylation activity compared to wild type CCHFV in cells with an intact interferon system but not in cells with an abolished interferon system (Scholte et al. 2017). These findings support an active role of the OTU domain in suppressing

interferon responses (Scholte et al. 2017). Further evidence for the role of the OTU domain as a virulence factor came from observations that the CCHFV OTU domain's affinity for mice ISG15 is reduced compared to human ISG15 (Capodagli et al. 2013).

CCHFV negatively affects the innate immune system thus delaying the induction of the adaptive immune response which is vital in clearing the viruses (Weber and Mirazimi 2008, Saksida et al. 2010). CCHFV has an array of strategies in which it blocks the immune response thereby allowing uncontrolled viral replication and subsequently systemic viral spread throughout the body. Partial activation of macrophages and DCs means they cannot fully function as antigen presenting cells resulting in lack of upregulation of major histocompatibility complex II and this has consequences in priming of naïve T cells (Bente et al. 2010). Hyperactivation of monocytes and macrophages with concomitant cytopenias due to excessive phagocytosis is the hallmark of the hemophagocytic syndrome. This syndrome has been reported in 50% of CCHF patients, being more common in those presenting with severe bleeding (Cagatay et al. 2007). Apart from that, CCHFV delays the induction of interferons (IFNs) rendering them ineffective once infection has been established. IFNs are an essential part of the innate immune system conferring an antiviral response thereby limiting the spread of infection. They promote expression of potent antiviral proteins, inhibit cell proliferation, regulate apoptosis and are involved in immunomodulation (Weber and Mirazimi 2008). An undetectable antibody response is a common feature in fatal cases and this is accompanied by higher viral loads. Decreased numbers of natural killer cells and lymphocytes were observed in a mouse model (Bente et al. 2010). Natural killer cells are responsible for detection and lysis of infected cells while lymphocytes are responsible for orchestrating immune responses (Akinici et al. 2013). The above viral strategies point to the disruption of the two arms of the immune system.

CCHFV modifies hemostasis in two ways: direct damage of cells involved in hemostasis like platelets and ECs and cell injury as a consequence of immune responses (Chen and Cosgriff 2000). A constellation of factors -vascular endothelial injury, DIC, thrombocytopenia, liver dysfunction and reduced levels of plasma coagulation factors lead to hemorrhage (Burt et al. 1997, Peters and Zaki 2002). Platelet adherence to damaged endothelium activates the coagulation pathway leading to DIC (Schnittler and Feldmann 2013). Depleted plasma coagulation factors are a result of either increased consumption in DIC or impaired synthesis emanating from liver dysfunction while thrombocytopenia could be due to increased platelet consumption as a result of DIC or bone marrow hypoplasia (Chen and Cosgriff 2000).

1.8 Laboratory diagnosis

Early diagnosis is critical for patient management as well as prevention of further transmission of disease. The following are indicators of CCHF: compatible clinical manifestations, epidemiological risk factors such as tick bite,

staying or traveling in endemic areas, exposure to blood/tissues of animal/human cases and compatible laboratory presentation such as leucopenia, thrombocytopenia (Appannanavar and Mishra 2011). The nonspecific symptoms and variable length of the incubation period make differential diagnostics necessary. Differential diagnosis depends on the geographical region of case presentation and it includes rickettsiosis, borreliosis, leptospirosis, malaria, viral infections and other hemorrhagic fevers (Appannanavar and Mishra 2011) caused by viruses from *Arenaviridae*, *Nairoviridae*, *Hantaviridae*, *Phenuiviridae*, *Filoviridae* and *Flaviviridae* families.

Clinical samples for CCHFV diagnosis include serum/plasma samples, midstream urine, and throat swab. For postmortem cases, liver, spleen and kidney tissue are desirable (Whitehouse 2004). The most common approaches of CCHFV diagnosis are detection of viral RNA (Drosten et al. 2003) detection of virus-specific antibodies/antigen (Saijo et al. 2005) and the isolation of virus (Zeller 2007).

1.8.1 Viral Isolation

Viral isolation is only performed in BSL-4 laboratories. This is the most definitive test and can be achieved by intracranial inoculation of day old mice or culture in mammalian cells (Zeller 2007). The latter is simpler and has shorter turnaround times. However, newborn mice inoculation is more sensitive, capable of isolating low viral concentrations. Cell culture is considered less sensitive for it is most effective in cases of high viral concentrations (Vanhomwegen et al. 2012). A number of cell lines support the growth of CCHFV and these include Vero, SW-13 and BHK-21 (Appannanavar and Mishra 2011). CCHFV is seldom cytopathic requiring viral detection and identification by the immunofluorescence test (Whitehouse 2004). The average turnaround time (TAT) in cell cultures is 3.3 days and 7.7 days in mice (Burt et al. 2011) and these TATs are not the best in the management of acute cases.

1.8.2 Serological Assays

Immunologically CCHF is diagnosed by demonstrating specific IgM and IgG antibodies. Antibody identification is frequently performed using enzyme-linked immunosorbent assays (ELISA) or immunofluorescence assays (Ergonul 2012). Seroconversion with detection of CCHFV IgM antibodies in a single specimen or an increase in antibody titer by a factor of four or more is indicative of recent infection in samples taken 2-4 weeks apart (Kubar et al. 2011). The earliest serological marker is the NP IgM becoming detectable 2-3 days after onset of symptoms followed by the GPC IgM (4-6 days) and IgG NP and GPC (5-6) days (Ergunay et al. 2014). IgM serum titer is at its peak 14-21 days after onset of illness. IgM antibody levels usually diminish with the progression of time reaching to levels that cannot be detected by available assays by the sixth month. IgG levels do decline as well but can be found in serum many years after resolution of infection (Burt et al. 1994, Shepherd et al. 1989). Fatal cases rarely produce a detectable antibody response (Ergonul et al. 2006, Ozturk et al. 2012). CCHFV delays induction of immune responses (Saksida et al. 2010) thus serological assays are not appropriate in early CCHF disease as antibody responses are absent.

Commercial serological assays are available for CCHFV diagnosis. ELISA kits for detecting IgM, IgG antibodies and CCHFV antigen in human serum (Vector-Best, Novosibirsk, Russia) are available. The manufacturer does not however state the target antigen for the ELISA IgM and IgG. Indirect immunofluorescence tests for determination of IgM or IgG against the CCHFV GP and NP in human serum are available commercially (Euroimmun, Luebeck, Germany). The EUROIMMUN kits contain BIOCHIPS coated with CCHFV transfected cells. The cells were transfected with plasmids encoding the CCHFV glycoprotein precursor and the nucleoprotein. Recently a competition competition ELISA for screening CCHFV specific antibodies from various animal species was developed for use in sero-epidemiological surveys. The assay uses a mouse monoclonal antibody to compete with test serum for the nucleoprotein antigen and an anti-mouse conjugate function as the detection system (Schuster et al 2016).

Serological cross-reactivity has been demonstrated between CCHFV, Dugbe and Hazara NP (Marriott et al. 1994). However, circulation of Hazara virus in South Africa has not been demonstrated in previous serologic surveys while a Dugbe virus human infection has been described (Burt et al. 1996). Dugbe virus is less pathogenic than CCHFV (Shi et al. 2018).

Detection of the CCHFV antigen in acute phase of disease has been described using antigen capture ELISA (Saijo et al. 2005) and the reversed passive hemagglutination test (Shepherd et al. 1988). The CCHFV NP which is the most abundant protein, most conserved and highly immunogenic makes is the ideal target antigen for detection. The CCHFV antigen was detected 2-11 days post development of symptoms mostly in patients with high viral loads and fatal cases. Although antigen detection is useful in the early course of disease, the antigen is not detected in survivors who develop an antibody response (Saijo et al. 2005) thus its lack of sensitivity in those with a non-fatal outcome should be considered.

1.8.3 Molecular Techniques

CCHFV nucleic acid is detected in serum samples in the early stage of disease by reverse transcriptase polymerase chain reaction (RT-PCR) assays. CCHFV RNA detection by RT-PCR based on the conventional PCR method was first described in 1996. A conserved region of the S segment was identified by aligning seven strains from different regions of the world (Schwarz et al. 1995, Rodriguez et al. 1997, Burt et al. 1998). Real time RT-PCR for CCHFV detection and quantification was first developed using primers designed from alignments of 36 CCHFV isolates from across the globe (Drosten et al. 2002a). The assay used SybrGreen® for detection of the amplicons. Thereafter a one step real time RT-PCR procedure targeting a conserved NP region of 19 CCHFV global strains and employing the Taqman based detection was developed (Yapar et al. 2005). Other real time RT-PCR assays described over the years and targeting the S segment are based on the fluorescence resonance energy transfer (FRET) probe technology (Duh et al. 2006), multiple probes (Wölfel et al. 2009), the Taqman ((R))-minor groove binding protein

probe technology (Garrison et al. 2007) which uses shorter probes and is more appropriate in cases of high nucleotide sequence diversity. To improve assay specificity which has been a challenge due to sequence variability amongst geographically distinct strains, an assay was developed with primers targeting the 5' and 3' non-coding region of the S segment which has reduced pressure for genetic variability (Atkinson et al. 2012). Further improvements in real time RT-PCR assays for CCHFV detection and quantification include an assay for detecting various CCHFV genotypes using chemically inactivated patient samples, possibly removing the requirement of BSL-4 facilities (Jääskeläinen et al. 2014) and a molecular beacon real time RT-PCR (Kamboj et al. 2014). Other variations of RT-PCRs for CCHFV diagnosis described in literature include nested PCR (Elata et al. 2011, Negredo et al. 2017), single round PCR (Deyde et al., 2006). Besides RT-PCR, isothermal molecular techniques for CCHFV diagnosis published in literature include reverse transcription loop-mediated isothermal amplification (RT-LAMP) (Osman et al. 2013) and recombinase polymerase amplification (RPA) (Bonney et al. 2017). Isothermal molecular techniques have advantages over RT-PCR in that they do not require specialized equipment thus they are suitable for use in the field or in poor resource settings. Besides that, absence of thermocycling in LAMP and RPA facilitates faster amplification and ultimately diagnosis (Bonney et al. 2017).

Diagnosis with molecular techniques is brought about by the amplification of the regions of the S segment of the viral genome that do not undergo mutation using consensus primers (Burt et al. 2011). The S segment with a nucleotide variation of 20% is considered the least variable of the three segments. CCHFV is therefore highly variable thus there isn't a single set of primers capable of detecting all known strains (Burt et al. 1998). Design of primers should, therefore, be continuously reviewed in light of newly published sequences of local circulating strains. However, molecular techniques offer many advantages. Laboratories without BSL-4 facilities can diagnose CCHFV and because of the high sensitivity of the assays, viral nucleic acid can be obtained from culture-negative samples (Schwarz et al. 1996). Results are available in a matter of hours as opposed to days with culture methods.

CCHFV nucleic acid can be detected in ticks and as such viral epidemiologic studies are enhanced (Whitehouse 2004). Genome sequencing techniques allow characterization of novel strains. Data from sequencing is used to identify strains causing regional outbreaks as well as pandemic strains. Moreover, the virus can be traced to how it is evolving thus the ability of CCHFV to reassort has been demonstrated (Hewson et al 2004a).

1.9 Treatment

1.9.1 Supportive Therapy

Specific antiviral therapy for CCHFV is yet to be established. Treatment is thus mainly supportive therapy, and this entails monitoring of full blood counts, levels of serum electrolytes, coagulation indices and replacement of blood and blood components like fresh frozen plasma and platelets. Consequences of increased vascular leakage such as

hypotension and reduced oxygen supply to tissues are managed by fluid replacement. However, caution should be exercised to prevent overloading the circulatory system which can cause pulmonary edema (Bente et al. 2013). Drugs which interfere with blood clotting mechanisms and administration of medicines via the intramuscular route should be avoided since patients tend to hemorrhage (Ergonul 2006). Supportive therapy on its own has been sufficient in some cases.

1.9.2 Ribavirin

The antiviral drug ribavirin has been in use for a long time for prophylaxis and therapy of CCHF. The drug's broad-spectrum antiviral activity has been explained through its direct mechanisms; immunomodulatory effects, inosine monophosphate dehydrogenase inhibition and direct mechanisms; polymerase inhibition, lethal mutagenesis and interference with mRNA capping (Graci and Cameron 2016). Antiviral activity has been demonstrated in virus-infected cells, newborn mice and STAT^{-/-} mice. Despite its widespread use in endemic areas, its efficacy for both prophylaxis and therapy remains debatable. Whilst some studies reported a high success rate in severely diseased cases if administered early in the course of infection (Metanat et al. 2006, Izadi 2009, Tasdelen Fisgin et al. 2009) other studies have found no difference in prognosis between recipients and non-recipients (Cevik et al. 2008, Bodur et al. 2011). Factors called to explain the limited value of many studies include variation in the patient population, small sample sizes and that variables like disease severity and stage of the disease when ribavirin was administered were not matched.

1.9.3 Specific immunoglobulin

Specific immunoglobulin derived from patients who recovered from infection has been used for therapy and prophylaxis on several occasions. Its use dates back to the Crimean outbreak of 1944-45. It is administered either intramuscularly or intravenously. However, its efficacy needs to be proved in clinical trials. There were no comparison groups in the limited studies that have reported its efficacy (Kubar et al. 2011, van Eeden et al. 1985b). Besides, supportive therapy was rendered in these cases thus the observed effects cannot be attributed to immunoglobulin therapy alone.

1.9.4 Monoclonal Antibodies

Monoclonal antibodies (mAb) offer another therapeutic approach given their specific antiviral activity and limited side effects. mAb against CCHFV targeting the nucleocapsid proteins were first described in 1987 (Blackburn et al. 1987). However, the mAb are unlikely to have neutralizing capacity even though immune correlates of CCHFV protection are not yet delineated. There have been attempts to develop anti-CCHFV mAb recognizing conformational epitopes within the Gn and Gc glycoproteins of CCHFV IbAr 10200 strain. mAb to Gn offered protection to mice 24 hours before and after virus administration while mAb to Gc could only confer protection 24 hours before virus

administration. Only anti-Gc mAb could neutralize CCHFV in cell culture (Bertolotti-Ciarlet et al. 2005). Neutralizing activity was thus concluded, not only to rely on the biological makeup of the antibody but other factors as well (Keshtkar-Jahromia et al. 2011).

1.10 Vaccines

1.10.1 Bulgarian Vaccine

There is no internationally licensed vaccine for CCHFV. The Bulgarian vaccine is recognized and used only in Bulgaria. It has its origins in the Union of Soviet Socialist Republics (USSR) and has been in use in Bulgaria since 1974. The vaccine is comprised of an inactivated CCHFV antigen as the active substance and other auxiliary substances (Keshtkar-Jahromia et al. 2011). The vaccine is credited for a fourfold reduction in reported cases to the Bulgarian Ministry of Health over 22 years (Christova et al. 2010). It has also been noted that there were no cases in vaccinated military and laboratory personnel. The latter worked with the virus and none contracted infection even after exposure through needle pricking. However, the reduction in Bulgarian cases observed could have been due to some other factors at play. Viral epidemiology and ecology could have changed over the same period without intervention. Reduction in tick exposure by behavior change due to heightened awareness or a change in case reporting after the introduction of the vaccine could be other possible factors. In a study to determine the clinical efficacy of the vaccine by Mousavi-Jazi and colleagues, they reported cellular and immune responses in vaccinated individuals, but the capacity of the antibodies to neutralize CCHFV was deemed low (Mousavi-Jazi et al. 2012).

Generation of virions for vaccine preparation requires BSL-4 facilities. Moreover, there are safety concerns over vaccines grown in mouse brains for there are concerns about adverse side effects caused by the myelin basic protein (Hemachuda et al. 1987, Jelinek et al. 2008). Repeated vaccinations at one year after vaccination and then after every five years (Keshtkar-Jahromi et al. 2011) to maintain immunity makes its administration labor intensive. Apart from that, the vaccine does not cater for all the population age groups since it can only be administered to persons above 16 years of age. Worse still, CCHFV divergence makes the efficacy of Bulgarian vaccine doubtful for the different viral strains found in different geographical locations. This calls for more vaccine platforms that consider all these factors.

1.10.2 Nucleic acid vaccines

1.10.2.1 History

The principle behind DNA vaccination came from the realization that DNA can be transferred to animals and the genes encoded can be expressed (Paschkis et al. 1955). The idea was boosted when the expressed genes were shown to elicit an immune response. DNA from polyomaviruses was demonstrated to induce tumors and specific

antibodies when introduced to animals (Atanasiu et al. 1962). Similar findings were observed by other researchers. Subsequent studies concentrated on the use of plasmids to deliver genes. In 1992, plasmid gene delivery was reported to generate cell-mediated immune responses against influenza and human immunodeficiency viruses (Ulmer et al. 1993) thus the foundations of genetic vaccination were laid. The field has since advanced with the licensure of platforms for veterinary use such as West Nile virus for horses and hematopoietic necrosis in fish (Flingai et al. 2013).

1.10.2.2 Construction of DNA vaccines

Genetic vaccines are principally made from bacterial plasmids combining gene sequences allowing replication and selection in bacterial cells with nucleotide sequences promoting expression of gene(s) of interest in vertebrate cells (Williams 2013). Viral particles composed of defective RNA genomes have also been described. These expression plasmids can be visualized as composed of two units. The antigen expression unit has sequences for the promoter, antigen of interest and polyadenylation (Azevedo et al 1999). The production unit has bacterial sequences for amplification and selection (Azevedo et al 1999). The plasmids are constructed using DNA recombinant technology. After construction, bacterial cells are transformed with the plasmids. The growth of bacterial cells allows production of multiple copies of plasmids which are purified before use.

1.10.2.3 Mechanism of action

Mimicking events that normally occur during a viral infection is the hallmark of nucleic acid vaccines. DNA vaccination provokes an immune response by introducing into the host cell, DNA coding the antigen of interest. Following uptake of transfected DNA, host cellular machinery facilitates endogenous production of the antigen encoded by the DNA. The synthesized foreign protein is regarded as foreign by the host immune system prompting humoral and cell-mediated immune responses (Flingai et al. 2013). Transfected nonantigen presenting cells excrete the antigen into the extracellular space and these are taken up, processed by antigen presenting cells (APC) and presented in context with major histocompatibility (MHC) II molecules. Antigens produced within APCs are presented by MHC I molecules. There is also cross-presentation of antigens produced within non-APCs through the MHC I pathway (Bins et al. 2013). In addition to the presence of antigen, APCs undergo extensive differentiation and maturation to present antigens to T lymphocytes effectively. However, the full repertoire of molecular structures that drive maturation and migration of APCs to lymphoid organs are yet to be delineated.

1.10.2.4 Advantages

DNA vaccines offer many attractive advantages. Traditional vaccines elicit antibody responses directed towards epitopes on the introduced inoculum. These surface antigens are bound to change as the virus evolves rendering the vaccine less effective. With DNA vaccines, conserved regions are selected and expressed thus multiple antigens can

be used to generate a broad spectrum vaccine (Redding and Werner 2009). Since particular epitopes are selected, immune responses to the particular antigen are generated thus it is possible to differentiate immune responses from natural infections and vaccination (Vander Veen et al. 2012). Even though the mechanisms of generating cytotoxic T lymphocyte responses are the same in live attenuated and DNA vaccines, the risk of reverting to virulence seen with attenuated vaccines is not present with DNA vaccines (Flingai et al. 2013). It is possible to administer multiple doses of vaccine without generating vector immunity. This makes them superior to bacterial or viral vectors where immune responses against the vector dampen the effectiveness of the vaccine (Bins et al. 2013).

1.10.2.5 Disadvantages

The greatest drawback with DNA vaccines has been their reduced immunogenicity in higher mammals. Thus investigating mechanisms of enhancing their immune responses is an area of intense research. Since DNA codes for proteins, it means DNA vaccines are limited to protein immunogens (Kindt et al. 2007). This in itself may not be much of a problem for proteins are the most immunogenic. There are also safety issues around the use of these vaccines. There is a possibility that the DNA introduced in vaccines can be integrated into host DNA thus modulating genes responsible for cell growth. Apart from that, anti-DNA antibodies can be elicited as a consequence of vaccination (Flingai et al. 2013). However, these fears are yet to be substantiated.

1.10.2.6 Strategies for enhancing immunogenicity

Despite their satisfactory immune responses in small animal models and variable vaccine efficacy in large animal models, their clinical ability remains unproven. DNA vaccines target innate signaling receptors, but the resulting immune responses have not been strong enough (Naslund et al. 2011). There have been however several strategies to improve humoral and cellular immune responses. These include co-administration of genetic adjuvants such as granulocyte macrophage colony stimulating factor and interleukin-15 (Loudon et al. 2010, Eickhoff et al. 2011, Fagone et al. 2011). Optimizing expression levels is another strategy and can be achieved through the use of viral promoters such as the human cytomegalovirus immediate early promoter (hCMV-IE) (Chatellard et al. 2007), codon optimization (Ko et al. 2005), addition of signal sequences (Brulet et al. 2007), genetic fusion to an entire protein or protein domain and targeting vaccine to dendritic cells.

1.10.2.7 Replicon vaccines

Even though the above strategies enhanced DNA vaccine immunogenicity, induction of robust immune responses in larger mammals was not frequently demonstrated. DNA vaccine potency could, however, be increased by using RNA replicons. Replicon vaccines make use of defective viral genomes incapable of producing infective virions to express proteins of interest. Alphavirus (Ljungberg 2007), flavivirus (Kortekaas et al. 2011) and measles virus (Singh et al. 1999) rhabdoviruses (Ryder et al. 2015, McKenna et al. 2007) adenoviruses (Holman et al. 2009) replicon vectors

are described in literature and alphavirus genomes are the most commonly used. Alphavirus genomes based on Venezuelan equine encephalitis virus (VEEV), Sindbis viruses, and Semliki Forest viruses (Gorchakov et al. 2007) have shown lots of promise in animal models. With alphavirus, the structural genes downstream of the 26S promoter are replaced with the gene(s) of interest. The replicon vaccine can be administered as viral particles capable of only infecting the transfected cell, naked RNA (Vander Veen et al. 2012) or can be launched from a DNA plasmid generating an alphavirus replicon-based DNA vector (DREP) (Ljungberg 2007). DREP vaccines have the advantage of being stable. The replicon can be self-amplifying or can be under the control of a promoter like hCMV-IE to drive the expression of the gene(s) of interest. Protein expression and interferon type 1 responses can be enhanced in a self-amplifying replicon by addition of alphavirus genomic promoter elements in the sub-genomic RNA (Kim et al. 2014).

These replicons are capable of producing copious amounts of the transgene product. Increased immunogenicity of alphavirus-based vectors is however due to the activation of the innate immune response as opposed to increased antigen production. Naslund and colleagues found similar T cell responses in DREP based vaccines and those composed of propagation-defective replicon particles thus they suggested activation of the same innate signaling pathways. However, it seems replicon vectors influence innate signaling pathways which dampen as well as those which activate the immune response as seen by the balanced immune responses generated (Naslund et al. 2011). Understanding the mechanisms that underpin this balance between inhibitory and stimulatory signals will inform researches that are seeking to improve the immunogenicity of DNA based replicon vaccines.

Stronger humoral and cell-mediated immune responses have been reported with replicon vaccines than conventional plasmid DNA vaccines. RNA replication intermediates are more effective at stimulating the innate immunity by engaging pattern recognition receptors thus stronger immune responses (Ulmer et al. 2012). Since RNA viruses replicate in the cytoplasm, there are no fears of vaccine integrating into the host genome as is the case with DNA vaccines. Moreover, viral particle delivery is more effective because of the ability of the virus particle to transverse membranes. DNA vaccines must cross plasma and nuclear membranes to reach the nucleus where transcription takes place. Vaccine uptake is reduced in cells which are not dividing because of intact membranes. Moreover, transient protein expression by RNA vaccines may better imitate antigen expression in acute infections thus are more poised to induce immune responses (Ulmer et al. 2012).

Even though viral particle delivery of alphavirus genomes has been effective in expressing heterologous proteins, virus production is costly. Cell lines to lower costs in alphavirus production have been generated though the titers are markedly lower (Polo et al. 1999). Besides, that gene expression is short-lived despite the development of replicons with lower cytopathogenicity capable of sustained protein expression. An extended therapeutic efficacy with alphavirus replicons, therefore, remains a dream. Moreover, there is the ever-present concern about safety and

potential development of anti-vector immunity. However further improvements in the efficacy of replicons based on VEEV are possible. VEEV capsid protein has been found to enhance synthesis of RNA intermediates. A role it performs as an element of the replication complexes and that it stabilizes RNA intermediates by packaging them into nucleocapsids (Kim et al. 2014). Despite excellent research on the use of viral vectors, little has been done to harness their superior immune responses and combine them with the advantages offered by DNA plasmids.

1.10.3 CCHF Vaccine development

Besides research in whole inactivated CCHF virus particles as vaccines, the glycoproteins and nucleoproteins which are the structural proteins of the virus are also being investigated as vaccine targets (Dowall et al. 2017).

1.10.3.1 Nucleoproteins

The nucleoprotein has a number of features which makes it a promising antigenic target for vaccine development. The nucleoprotein predominates in the virion and is believed to be highly capable of inducing an immune response. Moreover, the NP is the least variable protein (Hewson et al. 2004b) thus a vaccine produced in one part of the world could be effective against various CCHFV strains from around the globe. While complete protection in animal models for vaccines employing the NP has been demonstrated for other viral diseases; only partial protection has been demonstrated with the Rift Valley fever virus (Boshra et al. 2011) and Hantavirus (Maes et al. 2009) both of which belong to the *Bunyavirales* order. The two currently reported efficacy studies with CCHFV NP have reported conflicting findings (Dowall et al. 2016, Zivcec et al. 2018).

1.10.3.2 Glycoproteins

The M segment codes for the glycoprotein precursor, a polyprotein which undergoes processing by a series of host proteases giving rise to mature glycoproteins (Gn and Gc), which are found on the viral envelope, as well as secreted non-structural proteins. Most of the CCHF vaccine work has concentrated on the M segment maybe because the Gn and Gc are extracellular as opposed to the NP which is intracellular. Thus far neutralizing antibodies against Gn and Gc have been demonstrated (Ahmed et al. 2005) although some researchers restrict the neutralizing epitopes to the Gc regions (Bertolotti-Ciarlet et al. 2005). Even though the M segment is the most diverse, the differences are predominantly in the non-structural region which is not part of the mature proteins. It is therefore presumed that the neutralizing antibodies for mature proteins do cross-react amongst different CCHF strains. However, the effect brought by reassortment has not received much attention.

1.10.3.3 Inactivated Vaccines

A formaldehyde inactivated vaccine made from a CCHFV Turkish strain (Kelkit06) was published in 2015. The vaccine was formulated with the Imject Alum adjuvant (Canakoglu et al. 2015) which comprises of aluminum

hydroxide and magnesium hydroxide. In immunogenicity studies, the vaccine-induced neutralizing antibodies, but its effect on cellular immunity was not investigated possibly because inactivated vaccines are generally poor at activating cellular immunity. However, 80% of the vaccinated IFNAR^{-/-} mice were protected from a lethal dose of the Kelkit06 strain (Canakoglu et al. 2015).

1.10.3.4 CCHF vaccine candidates

CCHF vaccine development has recently accelerated with eight vaccine candidates published from the year 2011 to 2018. Previously there had been only two attempts recorded in literature. The investigated approaches include the use of whole virus particles (Canakoglu et al. 2015), viral vectors (Buttigieg et al. 2014, Dowall et al. 2016, Zivcec et al. 2018), DNA plasmids (Hinkula et al. 2017), virus-like particles (Hinkula et al. 2017) and transgenic plants (Ghiassi et al. 2011).

1.10.3.4.1 Viral vectors

Viral vectors that have been used in CCHF vaccine research include the Modified Vaccinia Ankara virus (MVA) and adenovirus human 5 serotype (AdHu5). The MVA was used in the delivery of the entire M and S segments of the Ibr 10200 CCHFV strain. The MVA vectored vaccine consisting of M segment elicited neutralizing antibodies as well as T cell responses and a 100% protection in an IFNAR^{-/-} mouse model (Buttigieg et al. 2014). The S segment delivered by MVA elicited antibody and T cell immune responses in mice which however failed to protect animals from a lethal virus challenge (Dowall et al. 2016). On the contrary, the AdHu5 vectored vaccine containing the entire M segment of the Ibr 10200 CCHFV strain failed to protect mice from a lethal virus challenge although the humoral and cellular immune responses were activated (Sahib 2010). The observed difference could be a reflection of the weakness of the STAT^{-/-} mouse model used in preference to IFNAR^{-/-} mouse model.

Viruses are very effective vectors in delivering genes of interest with concomitant high-level production of antigen and subsequent induction of robust immune responses. Use of viruses as vectors can backfire as was the case with MVA used in the smallpox vaccine when excessive stimulation of the immune responses led to fatalities in vaccine recipients. It should, however, be pointed out that these were rare cases, one to two in a million vaccines (Gilbert 2013). As with AdHu5 vectored vaccines, their immune responses are dampened by already existing immunity against the vector.

1.10.3.4.2 DNA vaccines

A plasmid DNA vaccine expressing the complete M segment of the 10200 CCHFV strain was published in 2005. The vaccine was either administered alone or in combination with other plasmid DNA vaccines for Hantaan virus, Rift Valley fever virus also expressing the M segment and tick-borne encephalitis virus expressing the preM and E genes. Half of the inoculated mice in a single group or combination group developed neutralizing antibodies (Spik et al.

2006). T cell responses were not investigated. Protective efficacy studies could not be carried at the time because of the absence of a suitable animal model. Another plasmid DNA vaccine coding the CCHFV Gn, Gc and NP of the 10200 CCHFV strain, induced humoral and cell-mediated immune responses which resulted in 100% protection against lethal CCHFV challenge in an IFNAR^{-/-} mouse model (Hinkula et al. 2017). Results from the study seem to suggest that neutralizing antibodies are not the sole predictor of immunity capable of resisting fatal infections. Mice that survived lethal viral challenge had lower neutralizing antibody titers compared to the group which had received a transcriptionally competent virus-like particle (tc-VLP) vaccine. Vaccinating with the tc-VLP was accompanied by a strong induction of neutralizing antibodies which proved not completely protective since only 40% of the mice were protected (Hinkula et al. 2017).

Garrison et al compared the immunogenicity and protection from a lethal disease in IFNAR^{-/-} and IS mouse models of a plasmid DNA vaccine coding the entire M segment of the 10200 CCHFV strain. While antibody induction was comparable in the two mouse models, the IS model had balanced T cell responses. Protection from lethal disease was not complete and not statistically different between the two models. (Garrison et al. 2017).

1.10.3.4.3 Plant-based vaccines

Animals, especially domestic animals occupy an essential niche in the viral transmission cycle. Decreasing viral amplification in animals would, therefore, reduce CCHFV transmission rate to human beings. Transgenic tobacco plants expressing the Gn and Gc of an Iranian CCHF M segment were fed to female BALB/c mice stimulated IgA and IgG antibody responses (Ghiasi et al. 2011). Of particular interest is the level of the mucosal immune response: Anti-Gn/Gc IgA titer was higher in fecal material (1:512) than in serum (1:256). Serum IgG responses were rather low (1:256) requiring boosting to magnify the response (1:32 000) (Ghiasi et al. 2011). The candidate vaccine could not, however, be assessed for protective efficacy since a suitable animal model was not available at the time.

1.11 Problem Statement

CCHFV is of public health importance -classified among biosafety level 4 pathogens and has the potential to expand its geographical distribution establishing new endemic zones especially in the wake of climate change (Papa et al. 2015). The virus is amongst emerging pathogens considered by the World Health Organization as serious epidemic threats. Though infections can be sporadic, they have the potential to be highly fatal especially in limited resource regions (Bente et al. 2013). CCHFV is endemic in South Africa and an increase in cases is inevitable. Such an increase will negatively impact the health delivery system already burdened with the scourge of HIV/AIDS. Moreover, outbreaks are often accompanied by hysteria and reluctance by health care workers to put their lives on the line. Despite its public health importance, currently, there is no internationally approved CCHF vaccine or antiviral therapy. Clinical efficacy of treatment options currently in use remains to be established while the available vaccine-only in

use in Bulgaria- an inactivated form, made from suckling mouse brain has been shown to lack clinical efficacy (Mousavi-Jazi et al. 2012). Its preparation requires the generation of virions thus needs maximum containment. Besides that, there are fears of autoimmune and allergic responses arising from vaccines grown in mice (Hemachuda et al. 1987 and Jelinek et al. 2008). The above-chronicled factors make its approval very unlikely.

DNA vaccines offer safer alternative platforms though satisfactory immune responses in non-human primates or human clinical trials are not frequently demonstrated. One of the approaches that have been investigated to improve the efficacy of DNA vaccines is by optimizing expression levels and this can be achieved through the use of replicon virus vectors. While this has been promising, there are challenges with the large scale manufacture of alphavirus replicons. This problem can be circumvented by launching the replicon from a DNA plasmid (Ljungberg et al. 2007). Sindbis replicons promote cell death through apoptosis and apoptosis is believed to enhance immune induction pathways (Leitner et al. 2006, Ljungberg et al. 2007). The apoptotic nature of these vectors reduces the chances of integration into the host genome by the introduced DNA thus making Sindbis virus vectors relatively safer than all vaccine vectors investigated so far. While there have been a number of attempts to prepare a plasmid DNA vaccine against CCHFV, none has considered the effect of reassortment of the CCHF M segment or used alphaviruses as vectors. A few studies have so far investigated the CCHF NP as a vaccine candidate independently. The CCHF GP and NP genes used so far in vaccine investigation have mostly come from the IbAr 10200 CCHF strain yet there are amino acid differences amongst CCHF various strains from across the globe. Besides that, the pathogenicity of the IbAr 10200 strain in humans is not known for the virus strain was isolated from a tick (Causey et al. 1970): thus the strain may not be the best model for CCHF viruses. Coverage of the various CCHF strains in vaccine investigation is therefore inadequate and so is the information about alphavirus DNA launched replicons against CCHFV. Delineating the mechanisms underpinning immunogenicity and immune responses by DNA launched alphavirus replicons is vital. This study investigated mechanisms of enhancing immunogenicity of alphavirus Sindbis replicons encoding South African CCHFV glycoproteins and nucleoproteins for future development of an efficacious vaccine.

1.12 Aim

To investigate mechanisms of immunogenicity of Sindbis replicons encoding CCHFV glycoproteins and nucleoproteins for future development of an efficacious vaccine.

1.13 Objectives

To prepare constructs expressing glycoprotein and nucleoprotein of different CCHFV strains.

To characterize the expression of CCHFV glycoprotein and nucleoprotein in mammalian cells.

To determine induction of apoptosis in mammalian cells.

To determine self-replication rates of CCHFV constructs in mammalian cells.

To evaluate immunogenicity of CCHFV candidate vaccine in mice.

CHAPTER 2

Preparation and expression of constructs expressing the glycoprotein and the nucleoprotein of different CCHFV strains.

2.1 Introduction

While considerable progress has been made in developing vaccines against infectious pathogens, there are instances where traditional vaccine approaches have either had poor safety profiles or are accompanied with suboptimal immune responses. Superior vaccine approaches in terms of safety and immunogenicity are therefore constantly sought. Vaccines are broadly classified into two groups, live and non-live. Live attenuated vaccines are known to activate humoral and cellular immune responses resulting in long-lasting immunity. The magnitude of the immune response though is inversely associated with the level of attenuation (Ferraro et al. 2011). On the other hand, non-live vaccines are mostly associated with humoral immune responses requiring repeated immunizations to maintain immunity. Genetic (DNA) vaccines have promised to be attractive vaccine candidates for intracellular pathogens and cancer. The interest in DNA vaccines has stemmed from observations that they can induce both the humoral and innate immune systems triggering immune responses akin to live attenuated vaccines (Ferraro et al. 2011). However, their most significant disadvantage to date has been suboptimal immune responses in higher mammals. Several strategies are therefore being investigated to enhance their immunogenicity. One such strategy is to augment gene expression and this is promising with replicon virus vectors derived from self-amplifying viral RNA. One of the viral genomes that have been investigated for replicon vaccines is the Sindbis virus belonging to the *Alphavirus* genus. Alphaviruses are mosquito-borne viruses classified in the *Togaviridae* family. Their genomes consist of single-stranded RNA of positive polarity coding for four non-structural proteins, capsid protein and envelope glycoproteins (Strauss and Strauss 1994). Separating the two open reading frames is the 26S promoter. The positive sense genome acts as mRNA and is translated at the 5' end giving rise to non-structural proteins whose function is genome replication, the formation of a negative sense RNA and transcription of sub-genomic RNA. The latter is translated to produce structural proteins. In Alphavirus replicons, structural proteins downstream of the 26S promoter are replaced with heterologous gene(s) of interest. Candidate vaccine replicons constructed using genomes based on Venezuelan equine encephalitis virus (VEEV), Sindbis viruses, and Semliki Forest viruses (Gorchakov et al. 2007) have shown lots of promise in animal models.

Alphavirus replicons are devoid of genes encoding the structural proteins: thus they are incapable of productive infections making them a safer option. Structural genes can, however, be supplied separately forming replicon particles. The supplied structural genes lack the packaging signals thus replicon particles achieve a single round of replication. Generation of replicon particles is initially made possible by packaging signals within the replicon RNA

facilitating its packaging into the provided structural proteins (Pushko et al. 1997). Studies have demonstrated that replicon particles are more effective in stimulating immune responses even though the manufacturing process is costly and safety issues remain a concern. One way to evade these challenges is to originate the replicon in a DNA plasmid. In this system, the Alphavirus sequence is converted to cDNA sequence which is driven by a promoter such as one derived from human cytomegalovirus (hCMV). Transcription begins in the nucleus with the production of the Alphavirus sequence which exits the nucleus into the cytoplasm where the translation of the viral replicase takes place. The replicase directs transcription of subgenomic mRNA encoding for the gene of interest (Herweijer et al. 1995, Dubensky et al. 1996). Compared to conventional plasmid DNA vectors, replicons are superior in terms of heterologous protein production. This is theoretically because the Alphavirus replication machinery generates numerous subgenomic mRNA from which the gene of interest is translated, in contrast to traditional DNA vectors in which fewer mRNA transcripts are generated.

Nevertheless, there are instances where researchers have not obtained differences *in vitro* in heterologous protein production between a Sindbis vector and a conventional DNA vector (Hariharan et al. 1998). Replicons contain 5' and 3' sequences responsible for RNA replication and these sequences are believed to improve immune responses by activating polymorphous immune pathways concurrently (Hikke and Pijlman 2017). Typically, 100 to 1000 fold lower Sindbis replicon doses induce similar levels of immune responses as with traditional plasmid DNA vaccines (Hariharan et al. 1998). The observed superior immune responses generated by replicons are however due to dsRNA intermediates produced during replication rather than enhanced protein production (Leitner et al. 2003). Sindbis replicon DNA vaccines have been used to express recombinant proteins; rabies glycoprotein (Saxena et al. 2008), influenza hemagglutinin (Miller et al. 2008), hantavirus M and S segments (Kamrud et al. 1999) and herpes simplex type 1 glycoprotein (Hariharan et al. 1998) resulting in protective immunity in animal models. Alphavirus replicons stimulate apoptotic pathways in transfected cells thus chances of integration of foreign DNA into a host are reduced (Frolov and Schlesinger 1994).

DNA-launched Sindbis replicons containing genes encoding for the green fluorescent protein (GFP) and glycoprotein precursor of CCHFV strain IbAr 10200, designated pSinGFP and pSin-DLR-CCHF, were developed and provided by Professor Mark Heise from the University of North Carolina in the United States of America (USA). The structural genes of Sindbis virus had been replaced with genes encoding for the GFP and the glycoprotein precursor of CCHFV strain IbAr 10200. The Sindbis cDNA sequence is under the control of the hCMV immediate-early promoter while the hCMV enhancer element complements gene transcription. The heterologous genes are driven by the Sindbis subgenomic promoter. This is different from traditional DNA vectors whose gene expression is under the direct control of a hCMV promoter. In this setup, the complimentary copy of the Sindbis virus genome under the control of the hCMV immediate-early promoter/enhancer element is transcribed by the RNA polymerase II in the nucleus to

produce the Sindbis replicon which egresses to the cytoplasm. Replication of the Sindbis replicon occurs in the cytoplasm originating from numerous Sindbis 26S subgenomic mRNA coding for the heterologous gene. This generates high-level protein production. The replicon contains pBR322, a bacterial origin of replication, to allow for propagation in bacterial cells. A bovine growth hormone (BGH) eukaryotic transcription terminator sequence is situated at the 3' end of the foreign gene. The polyadenine tail sequence stabilizes and safeguards the generated mRNA transcripts from degradation. The NeoR/KanR selectable marker sequence encodes for the transposon Tn5 aminoglycoside phosphotransferases which gives resistance to kanamycin and neomycin, allowing for selection during propagation in bacterial and mammalian cells respectively (Yenofsky et al. 1990).

2.2 Aim

To prepare constructs expressing CCHFV glycoprotein and nucleoprotein and their characterization in mammalian cells.

2.3 Methods and Materials

2.3.1 Primer design

Nucleotide sequences from four South African CCHFV strains (SPU45/88 Accession numbers KJ682809.1, KJ682819.1), SPU497/88 Accession numbers KJ682808.1, KJ682820.1, SPU48/90 Accession numbers KJ682813.1, KJ682822.1 and SPU187/90 Accession numbers KJ682814.1, KJ682823.1) coding for the full length open reading frames of the glycoprotein precursor (GP) and nucleoprotein (NP) genes were retrieved from GenBank. Of the four CCHFV strains, two have evidence of genetic reassortment involving the M segment (SPU 45/88 and SPU 497/88) while the other two (SPU48/90 and SPU187/90) show no evidence of genetic reassortment (Goedhals et al. 2014). The sequences were saved in FASTA format and aligned using Clustal Omega software version 1.2.4 (Sievers et al. 2011). Alignment of the glycoprotein precursor gene sequences demonstrated that the reassortant strains had an additional 15 bases at the 5' end. Moreover, the nucleotide sequences were markedly different thus different sets of primers were designed for the amplification of the open reading frame of the glycoprotein precursor gene for reassortant and non-reassortant viral strains. However, this was not the same with the nucleoprotein gene whose nucleotide sequences had little variation hence one set of primers was designed for the reassortant and non-reassortant strains. Primers capable of amplifying the entire open reading frame of the glycoprotein precursor gene were designed with *Not*I enzyme restriction sites at the 5' end whereas those amplifying the nucleoprotein gene were designed with *Not*I and *Cla*I enzyme restriction sites at the 5' end of the forward and reverse primers respectively. Sequences coding for a 6x histidine tag were also included in all the reverse primers. Glycoprotein precursor reassortant primers were designated CCHF-MR-F (forward primer) and CCHF-MR-RH (reverse primer),

glycoprotein precursor non-reassortant primers: CCHF-M-F (forward primer) and CCHF-M-RH (reverse primer), nucleoprotein primers: CCHF-NP-F (forward primer) and CCHF-NP-R (reverse primer). The nucleotide sequences for the designed primers are shown in Table 2.1 below.

Table 2. 1: Primer nucleotide sequences designed to amplify the CCHFV nucleoprotein open reading frame. *Not1* and *Cla1* restriction sites were added to the forward and reverse sequences respectively. **Not1 site** **Histidine tag** **stop codon** **Cla1 site** **Start codon**

Primer name	Tm	Primer Sequence from 5' to 3'
CCHF-MR-F	66.6°C	GCGGCCGCATGCCC(G/T)TCAACAT(T/C)ATGTAC
CCHF-MR-RH	72.9°C	GCGGCCGCCTAGTGGTGGTGGTGGTGGTGGCC(G/A)AT(A/G)TGT G(T/A)T TTTGT(G/A)GA
CCHF-M-F	62.1°C	GCGGCCGCATGCATATATC(G/A)TTAATGTATGC
CCHF-M-RH	76°C	GCGGCCGCCTAGTGGTGGTGGTGGTGGTGCCCAATGTGTGTTTTTGT(A/G)GAGAA
CCHF-NP-F	62.5°C	GCGGCCGCATGGAAAACAAAAT(T/C)GAGGTGAAT
CCHF-NP-R	70.2°C	ATCGATTCTAGTGGTGGTGGTGGTGGTGAT(G/A)ATGTT(G/A)GCACTGGTGGC

2.3.2 cDNA Synthesis

The National Institute of Communicable Diseases supplied aliquots of CCHFV RNA for the above strains from a previous study and were stored at -80°C. The RNA aliquots had been designated 31, 36, 44 and 52 for SPU45/88, SPU497/88, SPU48/90 and SPU187/90 respectively. RNA from each of the four CCHFV strains was reverse transcribed into cDNA using SuperScript™ III Reverse Transcriptase (RT) enzyme (Invitrogen, California, USA) with the corresponding designed forward primers according to manufacturer's instructions. The reaction mixture consisted of 1 µl primers (2 pmol/µl), 1 µl dNTP's (10 mM), 5 µl viral RNA and 6 µl nuclease-free water. The reaction mixture was heated at 65°C for 5 minutes and incubated at 4°C for two minutes. Midway in the incubation, the thermocycler was paused; 4 µl 5x first strand buffer, 1 µl 0.1 M dithiothreitol (DTT), 0.5 µl RNaseOUT™ Recombinant Ribonuclease Inhibitor (40U/µL), 0.5µl nuclease-free water and 1µl Superscript III RT enzyme were added. The reaction mixture was further heated at 50°C for 60 minutes and thereafter at 85°C for 5 minutes. The products were stored at -20°C.

2.3.3 Phusion High fidelity DNA PCR

The resultant cDNA from SPU45/88 and SPU187/90 RNA was amplified using Phusion® High fidelity (HF) DNA polymerase enzyme (New England Biolabs, Massachusetts, USA) to obtain the entire open reading frame of either the CCHFV nucleoprotein or the glycoprotein precursor genes. The reactions were set up as follows: 31.9 µl nuclease-free water, 10 µl 5x Phusion® HF buffer, 1 µl dNTP's (10 mM), 1 µl forward primer (20 pmol/µl), 1 µl reverse primer (20 pmol/µl), 2.5 µl template DNA (from cDNA synthesis), 1.5 µl dimethyl sulfoxide and 0.5 µl

Phusion® DNA polymerase (2 units/µl). The reactions were carried out in the ProFlex PCR System thermocycler (Applied Biosystems, New York, USA). The cycling conditions for the CCHF GP comprised of an initial denaturation 98°C for 30 seconds followed by 25 cycles of 98°C denaturation for 10 seconds, annealing at 68°C for 30 seconds, extension at 72°C for 4 minutes and a further 72°C final extension for 10 minutes. The cycling conditions for the CCHF NP comprised an initial denaturation 98°C for 30 seconds followed by 25 cycles of 98°C denaturation for 10 seconds, annealing at 68°C for 30 seconds, extension at 72°C for 1.5 minutes and a further 72°C final extension for 7 minutes. Samples were held at 4°C.

2.3.4 PCR product confirmation and purification

A 5µl aliquot of the PCR product was separated by electrophoresis on 1% agarose gel prepared in Tris-acetate-EDTA (TAE) buffer. Samples were mixed with 1µl 2000x gel red and loaded on the agarose gel. SM1173 DNA ladder mix (Fermentas, Illinois, USA) was used to determine the size of amplicons. Gel electrophoresis was carried out with the BioRad PowerPac Basic System (BioRad, California, USA) for 45 minutes at 10V/cm. DNA bands were visualized with the Molecular Imager® Gel Doc™ XR+ (Bio-rad California, USA).

DNA was purified using the Wizard® SV Gel and PCR Clean-Up System (Promega, Wisconsin, USA) as per the manufacturer's instructions. Briefly, DNA bands corresponding to the CCHF NP and GP genes were excised, transferred to 1.5 ml tubes whose mass had been pre-determined. The mass of tubes with the gel was determined and 1 µl of membrane binding solution per mg of gel was added to the tubes. The gel was melted by heating at 65°C for 15 minutes. After which, up to 800 µl of melted products were transferred at a time to the Wizard® SV Minicolumns, incubated at room temperature for one minute and centrifuged at 16 000 x g for a further one minute. Thereafter, the Wizard® SV Minicolumns were washed with 700 µl of membrane wash solution supplemented with ethanol by centrifuging at 16 000 x g for one minute. The washing step was repeated with 500 µl membrane wash solution at 16 000 x g for 5 minutes. To promote evaporation of residual ethanol, the columns were centrifuged with the microfuge lid open. The Wizard® SV Minicolumns were transferred to a clean 1.5 ml tube and DNA eluted in nuclease-free water.

2.3.5 Concentration of DNA

DNA concentration was quantified with the NanoDrop 2000 spectrophotometer (Thermo Scientific, Illinois, USA). The purity was based on 260/280 and 260/230 ratios. The DNA products were designated CCHF-31M, CCHF-52M, CCHF-31S, CCHF-52S and frozen at -20°C for further use.

2.3.6 Cloning CCHF-31M, CCHF-52M, CCHF-31S and CCHF-52S into the intermediate vector pMini T

The CCHFV NP and CCHF GP genes were cloned into pMini T plasmid vector (New England Biolabs, Massachusetts, USA) using the NEB® PCR cloning kit. The linearized pMiniT plasmid is 2525kb and allows cloning of blunt and PCR products with 3' adenosine overhangs. The vector has a pUC19 origin of replication, a Shine-Dalgarno sequence ribosome binding site, a toxic minigene, an IS10 tnpA gene encoding the transposase and ampicillin gene giving resistance to ampicillin, carbenicillin and associated antibiotics. The pMiniT vector map is shown in Figure 2.1. The cloning kit contains a ligation enhancer and uses the toxic minigene to disrupt *E. coli* translation machinery thus suppressing background growth of colonies. The ligation protocols were prepared according to Tables 2.2 and 2.3. An amplicon cloning control of 1kb in size supplied with the kit was used as a positive control.

Table 2. 2: Ligation reaction mixture for cloning CCHF-31S and CCHF-52S into pMiniT

Reagents	CCHF-31S	CCHF-52S	Positive Control	Background Control
pMini T vector	1 µl (25ng)	1 µl (25ng)	1 µl (25ng)	1 µl (25ng)
CCHFV DNA	1 µl (340ng)	1 µl (320ng)	-----	-----
Amplicon cloning control	-----	-----	2 µl (30ng)	-----
Nuclease-free water	3 µl	3 µl	2 µl	4 µl
Cloning mix 1	4 µl	4 µl	4 µl	4 µl
Cloning mix 2	1 µl	1 µl	1 µl	1 µl
Total volume	10 µl	10 µl	10 µl	10 µl

Table 2. 3: Ligation reaction mixture for cloning CCHF-31M and CCHF-52M into pMiniT

Reagents	CCHF-31M	CCHF-52M	Positive Control	Background Control
pMini T vector	1 µl (25 ng)	1 µl (25 ng)	1 µl (25 ng)	1 µl (25 ng)
CCHFV DNA	1 µl (400 ng)	1 µl (420 ng)	-----	-----
Amplicon cloning control	-----	-----	2 µl (30 ng)	-----
Nuclease-free fater	3 µl	3 µl	2 µl	4 µl
Cloning mix 1	4 µl	4 µl	4 µl	4 µl
Cloning mix 2	1 µl	1 µl	1 µl	1 µl
Total volume	10 µl	10 µl	10 µl	10 µl

The ligation reactions were incubated at 25°C in a heating block for 15 minutes. After that, reactions were kept on ice for 2 minutes before they were used to transform JM109 cells. Ligation products were designated pMiniTCCHF-31M, pMiniTCCHF-52M, pMiniTCCHF-31S and pMiniTCCHF-52S.

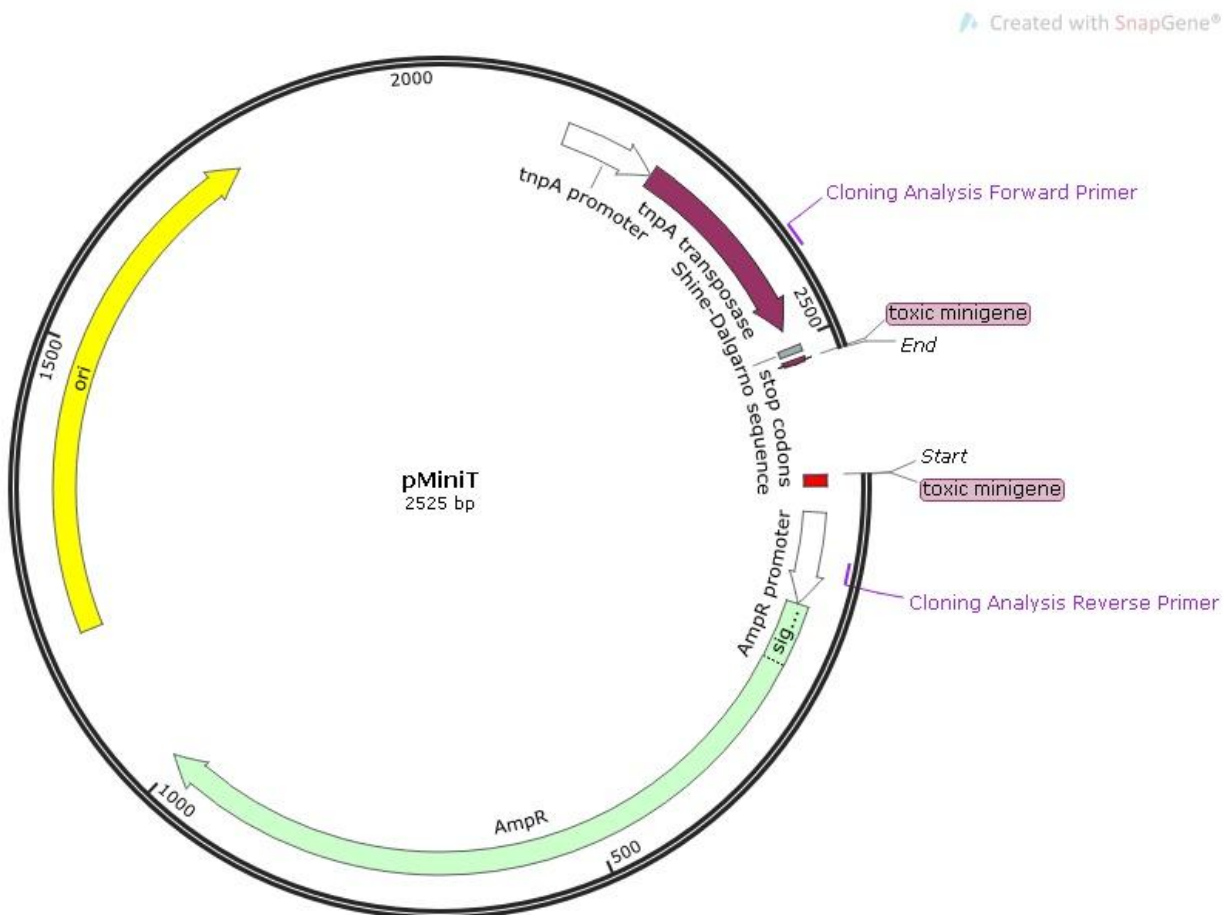


Figure 2. 1: Vector map for pMiniT drawn using SnapGene software version 2.2.2. The cloning analysis primers indicated are used for sequencing ligated nucleotide sequences. The vector allows cloning of blunt ended as well as PCR products with A overhangs. The vector has a pUC19 origin of replication, a Shine-Dalgarno sequence ribosome binding site, a toxic minigene, an IS10 tnpA gene encoding the transposase and ampicillin gene giving resistance to ampicillin, carbenicillin and associated antibiotics.

2.3.7 Transformation of JM109 Cells with pMiniTCCHF-31M, pMiniTCCHF-52M, pMiniTCCHF-31S and pMiniTCCHF-52S

Single-use JM109 competent cells (Promega, Wisconsin, USA) with a minimum transfection efficiency of 1×10^8 colony forming units (cfu/ μ g) were stored at -80°C . Vials of 50 μ l competent cells were retrieved from the -80°C freezer and thawed on ice for 5 minutes. A 10 μ l aliquot of ligation reaction mixture was added to the cells, gently mixed and incubated on ice for 20 minutes. Cells were heat shocked at 42°C for 50 seconds, incubated on ice for 5 minutes and 950 μ l of Super Optimal broth with Catabolite repression (SOC) media at room temperature was added. Cells were incubated at 37°C for 90 minutes with shaking at 150 rpm. A 1:10 dilution of the ligation mixture in SOC

media was plated on Luria-Bertani (LB) media plates with ampicillin antibiotic at a concentration of 100 µg/ml and incubated overnight at 37°C.

2.3.8 Plasmid purification

To confirm successful cloning, single bacterial colonies on LB plates were selected and incubated overnight at 37°C, shaking at 250 rpm in 5 ml LB ampicillin broth. DNA was purified with the PureYield™ Plasmid Miniprep System (Promega, Wisconsin, USA) as per the manufacturer's instructions. Briefly, 3 ml of overnight culture was spun at 16 000 x g for 30 seconds and the cell sediment was resuspended in 600 µl of distilled water. Bacterial cells were lysed by addition of 100 µl of cell lysis buffer, mixed and the lysing reaction was stopped by addition of 350 µl of the neutralization buffer. The mixture was centrifuged for 3 minutes at 16 000 x g following which the supernatant was transferred to PureYield™ minicolumns and centrifuged for 15 seconds at 16 000 x g. The flowthrough was discarded and the minicolumns were first washed with 200 µl endotoxin removal wash buffer for 15 seconds by centrifuging at 16 000 x g and then with 400 µl column wash solution by centrifuging at 16 000 x g for 30 seconds. The columns were each transferred to a clean 1.5 ml tube and DNA eluted in 30 µl nuclease-free water. The plasmid DNA was used in sequencing reactions. The remaining overnight culture was used to prepare glycerol stocks (823 µl overnight bacterial culture + 177 µl 85% glycerol) and stored in cryogenic vials (Corning, New York, USA) at -80°C.

2.3.9 DNA sequencing of CCHF-31M, CCHF-52M, CCHF-31S and CCHF-52S in pMini T

In order to check if the Phusion DNA polymerase enzyme did not introduce base changes during gene amplification, the CCHF NP and GP genes were sequenced using the Cloning Analysis Forward Primer (CAF) and Cloning Analysis Reverse Primer (CAR) supplied with the kit. Nucleotide sequences for CAF and CAR primers are shown in Table 2.4. Sanger sequencing was carried out using the Big® Dye Terminator V3.1 Sequencing kit (Applied Biosystems, New York, USA). Plasmid DNA was diluted to a final concentration of 400 ng/µl for all the transformants which were sequenced. The reactions consisted of 1 µl ready reaction, 4 µl sequencing primer (forward/reverse 0.8 pmol), 2 µl 5X sequencing buffer, 1 µl (400 ng) template DNA and 2 µl nuclease-free water. The sequencing reaction was carried out in the ProFlex PCR System thermocycler (Applied Biosystems, New York, USA). The cycling conditions comprised of an initial denaturation 96°C for 60 seconds followed by 25 cycles of 96°C denaturation for 10 seconds, annealing at 50°C for 5 seconds, extension at 60°C for 4 minutes.

Table 2. 4: Primers used for sequencing CCHF genes in pMiniT. Cloning primer sequence and primer position attachment on pMiniT vector

Primer	Primer Sequence from 5' to 3'	Tm	Position on pMiniT
CAF	ACCTGCCAACCAGCGAGAAC	66°C	2394 – 2415
CAR	TCAGGGTTATTGTCTCATGAGCG	62°C	92 – 114

The post reaction clean up was performed using EDTA/Ethanol precipitation. A 5 µl aliquot of 125mM EDTA and 60 µl of absolute ethanol were added to a 1.5 ml tube. The sequencing reaction mixture volume was adjusted to 20 µl by adding 10 µl nuclease-free water before it was added to the 1.5 ml tube. The mixture was vortexed for 5 minutes and incubated for 15 minutes at room temperature. Subsequently, the 1.5 ml tube was centrifuged at 14000 x g for 20 minutes at 4°C. The supernatant was aspirated and 500 µl of 70% ethanol added to tube followed by centrifugation at 14000 x g for 10 minutes at 4°C. The supernatant was decanted entirely and tubes were incubated at 37°C with the lids open to dry any residual ethanol completely. Samples were submitted to the Department of Microbial, Biochemical and Food Technology, University of Free State for sequencing.

The nucleotide sequences were assembled and analyzed with ChromasPro2 (Technelysium, South Brisbane, Australia). These were then saved in a FASTA format and together with sequences retrieved from *GenBank*, aligned using Clustal Omega version 1.2.4 (Sievers et al. 2011).

2.3.10 Restriction enzyme digestion of pMiniTCCHF-31M, pMiniTCCHF-52M, pMiniTCCHF-31S and pMiniTCCHF-52S

Plasmid DNA with the desired CCHF-31S and pSinCCHF-52S gene sequences were subjected to double restriction enzyme digestion using high-fidelity (HF) *Not*I-HF® and *Cla*I restriction enzymes (New England Biolabs, Massachusetts, United States) while those with the expected CCHF-31M and CCHF-52M gene sequences were digested with *Not*I-HF (New England Biolabs, Massachusetts, United States) in CutSmart® buffer (New England Biolabs). Restriction enzyme digestion reaction mixture for pMiniTCCHF-31S and pMiniTCCHF-52S genes consisted of 1 µl *Not*I-HF (20 units/µl), 1 µl *Cla*I (10 units/µl), 2.0 µl (1 µg) pMini T CCHF-31S/pMiniTCCHF-52S, 5 µl 10X NEBuffer and 41 µl nuclease-free water. Restriction enzyme digestion reaction mixture for pMiniTCCHF-31M and pMiniTCCHF-52M genes comprised of 1 µl *Not*I-HF (20 units/µl), 2.0 µl (1 µg) pMiniTCCHF-31M/pMiniTCCHF-52M, 5 µl 10X NEBuffer and 42 µl nuclease-free water. After 60 minutes of incubation at 37°C, the reaction was stopped by heating at 65°C for 20 minutes. Before samples were loaded on 1% agarose gel, they were mixed with 4000X GelRed® Nucleic Acid Gel Stain (Biotium, California, USA) at a ratio 1:5. SM1173 DNA ladder mix (Fermentas, Illinois, USA) was used to determine the size of digestion fragments. DNA was visualized with the Geldoc XR + System (Biorad, California, USA).

2.3.11 Gel Purification

After restriction enzyme digestion, the insertion of the gene of interest was confirmed, the remainder of digestion products was separated by electrophoresis on 1% agarose gel. Bands corresponding to the predicted size of the CCHF genes were excised and transferred to 1.5 ml tubes. Purification of restriction enzyme digestion products was carried out with Wizard® SV Gel and PCR Clean-Up System (Promega, Wisconsin, USA) according to

manufacturer's instructions as in section 2.3.4. DNA was eluted in 30 µl nuclease-free water, the concentration determined by the NanoDrop 2000 spectrophotometer and the DNA stored at -20°C.

2.3.12 Restriction enzyme digestion of pSinGFP and pSin-DLR-CCHF

DNA-launched Sindbis replicons containing genes encoding the green fluorescent protein (GFP) and glycoprotein precursor of CCHFV strain IbAr 10200, designated pSinGFP and pSin-DLR-CCHF, were developed and provided by Professor Mark Heise from the University of North Carolina in the United States of America (USA). The structural genes of the Sindbis virus have been replaced with heterologous genes: genes encoding for the GFP and the glycoprotein precursor of CCHFV strain IbAr 10200. A diagrammatic representation of pSin-DLR-CCHF is shown in **Figure 2.2**. The replicons contain human cytomegalovirus (hCMV) immediate-early promoter/enhancer element, consisting of a strong constitutive promoter and an enhancer element, essential for eukaryotic expression. The hCMV immediate-early promoter/enhancer element will facilitate the expression of the encoded Sindbis virus nonstructural and heterologous proteins in a eukaryotic host cell. Previously, the replicon containing the gene encoding GFP was modified to include *Cla*I restriction enzyme sites. The vector map for pSinGFP is shown in Figure 2.3. Glycerol stock aliquots of the modified pSinGFP were stored at -80°C.

An aliquot of pSinGFP was retrieved from the freezer, thawed and 5 µl of the plasmid was added to 5 ml 2XTY broth supplemented with kanamycin at a final concentration of 50 µg/ml. The plasmid was grown by incubating the mixture overnight at 37°C with shaking at 250 rpm. After the incubation period, plasmid DNA was purified with the PureYield™ Plasmid Miniprep System kit (Promega, Wisconsin, USA) as in section 2.3.8. DNA concentration was determined using the NanoDrop 2000 spectrophotometer. Using *Not*I and *Cla*I restriction enzyme sites identified, a double enzyme restriction digestion was set up to excise the GFP gene. Products of enzyme digestion were separated on an electrophoretic gel; the bands corresponding to the linearized replicon were excised and purified using a Wizard® SV Gel and PCR Clean-Up System (Promega, Wisconsin, USA) as in section 2.3.4. The vector was stored at -20°C and later used in cloning reactions for assembling replicons expressing the CCHF nucleoprotein gene.

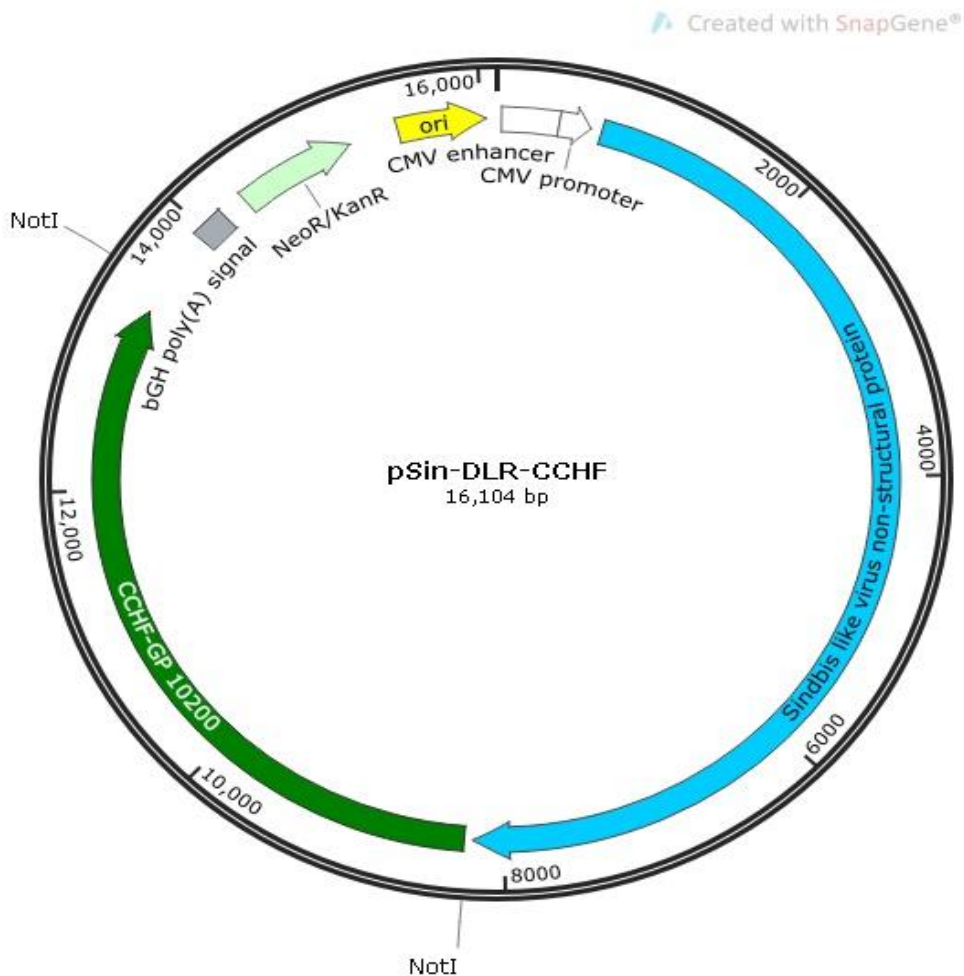


Figure 2. 2: Vector map for pSin-DLR-CCHF drawn using SnapGene software version 2.2.2. The replicons contain human cytomegalovirus (hCMV) immediate-early promoter/enhancer element, consisting of a strong constitutive promoter and an enhancer element, essential for eukaryotic expression, a bacterial origin of replication, a bovine growth hormone (BGH) eukaryotic transcription terminator sequence and the NeoR/KanR selectable marker sequence. The genome of Sindbis virus nonstructural proteins constitute the plasmid backbone while the structural genes have been replaced with genes encoding for the glycoprotein precursor of CCHFV strain IbAr 10200. The cloning site is flanked by *NotI* restriction sites.

Similarly, an aliquot of the pSin-DLR-CCHF glycerol stocks stored at -80°C was retrieved from the freezer, grown as above in 2XTY kanamycin supplemented broth, plasmid DNA purified and the CCHF IbAr 10200 GP gene digested out using *NotI*-HF restriction enzyme. A band of the required size of the linearized vector was excised from an agarose gel and cleaned with the Wizard® SV Gel and PCR Clean-Up System (Promega, Wisconsin, USA) as in section 2.3.4. Plasmid vector DNA was frozen at -20°C.

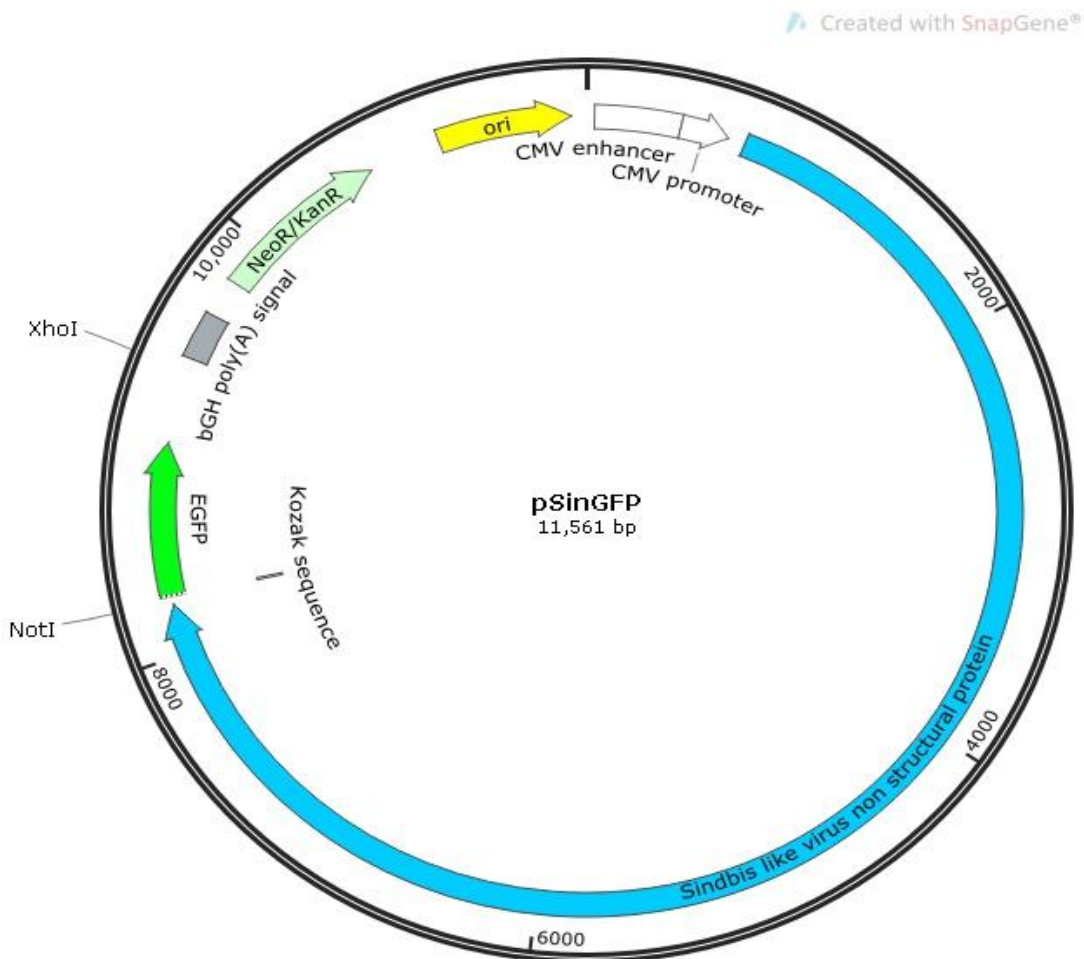


Figure 2. 3: Vector map for pSinGFP drawn using SnapGene software version 2.2.2 The replicons contain human cytomegalovirus (hCMV) immediate-early promoter/enhancer element, consisting of a strong constitutive promoter and an enhancer element, essential for eukaryotic expression, a bacterial origin of replication, a bovine growth hormone (BGH) eukaryotic transcription terminator sequence and the NeoR/KanR selectable marker sequence. The genome of Sindbis virus nonstructural proteins constitute the plasmid backbone while the structural genes of the have been replaced with genes encoding for the GFP. The cloning site is flanked by *NotI* restriction sites.

2.3.13 Dephosphorylating the linearized replicon from pSin-DLR-CCHF

A plasmid vector linearized by a single restriction enzyme as is the case with *NotI* is prone to religate to itself during cloning because of the compatible sticky ends. This reduces the chances of an insert ligating into the vector when the insert is as big as the CCHF GP gene. To prevent plasmid vector re-ligation, the linearized replicon was dephosphorylated using the Antarctic phosphatase enzyme (New England Biolabs, Massachusetts, United States). The enzyme cleaves the phosphate groups at the 5' and 3' ends of the plasmid vector. Once the phosphate groups

are removed, the 3' OH groups at the ends of the plasmid vector can only combine with the 5' phosphate groups from the insert. The dephosphorylation reaction was set up as follows, 1 μ l Antarctic phosphatase enzyme (5000 U/ml), 1 μ l 10X Antarctic phosphatase reaction buffer, 6 μ l (340ng) linearised replicon and 2 μ l nuclease-free water. After 30 minutes of incubation at 37°C, the enzyme was inactivated by heating at 70°C for 5 minutes. The reaction mixture was used in cloning reactions for the preparation of replicons expressing the CCHF glycoprotein precursor gene.

2.3.14 Construction of vaccine candidates

CCHF-52S, CCHF-31S, CCHF-52M and CCHF-31M genes excised from the intermediate vector by restriction endonuclease digestion were cloned into the linearized DNA launched vector using recombinant technology. The ligation reactions were set up as shown in Tables 2.5 and 2.6 below.

Table 2. 5: Reaction composition mixture for ligating CCHF-31S and CCHF-52S into pSin vector

Reagent	CCHF-31S	CCHF-52S	Background Control
2X Rapid ligation buffer	5 μ l	5 μ l	5 μ l
pSin vector	1 μ l (39.9 ng)	1 μ l (39.9 ng)	1 μ l (39.9 ng)
CCHFV gene	3 μ l (54 ng)	3 μ l (57 ng)	-----
T4 DNA Ligase (3 units/ μ l)	1 μ l	1 μ l	1 μ l
Nuclease-free water	-----	-----	3 μ l
Total volume	10 μl	10 μl	10 μl

The ligation reaction was incubated overnight at 4°C. Thereafter, the reaction volume was heated at 70°C for 15 minutes to inactivate the ligase enzyme.

Table 2. 6: Reaction composition mixture for ligating CCHF-31M and CCHF-52M into pSin vector

Reagent	CCHF-31M	CCHF-52M	Background Control
2X Rapid ligation buffer	5 μ l	5 μ l	5 μ l
pSin vector	1 μ l (34 ng)	1 μ l (34 ng)	1 μ l (34 ng)
CCHFV gene	3 μ l (120 ng)	3 μ l (130 ng)	-----
T4 DNA Ligase (3 units/ μ l)	1 μ l	1 μ l	1 μ l
Nuclease-free water	-----	-----	3 μ l
Total volume	10 μl	10 μl	10 μl

2.3.15 Transformation of JM109 cells

The products of the ligation experiment were used to transform 50 μ l of JM109 *E. coli* cells. A 10 μ l aliquot of the ligation reaction was added to cells and incubated on ice for 20 minutes. After that, the cells were heat shocked at 42°C for 50 seconds and immediately returned on ice for 2 minutes. A 950 μ l aliquot of SOC media was added to

cells and incubated at 37°C for 90 minutes shaking at 150 rpm. Subsequently, cells were plated and grown overnight at 37°C on 2X TY agar plates enriched with kanamycin antibiotic at a final concentration of 50 µg/ml for the selection of positive transformants.

2.3.16 Plasmid purification

To confirm successful cloning of the CCHF genes into the replicon, single bacterial colonies on transformation plates were selected and grown overnight at 37°C, shaking at 250 rpm in 5 µl 2XTY broth. DNA was purified with the PureYield™ Plasmid Miniprep System (Promega, Wisconsin, USA) as in section 2.3.8. The remainder of the overnight culture media was used to prepare glycerol stocks which were stored at -80°C.

2.3.17 Vaccine constructs confirmation

Confirmation of constructs was done by performing a PCR using a primer targeting a region on the plasmid designated FW-pSin and one of the reverse primers CCHF-NP-R, CCHF-M-RH, and CCHF-MR-RH. The reactions consisted of 10 µl 5X Green Go Taq® flexi buffer, 8 µl MgCl₂ (25 mM), 2.5 µl dNTPs (10 mM each), 1 µl forward primer (20 pmol/µl), 1 µl reverse primer (20 pmol/µl), 0.25 µl GoTaq polymerase enzyme (5 u/µl), 5 µl template (5 ng) and 22.25 µl nuclease-free water. GoTaq polymerase enzyme (Promega, Wisconsin, USA) was used for the PCR amplification reaction with the ProFlex PCR System. While the enzyme is not ideal (because it lacks the 3'-5' exonuclease activity) in amplifying genes used for expression studies, it was used for PCR experiments to confirm the presence and size of amplified PCR products. The cycling reaction conditions comprised of 60 seconds initial denaturation at 95°C followed by 25 cycles of denaturation 95°C for 30 seconds, annealing at 50°C for 30 seconds, extension at 72°C for 1.5 minutes and final extension 72°C for 7 minutes. On completion of the PCR reaction, an electrophoretic gel was run to ascertain the size of amplicons. Glycerol stocks were made from overnight cultures with positive transformants and stored at -80°C.

2.3.18 DNA Sequencing of CCHF genes in Sindbis replicon vector

Nucleotide sequences of the CCHFV genes were confirmed by the Big Dye™ Terminator Sequencing Ready Reaction kits with the AmpliTaq DNA polymerase FS (Applied Biosystems) according to the manufacturers' instructions. Sequencing was carried out using Sindbis primers FW-pSin and RP-pSin whose nucleotide sequences are shown in Table 2.7. These primers had been designed by a colleague in the department and had been used in a previous study. Four vaccine constructs (two encoding the nucleoprotein genes and two encoding the glycoprotein precursor genes) had the sequences confirmed by Sanger sequencing and BLAST analysis.

Table 2. 7: Primers used for CCHF gene sequencing in Sindbis replicon vector

Primer Designation	Primer Sequence from 5' to 3'	Tm	Position on plasmid pSin-DLR-CCHF, base pairs (bp)
FW-pSin	AAATAGTCAGCATAGTACATT	46.5°C	8 199 - 8 219
RP-pSin	TGCAATTCCTCATTTTATTA	45.6°C	9 089 – 9 069

The sequencing reaction mixture for transformants was made up of 1 µl ready reaction mix, 4 µl sequencing primer (forward/reverse 0.8 pmol), 2 µl 5X sequencing buffer, 1 µl (500 ng) template DNA, and 2 µl nuclease-free water. PCR cycling conditions for the sequencing reaction consisted of 60 seconds initial denaturation at 96°C followed by 25 cycles of denaturation 96°C for 10 seconds, annealing at 50°C for 5 seconds and extension at 60°C for 4. The post reaction clean up was performed using EDTA/Ethanol precipitation as described in section 2.3.9. Samples were submitted to the Department of Microbial, Biochemical and Food Technology, University of Free State for sequencing.

2.3.19 Next-generation sequencing of vaccine constructs and data analysis

The complete nucleotide sequences for pSinCCHF-31S, pSinCCHF-52S, pSinCCHF-31M and pSinCCHF-52M, were determined using the MiSeq® (Illumina, California, USA) by the Next Generation Sequencing unit, University of the Free State. Raw sequencing data in FASTQ files were trimmed and filtered using PRINSEQ (Schmieder and Edwards 2011). K-mer based genome assembly was performed by SPAdes assembler (Bankevich et al. 2012). Using MARS software, the consensus sequences were mapped to reference sequences (Ayad and Pissis 2017).

2.3.20 Plasmid DNA purification for transfection experiments

DNA extraction and purification were performed using the QIAGEN® Plasmid Plus Midi Kit (Qiagen, Hilden, Germany) according to manufacturers' instructions. Glycerol stocks consisting of the confirmed vaccine constructs were retrieved from the -80°C freezer, thawed at room temperature and grown overnight 37°C in 5 ml of 2X TY media with kanamycin at a final concentration of 50 µg/ml. The following day, 350 µl of the overnight culture was subcultured in 35 ml of fresh 2X TY media and further incubated at 37°C for 10 hours. The bacterial culture was harvested by centrifuging at 6000 x g for 15 minutes at 4°C before it was resuspended in 4 ml buffer P1. Bacterial cells were lysed by adding 4 ml buffer P2 followed by incubation at room temperature for 3 minutes. Cell lysis was stopped by adding 4 ml of buffer S3 to the lysate and mixing the solution until it became colourless. The lysate was transferred to a QIAfilter Cartridge and incubated for 10 minutes at room temperature. Thereafter, the lysate was filtered into a 15 ml falcon tube and 2 ml buffer BB was added and mixed with the lysate. The lysate was transferred to QIAGEN Plasmid Plus spin columns and drawn through the column by applying vacuum pressure. The DNA was washed using buffer ETR and buffer PE supplied in the kit. A centrifugation step at 10 000 x g for 60 seconds was

carried out to remove residual wash buffer. DNA was eventually eluted in 200 µl nuclease-free water. The concentration was quantified by the NanoDrop 2000 spectrophotometer and labeled aliquots were stored at -20 °C.

2.3.21 Transfection experiments

2.3.21.1 Cell maintenance

Human embryonic kidney cells (HEK-293) and baby hamster kidney cells (BHK-21) were procured from the American Type Culture Collection (ATCC) CRL-1573 and CCL-10 respectively. Cells were stored in liquid nitrogen. Aliquots of HEK-293 and BHK-21 cells were retrieved from liquid nitrogen and grown in Dulbecco's Modified Eagle Medium (DMEM) supplemented with 10% gamma irradiated Fetal Bovine Serum (FBS) (Gibco), 1% L-glutamine (Lonza, Verviers, Belgium), 1% penicillin-streptomycin (Lonza, Verviers, Belgium) and 1% non-essential amino acids (Lonza, Verviers, Belgium) in T-25cm² cell culture flasks (NEST, Jiangsu, China). Cells were passaged at least three more times before they were used in transfection experiments.

2.3.21.2 Transfection of HEK-293 cells

A day before transfection, HEK-293 cells were seeded on coverslips in 24 well cell culture plates (NEST, Jiangsu, China) at a seeding rate of 2×10^5 per well and incubated at 37°C in a 5% carbon dioxide-enriched atmosphere. On the day of transfection, an hour before the transfection experiment, growth media was replaced with transfection media, i.e. DMEM supplemented with 10% gamma irradiated FBS (Gibco), 1% L-glutamine (Lonza, Verviers, Belgium) and 1% non-essential amino acids (Lonza, Verviers, Belgium). Cells grown in a T-25 cm² flask (NEST, Jiangsu, China) were rinsed with phosphate buffered saline (PBS) and detached from cell culture flask using 250 µl of trypsin versiene (Lonza, Verviers, Belgium). All cell washes were done with PBS short of magnesium and calcium. After incubation at 37°C, 2 ml DMEM transfection media were added to the flask. A 10 µl aliquot of HEK-293 cells was mixed with 10 µl of 0.4% trypan blue and a cell count was performed with the Countess™ II FL Automated cell counter (Invitrogen, California, USA). Plasmid DNA was diluted in a mixture of Opti-MEM media (Gibco, Paisley, UK) and P3000™ reagent (Invitrogen, California, USA). Lipofectamine® 3000 (Invitrogen, California, USA) reagent was diluted in Opti-MEM media. The diluted plasmid DNA and the Lipofectamine reagent were combined and incubated at room temperature for 30 minutes. After that, the DNA-lipid complexes were added to HEK-293 cells in 24 well cell culture plates (NEST, Jiangsu, China) and incubated at 37°C for 24 hours. The DNA-launched Sindbis replicon containing a gene encoding for green fluorescent protein (pSinGFP) was used as a positive control.

2.3.21.3 Transfection of BHK-21 cells

Approximately 24 hours before transfection, BHK-21 cells were seeded on coverslips in 24 well cell culture plates at a seeding rate of 1×10^5 and incubated at 37°C. An hour before the transfection experiment, growth media was

replaced with transfection media. BHK-21 cells in T-25cm² (NEST, Jiangsu, China) flasks between 70-90% confluent were rinsed with PBS and detached by the addition of 2.5% trypsin (Gibco, Paisley, UK) followed by a three-minute incubation at 37°C. Afterwards, the reaction was stopped by adding 2 ml of transfection media. A single cell suspension was achieved by gently pipetting up and down. A 10 µl aliquot of BHK-21 cells was mixed with 10 µl of 0.4% trypan blue and cell count was performed with the Countess™ II FL Automated cell counter (Invitrogen). DNA-lipid complexes were prepared as above and were added to BHK-21 cells at the end of a 30 minute incubation period. Transfectants were incubated at 37°C for 24 hours. Control plasmid pSinGFP was used as a positive control.

2.3.21.4 Optimizing transfection reactions

Various plasmid DNA Lipofectamine ratios as illustrated in Table 2.8 were tried in order to find the optimum transfection efficiencies. A starting DNA: Lipofectamine ratio of 1:1.5 was chosen since this had been proven effective by various researchers in our laboratory. Optimization was carried out with both BHK-21 and HEK-293 cell lines and the optimization parameters are shown in Table 2.8.

Table 2. 8: Optimisation parameters of DNA plasmids in BHK-21 and HEK-293 cells

Amount of plasmid DNA	Optimem Media	P3000 reagent	Lipofectamine 3000 reagent	DNA:Lipofectamine ratio
2µg	50 µl	4 µl	3 µl	1:1.5
2µg	50 µl	4 µl	4 µl	1:2
2µg	50 µl	4 µl	6 µl	1:3
2.5µg	50 µl	6 µl	3.75 µl	1:1.5
2.5µg	50 µl	5 µl	5 µl	1:2
2.5µg	50 µl	5 µl	7.5 µl	1:3
3µg	50 µl	6 µl	3 µl	1:1
3µg	50 µl	6 µl	4.5 µl	1:1.5
3µg	50 µl	6 µl	6 µl	1:2
3µg	50 µl	6 µl	9 µl	1:3
3.5µg	50 µl	7 µl	3.5 µl	1:1
3.5µg	50 µl	7 µl	5.25 µl	1:1.5
3.5µg	50 µl	7 µl	7 µl	1:2
3.5µg	50 µl	7 µl	10.5 µl	1:3
4µg	50 µl	8 µl	6 µl	1:1.5
5µg	50 µl	10 µl	7.5 µl	1:1.5
6µg	50 µl	12 µl	9 µl	1:1.5

2.3.21.5 Cell preparation for electroporation

Approximately 48 hours before electroporation, low passage BHK-21/HEK-293 cells were passaged in T-75cm² flasks (NEST, Jiangsu, China) such that they were 80-90% confluent prior transfection. On the day of the electroporation experiment, growth media was decanted and cells rinsed with PBS (Lonza, Verviers, Belgium). A 1 ml aliquot of trypsin versiene (Lonza, Verviers, Belgium) was applied to HEK-293 cells while 1 ml of 2.5% trypsin (Gibco, Paisley, UK) was added to BHK-21 cells and incubated for three minutes at 37°C. Subsequently, the detached cells were resuspended in 3 ml of DMEM recovery media enriched with 10% gamma irradiated FBS (Gibco, Paisley, UK), 1% L-glutamine (Lonza, Verviers, Belgium), 1% sodium pyruvate (Lonza, Verviers, Belgium) without antibiotics. A 10 µl aliquot of BHK-21 or HEK-293 cells was mixed with 10 µl of 0.4% trypan blue and cell count was performed with the Countess™ II FL Automated cell counter (Invitrogen). BHK-21 and HEK-293 cells at a cell density of 5.5×10^6 cells/ml and 5×10^6 cells/ml respectively were transferred to 1.5 ml tubes and spun for 5 minutes. All centrifugation steps were carried out at $400 \times g$ at a temperature of 4°C. The supernatant was discarded and cells were washed with 200 µl of PBS (Lonza, Verviers, Belgium) by centrifuging for 5 minutes. The supernatant was aspirated and discarded while cells were resuspended in 100 µl of Resuspension Buffer R. A 15 µg aliquot of plasmid DNA resuspended in ≤ 10 µl of nuclease-free water was added to the cell suspension and mixed briefly. T-25 cm² flasks (NEST, Jiangsu, China) and 24 well plates NEST, Jiangsu, China) were prepared by adding 5 ml into the former and 0.5 ml into the latter of DMEM recovery medium.

2.3.21.6 Electroporation procedure

Electroporation of cells using purified vaccine constructs were carried out with the Neon® Transfection System MPK5000 (Invitrogen, California, USA). The Neon pipette station was set up before cell preparation. A 3 ml aliquot of buffer E2 was dispensed to the Neon tube inserted into the pipette station. The desired pulse conditions were selected on the Neon device. The mixture of plasmid DNA and cell suspension prepared above was gently mixed. With the Neon tip connected to the pipette, the plasmid DNA/ cell suspension was aspirated making sure there are no air bubbles. The Neon pipette with the sample was inserted into the Neon tube with the buffer E2. Subsequently, an electric pulse was delivered to the mixture. Afterwards, 20 µl of the electroporated cells were transferred to 500 µl recovery media in a 24 well plate (NEST, Jiangsu, China) and 80 µl was transferred to 5 ml recovery media in a T-25 cm² flask (NEST, Jiangsu, China) and both were incubated at 37°C in a 5% CO₂ incubator for 24 and 48 hours respectively.

2.3.21.7 Optimizing electroporation

The control plasmid, pSinGFP, was used as a positive control. Varying amounts of plasmid DNA vaccine constructs were electroporated using different sets of electroporating parameters with a Neon® Transfection System MPK5000 (Invitrogen, California, USA) as per manufacturer's instructions. Different sets of electroporation parameters investigated are shown in Table 2.9. These parameters had been used with the Neon transfection system and yielded high transfection efficiencies and cell viability by various researchers in HEK-293, BHK-21 and PC-12 cell lines (Kim et al. 2008, Covello et al. 2014). Cell viability was however low with higher voltages. To improve cell survival rate post-electroporation, cells were transferred to a 1.5 ml tube and allowed to incubate at room temperature for 5, 10, 15, 30 and 45 minutes before they were added to the recovery media. After the respective incubation periods, 20 µl of the electroporated sample was added to 500 µl recovery media in a 24 well plate and 80µl was transferred to 5 ml recovery media in a T25 flask and both were incubated at 37°C for 24 and 48 hours respectively.

Table 2. 9: Electroporation parameters investigated for optimizing transfection experiments

Pulse Voltage (V)	Pulse Width (ms)	Pulse Number
1 100	20	2
1 200	30	1
1 300	10	3
1 300	30	1
1 500	20	1
1 500	10	3

2.3.21.8 Indirect Immunofluorescence assay

After a 24 hour incubation period, transfected cells grown on 14 mm glass coverslips were briefly rinsed in PBS and fixed at -20°C in a 1:1 methanol-acetone solution. Following fixation, cells transfected with pSinGFP were examined for fluorescence while CCHF vaccine constructs transfected cells were briefly rinsed with PBS and blocked for 60 minutes at room temperature by a solution consisting of 10% sucrose, 0.5% Triton X-100 (Promega, Wisconsin, USA) in 1% PBS. Excess blocking solution was tipped off the cover-slip and cells were reacted with mouse anti-His₆ antibody (Roche, Basel, Switzerland) (diluted 1:100 in blocking solution) at 37°C in a humidified container. Unbound antibody was washed off with 1% Tween® 20 (VWR™ Life sciences, Pennsylvania, USA) in phosphate buffered

saline (PBST) solution and cells were reacted with fluorescein labeled goat anti-mouse IgG antibody (SeraCare Life Sciences, Massachusetts, USA) (diluted 1:20 in 0.1% Evans blue) for 30 minutes at 37°C. Coverslips were washed with 1% PBST, air dried, mounted with a 90% glycerol-PBS solution and visualized with an OPTIPHOT fluorescent microscope (Nikon, Tokyo, Japan).

The numbers of fluorescing cells were counted in five random fields. Percentage transfection rate was determined by dividing the number of fluorescing cells by the total number of cells per field and multiplying by 100.

2.3.21.9 Confirming glycoproteins and nucleoprotein expression using CCHF serum

Confirmation of CCHFV Gn, Gc and NP expression was carried out in the BHK-21 and HEK-293 cell lines. Electroporated BHK-21 cells on coverslips in 24 well plates were incubated for 24 hours at 37°C 5% CO₂. At the end of the incubation period, cells were fixed in a methanol-acetone solution at a temperature of -20°C. Blocking for 20 minutes at room temperature was achieved by a solution comprising of 10% sucrose, 0.5% Triton X-100 (Promega, Wisconsin, USA) in 1% PBS. Thereafter, cells were reacted with anti-CCHF IgG human serum (diluted 1:10 in blocking solution) at 37°C in a moisturized container for 90 minutes. Non-specific binding antibodies were washed off coverslips by 1% PBST. Immediately after washing, coverslips were overlaid with goat anti-human IgG antibody conjugated to a fluorescein isothiocyanate molecule (SeraCare Life Sciences, Massachusetts, USA) (diluted 1:40 in 0.1% Evans blue) for 30 minutes in a moist container at 37°C. The excess secondary antibody was removed by washing with 1% PBST. After coverslips had dried, they were mounted with 90% glycerol in 1% PBS and visualized.

2.3.21.10 Sodium dodecyl sulfate polyacrylamide gel (SDS-PAGE) analysis

Electroporated cells were grown in a T-25 cm² flask at 37°C for 48 hours. After that, the culture media was aspirated and the cell monolayer rinsed with 5ml cold PBS. A 250µl aliquot of NET/BSA lysis buffer was added to the cells and the flask was incubated on ice for 30 minutes with shaking. Cells were scraped off, collected in a 1.5 ml tube and centrifuged at 1300 x g for 5 minutes at 4°C. The supernatant was stored at -20°C.

On the day of the experiment, the cell lysates were thawed, 40 µl of each sample was mixed with 10 µl of Lane Marker Reducing Sample Buffer (Thermo Scientific, Illinois, USA) and the mixture was boiled for 5 minutes. The mixture was divided into two aliquots and allowed to cool at room temperature. An SDS-PAGE experiment was set up. Reaction components for the preparation of the gels are detailed in Table 2.10. The resolving gel monomer solution was first prepared and transferred into glass plates. A layer of Amyl alcohol was overlaid on top of the gel to allow the gel to set in an even layer. After the resolving gel was set, amyl alcohol was removed with an absorbent paper following which the stacking gel monomer solution was prepared, added on top of the resolving gel and combs inserted. When the gels were fully set, the gels were submerged in a Mini-PROTEAN Tetra cell tank with Tris-Glycine SDS buffer (Melford laboratories, Ipswich I, UK), pH 8.5. The combs were removed and samples prepared

above were loaded onto the SDS-PAGE gel (4% stacking, 12% resolving). A 5µl aliquot of the PageRuler™ prestained protein ladder (Thermo Scientific, Illinois, USA) was mixed with 5µl MagicMark XP Western Protein Standard (Thermo Scientific, Illinois, USA) and the mixture was used to estimate the sizes of proteins separated. The two gels were run for 1 hour and 50 minutes at 140V.

Table 2. 10: 12% and 4% resolving gel components using 30% Bis-acrylamide (Sigma-Aldrich, Missouri, USA)

	12% resolving gel	4% resolving gel
Component	Volume	Volume
1.5 Tris-HCL (pH 8.8)	2.75 ml	-----
1.5 Tris-HCL (pH 6.8)	-----	1.375 ml
30% Bis-acrylamide	4 ml	0.667 ml
10% SDS	100 ul	50 ul
50% Glycerol	2 ml	1 ml
Distilled water	1.065 ml	1.861 ml
10% APS	75 ul	37 ul
TEMED	10 ul	10 ul
Final Volume	10 mL	5 mL

On completion of the run, gels were soaked in transfer buffer (refer to appendix H) for 15 minutes. A BioTrace polyvinylidene fluoride (PVDF) transfer membrane (Pall Corporation, New York, USA) membrane corresponding to the size of the gel was cut and first soaked in 100% methanol for 5 minutes, then distilled water for two minutes and finally transfer buffer. A sandwich consisting of sponge, PVDF membrane and the gel was assembled. Protein transfer was carried out at 20V (0.06 Amps) for 1 hour 50 minutes using the Trans-Blot® SD semi-dry electrophoretic transfer cell (Bio-rad, California, USA).

2.3.21.11 Immunoblot analysis

2.3.21.11.1 Immunoblot using anti-His₆ antibody

A protein immunoblot was carried out to detect the C-terminal histidine tag fused to the CCHFV nucleoprotein and Gc mature glycoprotein by making use of the Pierce® Fast Western Blotting kit (Thermo Scientific, Illinois, USA). Subsequent to protein transfer the polyvinylidene difluoride (PVDF) transfer membrane was washed in 0.05%

Tween® 20 (VWR™ Life sciences, Pennsylvania, USA) in Tris-buffered saline (TBST) pH 7.5 for 10 minutes three times before it was incubated overnight with primary antibody diluted in equal volumes of TBS and Fast western antibody diluents (Thermo Scientific, Illinois, USA). At the end of the incubation period, the membrane was washed with 0.05% Tween® 20 in Tris-buffered saline (TBST) (pH 7.5) three times. The membrane was incubated in a 1:10 dilution of the horseradish peroxidase (HRPO) reagent in antibody diluent and TBS at room temperature for 15 minutes. Subsequently, the membrane was washed with 0.05% TBST for 10 minutes three times and once with TBS. A 1:1 mixture of luminol and peroxidase was prepared as per manufacturers' instruction. A 5 ml aliquot of SuperSignal® West Pico Plus Luminol/Enhancer solution (Thermo Scientific, Illinois, USA) was mixed with 5 ml of SuperSignal® West Pico Plus stable peroxide solution (Thermo Scientific, Illinois, USA). The membrane was incubated in the mixture for 5 minutes with shaking. Subsequently, the membrane was removed from the solution, excess reagent tipped off and the image was captured with the C-DiGit® Blot Scanner (LI-COR®, Bad Homburg, Germany).

2.3.21.11.2 Immunoblot using CCHF serum

The protein was transferred to a PVDF membrane as in section 2.3.21.11.1. After protein transfer the membrane was blocked with 5% bovine serum albumin/0.1% TBST for 60 minutes at room temperature with shaking. All subsequent incubations were carried out at room temperature with shaking and 10 minute washes were performed. After the incubation period, the membrane was washed three times with 0.1% TBST and incubated in a 1:100 dilution of CCHF serum for a further 60 minutes. Thereafter the membrane was washed in 0.1% TBST three times and incubated in a 1:4000 dilution of goat anti-human IgG HRP (SeraCare Life Sciences, Massachusetts, USA) for 60 minutes. Following this, the membrane was washed three times with 0.1% TBST and once in TBS for 10 minutes. The membrane was exposed to a 1:1 mixture of SuperSignal® West Pico Plus Luminol/Enhancer solution and SuperSignal® West Pico Plus stable peroxide solution for 1 second and the image was captured with the C-DiGit® Blot Scanner (LI-COR®, Bad Homburg, Germany).

2.4 Results

2.4.1 PCR Amplification of CCHF-31S, CCHF-52S, CCHF-31M and CCHF-52M

CCHF- 31S, CCHF-52S, CCHF-31M and CCHF-52M were PCR amplified using Phusion DNA polymerase. After running 5 μ l of the PCR products on an agarose gel, bands corresponding to 1449 bp which are the predicted size of CCHF NP gene, 5070 bp and 5055 bp for CCHF-31M and CCHF-52M respectively the predicted size of CCHF GP gene were visualized as shown in Figure 2.4. Following confirmation, the remainder of the PCR products was separated by electrophoresis on agarose gel, the bands excised, purified and then pooled together. Thereafter the DNA concentrations as measured by the NanoDrop 2000 spectrophotometer were CCHF-52S = 320 ng/ μ l, CCHF-31S = 340 ng/ μ l, CCHF-52M = 420 ng/ μ l and CCHF-31M = 400 ng/ μ l.

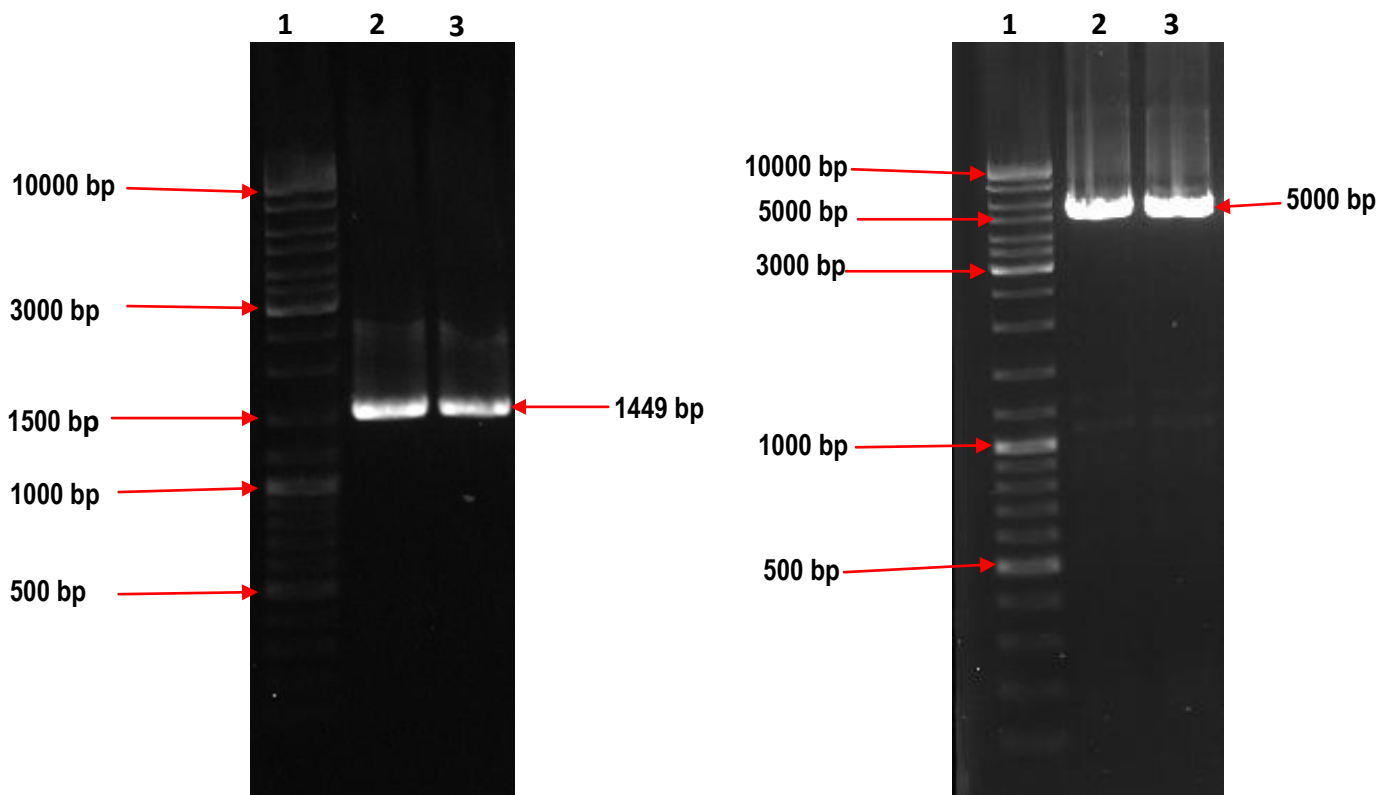


Figure 2. 4: Agarose gel electrophoretic analysis of CCHF NP (left) and GP (right) PCR products. Left, Lane 1: Molecular marker SM 1173, Lane 2: CCHF-31S, Lane 3: CCHF-52S. Right, Lane 1: Molecular marker SM 1173, Lane 2: CCHF-31M, Lane 3: CCHF-52M

The purified PCR products were also analyzed on an electrophoretic gel to confirm the size of the bands. The expected band sizes of approximately 1500 bp and 5000 bp were obtained for nucleoprotein and glycoprotein precursor genes as shown in Figures 2.5 and 2.6 respectively.

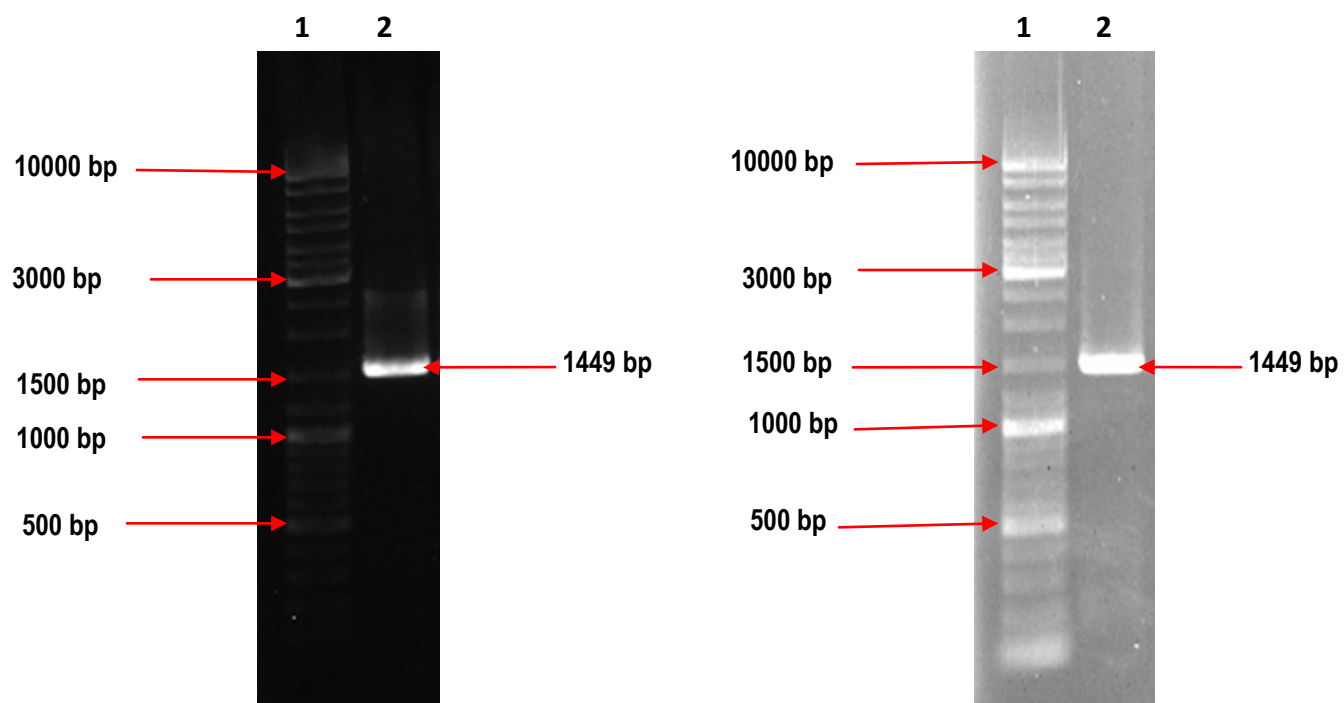


Figure 2. 5: Agarose gel electrophoretic analysis of CCHF NP purified PCR products. CCHF-31S (Left) and CCHF-52S (Right). Lane 1: Molecular marker SM 1173, Lane 2: Purified PCR amplicon

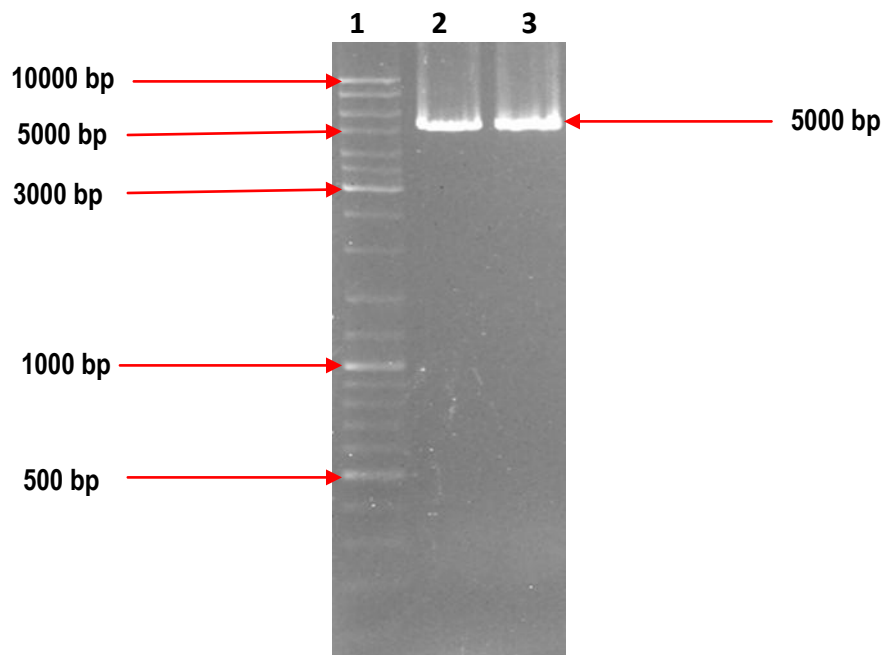


Figure 2. 6: Agarose gel electrophoretic analysis of CCHF GP purified PCR products. Lane 1: Molecular marker SM 1173, Lane 2: Purified CCHF-31M PCR amplicon. Lane 3: Purified CCHF-52M PCR amplicon

2.4.2 Cloning CCHF-31S and CCHF-52S into pMiniT

The PCR products generated had blunt ends and did not have phosphate groups thus they could not be ligated directly into the replicon vector. There was, therefore, the need of an intermediate vector and pMiniT was used for this purpose. pMiniT is a prokaryotic vector and as such, it cannot support protein expression in mammalian cells. A ligation reaction was carried out to ligate the CCHF-31S and CCHF-52S PCR products. The blunt PCR amplicons with the *Not*I restriction enzyme site at the 5' end and *Cla*I restriction enzyme site at the 3' end were cloned into pMiniT and propagated in bacterial cells. Four colonies (pMiniTCCHF-52S) were selected, grown overnight at 37°C, purified and the plasmid DNA was subjected to double restriction enzyme digestion using *Not*I-HF and *Cla*I to confirm positive transformants. Products were analyzed on 1% agarose and all four colonies did not yield the expected insert sizes after restriction enzyme digestion. It was suspected that one of the enzymes was not digesting and when the restriction activity of the enzymes was checked separately, it was observed that *Cla*I was not digesting. A sequencing reaction was performed with primers provided with the pMiniT kit to confirm if the *Cla*I restriction site had been incorporated into the PCR amplicons. All the four clones had the *Cla*I enzyme restriction site (ATCGAT). On further analysis of the sequences, it was observed that amplicons ligating in a forward orientation into the pMiniT vector had the activity of *Cla*I blocked due to Deoxyadenosine methylation (*dam*). The first three bases downstream of the insert site on pMiniT vector are CTG. If the CCHF NP gene is cloned in the forward orientation, the *Cla*I enzyme site will precede the CTG sequence. This gives rise to a 5'- ATCGATCTG-3' sequence and

methylation of the second adenine base in this sequence prevents the restriction enzyme activity of *Cla*I as demonstrated in Figure 2.7.

```

11F      TGT TTGAAATTCAGAAAACAGGGTTCAACATTCAGGACATGGACATAGTGGCCTCTGAGC
5R      TGT TTGAAATTCAGAAAACAGGGTTCAACATTCAGGACATGGACATAGTGGCCTCTGAGC
3R      TGT TTGAAATTCAGAAAACAGGGTTCAACATTCAGGACATGGACATAGTGGCCTCTGAGC
7R      TGT TTGAAATTCAGAAAACAGGGTTCAACATTCAGGACATGGACATAGTGGCCTCTGAGC
          *****

11F      ACCTGCTGCACCAGTCTCTTGTGGCAAGCAATCTCCATTCCAGAACGCCTACAACGTCA
5R      ACCTGCTGCACCAGTCTCTTGTGGCAAGCAATCTCCATTCCAGAACGCCTACAACGTCA
3R      ACCTGCTGCACCAGTCTCTTGTGGCAAGCAATCTCCATTCCAGAACGCCTACAACGTCA
7R      ACCTGCTGCACCAGTCTCTTGTGGCAAGCAATCTCCATTCCAGAACGCCTACAACGTCA
          *****

11F      AAGGCAATGCCACCAGTGCCAACATCATCCACCACCACCACCACCTAAATCGATATCA
5R      AAGGCAATGCCACCAGTGCCAACATTATCCACCACCACCACCACCACCTAAATCGATCTGA
3R      AAGGCAATGCCACCAGTGCTAATATTATCCACCACCACCACCACCACCTAAATCGATCTGA
7R      AAGGCAATGCCACCAGTGCCAACATTATCCACCACCACCACCACCACCTAAATCGATCTGA
          *****

11F      TGGTTTACCTCC
5R      TAATAATGACGTCA
3R      TAATAATGACGTCA
7R      TAATAATGACGTCA
          *  *  *  *  *

```

Figure 2. 7: Representative CCHF-52S sequences showing the *Cla*I restriction site overlapped with the *dam* methylation site. CCHF-52S sequences, Stop codon, *Cla*I enzyme site, *dam* methylation site, pMiniT vector. F and R denote the forward and reverse pMiniT sequencing primers. Sample 11 was cloned in a reverse orientation while the rest cloned in a forward orientation resulting in the GATC sequence which is a *dam* methylation site.

Another set of 12 colonies were selected, numbered one to 12, cultured as above, plasmid DNA purified and sent for Sanger sequencing. Sequences were assembled and analyzed with ChromosPro version 2.0.0 (Technelysium, Brisbane, Australia). Colonies number 1, 2, 3, 4, 5, 7, 9, 10 and 12 were ligated in a forward orientation and these were discarded. Colonies 6, 8 and 11 had been ligated in a reverse orientation. Colony number 6 and 8 had a nucleotide base missing in the primer site and was discarded. Colony 11 had identical genome sequences with representative sequences on GenBank. Moreover, the translation of the amplified genome with the ExPASy translate tool (Appel et al. 1994) yielded the desired CCHF NP amino acid sequence. Plasmid DNA from colony 11 was subjected to double restriction enzyme digestion and products analyzed on 1% agarose are shown in Figure 2.8. Bands corresponding to the CCHF NP were excised and purified. The DNA concentration after purification was 19ng/μl.

Cloning CCHF-31S into pMiniT proved to be as efficient as was the cloning of CCHF-52S. However, the cloning orientation remained a challenge. Following the ligation reaction, streaking of the transformed JM109 cells on LB/Amp agar plates and incubation of the plates overnight at 37°C, colonies were picked, designated number one up

to 12. Plasmid DNA was purified as above and sent for Sanger sequencing. Although all the 12 colonies were positive transformants, colony number 3, 6, 10 and 12 had CCHF-52S gene in the reverse orientation in pMiniT vector. On close examination of the sequences, plasmid DNA from samples 6, 10 and 12 had a mutation in the *Cla*I restriction site. Plasmid DNA from sample 3 had the *Not*I and *Cla*I enzyme restriction sites as well as the particular nucleoprotein sequences. The plasmids (pSinCCHF-31S and pSinCCHF-52S) were double digested as illustrated in Figure 2.8, cleaned up and the concentrations as measured by the NanoDrop 2000 spectrophotometer were 18ng/μl and 19ng/μl respectively. These were stored at -20°C for use in downstream reactions.

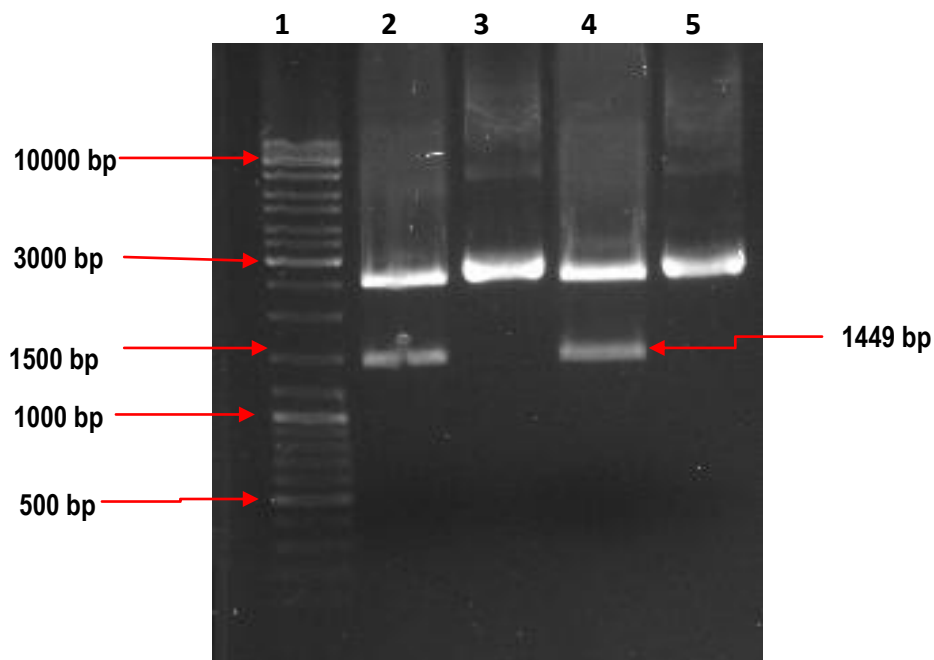


Figure 2. 8: Agarose gel electrophoretic analysis of pMiniTCCHF-31S and pMiniTCCHF-52S double digestion using *Not*I-HF and *Cla*I. Lane 1: Molecular marker SM 1173. Lane 2: pMiniTCCHF-31S double restriction digestion with *Not*I-HF and *Cla*I. Lane 3: Undigested plasmid pMiniTCCHF-31S Lane 4: pMiniTCCHF-52S double restriction digestion with *Cla*I and *Not*I-HF. Lane 5: Undigested pMiniTCCHF-52S plasmid

2.4.3 Cloning CCHF-31M and CCHF-52M into pMiniT

Cloning the CCHF glycoprotein precursor genes into the pMiniT vector was less efficient than cloning the CCHF nucleoprotein gene. This was evidenced by a low number of colonies growing on the agar plate after transformation, an average of 30 colonies compared to more than 500 colonies. Positive transformants were found on average in two out of 12 colonies picked on the LB/Amp plate. Colonies consisting of the self-ligated pMiniT vector grew on the agar plate despite the presence of the toxic minigene. Sequencing results revealed transformants with incomplete CCHF-GP genes which could have been a consequence of the CCHF-GP gene fragmenting. Sanger sequencing provided

800 bases with each of the primers. Although this was not enough to cover the full glycoprotein precursor gene, the start and stop codons, as well as the polyhistidine tag, were present. Alignment of the 800 nucleotide sequences with the original sequences on GenBank displayed 100% identity. The sequences were therefore used in downstream experiments with confirmation of the complete genes in the final constructs. DNA concentrations of 43.3 ng/μl and 40 ng/μl for CCHF-52M and CCHF-31M respectively were obtained after *Not*I restriction enzyme digestion of inserts in pMiniT. Figure 2.9 shows the restriction digestion of pSinCCHF-31M and pSinCCHF-52M.

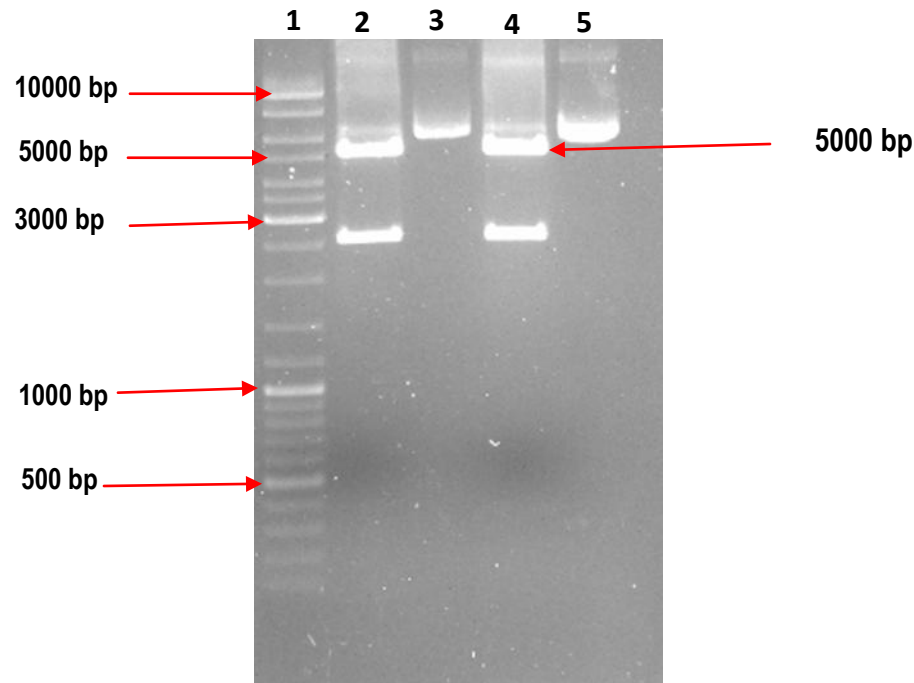


Figure 2. 9: Agarose gel electrophoretic analysis of pSinCCHF-31M and pSinCCHF-52M restriction digestion using *Not*I-HF restriction enzyme. Lane 1: Molecular marker SM 1173. Lane 2: pSinCCHF-31M restriction digestion with *Not*I-HF. Lane 3: Undigested plasmid pSinCCHF-31M Lane 4: pSinCCHF-52M digestion restriction digestion with *Not*I-HF. Lane 5: Undigested pSinCCHF-52M plasmid

2.4.4 Sub-cloning CCHF-31S, CCHF-52S, CCHF-31M and CCHF-52M genes into pSin replicon vector

The pSinGFP vector is a DNA-launched Sindbis replicon that utilizes the hCMV immediate-early promoter/enhancer element to drive recombinant protein expression. The vector had been previously modified to include *Cla*I restriction sites. In the current study, the modified pSinGFP plasmid was linearized using *Not*I-HF and *Cla*I restriction enzymes. Products of restriction enzyme digestion were separated on an agarose gel and the band corresponding to the linearized plasmid (10812 bp) was excised, purified and used in downstream experiments.

The *Not*I-HF/*Cla*I digested CCHF-52S and CCHF-31S PCR products from pMiniT were cloned into *Not*I and *Cla*I restriction enzyme sites on the replicon vector using an insert: vector molar ratio of 10:1. To confirm ligation of CCHF-52S and CCHF-31S into the linearized replicon vector, purified plasmid DNA from two single colonies (for each of the plasmid) were picked on agar plates and incubated overnight in 2XTY kanamycin supplemented broth. Purified DNA plasmids were subjected to PCR amplification. All the PCR products obtained had a band size corresponding to 1449 bp after analysis on an agarose gel as shown in Figure 2.10. The prepared constructs were designated pSinCCHF-31S and pSinCCHF-52S.

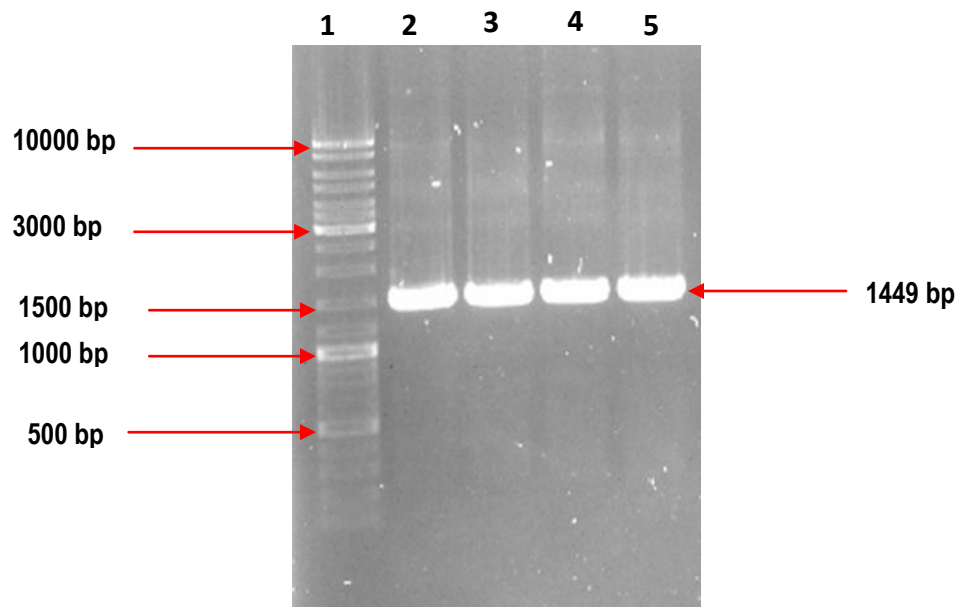


Figure 2. 10: Agarose gel PCR confirmation of pSinCCHF-31S and pSinCCHF-52S. Lane 1: Molecular marker SM 1173. Lanes 2-3 CCHF-31S, Lanes 4-5 CCHF-52S PCR products

The linearised replicon from pSin-DLR-CCHF was dephosphorylated by antarctic phosphatase before the PCR amplicons (CCHF-52M and CCHF-31M) digested from pMiniT were ligated into the replicon using an insert: vector molar ratio of 1:8. The self-ligation reaction yielded no growth of colonies. The constructs were designated pSinCCHF-31M (encoding glycoprotein precursor gene from a reassortant strain), pSinCCHF-52M (encoding the glycoprotein precursor gene from a non-reassortant strain). Cloning of the CCHF glycoprotein precursor genes into the replicon was non-directional, so there was a possibility of the genes not cloning in frame with the replicon components. To check if the cloned glycoprotein precursor genes were in the correct orientation, plasmid DNA purified from colonies picked on agar plates were subjected to a PCR using either of the forward primers (CCHF-MR-F or CCHF-M-F) and a replicon reverse primer (RP-pSin). Of the five colonies picked for pSinCCHF-52M, two were in

the correct orientation while three were not as shown in Figure 2.11. For the plasmid pSinCCHF-31M, three of the five colonies had plasmid DNA cloned in the correct orientation as shown in Figure 2.12.

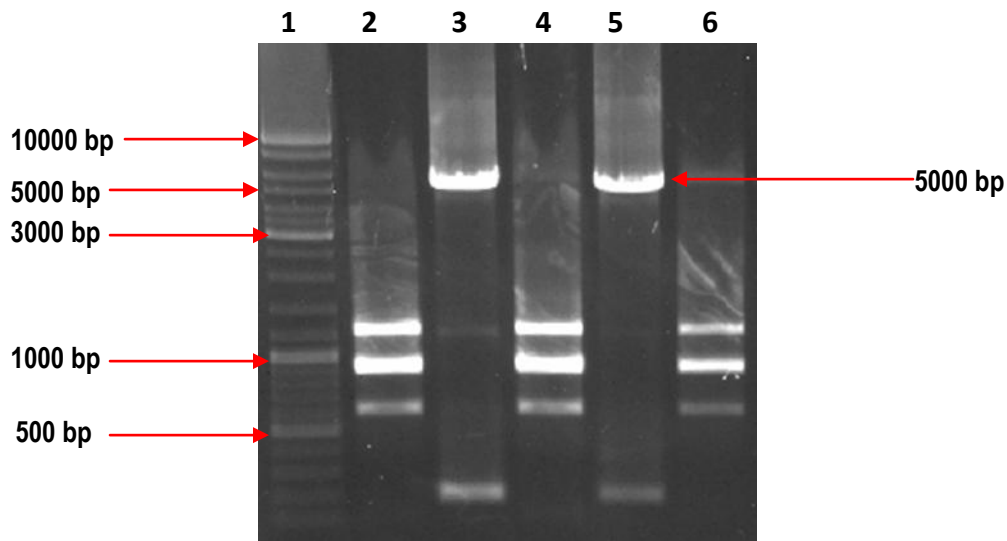


Figure 2. 11: Agarose gel analysis for PCR confirmation of CCHF-52M alignment in the replicon vector. Lane 1: Molecular marker SM 1173. Lanes 2-6: CCHFV GP PCR products. Lanes 3 and 5 show PCR products from plasmids with the insert in the correct orientation and of the expected size while lanes 2, 4 and 6 show PCR products from plasmids without the required insert sizes or correct orientation. Bands observed in lanes 2,4 and 6 could have resulted from non-specific PCR amplification in plasmids with inserts in the reverse orientation or plasmids with the correct orientation but with inserts smaller than the expected size of 5000 bp.

2.4.5 DNA Sequencing of CCHF-31S, CCHF-31M, CCHF-52S and CCHF-52M genes in Sindbis replicon vector

Nucleotide sequences of the CCHF genes in the replicon vector were determined from plasmid DNA purified from positive transformants from the PCR confirmation reaction. The crude data were assembled and analyzed with ChromasPro. The chromatogram had discrete, distinct and uniformly spaced peaks as shown in Figure 2.13 for CCHFV-52S. After trimming the first and last base sequences whose peaks were small and not well defined, 800 base sequences were obtained with each of the forward and reverse primers. This meant that the full open reading frame of CCHF-31S and CCHF-52S was obtained (1449 bp) but not the CCHF-31M gene which is 5070 bp from a reassortant strain and 5055 bp (CCHF-52M) from a non-reassortant strain. The start and stop codons, as well as the polyhistidine tag, were present in all the constructs. This was evidence that the genes had been cloned in the correct orientation with the replicon components. When aligned with the original nucleotide sequences on GenBank, the full-length CCHF-31S was 100% identical while CCHF-52S had three base differences at different positions. The

amplified sequences were then translated into amino acid sequences with the Expasy translate tool (Appel et al. 1994). The translated sequences for the two constructs (pSinCCHF-31S and pSinCCHF-52S) yielded 100% similarity with the original amino acid sequences on GenBank.

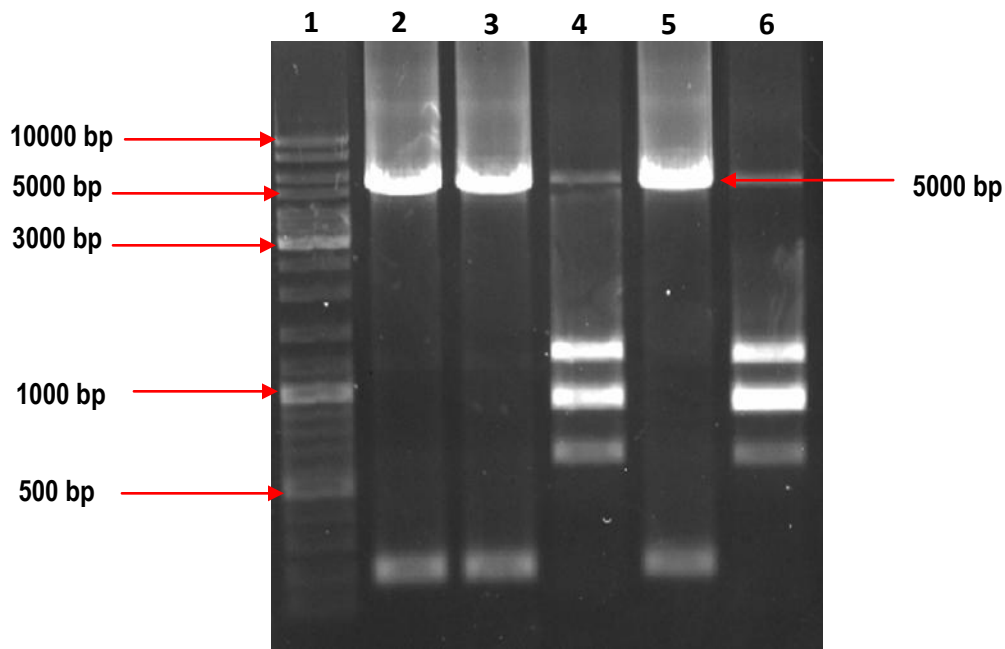


Figure 2. 12: Agarose gel analysis for PCR confirmation of CCHF-31M alignment in the replicon vector. Lane 1: Molecular marker SM 1173. Lanes 2-6: CCHFV PCR products. Lanes 2, 3 and 5 show PCR products from plasmids with the insert in the correct orientation and of the expected size while lanes 4 and 6 show PCR products from plasmids without the required insert sizes or correct orientation. Bands observed in lanes 4 and 6 could have resulted from non-specific PCR amplification in plasmids with inserts in the reverse orientation or plasmids with the correct orientation but with inserts smaller than the expected size of 5000 bp.

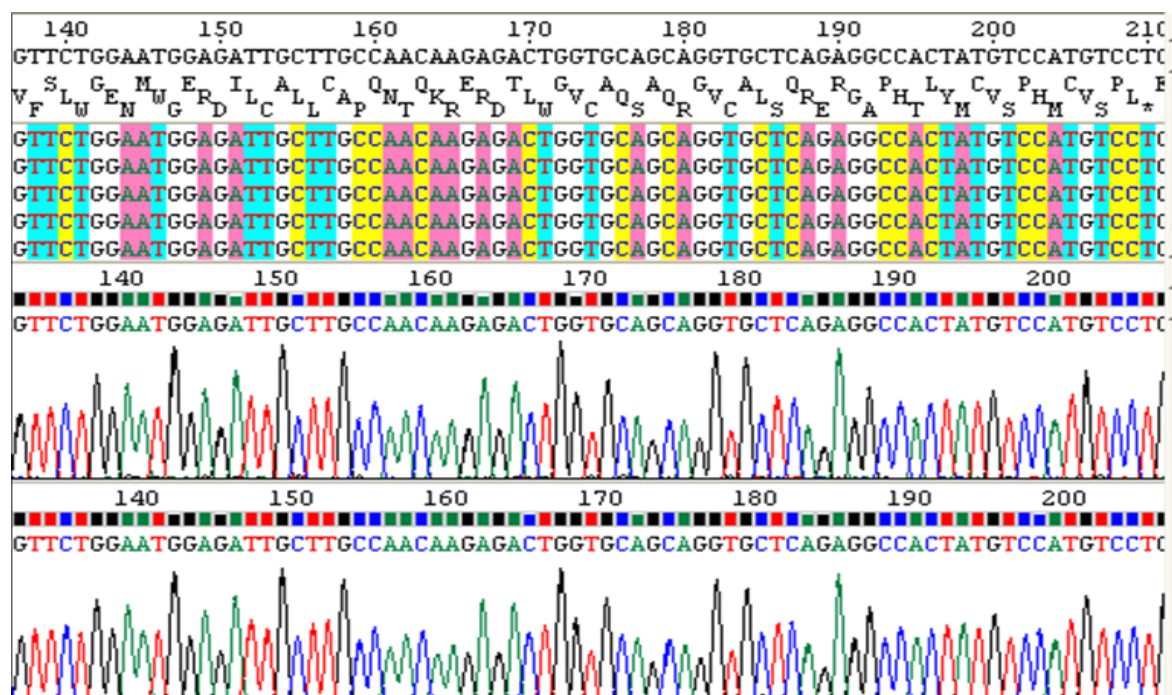


Figure 2. 13: DNA sequencing chromatogram for CCHFV-52S obtained after Sanger sequencing

2.4.6 Next-generation sequencing of vaccine constructs

Full coverage for the prepared vaccine constructs was obtained and aligned with original sequences available on GenBank. Alignment of the sequenced CCHF-31M and the original sequences on GenBank revealed a deletion in the coding GP sequence of pSinCCHF-31M at position 2919 and base changes at positions 7 and 2677. The coding GP sequence in pSinCCHF-52M had two base mutations at positions 1122 and 2720, the NP sequence in pSinCCHF-52S had three base mutations at positions 516, 1437 and 1443 while there were no base changes with the NP sequence in pSinCCHF-31S. The nucleotide sequences were translated to amino acid sequence using the ExPASy translate tool (Appel et al. 1994) and aligned with respective amino acid sequences available in GenBank. Alignment of the translated NP amino acid sequences revealed 100% identity with respective amino acid sequences available in GenBank. Alignment of the GP amino acid sequence from pSinCCHF-52M displayed one amino acid difference (isoleucine replaced with asparagine) with sequences in GenBank. The GP nucleotide sequence in vaccine construct pSinCCHF-31M had a frameshift as a result of the deletion and was therefore not used in downstream experiments.

2.4.7 Optimization of transfection with Lipofectamine reagent

A series of transfection experiments were carried out to determine optimal conditions regarding cell count and plasmid concentrations. The procedure had been optimized previously in our laboratory but the plasmids used then

were smaller than the ones used in the study and such the conditions did not yield desirable results. After attempting various permutations of plasmids and transfection reagent ratios, transfection efficiencies were by observation still very low for the glycoprotein and nucleoprotein constructs. Higher concentrations of the Lipofectamine reagent and DNA plasmids gave better transfection efficiencies, but these were accompanied by lower cell viability. As shown in Table 2.11 nucleoprotein transfection efficiency was around 8% while transfection efficiencies with the glycoproteins were significantly lower, around 3%. Besides that, the results were not consistent.

Table 2. 11: Percentage transfection efficiency rate in BHK-21 and HEK-293 cells after transfections with the Lipofectamine 3000 reagent

		Transfection efficiency		
Amount of plasmid DNA	DNA:Lipofectamine ratio	pSinCCHF-31S	pSinCCHF-52S	pSinCCHF-52M
2 µg	1:1.5	0%	0%	0%
2 µg	1:2	0%	0%	0%
2 µg	1:3	0%	0%	0%
2.5 µg	1:1.5	3%	3%	0%
2.5 µg	1:2	5%	5%	0%
2.5 µg	1:3	5%	5%	0%
3 µg	1:1	6%	6%	2%
3 µg	1:1.5	6%	6%	2%
3 µg	1:2	6%	6%	2%
3 µg	1:3	6%	6%	3%
3.5 µg	1:1	6%	6%	3%
3.5 µg	1:1.5	6%	6%	3%
3.5 µg	1:2	6%	6%	3%
3.5 µg	1:3	8%	8%	3%
4 µg	1:1.5	8%	8%	3%
5 µg	1:1.5	8%	8%	3%
6 µg	1:1.5	8%	8%	3%

2.4.8 Optimization of electroporation experiments

In order to evaluate CCHFV Gn, Gc and NP expression, gene expression was demonstrated in a transient expression system. A high level of heterologous protein expression is mandatory in demonstrating the functionality of the replicon and as such, electroporation experiments were optimized to establish optimal electroporation parameters and the amount of plasmid DNA. The recommended electroporation parameters by the manufacturer (Neon® Transfection System) for HEK-293 and BHK-21 cell lines yielded low transfection efficiencies thus parameters with better transfection efficiencies were sought. Plasmids investigated in this study are more than 10 kb which are bigger than plasmids mostly used for optimization by manufacturers. It, therefore, needed higher voltage

parameters, but then these are accompanied by lower cell viability. Protein expression was demonstrated in BHK-21 and HEK-293 mammalian cell lines at 24 hours post electroporation. A 15 µg aliquot of plasmid DNA yielded optimum results with the investigated electroporation parameters. The percentage transfection efficiencies obtained using various electroporation parameters are shown in Table 2.12. A pulsing voltage of 1500V, pulse width 20 ms and pulse number one yielded high levels of the nucleoprotein and glycoprotein expression with the least cell death (visually). Increasing recovery time of cells shortly after exposure to an electric current before returning cells to culture media has been reported to increase cell survival and transfection efficacy with large plasmids (Lesueur et al. 2016). This was also investigated in the study to enhance cell survival and transfection efficiency which was a challenge with the over 15 kb plasmid (pSinCCHF-52M). Incubating cells at room temperature in electroporation buffer for 30 minutes before transferring them to growth media gave maximum cell viability and transfection efficiency.

2.4.9 Indirect Immunofluorescent Assays

CCHFV Gn, Gc and NP expression were demonstrated by performing indirect immunofluorescent assay (IFA) on pSinGFP, pSinCCHF-52S, pSinCCHF-31S and pSinCCHF-52M transfected BHK-21 and HEK-293 cells. Approximately 24 hours post electroporation, transfected cells grown on glass cover-slips were used as antigen slides. The slides were fixed in methanol-acetone and an IFA was performed. Expression of the GFP was demonstrated by fluorescence as visualized under the microscope on fixed cells while CCHF NP and GP expression was confirmed by demonstrating the presence of the C-terminal histidine tag fused to the NP and Gc by using the commercial mouse anti-His₆ antibody. Images are shown in Figures 2.14-2.17. In the absence of a pSin vector containing all the replicon elements, cells used as controls underwent the preparation process for electroporation just as the transfected cells. Controls cells were resuspended in the electroporation buffer in the presence of plasmid DNA and did not receive an electric pulse. This was to demonstrate that plasmids were not transferred into cells in the absence of an electric pulse. Expression of CCHFV structural proteins was further confirmed using serum from CCHF survivors. Transfection efficiencies were determined by counting the number of fluorescing cells per field divided by the total number of cells in the field multiplied by 100. The obtained transfection efficiencies obtained after electroporating plasmids using different electroporation parameters are shown in Table 2.12. Incubation of transfected cells beyond 24 hours before assaying for protein expression did not improve CCHFV Gn, Gc and NP protein expression. CCHFV protein expression was confirmed by immunofluorescence assays using serum from CCHF survivors.

Table 2. 12: Percentage transfection efficiency rate in BHK-21 and HEK-293 cells after electroporation

Electroporation parameter			Percentage transfection rate		
Pulse Voltage (V)	Pulse Width (ms)	Pulse Number	pSinCCHF-31S	pSinCCHF-52S	pSinCCHF-52M
1 100	20	2	40%	40%	20%
1 200	30	1	45%	45%	25%
1 300	10	3	50%	52%	30%
1 300	30	1	62%	65%	30%
1 500	20	1	58%	60%	30%
1 500	10	3	58%	60%	30%

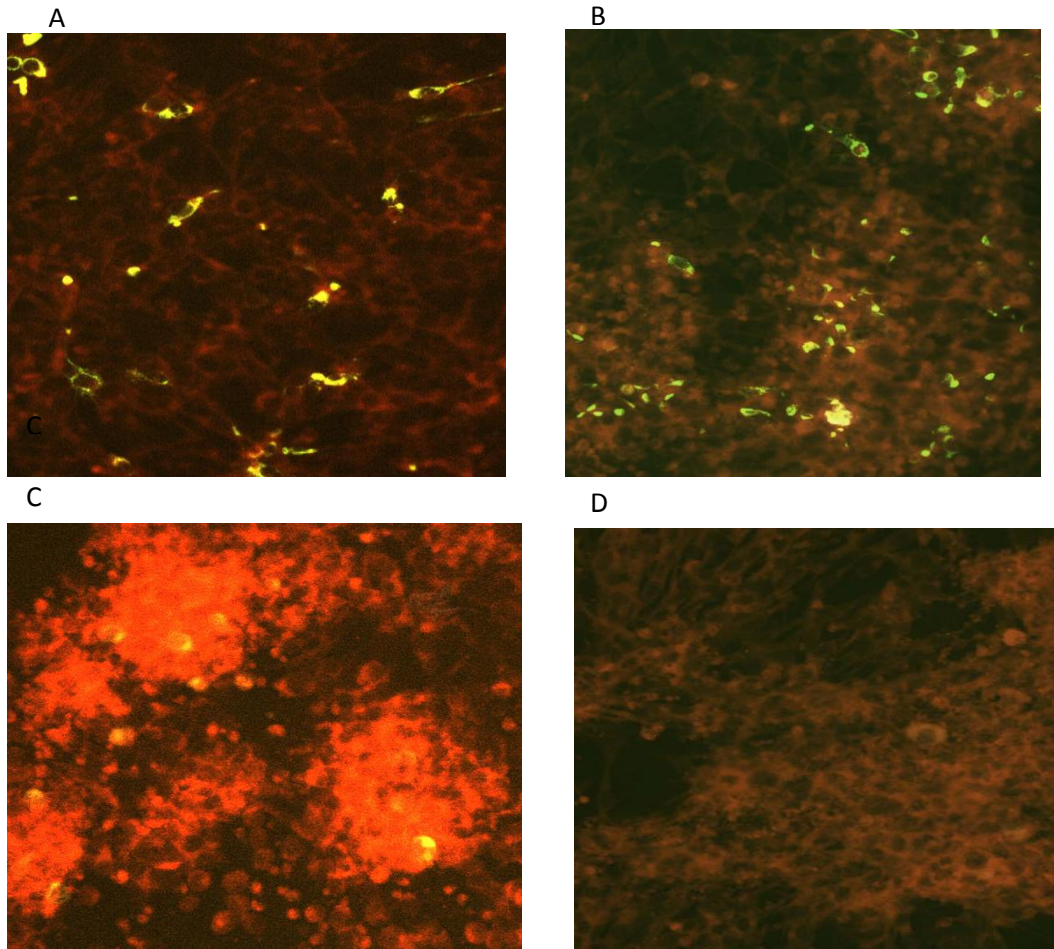


Figure 2. 14: Confirmation of CCHFV nucleoprotein and glycoprotein expression in BHK-21 cells using commercial mouse anti-His₆ antibody. **(A):** BHK-21 cells transfected with replicon pSinCCHF-31S. **(B):** BHK-21 cells transfected with replicon pSinCCHF-52S. **(C):** BHK-21 cells transfected with replicon pSinCCHF-52M **(D):** untransfected BHK-21 cells

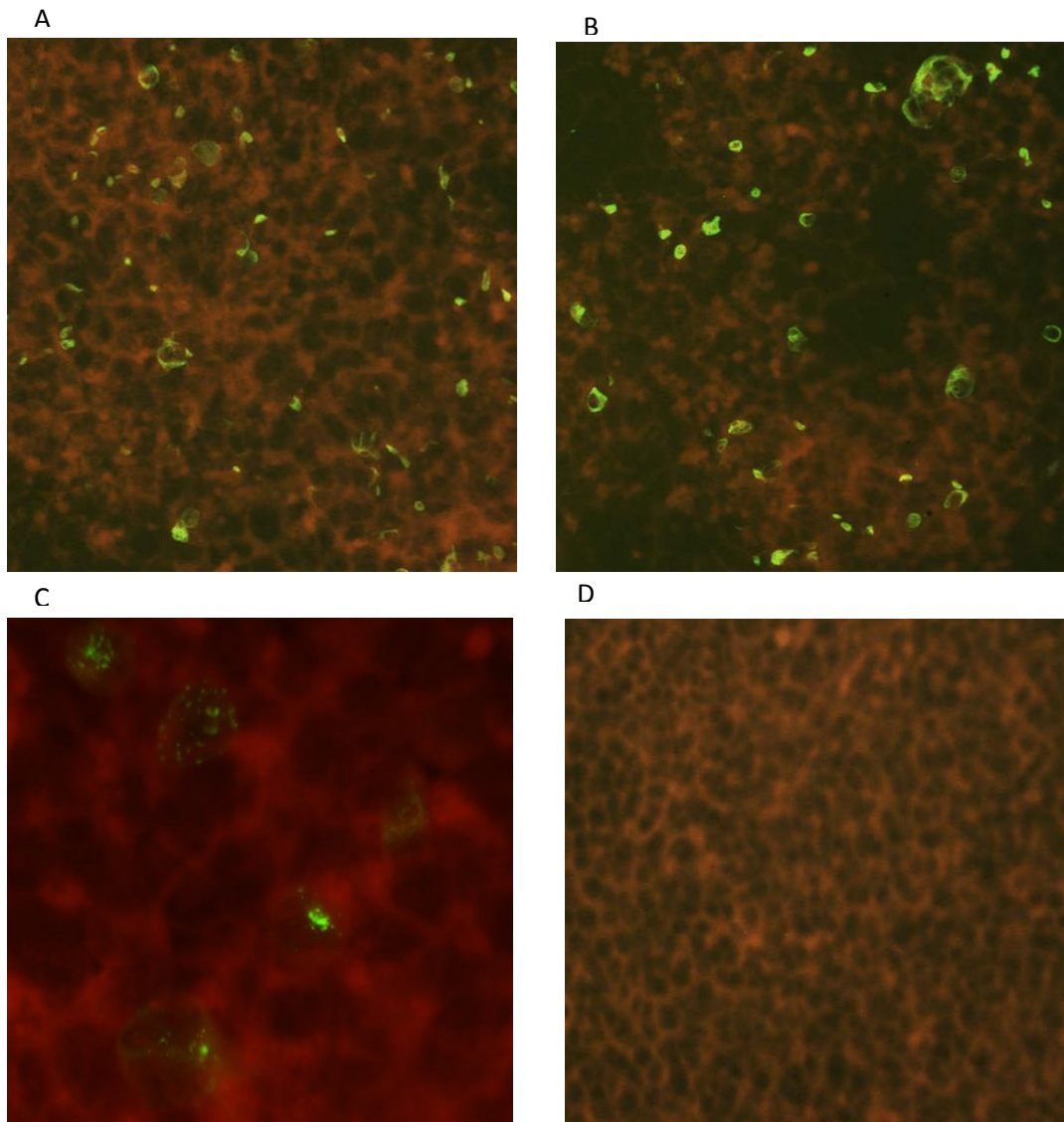


Figure 2. 15: Confirmation of CCHFV nucleoprotein and glycoprotein expression in HEK-293 cells using commercial mouse anti-His₆ antibody. **(A):** HEK-293 cells transfected with replicon pSinCCHF-31S. **(B):** HEK-293 cells transfected with replicon pSinCCHF-52S. **(C):** HEK-293 cells transfected with replicon pSinCCHF-52M **(D):** untransfected HEK-293 cells

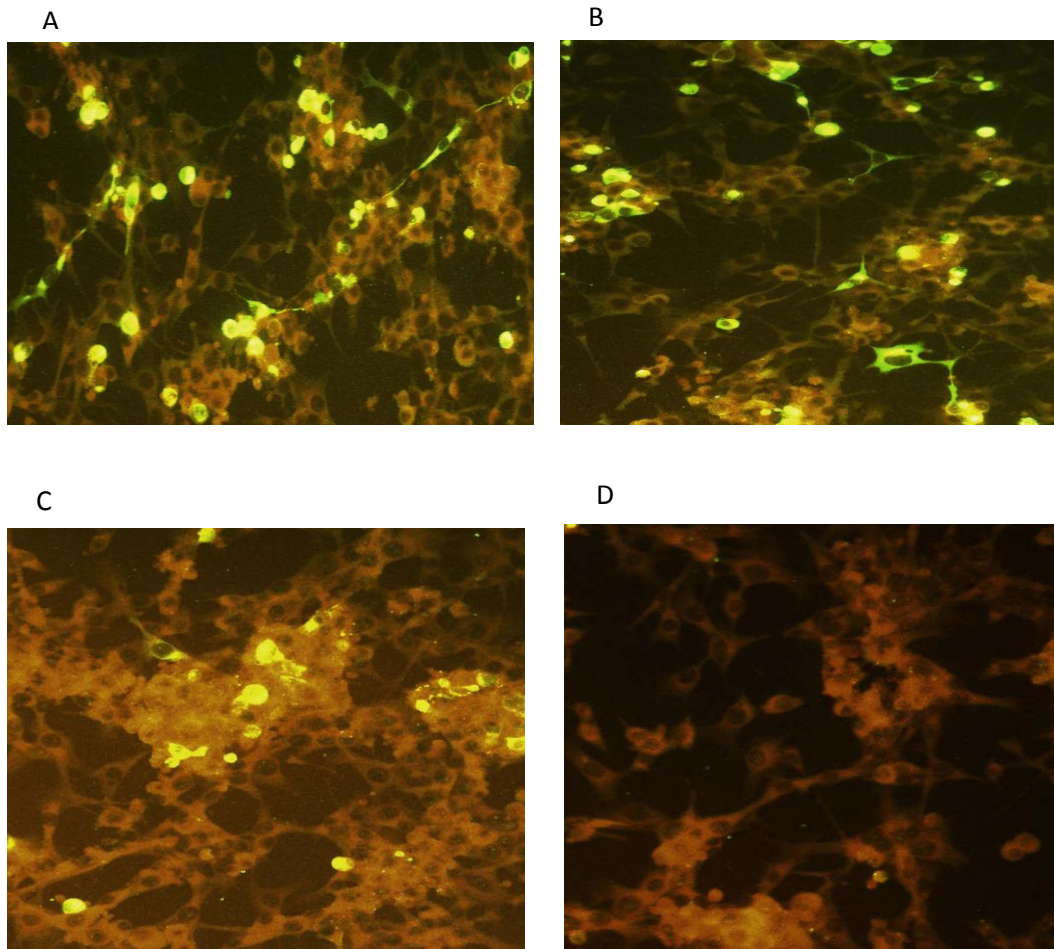


Figure 2. 16: Confirmation of CCHFV glycoprotein and nucleoprotein expression in BHK-21 cells using anti-CCHF IgG human serum. **(A):** BHK-21 cells transfected with replicon pSinCCHFV-52M. **(B):** BHK-21 cells transfected with replicon pSinCCHFV-31S. **(C):** BHK-21 cells transfected with replicon pSinCCHFV-52M. **(D):** untransfected BHK-21 cells

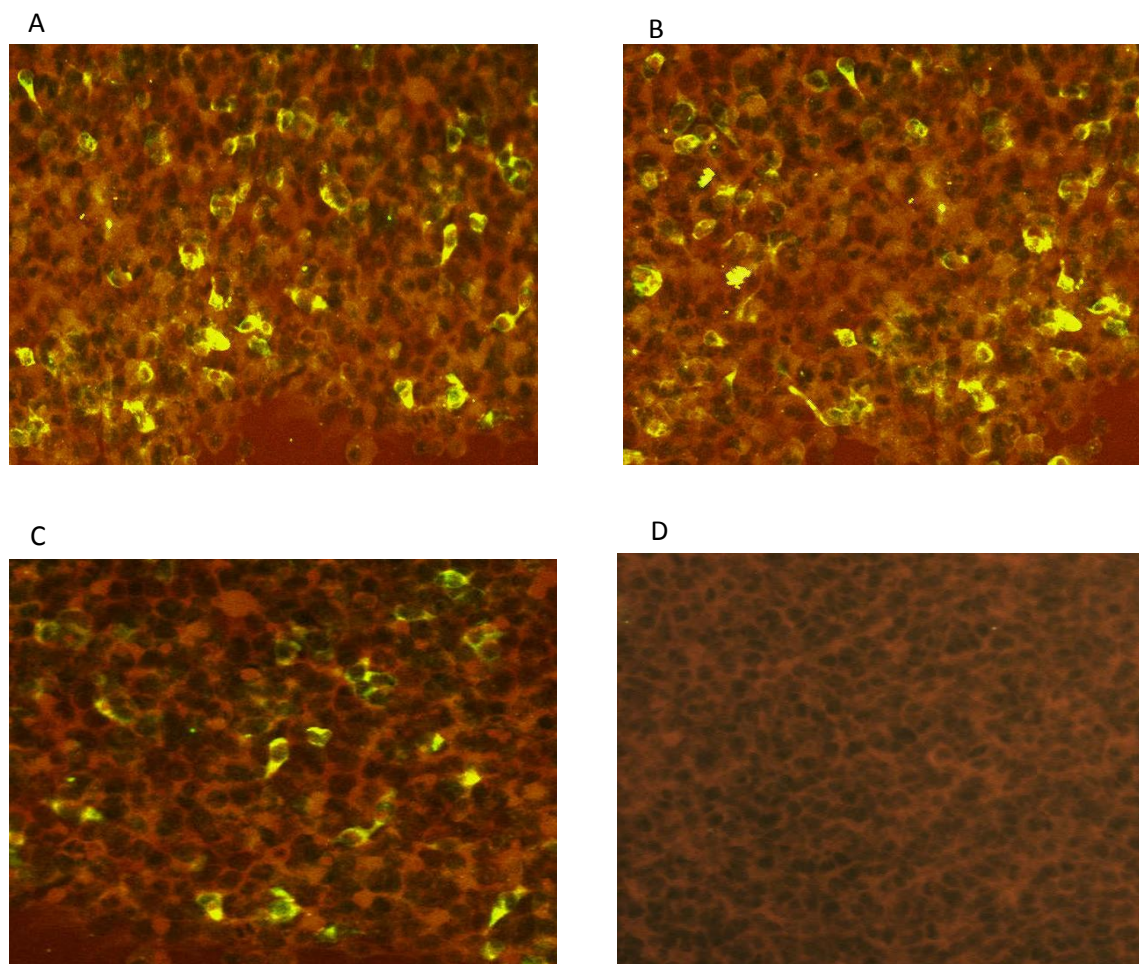


Figure 2. 17: Confirmation of CCHFV glycoprotein and nucleoprotein expression in HEK-293 cells using anti-CCHF IgG human serum. **(A):** HEK-293 cells transfected with replicon pSinCCHFV-52M. **(B):** HEK-293 cells transfected with replicon pSinCCHFV-31S. **(C):** HEK-293 cells transfected with replicon pSinCCHFV-52M. **(D):** untransfected BHK-21 cells.

2.4.10 Western Blot analysis of CCHFV NP and GP

To further characterize the expression of CCHFV NP and GP, cell lysates from transfected cells were examined using anti-His₆ antibody and CCHF serum. The expected sizes of the CCHFV Gn, Gc and NP, are 75 kDa, 37 kDa (Vincent et al., 2003) and 52 kDa (Marriott and Nuttall, 1992) respectively. Studies described in the literature have shown that BHK-21 cells are superior to HEK-293 with regards to protein production after transfection with alphavirus replicons (Kim et al. 2014; Benmaamar et al., 2009) thus lysates from electroporated BHK-21 cells were analyzed. Forty-eight hours after transfection lysed cell supernatants were harvested and subjected to western blot analysis using the anti-His₆ antibody. Protein bands corresponding to 52 kDa which is the estimated size of CCHFV NP were

observed as shown in Figure 2.18 below. Repeated efforts to visualize the glycoproteins on a western blot using both the anti-His₆ antibody and CCHF serum were unsuccessful.

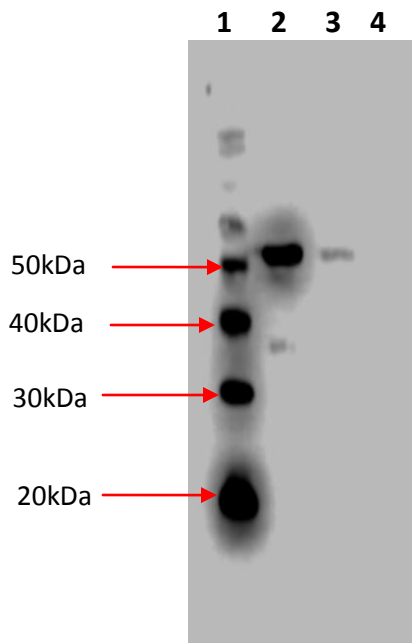


Figure 2. 18: Western blot analysis of CCHFV NP. From left to right; Lane 1: MagicMark XP Western Protein Standard, lane 2 CCHF-52S , Lane 3 CCHF-31S, Lane 4 mock electroporated cells

2.5 Discussion

Alphavirus replicons have underscored their utility as expression vectors. In this study, Sindbis replicons expressing CCHFV glycoproteins and nucleoproteins of two South African strains (SPU45/88 and SPU187/90) were prepared using recombinant molecular technology. The complete genome sequences available for South African strains are limited. Some South African strains have evidence of reassortment in the M segment and clusters with the Asian and the Middle East strains while the S and L segments cluster with South African and West African strains (Goedhals et al. 2014). The SPU45/88 is a reassortant strain and is representative of the Asian/Middle East strains while the SPU187/90 strain is a non-reassortant and is representative of South African strains. Primers capable of amplifying the entire open reading frame of CCHFV glycoprotein precursor were designed with *Not*I endonuclease sites at the 5' end while primers amplifying the complete open reading frame of the nucleoprotein genes were designed with *Not*I and *Cla*I enzyme restriction sites at 5' end of the forward and reverse primers respectively. Sequences coding for a 6x histidine tag were included in the reverse primers. The GP sequences were from reassortant and non-reassortant strains and because of the major differences in the nucleotide sequences, different sets of primers were designed. This was not the case with the NP whose nucleotide sequences exhibited minimal differences thus one set

of primers was designed. Viral RNA was supplied by the National Institute of Communicable Disease, South Africa. Genes encoding the full length of CCHFV nucleoprotein and glycoprotein of South African strains were amplified by the RT-PCR. To ensure errors during amplification were kept to a minimum, a high fidelity DNA polymerase enzyme was used. High fidelity enzymes have mechanisms to safeguard against the addition of incorrect bases during amplification (Joyce and Benkovic 2004). However, the fidelity of polymerase enzymes decreases with increase in PCR cycles thus a maximum of 25 PCR cycles were used. In addition to that, the primer annealing temperature was set at 68°C which is close to the polymerase extension temperature of 72 °C. Amplicons generated were blunt-ended and these were first ligated into an intermediate vector, pMiniT. The vector has a Shine-Dalgarno sequence thus it can only support transcription in bacterial cells. Assembly of the bigger CCHFV GP genes (5055 bp and 5070 bp) into pMiniT was less efficient compared to the smaller CCHFV NP genes (1449 bp). Genetic transformation efficiency of *E. Coli* decreases with increase in DNA size (Hanahan 1983).

CCHFV gene sequences in the pMiniT vector were confirmed by Sanger sequencing by employing bi-directional sequencing. The inserted genes were removed using restriction digestion digested out of the cloned pMiniT vector. Digesting CCHFV NP genes from pMiniT vector was complicated by *dam* methylation which blocks the restriction activity of *Cla1* but not *Not1*. CCHF NP inserts which ligated in the forward orientation in pMiniT could not be digested with *Cla1* due to *dam* methylation. Inserts ligating in the reverse orientation were free from *dam* methylation. Clones in this format (reverse orientation) were few thus several clones were screened. However, restriction enzyme digestion of CCHFV GP genes in pMiniT was not affected by this phenomenon because of the absence of ATCGAT sequences which precipitated *dam* methylation. *Not1* restriction enzyme digestion of GP genes generated compatible ends with both the insert and replicon vector and this presented intramolecular ligation as a challenge. To circumvent this problem, the replicon vector was dephosphorylated to minimize re-ligation. Besides that, this meant that the correct orientation of GP inserts in the replicon expression vector had to be confirmed because cloning was not directional. Restriction enzyme digestion of NP genes with *Not1* and *Cla1* yielded non-compatible ends thus inserts were ligated directionally. A number of strategies were employed to enhance the ligation efficiency of GP inserts into the Sindbis replicon vector. Incubating ligation reactions at 4°C overnight had the positive effect of increasing transformants. In addition to that, heat inactivating the T4 DNA ligase enzyme before transforming cells also increased the number of transformants. The effect of these approaches was not noticeable with the NP inserts since ligations were very efficient before ligase enzyme inactivation.

Four vaccine constructs were prepared and these were designated pSinCCHF-31S, pSinCCHF-52S for the constructs expressing CCHFV nucleoprotein while the constructs expressing the CCHFV glycoprotein precursor were designated pSinCCHF-31M and pSinCCHF-52M. Gene sequences were confirmed by Sanger sequencing and next-generation sequencing after cloning into the Sindbis replicon vector. Next-generation sequencing was necessary

especially for the GP inserts whose full gene sequence could not be determined by Sanger sequencing due to their nucleotide length. After translating the nucleotide sequences to amino acid sequences, and aligning them with the original sequences on GenBank, a 100% identity was observed with the constructs coding the nucleoprotein (pSinCCHF-31 and pSinCCHF-52S). The GP amino acid sequence in pSinCCHF-52M had one amino acid difference. Several clones were screened and Sanger sequencing was performed but the mutation was in a region where sequences were not obtained because we had one set of primers annealing at the 5' and 3' ends of the GP sequence. Because of the costs associated with next-generation sequencing, we sequenced the clone which had no mutations with the sequences generated by Sanger sequencing. The mutation (Isoleucine to Asparagine) occurred at amino acid position 907 of the GP sequence in pSinCCHF-52M. This region codes for the non-structural M protein (NS_M) whose function is not yet described. The potential impact of the mutation is thus not known. Vaccine construct pSinCCHF-31M had a nucleotide deletion in the coding GP sequence and could not be used in downstream investigations. The nucleotide deletion could have been introduced during the RT-PCR amplification. Sequencing errors are unlikely because of the deep coverage observed with next-generation sequencing. The construct pSinCCHF-31M could not be recloned because of limited time. Preparing the constructs expressing the glycoprotein precursor took lots of time because ligation efficiencies into pMiniT and the expression vector and transformation of competent cells were poor with an average of 10 colonies growing per plate. Several ligation reactions were thus performed and several colonies were screened to obtain positive transformants. Some positive transformants had incomplete nucleotide sequences and the GP genes being large (over 5000 bp), it is likely that the gene sequences fragmented prior to ligation. Repeating experiments meant using more reagents and this was costly.

The functionality of prepared constructs was verified by demonstrating protein expression in BHK-21 and HEK-293 cell lines. The 260/280 absorbance ratios of plasmids used in transfection experiments were all greater than 1.8. Plasmids were prepared from the same kit (QIAGEN® Plasmid Plus Midi Kit) and purifications were done the same day. The cell membrane, however, functions as a barrier blocking the passive movement of large hydrophilic molecules such as plasmid DNA. Transfection was therefore achieved by using the Lipofectamine 3000 reagent and the electroporation technique. Optimization experiments were first carried with the Lipofectamine reagent and when transfection efficiencies remained consistently low, the focus shifted to the electroporation technique. The latter technique required a higher density of mammalian cells and higher amounts of plasmid DNA per transfection experiment. Transfection efficiencies were higher with high voltages but this was accompanied by low cell viability. On the other hand, low voltages had lower transfection efficiencies and high cell viabilities. Incubating transfected cells at a lower temperature (30°C) did not improve transfection efficiencies. Recombinant protein production was assayed by performing IFA's using a commercial antibody to the histidine tag as the primary antibody. Protein expression of CCHF specific viral proteins was confirmed using anti-CCHF IgG human serum. Electroporation yielded superior transfection efficiencies compared to the Lipofectamine reagent. There were no visual differences in

protein expression rates by the two cell lines though cell viability was higher in BHK-21 cells at the high voltage and high plasmid DNA concentrations used in electroporation experiments. The nucleoprotein had superior expression rates compared to the glycoproteins. Mature glycoproteins could, however, could not be demonstrated on a western blot both with the anti-His₆ antibody and anti-CCHF IgG human serum, possibly due to low expression levels. It is unlikely that the histidine tag fused to the Gc protein was not accessible because IFA experiments using mouse anti-His6 antibody and anti-CCHF primary antibody confirmed Gc expression. Western blot analysis of lysates from BHK-21 cells transfected with NP constructs revealed bands corresponding to the nucleoprotein.

CHAPTER 3

Self-replication rates and induction of apoptosis in cells transfected *in vitro* with DNA launched replicons expressing the glycoprotein and the nucleoprotein of different CCHFV strains.

3.1 Introduction

Alphaviruses possess a single-stranded, positive oriented RNA genome in the region of 12 kb in size (Strauss et al. 1984). The genome comprises of two open reading frames (ORFs) separated by a subgenomic promoter. The ORF downstream of the subgenomic promoter encodes the structural polyprotein while the upstream ORF encodes the non-structural polyprotein. The structural polyprotein is processed into five structural proteins whose function together with the transient non-structural proteins is packaging genomic RNA into viral capsid protein and budding of viral particles from host cells (Strauss et al. 1984). The non-structural polyprotein is post-translationally cleaved into non-structural protein 1 (nsP1), nsP2, nsP3 and nsP4 which are responsible for viral replication. nsP1 participates in capping and addition of methyl groups to the newly generated genomic and subgenomic RNA as well as anchoring replication complexes to membranes. nsP2 has RNA triphosphatase and protease activities within the N and C-terminal half respectively. The function of nsP3 is poorly characterized while nsP4 has RNA-dependent RNA polymerase activity (Kallio et al. 2016). Cleavage of the non-structural polyprotein begins by yielding P123 and nsP4 (de Groot et al., 1990). The two form a replicase complex synthesizing the complementary RNA (Shirako and Strauss 1994). Further cleavage of P123 polyprotein generates the nsP1 and P23 polyprotein. Following total cleavage of the non-structural polyprotein to the four functional proteins, the formation of the complementary RNA is inhibited promoting instead production of genomic and subgenomic RNA from the complementary RNA (Shirako and Strauss 1994). In this study, the prepared vaccine constructs in chapter 2, possessing Sindbis virus non-structural proteins, and were analyzed for their self-replicative capacity by assaying for CCHFV RNA using the quantitative polymerase chain technique qPCR.

The qPCR technique is a common technique and was developed in 1992 (Higuchi et al. 1992). The technique originated as a result of the need to quantify the original amount of DNA molecules in a particular sample. Quantitation with the original PCR technique has drawbacks in the sense that it has lower sensitivities, specificities and is less rapid (Kubista et al. 2006). qPCR, however, employs concurrent amplification and detection of target DNA sequences. Initially, ethidium bromide was used to stain the DNA and hence allowing the detection of amplicons (Higuchi et al. 1992).

Fluorescence is currently the sole detection method in qPCR and the source of fluorescence can be DNA binding molecules which can be intercalators such as ethidium bromide or cyanine dyes for instance SYBR. Besides DNA

binding molecules, fluorogenic tagged probes are also a source of fluorescence. Among the DNA binding molecules, cyanine dyes are more popular. One common property with these molecules is that they only fluoresce when they bind DNA. The obvious disadvantage with the DNA binding molecules is that they cannot discriminate specific from non-specific double-stranded DNA. Non-specific products can, however, be detected by performing a melting curve analysis on completion of the PCR. Fluorogenic tagged probes are derived from nucleic acid or their artificial analogs which include the peptide and locked nucleic acids (Nielsen et al. 1992, Singh et al. 1998). These probes consist of a reporter molecule at the 5' of the sequence and a quencher molecule at the 3' end. With this arrangement, fluorescence from the reporter molecule is quenched. On annealing to the specific sequence and subsequent DNA amplification, the reporter molecule is cleaved by the *Taq* polymerase increasing the distance from the quencher molecule and the result is an increase in fluorescence signal. A qRT-PCR was developed and used to confirm self-replication of the alphavirus replicon.

Apoptosis is a programmed biochemical cell death that is activated by a number of stimuli. Two apoptotic pathways are recognized, specifically the extrinsic and intrinsic pathways. Apoptosis can be categorized into bland, inflammatory and immune apoptosis (Restifo 2000). This characterization seeks to explain how apoptosis can lead to antigen tolerance which results when host cells die and the antigens are presented to immune cells, antigen ignorance as a consequence of developmental processes or immunity as a result of viral infection (Leitner et al. 2004). Apoptosis triggered by viral infection can act to suppress viral replication by eliminating virally infected cells or promote dissemination of progeny viruses. Elimination of virally infected cells is one of the mechanisms evolved by mammalian cells to counteract viral infections. Viral replication produces dsRNA intermediates which are potent inducers of the ds-RNA dependent protein kinase (PKR) and RNase L antiviral pathways (Leitner et al. 2004) which in turn trigger apoptosis in infected cells. Activation of these antiviral pathways is also known to elicit both innate and adaptive immunity (Restifo 2000). Alphavirus replicons have been demonstrated to induce apoptosis in transfected cells by triggering similar antiviral pathways as activated during infections with alphaviruses (Leitner et al. 2004). Stronger immune responses induced by alphavirus replicons have been attributed to their role in apoptosis induction thus they act as adjuvants enhancing immunogenicity of encoded antigens. Apoptosis induction in plasmid DNA vaccines has also been demonstrated to induce stronger immune responses (Sasaki et al. 2001). However, activation of antiviral pathways by replicase based vaccines may inhibit antigen production by restricting viral replication (Terenzi et al. 1999).

Apoptosis detection assays are based on structural and functional modification of cells occurring during apoptosis (Banfalvi 2017). Structural changes during apoptosis pertain to membrane alterations and these can be detected using annexin V assays. Functional changes are a product of intracellular biochemical reactions which result in damage to the nucleus, mitochondrial alterations and cytoplasmic changes such as activation of endonucleases

(Banfalvi 2017). One functional cellular change which occurs during apoptosis is DNA fragmentation. DNA fragmentation is mediated by endonucleases and results from activation of both extrinsic and intrinsic pathways (Elmore 2007). It occurs early during apoptosis before the plasma membrane breaks down and is accompanied by enrichment of nucleosomes in the cytoplasm (Salgame et al. 1997). Induction of apoptosis is considered one of the mechanisms that contribute towards the induction of immune responses. Hence if apoptosis is induced, it suggests stronger immunogenicity of the replicon system. To determine if apoptosis was induced in transfected cells expressing CCHF viral proteins *in vitro* a commercial ELISA based on the double antibody sandwich principle was used to quantitate cytoplasmic nucleosomes. An immune complex composed of anti-histone biotin and cytoplasmic nucleosomes was captured onto streptavidin-coated plates. The nucleosomes were detected with anti-DNA-peroxidase conjugate which binds to the DNA portion of the nucleosomes.

3.2 Aim

To determine self-replication rates and induction of apoptosis in cells transfected with Sindbis based DNA launched replicons transiently expressing CCHFV glycoprotein precursor and nucleoprotein genes.

3.3 Methods and Materials

3.3.1 Primer design

Primer pairs and hydrolysis probes that could be used to quantitate the replication of the three constructs prepared in chapter 2 were designed. Briefly, there were two DNA launched replicons expressing the NP of South African isolates SPU 45/88 and SPU 187/90 and one DNA launched replicon expressing the GP precursor of South African isolate SPU 187/90. The nucleotide sequences for the South African CCHFV strain (SPU45/88, Accession number: KJ682819.1) coding the full-length open reading frame nucleoprotein (NP) and SPU187/90 (Accession numbers KJ682814.1 and KJ682823.1) coding the open reading frame of the glycoprotein precursor (GP) and NP genes respectively were previously retrieved from *GenBank*. The sequences were saved in FASTA format and aligned using Clustal Omega software version 1.2.4 (Sievers et al. 2011). Primers amplifying a 592 base pair region of the glycoprotein precursor gene and a 536 base pair region of the nucleoprotein gene were designed. Hydrolysis probes were identified which annealed within the targeted regions. Glycoprotein precursor primers and probe were designated CCHF-TGPF (forward primer), CCHF-TGPR (reverse primer), and CCHF-GP_52 (hydrolysis probe) respectively. Nucleoprotein primers and probe were designated CCHF-TNPF (forward primer), CCHF-TNPR (reverse primer) and CCHF-NP31_52 (hydrolysis probe) respectively. The nucleotide sequences are shown in Table 3.1 below.

Table 3. 1: Nucleotide sequences for primers and probes

Primer	Tm	Primer Sequence 5' to 3'	Position relative to gene
CCHF-TGPF	53.1°C	ATCTGCAACGGCTCAACTAT	1663-1682
CCHF-TGPR	53.1°C	GCATCTCAGCATCTATTGCAT	2254-2234
*CCHF-GP_52	61.9°C	CATCCTAGTTGACTGTTTCAGGTGGGCA	1935-1962
CCHF-TNPF	52.3°C	TGGACACCTTCACAACTC	80-98
CCHF-TNPR	55.2°C	GACAAACTCCCTGCACCA	615-597
*CCHF-NP31_52	59.1°C	CTGAGCTAAAAGTTGACGTCCCGAAAAT	332-359

* Indicate nucleotide sequences for probes

3.3.2 Vaccine constructs preparation for transfection

Glycerol stocks of cells containing vaccine constructs pSinCCHF-31S, pSinCCHF-52S and pSinCCHF-52M stored at -80°C were thawed and 10 µl of the cells was inoculated into 5 ml 2XTY broth supplemented with kanamycin at a final concentration of 50 µg/ml. The cultures were incubated for 8 hours at 37°C with shaking and subcultured by dilution of 1:100 in fresh 2XTY kanamycin supplemented broth and grown for a further 16 hours at 37°C. Bacterial cells were harvested by centrifugation at 5000 x *g* for 15 minutes. The supernatant was discarded and DNA extraction and purification was performed using the QIAGEN® Plasmid Plus Midi Kit (Qiagen, Hilden, Germany) according to manufacturers' instructions. DNA plasmid concentrations were measured with the NanoDrop 2000 spectrophotometer (Thermo Scientific, Illinois, USA). Confirmatory restriction enzyme digestion was performed with *Not*I-HF (New England Biolabs, Massachusetts, USA) for pSinCCHF-52M while pSinCCHF-31S and pSinCCHF-52S were confirmed with *Not*I and *Cla*I (Promega, Wisconsin, USA). Purified plasmid DNA was stored at -20°C.

3.3.3 Cell maintenance

Baby hamster kidney cells (BHK-21) were grown in Dulbecco's Modified Eagle Medium (DMEM) (Lonza, Verviers, Belgium) supplemented with 10% gamma irradiated fetal bovine serum (FBS) (Gibco, Paisley, UK), 1% L-glutamine (Lonza, Verviers, Belgium), 1% penicillin-streptomycin (Lonza, Verviers, Belgium) and 1% non-essential amino acids (Lonza, Verviers, Belgium) in T-25 cm² cell culture flasks (NEST, Jiangsu, China). Cells were passaged a minimum of three times before they were used in transfection experiments.

3.3.4 Cell preparation and electroporation

Approximately 48 hours before electroporation, low passage BHK-21 cells were seeded in T-75cm² flasks (NEST, Jiangsu, China) such that they were 80-90% confluent prior transfection. On the day of performing the electroporation experiment, growth media was decanted and cells rinsed with PBS (Lonza, Verviers, Belgium). A 1 ml aliquot of 2.5% trypsin (Gibco, Paisley, UK) was added to BHK-21 cells and incubated for three minutes at 37°C. Subsequently, the detached cells were resuspended in 3 ml of DMEM recovery media enriched with 10% gamma irradiated FBS, 1% L-glutamine, 1% sodium pyruvate (Lonza, Verviers, Belgium) without antibiotics. A 10 µl aliquot of BHK-21 cells in DMEM recovery media was mixed with 10 µl of 0.4% trypan blue and a cell count was performed with the Countess™ II FL Automated cell counter (Invitrogen, California, USA). Cells at a density of 5.5×10^6 cells/ml were transferred to 1.5 ml tubes and spun for 5 minutes. All centrifugation steps were carried out at $400 \times g$ at 4°C. The supernatant was discarded, re-suspended in 200 µl of PBS and centrifuged for 5 minutes. The supernatant was aspirated and discarded while cells were re-suspended in 100 µl of Resuspension Buffer R. A 15 µg aliquot of plasmid DNA re-suspended in ≤ 10 µl of nuclease-free water was added to the cell suspension and mixed briefly. Six well cell culture plates (NEST, Jiangsu, China) were prepared by adding 2 ml of DMEM recovery media. Cells were electroporated using the Neon® Transfection System MPK5000 (Invitrogen, California, USA) at a pulsing voltage of 1500V, pulse width 20 ms and pulse number one (optimized in chapter 2). A construct expressing the green fluorescence protein (GFP) was used as a negative control. Transfected cells were incubated for 30 minutes at room temperature in electroporation buffer. Afterwards cells were seeded at a rate of 2.0×10^6 cells/well in six-well culture plates with recovery media and incubated at 37°C in a 5% CO₂ enriched atmosphere.

3.3.5 Cell harvesting

Cells were harvested at 4 hrs, 8 hrs, 12 hrs, 24 hrs and 48 hrs post electroporation. At each time point, culture media was completely removed. Immediately 700 µl of RNeasy Protect® cell reagent (Qiagen, Hilden, Germany) was added to the attached cells. To facilitate cell detachment, the RNeasy Protect® cell reagent was pipetted up and down gently several times. Cells were thereafter transferred to RNase free 1.5 ml tubes and stored at -80°C until RNA extraction.

3.3.6 RNA extraction from transfected cells

RNA extraction was carried out with the RNeasy® Plus Mini Kit (Qiagen, Hilden, Germany) according to the manufacturer's instructions. Cells were retrieved from the freezer and the 1.5ml tubes were spun at $500 \times g$ for 5 minutes. After decanting the supernatant, cells were lysed in Buffer RLT supplemented with 10 µl/ml of β -mercaptoethanol (Sigma-Aldrich, Missouri, USA). The lysate was transferred to a gDNA Eliminator spin column and centrifuged at $10\,000 \times g$ for 30 seconds. To the flow through, 600 µl of 70% ethanol was added followed by gentle mixing before being transferred to an RNeasy spin column. Following centrifugation at $10\,000 \times g$ the RNeasy spin columns were washed twice with 500 µl of Buffer RPE by centrifuging at $10\,000 \times g$ for 15 seconds. Further

centrifugation at 10 000 x g for 60 seconds was carried out to ensure ethanol was completely removed from the spin columns. RNA was eluted in 45 µl of RNase-free water (supplied with the kit).

Plasmid DNA was eliminated from RNA samples using the RQ1 RNase-free DNase kit (Promega, Wisconsin, USA). CCHF-52S and CCHF-52M PCR amplicons were used as a positive control. The reactions consisted of 1 µl total RNA sample/positive control, 1 µl RQ1 RNase-Free DNase 10x reaction buffer, 1 µl RQ1 RNase DNase enzyme (1 u/µl) and 7 µl of nuclease-free water. After mixing by gently pipetting up and down, the mixture was incubated at 37°C for 30 minutes. Thereafter, the reactions were stopped by adding 1 µl of RQ1 DNase Stop solution. The DNase enzyme was inactivated by heating the reaction mixture at 65°C for 10 minutes.

To confirm that all the plasmid DNA was eliminated, 1 µl of the DNase treated RNA samples were used as a template in a PCR. The reaction mixture comprised of 10 µl 5X Green Go Taq® flexi buffer, 8µl MgCl₂ (25mM), 1 µl dNTP (10 mM), 1 µl forward primers (CCHF-TGPF and CCHF-TNPF) (20 pmol/µl), 1 µl reverse primers (CCHF-TGPR and CCHF-TNPR) (20 pmol/µl), 0.25 µl Go Taq® G2 Hot Start polymerase enzyme (5 u/µl) (Promega, Wisconsin, USA), 1 µl DNase treated RNA samples and 27.75 µl nuclease-free water. The PCR was carried out with the following cycling conditions: 2 minutes at 95°C, followed by 35 cycles of 30 seconds at 95°C, 30 seconds at 50°C, 45 seconds at 72°C, final extension of 2 minutes at 72°C and cooling at 4°C.

3.3.7 Development of two-step quantitative RT-PCR

3.3.7.1 Preparation of DNA controls for development of RT-qPCR

cDNA was prepared from SPU187/90 viral RNA (available in the laboratory) and was used as a template in a PCR with primers CCHF-TNPF and CCHF-TNPR or CCHF-TGPF and CCHF-TGPR to generate CCHF NP and GP amplicons using the Phusion® High fidelity (HF) DNA polymerase enzyme (New England Biolabs, Massachusetts, USA). DNA was purified using the Wizard® SV Gel and PCR Clean-Up System (Promega, Wisconsin, USA) as per the manufacturer's instructions. The DNA concentration was measured using the Qubit® dsDNA BR Assay Kit (Invitrogen, California, USA) according to the manufacturer's instructions. The Qubit® working solution was prepared by mixing 5 µl of Qubit® dsDNA BR Reagent with 995 µl Qubit® dsDNA BR Buffer. Qubit® Standards were prepared by adding 10 µl of the respective Qubit® Standards to 190 µl Qubit® working solution followed by vortexing to homogenize the mixture. Sample preparation was achieved by adding 2 µl of PCR amplicons to 198 µl of the Qubit® working solution. Samples and standards were incubated for 2 minutes at room temperature according to the manufacturer's instructions. Thereafter, the Qubit® Fluorometer (Invitrogen, California, USA) was calibrated and subsequently, samples were analyzed. Sample concentrations given by the Qubit® Fluorometer corresponds to the diluted sample. The undiluted sample concentrations were calculated using the following equation;

$$\text{Sample concentration} = \frac{\text{QV} \times 200}{X}$$

QV = the read-out value given by the Qubit® Fluorometer

X = volume of the sample added to the assay tube

The sample concentrations were converted to copy numbers using a dsDNA copy number calculator (<https://cels.uri.edu/gsc/cndna.html>). Subsequently, 10-fold serial dilutions of PCR amplicons were made with nuclease-free water. The dilutions were frozen at -20°C until use.

Using ten-fold dilutions of the DNA standards, standard curves were generated for the nucleoprotein and glycoprotein precursor genes. Five diluted standards whose concentrations ranged from 1.77×10^1 to 1.77×10^5 copies for the gene encoding the CCHF glycoprotein precursor and 1.28×10^3 to 1.28×10^7 copies for the gene encoding the CCHF nucleoprotein were used to create standard curves. Amplification efficiencies from the standard curves were reviewed and saved on the LightCycler. By making use of the computer program of the LightCycler® 2.0 Instrument (Roche Diagnostics GmbH, Mannheim, Germany), the standard curves were prepared by plotting cycle threshold values against the proportionate logarithmic DNA concentrations. The computer program also calculated PCR efficiencies from the resultant standard curves with acceptable efficiencies ranging from 1.8 to 2.

3.3.7.2 cDNA synthesis

A 2.5 µl aliquot of each of the DNase treated RNA samples were used to prepare cDNA in a 20 µl reaction using SuperScript™ III reverse transcriptase (RT) enzyme (Invitrogen, California, USA). The forward primers CCHF-TGPF (glycoprotein precursor) (2 pmol/µl) or CCHF-TNPF (nucleoprotein) (2 pmol/µl) were used. The reaction mixture consisted of 1 µl primer, 1 µl dNTP's (10 mM), 2.5 µl RNA and 8.5 µl nuclease-free water. The reaction mixture was heated at 65°C for 5 minutes and incubated at 4°C for two minutes. Midway in the incubation period, the thermocycler was paused; 4 µl 5x first strand buffer, 1 µl DTT (0.1M), 0.5 µl RNaseOUT™ Recombinant Ribonuclease Inhibitor (40 U/µL), 0.5 µl nuclease-free water and 1 µl Superscript™ III RT enzyme (200 U/µL) were added. The reaction mixture was further heated at 50°C for 60 minutes and after that at 85°C for 5 minutes. The products were stored at -20°C.

3.3.7.3 Quantitative real-time PCR assays

Total RNA was quantified using the LightCycler® TaqMan® Master kit (Roche Diagnostics GmbH, Mannheim, Germany) according to the manufacturer's instructions. Quantitative real-time in a two-step RT-PCR was performed using the LightCycler® 2.0 Instrument (Roche). Optimization was performed to determine the PCR cycling conditions, the concentrations of primers and probes for the real time PCR assays. The master mix was prepared by adding 10 µl of the LightCycler® FastStart Enzyme to the LightCycler® FastStart TaqMan® Reaction Mix containing reaction buffer, MgCl₂ and dNTP mix, all supplied with the kit. The reactions consisted of 4 µl master mix, 2 µl (10 pmol/µl)

each of CCHF-TNPF and CCHF-TNPR, 1 µl (2 pmol/µl) CCHF-NP31_52 (hydrolysis probe), 1 µl cDNA/diluted standards and 10 µl nuclease-free water. Thermocycling conditions used comprised of a pre-incubation step at 95°C, followed by 35 cycles of denaturation at 95°C for 10 seconds, annealing and extension at 55°C for 60 seconds and a cooling step at 40°C for 30 seconds. Fluorescence signal was gathered at the end of the combined annealing and extension step of each cycle. A temperature transition rate of 20°C/sec was utilized. Primers and probes listed in Table 3.1 above were used in qPCR. Samples were analysed in duplicate and each run included one of the DNA standards as a sample. The concentrations of samples were determined using standard curves generated above.

3.3.11 Induction of apoptosis

BHK-21 cells were maintained and electroporated as described in sections 3.3.3 and 3.3.4 respectively. Apoptosis induction by vaccine constructs was analyzed using the Cell Death Detection ELISA Plus kit (Roche Diagnostics GmbH, Mannheim, Germany) as per manufacturer's instructions. Briefly, electroporated BHK-21 cells were seeded into 96 well plates at 10⁴ cells/well and incubated at 37°C, 5% CO₂. Unelectroporated BHK-21 cells were seeded at the same seeding rate and served as a negative control while BHK-21 cells electroporated in the absence of plasmid DNA were included to determine the effect of the electroporation technique on apoptosis. Cells were harvested at 24 hours, 36 hours, 48 hours, 60 hours and 72 hours post electroporation. At the end of the respective incubation period, the 96 well plate was centrifuged at 200 x g for 10 minutes. The supernatant was discarded and the cell sediment was re-suspended in 200 µl lysis buffer. Following an incubation step of 30 minutes at room temperature, the lysate was centrifuged at 200 x g for a period of 10 minutes. A 20 µl aliquot of the supernatant was transferred into microplates coated with streptavidin. Samples were analyzed in duplicate. Into each microplate well 80 µl of the immuno-reagent was added. The immune reagent was prepared by mixing 0.9 volumes of the supplied incubation buffer, 0.05 volumes of biotin-labeled mouse anti-histone (anti-histone-biotin) and 0.05 volumes of peroxidase conjugated mouse anti-DNA (anti-DNA-POD). After covering the well plate with an adhesive foil, the well plate was incubated on a 300 rpm shaking plate for 2 hours at room temperature. Thereafter, the solution was removed and incubated wells were rinsed three times with 300 µl incubation buffer. Subsequently, the incubation buffer was replaced with 100 µl 2,2'-azinobis-(3-ethylbenzothiazoline-6-sulfonate) (ABTS) solution. Succeeding incubation with shaking at 250 rpm, the reactions were stopped by adding 100 µl ABTS stop solution and absorbance measured at 405 nm.

Average absorbance values were calculated and the background value (Incubation buffer + ABTS Stop solution) was subtracted from each of the averaged absorbance value. The specific enrichment of mono and oligonucleosomes released into the cytoplasm following cell death was calculated with the formula below.

$$\text{Enrichment factor} = \frac{\text{Absorbance of sample}}{\text{Absorbance of negative control}}$$

3.3.12 Statistical analysis

Pairwise comparisons between groups were assessed with the Kruskal-Wallis test. Statistical significance was set at $p < 0.05$. Analyses were performed with the SAS software Version 9.3.

3.4 Results

3.4.1 DNase treatment and plasmid DNA contamination check (Post DNase treatment)

To confirm elimination of plasmid DNA from RNA samples after digestion with the RQ1 RNase-free DNase kit (Promega, Wisconsin, USA), a PCR was set up and the DNase treated RNA samples were used as a template. Absence of bands specific to the CCHF NP and GP as shown in Figure 3.1 below demonstrated that the RNA samples were free of plasmid DNA contamination. A positive control was included in each PCR run.

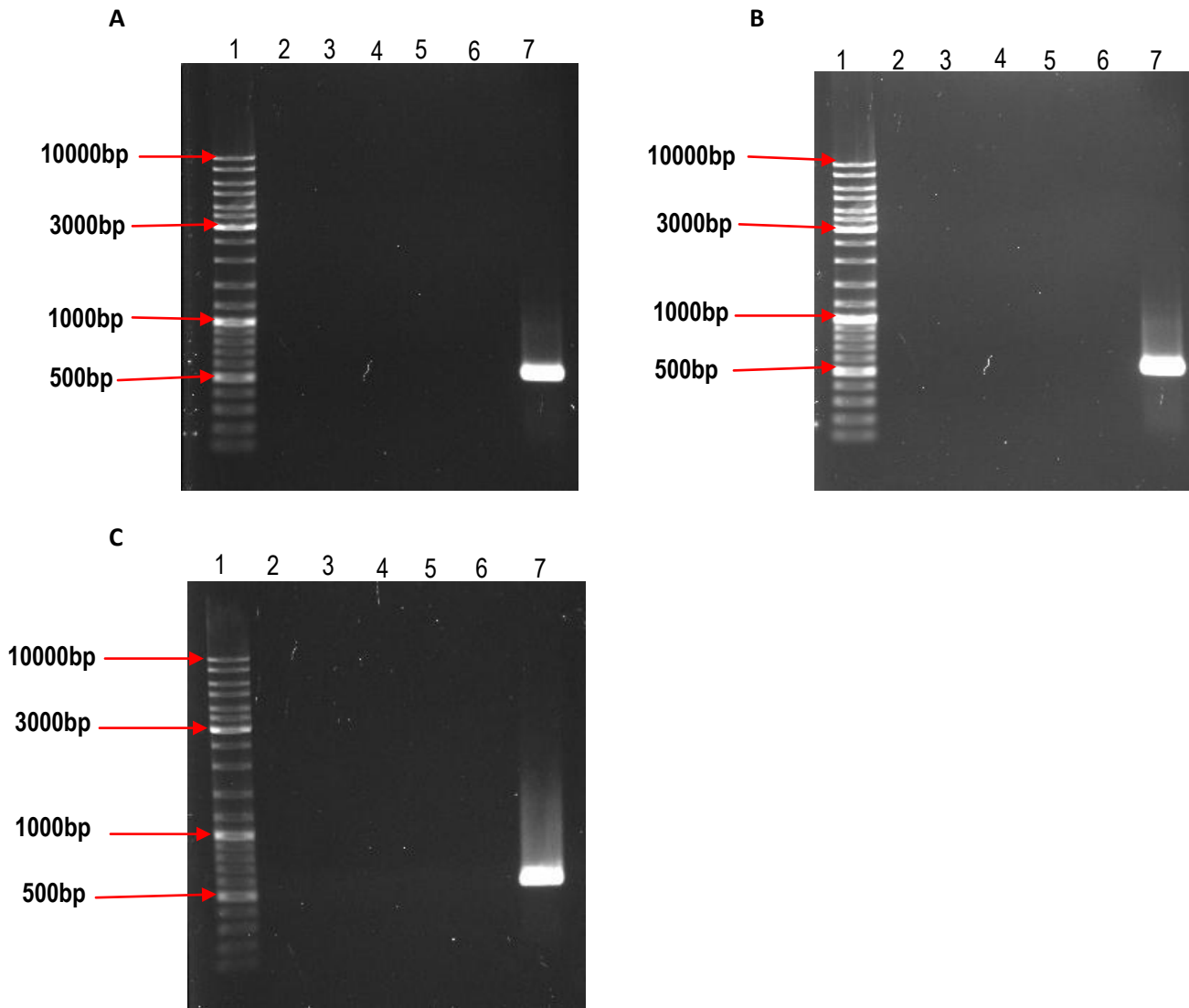


Figure 3. 1: Post DNase treatment of RNA samples. Plasmid DNA contamination check of extracted RNA from transfected cells. CCHF-31S RNA (**A**), CCHF-52S RNA (**B**) and CCHF-52M RNA (**C**) Lane 1: Molecular marker SM 1173. Lane 2: RNA at 4 hours. Lane 3: RNA at 8 hours. Lane 4: RNA at 12 hours. Lane 5: RNA at 24 hours. Lane 6: RNA at 48 hours. Lane 7: Positive control

3.4.2 Standard curve for two-step RT-qPCR

CCHF-52S and CCHF-52M PCR amplicons were used to generate standard curves for the amplification of nucleoprotein and glycoprotein precursor genes respectively. The concentration of CCHF-52S and CCHF-52M amplicons obtained on the Qubit® Fluorometer were 200 µg/ml and 260 µg/ml respectively. These DNA concentrations were converted to copy numbers using a dsDNA copy number calculator yielding 1.28×10^{11} for CCHF-52S and 4.77×10^{10} for CCHF-52M. Five ten-fold serial dilutions of each of the CCHF-52S and CCHF-52M standards were analyzed with the LightCycler® 2.0 Instrument (Roche) to generate a standard curve. Single set of data was used to generate the standard curves and the LightCycler® 2.0 Instrument calculated the efficiency and the error. The standard curves obtained are shown in Figure 3.2 for CCHF-NP and Figure 3.3 for CCHF-GP.

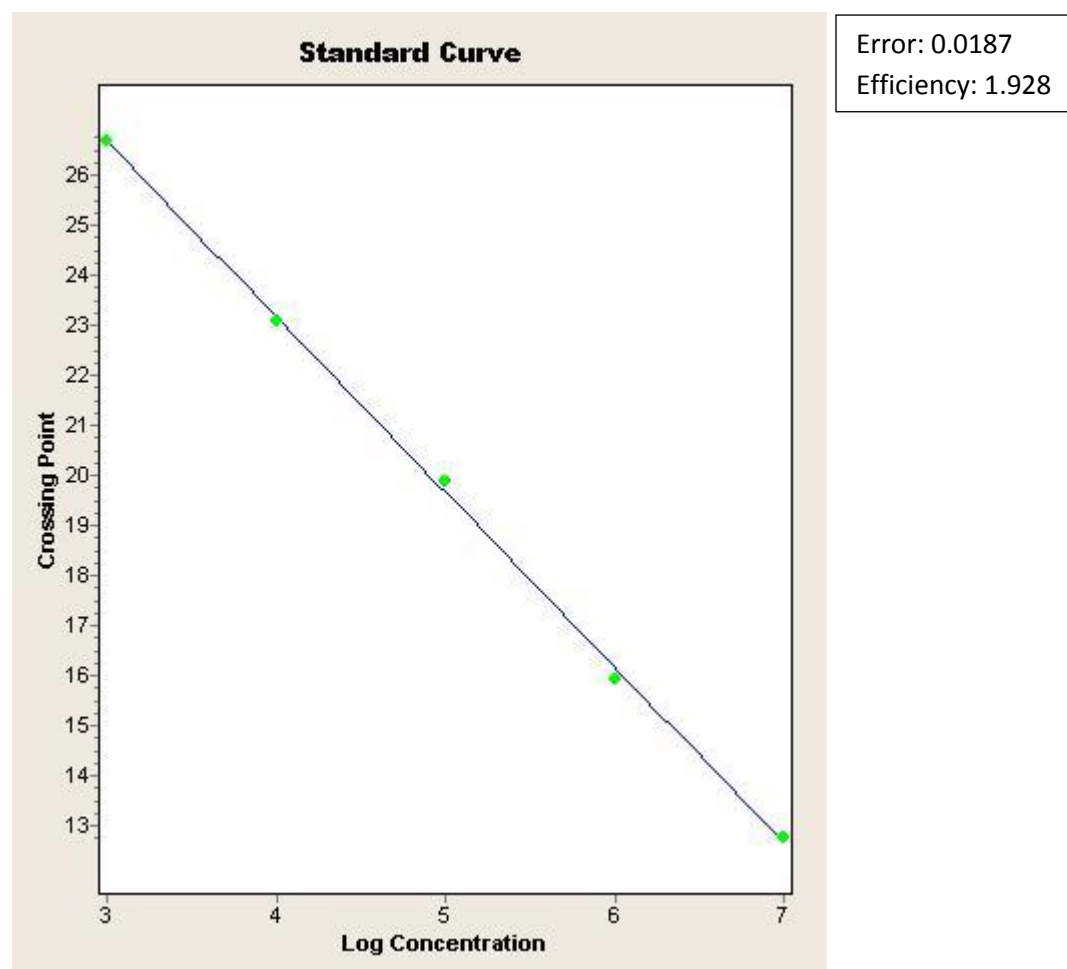


Figure 3. 2: Standard curve for quantifying CCHF-31S and CCHF-52S genes generated using log concentration of CCHF-52S standards plotted against the crossing points

As was expected higher CCHF-52S DNA concentrations resulted in lower cycle threshold values and lower CCHF-52S DNA concentrations were accompanied with higher cycle threshold values. The obtained amplification efficiency of 1.928 is close to 2 which is the ideal efficiency since the amplified sequence is expected to double in each cycle.

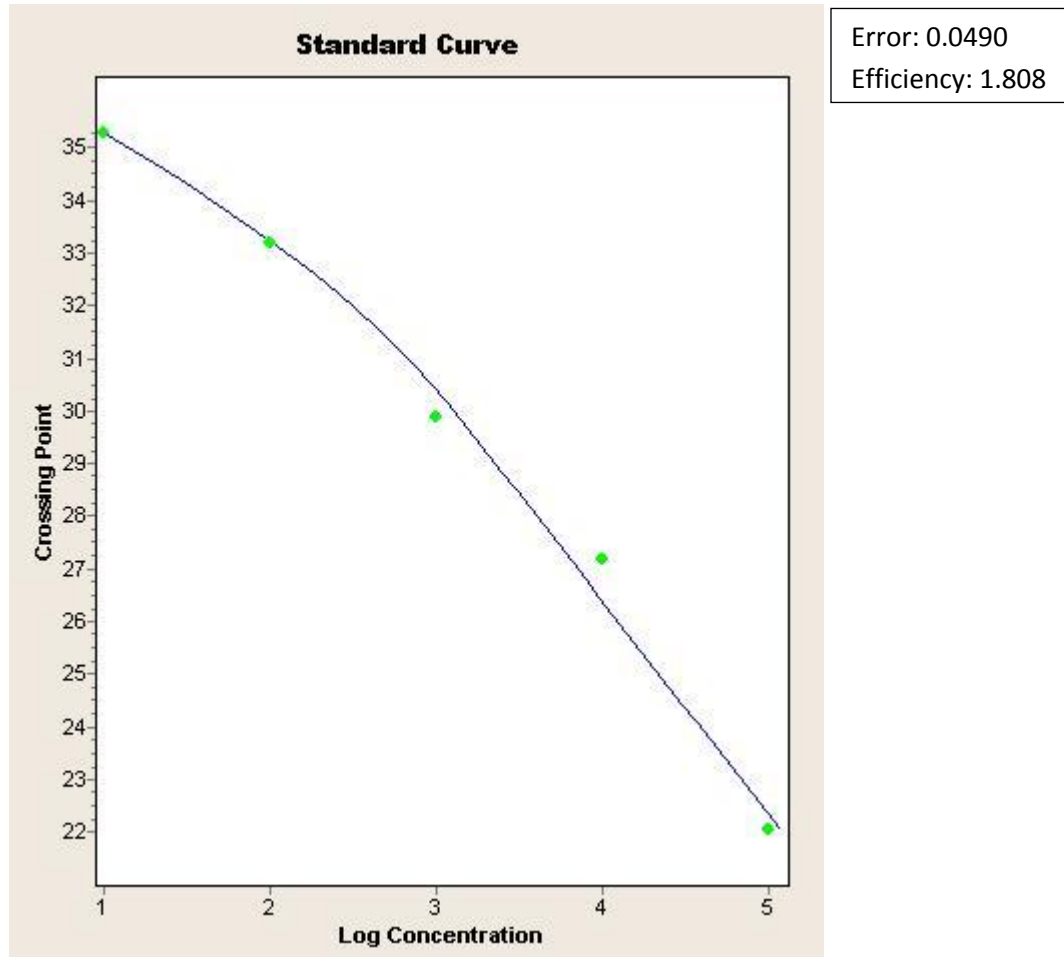


Figure 3. 3: Standard curve for quantifying CCHF-52M genes generated using log concentration of CCHF-52M standards plotted against the crossing points.

Higher CCHF-52M plasmid DNA concentrations resulted in lower cycle threshold values and lower CCHF-52M DNA concentrations yielded higher cycle threshold values. The obtained geometric efficiency of 1.808 was within the 1.8 to 2 recommended range.

3.4.3 Vaccine constructs self-replication

The kinetics of the Sindbis replicon activity was performed in BHK-21 cells. Electroporated cells were harvested at various time points. Recombinant protein expression was confirmed by performing IFA. The percentage transfection efficiencies were not determined. Total CCHFV RNA was converted to cDNA and quantified by qPCR. The resultant

amplification curves are shown in Figure 3.4. By making use of the LightCycler® software, the generated standard curves were used to determine, the CCHFV RNA copy number of samples collected at various time points. The calculated average CCHFV RNA copy numbers are shown in Tables 3.2 and 3.3. Using the GraphPad software, the total CCHFV RNA copy numbers were plotted against hours after electroporation yielding Figures 3.5 and 3.6. All vaccine constructs investigated were transcriptionally active as evidenced by total viral RNA generated. CCHFV RNA was detected 4 hours after transfection and it increased sharply by 24 hours. Total viral RNA concentration by vaccine constructs pSinCCHF-52S and pSinCCHF-52M peaked at 24 hours and by the 48-hour mark the concentration was decreasing. This is in contrast to pSinCCHF-31S whose RNA concentration kept an upward trend throughout the whole sampling period. Vaccine construct pSinCCHF-52S exhibited slower replication kinetics compared to pSinCCHF-31S. The RNA concentration for all the vaccine constructs increased by more than 15 fold between 4 and 8 hours. The highest RNA concentrations were attained by pSinCCHF-31S while pSinCCHF-52M demonstrated the least replicative capacity.

Table 3. 2: RT-qPCR viral load results following transfection of pSinCCHF-52S and pSinCCHF-31S in BHK-21 cells. Samples were analyzed in duplicate.

pSinCCHF-52S				pSinCCHF-31S			
Time after electroporation	Cq value	Estimated RNA copy number	Average RNA copy number	Time after electroporation	Cq value	RNA copy number	Average RNA copy number
4 hrs 4 hrs	28.52 28.68	*NE	*NE	4 hrs 4 hrs	27.48 27.24	*NE	*NE
8 hrs 8 hrs	24.31 24.21	4.09 x 10 ³ 4.31 x 10 ³	4.23 x 10 ³	8 hrs 8 hrs	22.05 21.99	2.41 x 10 ⁴ 2.52 x 10 ⁴	2.46 x 10 ⁴
12 hrs 12 hrs	22.86 23.01	1.06 x 10 ⁴ 9.6 x 10 ³	9.65 x 10 ³	12 hrs 12 hrs	21.66 21.67	3.12 x 10 ⁴ 3.10 x 10 ⁴	3.11 x 10 ⁴
24 hrs 24 hrs	22.01 21.96	1.85 x 10 ⁴ 1.91 x 10 ⁴	1.88 x 10 ⁴	24 hrs 24 hrs	20.69 20.53	5.88 x 10 ⁴ 6.57 x 10 ⁴	6.22 x 10 ⁴
48 hrs 48 hrs	22.98 23.16	9.78 x 10 ³ 8.7 x 10 ³	9.24 x 10 ³	48 hrs 48 hrs	20.44 20.31	6.93 x 10 ⁴ 7.58 x 10 ⁴	7.25 x 10 ⁴

*NE – CCHFV RNA copy numbers not estimated

Table 3. 3: RT-qPCR viral load results following transfection of pSinCCHF-52M in BHK-21 cells. Samples were analyzed in duplicate

pSinCCHF-52M			
Time after electroporation	Cq value	RNA copy number	Average RNA copy number
4 hrs 4 hrs	37.79 37.50	*NE	*NE
8 hrs 8 hrs	35.44 35.96	*NE	*NE
12 hrs 12 hrs	35.12 35.01	1.58 x 10 ¹ 1.82 x 10 ¹	1.7 x 10 ¹
24 hrs 24 hrs	33.78 33.75	7.38 x 10 ¹ 7.45 x 10 ¹	7.41 x 10 ¹
48 hrs 48 hrs	33.53 33.48	9.62 x 10 ¹ 9.72 x 10 ¹	9.67 x 10 ¹

*NE – CCHFV RNA copy numbers not estimated

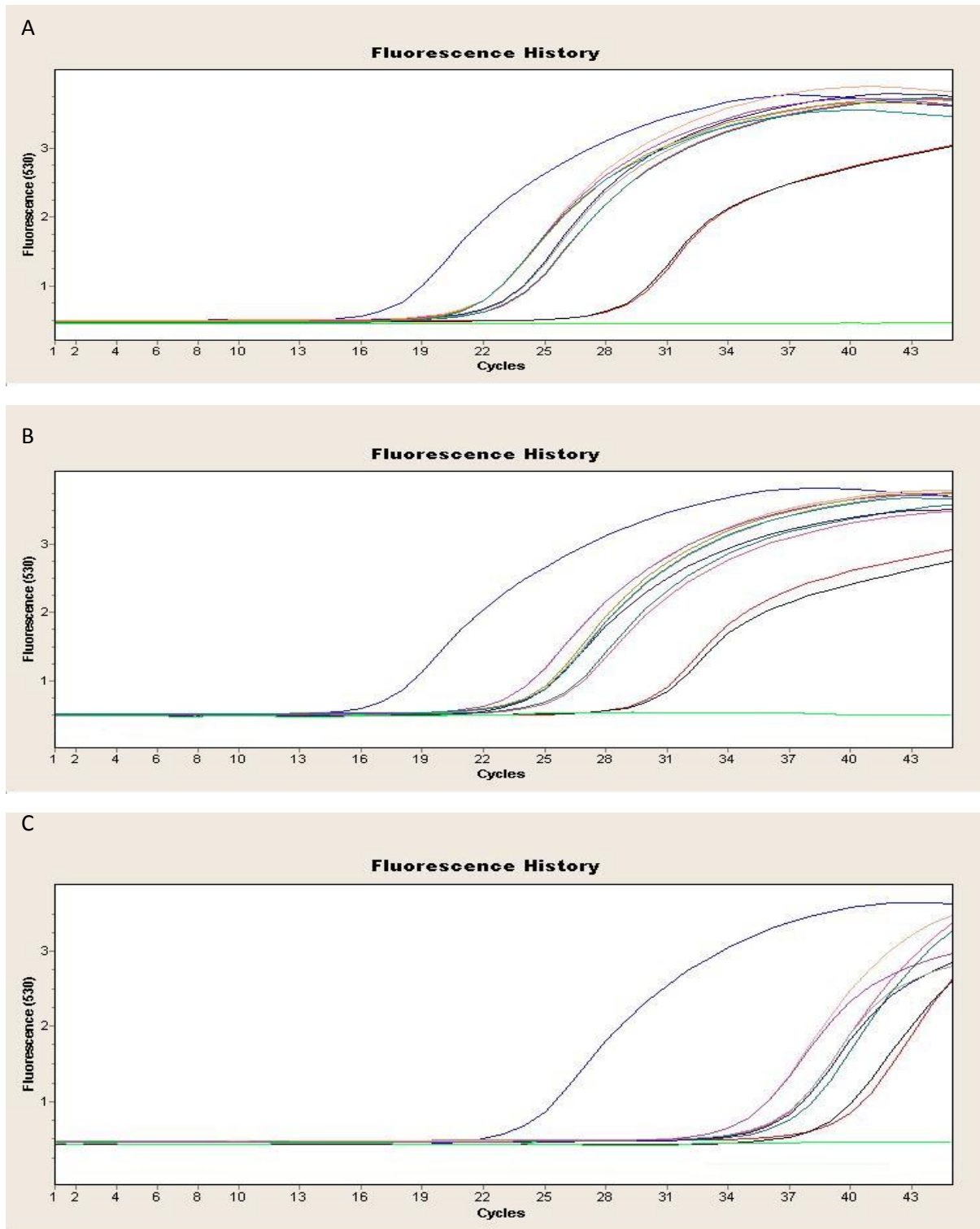


Figure 3. 4: Amplification curves for CCHFV RNA. **(A)** CCHF-31S **(B)**, CCHF-52S **(C)** and CCHF-52M RNA. CCHFV RNA collected at various time points was converted to cDNA using SuperScript™ III reverse transcriptase enzyme and amplified using the qPCR.

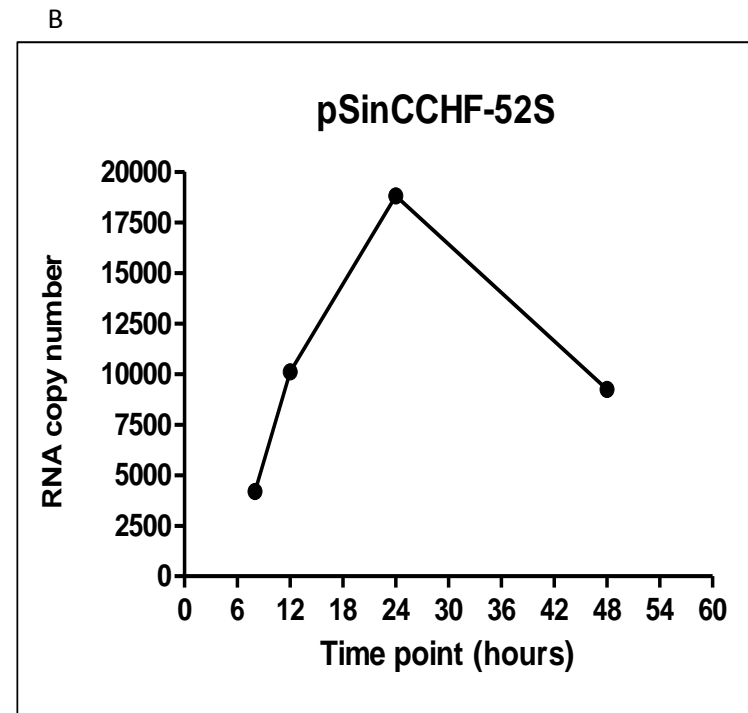
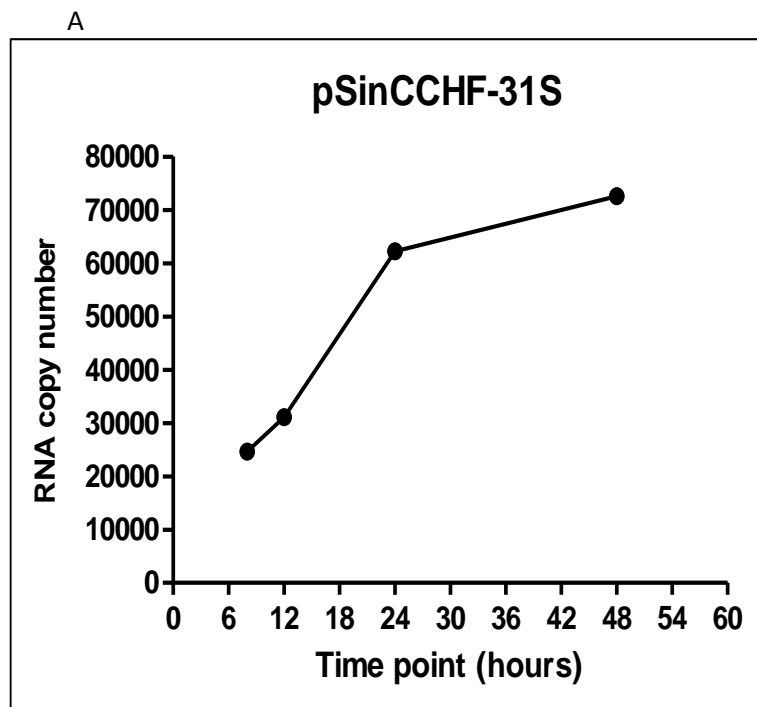


Figure 3. 5: Replication kinetics of CCHF NP total RNA expression in BHK-21 cells electroporated with pSinCCHF-31S and pSinCCHF-52S over 48 hours. **(A)** pSinCCHF-31S **(B)** and pSinCCHF-52S

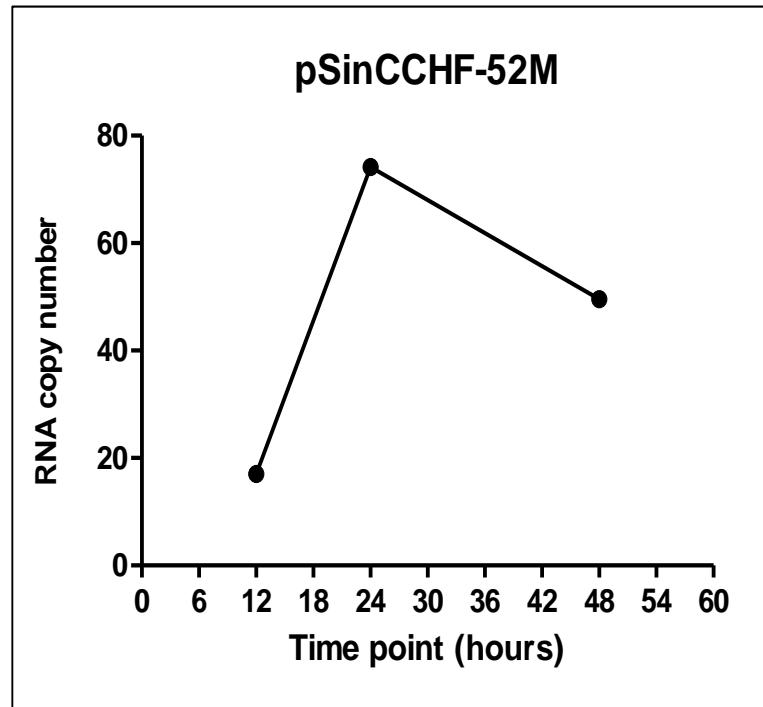


Figure 3. 6: Replication kinetics of CCHF GP total RNA expression in BHK-21 cells electroporated with pSinCCHF-52M over 48 hours.

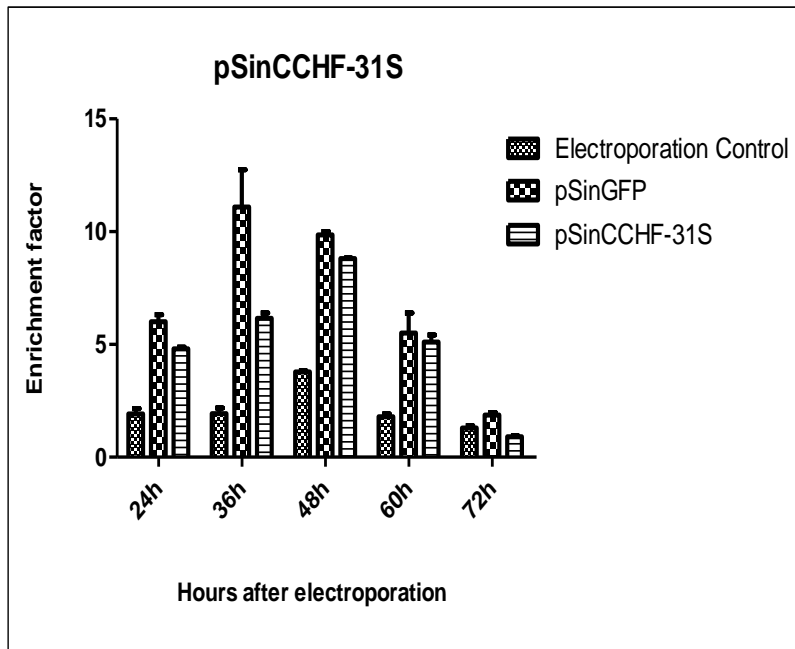
3.4.4 Apoptosis induction

The degree of apoptosis induced by vaccine constructs after electroporation was quantitated by ELISA. Cells were harvested 12 hourly starting at 24 hours post electroporation. The amount of mono and oligonucleosomes released into the cytoplasm after induction of apoptosis was analyzed as an index of apoptosis. BHK-21 cells electroporated in the absence of DNA were taken as the electroporation control. The enrichment of mono and oligonucleosomes in the cytoplasm was calculated as the ratio of electroporated cells to the ratio of unelectroporated cells. The calculated enrichment factors after electroporation of BHK-21 cells are shown in Table 3.4. An enrichment factor above one thus demonstrates a higher amount of cell death in electroporated cells compared to the unelectroporated cells. The absorbance signal from the positive control supplied with the kit was above 0.6 after subtracting background absorbance as recommended by the kit's manufacturer. The amount of cell death in electroporated BHK-21 cells followed a similar pattern with the constructs expressing CCHFV GP and NP peaking after 48 hours post electroporation declining to similar levels with the electroporation control by 72 hours. The construct expressing the GFP, however, peaked 12 hours earlier, recording the highest nucleosome release into the cytoplasm 36 hours after electroporation declining to comparable levels to the electroporation control after 72 hours. Cells electroporated with a construct expressing the CCHFV GP gene (pSinCCHF-52M) demonstrated a higher amount of cell death compared to those electroporated with constructs expressing the CCHFV NP gene. There was no statistical difference between nucleosome release by the electroporation control and nucleosome release by the constructs at all time points ($p>0.05$). Figure 3.7 and 3.8 shows the kinetics of cell death after electroporation. Data for pSinGFP and electroporation control was plotted against data for each of the prepared vaccine constructs (pSinCCHF-31S, pSinCCHF-52S and pSinCCHF-52M).

Table 3. 4: Calculated enrichment factors after electroporation of BHK-21 cells

Vaccine Construct	Enrichment factor				
	24 hours	36 hours	48 hours	60 hours	72 hours
Electroporation control	2.16	1.68	3.74	1.92	1.40
	1.68	2.18	3.83	1.67	1.18
pSinGFP	6.32	9.44	9.70	6.39	1.98
	5.68	12.74	10.0	4.63	1.75
pSinCCHF-31S	4.88	5.93	8.78	5.42	0.94
	4.72	6.39	8.83	4.80	0.87
pSinCCHF-52S	4.16	9.26	11.17	6.17	1.06
	4.16	8.81	10.17	4.77	1.15
pSinCCHF-52M	10.48	10.91	16.09	4.11	1.99
	11.6	15.09	17.17	3.50	1.92

A



B

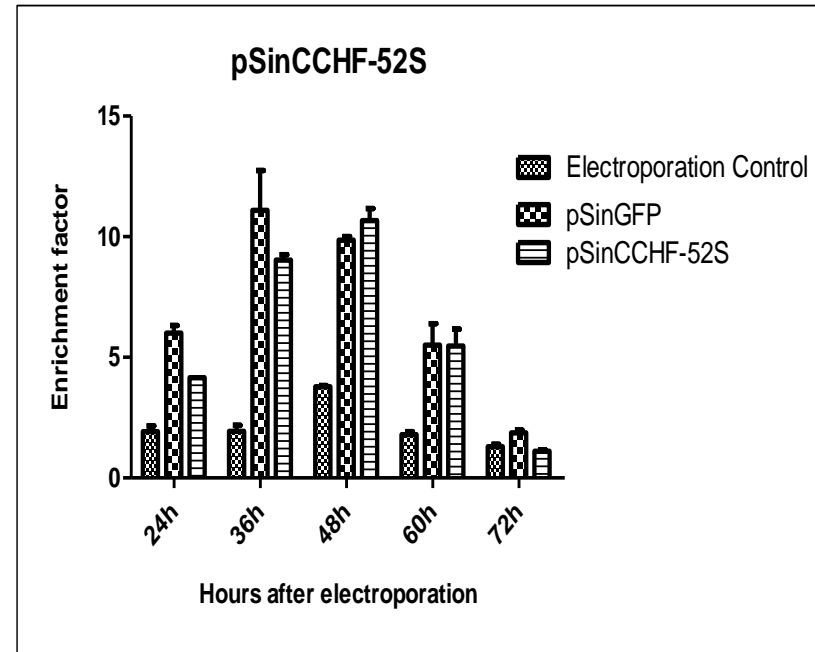


Figure 3. 7: Vaccine constructs apoptosis induction in BHK-21 cells transfected with pSinCCHF-31S and pSinCCHF-52S. To assess release of mono and oligonucleosomes in cells undergoing apoptosis following electroporation with (A) pSinCCHF-31S, (B) pSinCCHF-52S as well as control plasmid pSinGFP and electroporation in the absence of DNA (electroporation control) was analyzed using the ELISA technique. All values represent an average of two readings.

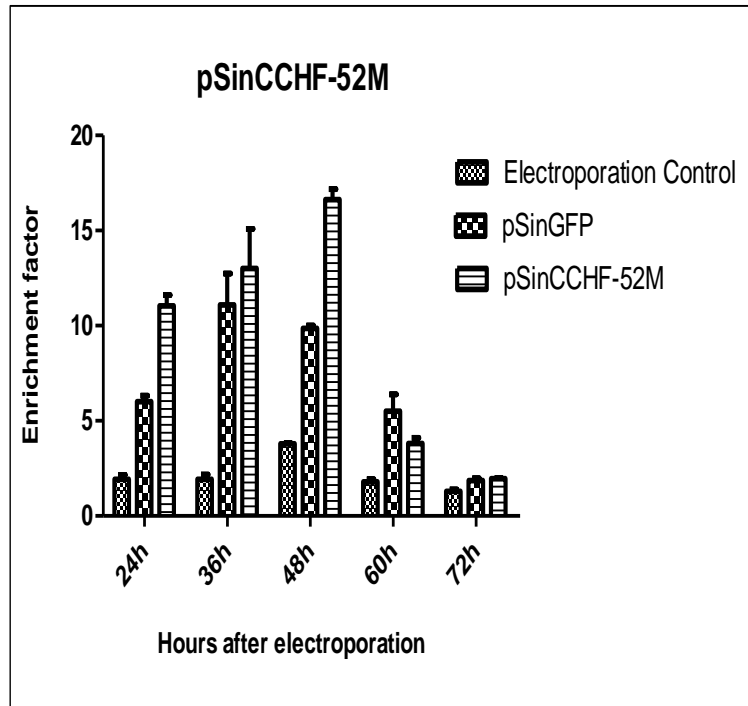


Figure 3. 8: Vaccine constructs apoptosis induction in BHK-21 cells transfected with pSinCCHF-52M. To assess the release of mono and oligonucleosomes in cells undergoing apoptosis following electroporation with pSinCCHF-52M as well as control plasmid pSinGFP and electroporation in the absence of DNA (electroporation control) was analyzed using the ELISA technique. All values represent an average of two readings.

3.5 Discussion

Heterologous gene expression in mammalian cells requires expression vectors which facilitate transcription and translation of foreign genes cloned into them. One class of such expression vectors that are increasingly being investigated belong to the Alphaviruses. Alphaviruses replicate efficiently in a wide range of host cells including mammalian cells (Frolov et al. 1996). Prepared vaccine constructs based on the Sindbis virus genome were investigated for their capability to transcribe CCHFV RNA. The aim of this study was to demonstrate that the prepared vaccine constructs were capable of undergoing self-replication and inducing apoptosis. Self-replication is vital in underscoring the prepared vaccine constructs as efficient vectors to express the CCHFV genes both for recombinant protein production purposes and in vaccine studies. Using qPCR, gene expression and copy number can be quantified. This entails amplifying the gene with an unknown copy number and the gene with known copy number. A standard curve generated from amplifying the gene with a known copy number is used to determine the concentration of test samples. Since quantitation and amplification occur simultaneously, the original copy number in test samples is deduced from the PCR cycle number at which fluorescence generated appreciably exceeds background level. Self-replication rates of prepared Sindbis replicon vaccine constructs were analyzed by measuring CCHFV specific RNA using the qPCR technique. A two step PCR was performed so we thought it necessary to generate DNA standard curves for quantification of RNA rather than generating RNA transcripts and setting up RNA standard curves. To assist in gene quantification, primers amplifying segments of the GP and NP genes for two South African CCHFV strains were designed. Hydrolysis probes specific for the targeted GP and NP genes were also designed. Glycerol stocks of prepared vaccine constructs stored at -80°C were retrieved, grown and purified using a commercial kit. Vaccine construct DNA concentrations were measured and constructs were identified using restriction enzyme digestion.

Selection of a suitable cell line is vital for the success of gene expression. Numerous mammalian cell lines are available and these differ in their ability to take up and express foreign genes (Zhao et al. 2016, Kim et al. 2008). BHK-21 cells were used because of their availability, they had yielded relatively high transfection efficiencies with the vaccine constructs and had relatively higher viability rates compared to HEK-293 cells in this study. BHK-21 cells were maintained in T25 cell culture flasks in preparation for electroporation. After electroporation with replicon DNA, samples were harvested periodically and stabilized using an RNeasy Protect reagent before storage at -80°C. Extraction of CCHFV RNA from cells was performed using a commercial kit. To ensure total elimination of replicon DNA from extracted RNA samples, an equal volume of the samples were DNase treated. Afterwards, a portion of the DNase treated samples was used as template in a PCR. After confirming the absence of replicon DNA from RNA samples, cDNA synthesis using gene-specific primers ensued. Amplicons generated were used in the preparation of standard curves which were used to estimate the amount of viral RNA in samples. Standard curves were evaluated for

amplification efficiency and error. Optimization of the qPCR assays was achieved by performing the annealing and the extension steps at the same temperature of 55°C.

An online calculator for determining the number of copies of a template developed by Andrew Staroscik was used to estimate CCHFV RNA. The tool has previously been used by other researchers as there are published articles which reference the online calculator (Nga et al. 2010, Abdelmotelb et al. 2013, Laakso et al. 2013). Hence we selected to use the calculator to estimate the CCHFV RNA copy numbers. The tool is based on the formula: number of copies = (amount of amplicon (ng) * 6.022×10^{23}) / (length * 1×10^9 * 650). CCHFV total RNA was detected starting 8 hours after electroporation for pSinCCHF-31S and pSinCCHF-52S, and 12 hours for pSinCCHF-52M. Total RNA at 4 hours for pSinCCHF-31S and pSinCCHF-52S and total RNA for pSinCCHF-52M at 4 and 8 hours could not be estimated as the values did not fall within the standard curve data points. Construct pSinCCHF-52M however achieved the lowest RNA concentration throughout the 48 hour sampling period. The kinetics however of RNA expression for the constructs followed a similar pattern, a sharp increase during the early hour's post-electroporation and reaching the peak at 24 hours. Higher RNA concentrations were observed with constructs expressing the nucleoprotein gene compared to the constructs expressing the GP gene. We therefore concluded that constructs expressing the nucleoprotein gene had superior self-replication rates resulting in higher viral loads compared to the construct expressing the glycoprotein precursor.

Eukaryotic DNA is organized into repeating units called nucleosomes. The central part of nucleosomes is made up of approximately 147 bp of DNA wrapping eight histone proteins (McGinty and Tan 2015). These histone proteins are designated H2A, H2b, H3 and H4 existing in duplicate. H1 histone also known as linker histone binds DNA molecules at cross points thus preventing DNA from unwinding from the nucleosome core. H1 histone too is wrapped with an additional 20 bp of DNA and the nucleosome core plus the linker histone form a chromatosome. Adjacent chromatosomes are linked with DNA ranging 20-80 bp bound to H1 histone forming a nucleosome. However, the nucleosome core is often loosely termed the nucleosome. A chromosome, therefore, consists of multiple chromatosomes joined together. During apoptosis, DNA is cleaved at the linker region producing mono and oligonucleosomes. The structures generated shows as regularly spaced DNA bands when analyzed electrophoretically on an agarose gel. Generation of the mono and oligonucleosomes were quantitated using the ELISA technique. All the prepared vaccine constructs induced apoptosis reaching peak nucleosome release into the cell cytoplasm at 48 hours after electroporation and declining to comparable levels with cells electroporated in the absence of DNA at 72 hours.

CHAPTER 4

Immunogenicity of DNA-launched Sindbis replicons expressing the glycoprotein and the nucleoprotein of different CCHFV strains.

4.1 Introduction

Currently, there are no internationally recognized specific therapies or vaccine against CCHF. There is, however, a vaccine used on a small scale in Eastern Europe, in Bulgaria. This is an inactivated vaccine grown in mouse brains and is formulated with adjuvant aluminium hydroxide (Mousavi-Jazi et al. 2012). Although the vaccine has been attributed with a reduction in CCHF cases in Bulgaria, its immunogenicity is yet to be established in controlled protective studies and there are safety concerns as it is prepared from mouse brain tissue. As such, the search for a vaccine is an area of intense research. The CCHFV nucleoprotein and glycoproteins have been targets for DNA based, viral vectored or subunit vaccines. These two structural proteins contain B and T cell epitopes (Moming et al. 2018, Goedhals et al. 2017, Fritzen et al. 2018). A number of vaccine candidates have been reported based on the two major structural proteins, the nucleoprotein and the full length glycoprotein precursor or the mature glycoproteins (Gn and Gc) (Hinkula et al. 2017, Spik et al. 2006, Sahib 2010, Kortekaas et al. 2015, Buttigieg et al. 2014, Dowal et al. 2016).

The development of vaccines was previously limited due to the lack of suitable animal models for efficacy protection studies. Identification of knock out species that succumb to the virus has promoted vaccine development although the availability of these mice is still limited. For immunogenicity studies, these species are however not necessary as any other mice species can be used. Animal welfare during research relies on a set of principles guiding the ethical evaluation of animal use (Fenwick et al. 2009). These set of principles are commonly known as the 3Rs namely replacement, reduction and refinement (Russel and Burch 1959). Replacement concerns the use of animals in research only in cases when an alternative is not available. In such cases, the minimum number of animals necessary to achieve valid scientific results should be used with humane methods (Fenwick et al. 2009). Replacement alternatives can either be absolute in which animals are replaced with inanimate systems or partial in which animals scientifically proved to possess lower pain perception are used. Reduction alternatives include any strategy that reduces the number of research animals but still answering research objectives or obtaining more data by maintaining the number of animals in the absence of increased pain (Fenwick et al. 2009).

Some aspects of infectious disease research such as vaccine development and testing cannot be ethically performed in human beings (Colby et al. 2017). Neither can they be achieved by using inanimate systems despite technological advancements permitting the design of vaccines *in silico*, eliciting a protective immune response requires an intact immune system (Gerdtts et al. 2015). The use of animal models is therefore appropriate in this regard. The choice of

the animal model has a bearing on the nature and magnitude of the immune response elicited. Mice are commonly used in vaccine development and testing because of a number of reasons including their small size allowing ease of handling, ease of breeding, availability of a wide range of mouse types and strains and similar evolutionary history to human beings (Perlman 2016). NIH mice available at the animal house, University of Free State were used to investigate the immunogenicity of the prepared vaccine constructs.

The ultimate goal of vaccination is the induction of a protective immune response. However, the correlates of protection differ amongst pathogens. The success of a vaccine thus depends on stimulation of the desired immune response. Differentiation of hematopoietic stem cells into different white blood cell population is governed by stimuli mostly in primary immune organs (Yamaguchi et al. 2015). After activation, the immunologically naive cells differentiate towards distinct cell populations whose function is also modeled by epigenetic processes (Wilson et al. 2009). In mice and human beings, CD4⁺ T helper cells polarize into two subsets which are recognized as Th1 and Th2 cells. Th1 cells promote type 1 immunity by secreting interferon gamma (IFN- γ), interleukin (IL)-2 and tumor necrosis factor alpha (TNF- α). On the other hand, Th2 cells support type 2 immunity by secreting IL-4, IL-5, IL-6 and IL-10 (Spellberg and Edwards 2001). Although this dichotomy is clear in inbred mice, there is cytokine secretion overlap in human beings and such the principal recognized Th1 cytokine is IFN- γ while IL-4 is regarded as the signature cytokine for Th2 cells. IFN- γ enhances microbicidal actions of macrophages and promotes the production of Fc receptor (Fc γ Rs) and complement binding IgG antibodies which are effective at the elimination of intracellular pathogens (Abbas et al. 1996). These IgG isotypes are IgG2a and IgG3 in mice (Coffman et al. 1993). Besides that IFN- γ and IL-2 promote the cytolytic capacity of CD8⁺ T cells by transforming them into active cells (Abbas et al., 1996). Th2 cytokines principally IL-4 favor antibody production and class switching (Lundgen et al. 1984). While Th1 cytokines are pro-inflammatory, Th2 cytokines are anti-inflammatory. The net result is that the two CD4⁺ T cell subpopulations regulate one another (Abbas et al. 1996). IFN- γ thus promotes the development of type 1 immunity and acts to suppress IL-4 secretion. On the contrary, IL-4 inhibits secretion of IFN by blocking polarization of naïve T cells into Th1 cells (Spellberg and Edwards 2001). IL-10 is known to have anti-inflammatory properties counteracting the effects of type 1 immunity (Rennick et al. 1995).

Adjuvants can be used to direct immune responses towards type 1 or type 2 immunity depending on the immune correlates of protection. Adjuvants do possess immunostimulatory markers which activate the innate immune system thus guiding a robust adaptive immune response. One promising class of adjuvants belong to the Toll-like receptor (TLR) agonists such as polyinosinic-polycytidylic acid (poly (I:C)). These molecules are known to activate the innate immunity and thus enhance the immunogenicity of vaccines (Pasare and Medzhitov 2004). Endosomal and cytosolic poly(I:C) activate TLR3 and MDA-5 respectively. Stimulation of the TLR3 pathway in dendritic cells is associated with induction of IL-12 and type 1 interferons (IFNs), improved MHC II expression and antigen cross-presentation

(Coffman et al. 2010). Triggering the MDA-5 pathway promotes secretion of type 1 IFNs (Coffman et al. 2010). Poly (I:C) has mostly been investigated as an adjuvant with peptide vaccines (Pulko et al. 2009, Currie et al. 2008, Salem et al. 2005; Celis 2007).

Development of candidate vaccines for viral hemorrhagic fevers such as CCHFV requires access to biosafety level 4 facilities for challenge studies, and expensive knockout mice as animal models. Hence there is a definite role for investigating the immunogenicity before taking candidate vaccines into challenge and protection studies. Hence it was considered justified to determine the immune responses induced by replicon candidate vaccines using readily available laboratory animals.

4.2 Aim

To evaluate immune responses induced by DNA launched Sindbis replicons expressing the glycoprotein and nucleoprotein of different CCHFV strains.

4.3 Methods and Materials

4.3.1 Plasmid DNA purification and confirmation for immunogenicity studies

Plasmid DNA purification for immunization of mice was carried out using the Endofree Plasmid Maxi Kit (Qiagen, Hilden, Germany) according to manufacturers instructions. Glycerol stocks of vaccine constructs stored at -80°C were thawed at room temperature and 10 µl of vaccine construct was inoculated in 5 ml of 2XTY media enriched with 50 µg/ml kanamycin antibiotic. The inoculate was grown for 8 hours at 37°C shaking at 250 rpm after which 200 µl of starter culture was diluted into 100 ml fresh 2XTY media and further grown for 16 hours at 37°C shaking at 250 rpm. Thereafter, bacterial cells were harvested by pelleting culture media at 600 x g for 15 minutes at 4°C before resuspending the cell pellet in 10 ml buffer P1. The resuspended bacterial cells were lysed by addition of 10 ml buffer P2 followed by incubation at room temperature for 5 minutes. Cell lysis was stopped by the addition of 10 ml buffer P3 pre-stored at 4°C. The lysate was transferred to a Qiafilter cartridge which was incubated for 10 minutes at room temperature. Subsequently, the lysate was filtered into a sterile falcon tube and to it was added 2.5 ml buffer ER in preparation for 30 minutes incubation on ice. Meanwhile, a Qiagen tip was equilibrated with 10 ml of buffer QBT by draining through it. At the end of the 30 minute incubation period, the filtered lysate was applied to the equilibrated tip and allowed to drain by gravity flow. The tip was washed twice with 30 ml buffer QC and plasmid DNA was eluted with 15 ml of buffer QN. To precipitate the eluted plasmid DNA, 10.5 ml of isopropanol was added to the eluate, briefly homogenized and spun at 5000 x g for an hour at 4°C. Subsequently, the supernatant was decanted and the DNA pellets washed by centrifugation at 5000 x g in endotoxin-free 70% ethanol for 60 minutes. The supernatant was discarded, the DNA pellet air dried and resuspended in 250 µl of nuclease-free water. The DNA concentration

was quantified using the NanoDrop 2000 spectrophotometer (Thermo Scientific, Illinois, USA) and constructs were stored at -20°C.

Vaccine constructs pSinCCHF-31S and pSinCCHF-52S were confirmed by double restriction enzyme digestion using *Not1* and *Cla1* (New England Biolabs, Massachusetts, United States) and pSinCCHF-52M confirmation was achieved by digestion with *Not1* restriction enzyme (New England Biolabs, Massachusetts, United States) while pSinGFP confirmation was achieved by double restriction digestion using *Not1* and *Xho1* restriction enzymes (Promega, Wisconsin, USA). The restriction enzyme experiments were set up as shown in Table 4.1.

Table 4. 1: Restriction enzyme digestion for confirmation of vaccine constructs

Reagents	pSinCCHF31S	pSinCCHF52S	pSinCCHF52M	pSinGFP
Not1-HF (20 u/μl)	1 μl	1 μl	1 μl	-----
Not1 (10 u/μl)	-----	-----	-----	1 μl
Cla1 (10 u/μl)	1 μl	1 μl	-----	-----
Xho1 (10 u/μl)	-----	-----	-----	1 μl
Vaccine construct	2 μl (1 μg)	2 μl (1 μg)	2 μl (1 μg)	2 μl (1 μg)
10X NEBuffer	5 μl	5 μl	5 μl	-----
Buffer D	-----	-----	-----	2 μl
Nuclease-free water	41 μl	41 μl	42 μl	16 μl
Total volume	50 μl	50 μl	50 μl	20 μl

4.3.2 Animal immunizations

An animal experiment was designed to evaluate the immune response induced by each vaccine. Ethical clearance was obtained from the Animal Ethics Research Committee (Ethics number, UFS-AED2017/0066), University of the Free State. Groups of three, 6-8 week old NIH mice were immunized with each of the candidate vaccines into the tibia anterior muscle. Mice were randomly assigned into four groups as shown in Table 4.2. Mice in the control group were immunized with a control construct (pSinGFP).

Table 4. 2: Route of administration, dose and amount of dosages for different plasmids

Group	Plasmid DNA construct	Dose/mouse and schedule	Route
1	PSinGFP	100 μg, 3 doses*	Intramuscular
2	pSinCCHF-31S	100 μg, 3 doses	Intramuscular
3	pSinCCHF-52S	100 μg, 3 doses	Intramuscular
4	pSinCCHF-52M	100 μg, 3 doses	Intramuscular

*All groups were vaccinated on days 0, 21 and 42. The experiment was completed on day 56. See Figure 4.1 for allocation of mice into different groups.

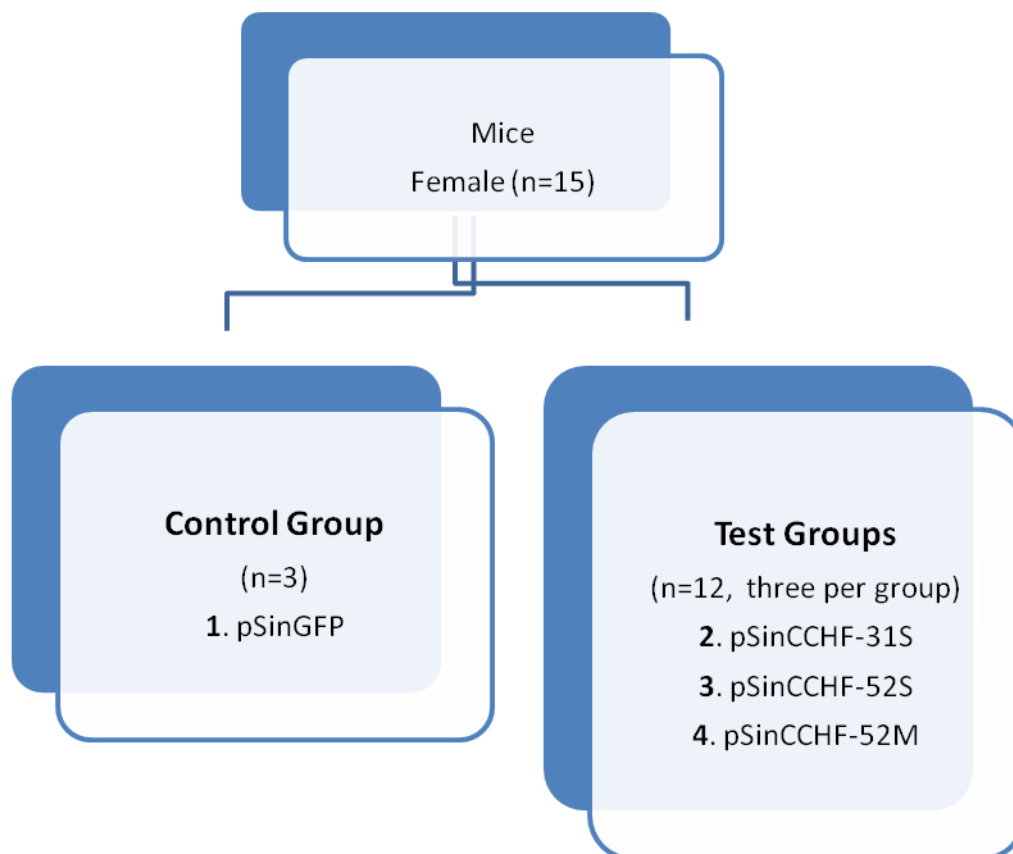


Figure 4. 1: Allocation of mice into different groups. A total of 15 mice were used in the experiment. Mice were randomly assigned to the control group and test groups. Three mice were used per group.

Based on the outcome of the pilot mouse study, one construct expressing CCHFV glycoprotein (pSinCCHF-52M) and one construct expressing CCHFV nucleoprotein (pSinCCHF-52S) induced the most promising results with regard to humoral and/or cellular responses. The two constructs were selected and a mouse experiment was performed in which the adjuvant polyinosinic-polycytidylic (poly (I:C) HMW VacciGrade was used to determine if the administration of the adjuvant with the constructs could increase the immunogenicity of the vaccine constructs. Also, the two constructs were co-administered with and without poly (I:C) to induce a response against both proteins simultaneously. Mice were grouped into 6 groups as detailed in Table 4.3 below. Each group had three mice with group 1 as a control group while groups 2, 3, 4, 5 and 6 constituted the test groups. Allocation of mice into groups is described in Figure 4.2. Groups 1, 3, and 4 were immunized with 100 micrograms of DNA plasmid and 50 micrograms of poly (I:C)/immunization/mouse. Group 2 mice received 100 micrograms of DNA plasmid/immunization/mouse while those in group 5 received 50 micrograms of each of the plasmid DNA/immunization/mouse. Mice assigned to group 6 were vaccinated with 50 micrograms of each of the DNA

vaccine construct and 50 micrograms of poly (I:C)/immunization/mouse. DNA plasmids and poly (I:C) were dissolved in a total volume of 100 μ l. Immunization with pSinGFP and pSinCCHF-52S in the absence of poly (I:C) were not repeated to reduce the number of animals required.

Stock poly (I:C) HMW Vaccigrade™ was prepared according to the manufacturer's instructions. Briefly, 10 mg poly (I:C) HMW Vaccigrade™ was dissolved in 10 ml endotoxin-free water. To ensure complete homogenization, the solution was gently pipetted up and down. Thereafter, the mixture was heated for 10 minutes at 65°C. Proper annealing was promoted by cooling the suspension for 60 minutes between 15-25°C.

Table 4. 3: Route of administration, dose and amount of dosages for different plasmids

Group	Plasmid DNA construct	Adjuvant	Dose (μ g)/mouse	Route Dosage
1	PSinGFP	Poly(I:C)	pSinGFP:100 Poly(I:C):50	Intramuscular*
2	pSinCCHF-52M	————	pSinCCHF-52M:100	Intramuscular
3	pSinCCHF-52M	Poly(I:C)	pSinCCHF-52M:100 Poly(I:C):50	Intramuscular
4	pSinCCHF-52S	Poly(I:C)	pSinCCHF-52S:100 Poly(I:C):50	Intramuscular
5	pSinCCHF-52M + pSinCCHF-52S	————	pSinCCHF-52M:50 pSinCCHF-52S:50	Intramuscular
6	pSinCCHF-52M + pSinCCHF-52S	Poly(I:C)	pSinCCHF-52M:50 pSinCCHF-52S:50 Poly(I:C):50	Intramuscular

*All groups were inoculated on days 0, 21 and 42. The experiment was completed on day 56. See Figure 4.2 for allocation of mice into different groups.

Mice were housed in small cages (shoe box), each cage accommodating three mice. For environment richness, bedding consisted of saw dust, corn cob and shredded tissue. The cages were labeled for identification purposes. Bedding was changed weekly and animals were fed *ad libitum*. The temperature in the room was maintained between 19-24°C with humidity of 45-75%. Animals were provided with 12 hours of light (6 am to 6 pm) and 12 hours of darkness (6 pm to 6 am). An automatic light switch regulated the light. Animal handling was performed only when changing cages (which was done weekly throughout the study) and inoculation of plasmids. During this time, mice were held by the base of the tail.

At the end of the study, mice were anesthetized with drug halothane, bled from the orbital eye and euthanized by dislocation of the neck. Blood was collected in plain tubes and left to stand overnight at 4°C. After the incubation period, tubes containing blood were spun at 1500 × g at 4°C for 15 minutes. Thereafter, serum was carefully transferred to 1.5 ml tubes and stored at -80°C till antibody assaying. Trained personnel from the Animal Unit at the University of the Free State performed the bleeding, anesthetizing and euthanizing of the mice.

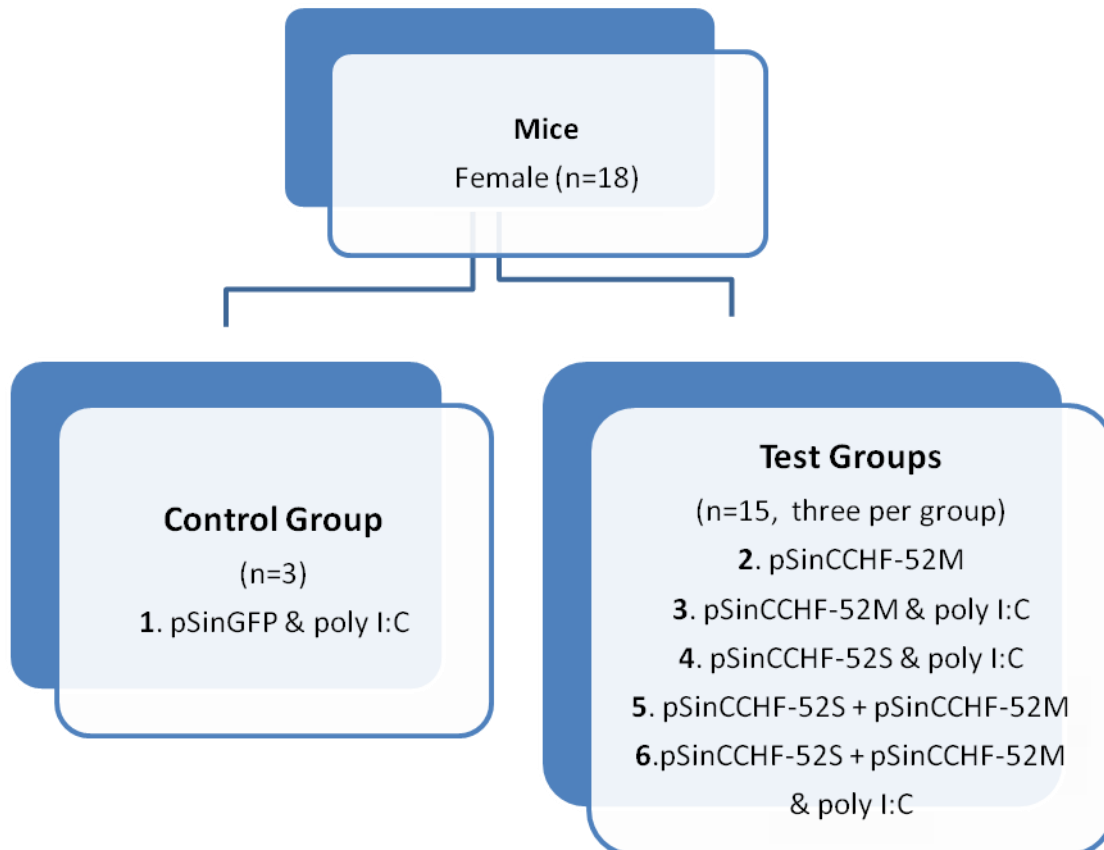


Figure 4. 2: Allocation of mice into various groups. A total of 18 mice were used in the experiment. Mice were randomly assigned to the control group and test groups. Three mice were used per group. Vaccine constructs administered to mice in control group 1 and test groups 3, 4 and 6 were co-immunized with adjuvant poly(I:C). Group 2 animals received vaccine construct pSinCCHF-52M in the absence of poly(I:C). Mice in test groups 5 and 6 were administered with the two constructs pSinCCHF-52S and pSinCCHF-52M.

4.3.3 Determination of cellular immune responses

To determine if the vaccine constructs induced a cellular immune response to the proliferation of T cells in splenocytes was determined using a specific CCHFV protein-T cell proliferation assay. Splenectomy was performed and spleens were placed in petri dishes with 10 ml phosphate buffered saline (PBS). Using sterile scissors, the spleens were cut into small pieces and rolled between sterile frosted glass ends of microscope slides. The cell

suspension with fragments of tissue was transferred to 15 ml tubes and centrifuged at 300 x g for 8 minutes at 4°C. After discarding the supernatant, cells were resuspended in 7ml cold PBS and centrifuged as above. The resultant cell pellet was resuspended in RPMI 1640 media (Gibco, Paisley, UK) supplemented with 1% L-glutamine (Lonza, Verviers, Belgium), 1% penicillin-streptomycin (Lonza, Verviers, Belgium) and 10% fetal bovine serum (Lonza, Verviers, Belgium) and passed through 70 µm mesh filters (BD Falcon™, New Jersey, USA). Cells were counted with a hemocytometer and cell counts confirmed with the Countess™ II FL Automated cell counter (Invitrogen, California, USA). Thereafter cells were transferred to 96 well plates (NEST, Jiangsu, China) at a seeding density of 5 x10⁵ cells per well in a total volume of 250 µl RPMI 1640 media. A 10 µg per well of CCHFV antigen (kindly donated by Prof J Paweska from the National Institute of Communicable Diseases, South Africa) composed of inactivated virus particle was used to stimulate cells, concanavalin A antigen (Calbiochem, California, USA) (0.25µg/well) functioned as a positive control while sterile PBS served as a negative control. Cells were stimulated for 48 hours at 37°C in a 5% CO₂ enriched incubator. At the end of the incubation period cell culture supernatants were harvested and frozen at -80°C till cytokine profiling.

Levels of cytokines secreted by splenocytes, interleukin (IL) 2, IL-4, IL-6, IL-10, tumor necrosis factor alpha (TNF-α) and interferon gamma (IFN-γ) were quantitated using a commercially available ELISA (eBioscience, California, USA). Nunc MaxiSorp™ ELISA plates (Nunc™, Roskilde, Denmark) were coated overnight at 4°C with capture antibodies specific to IL-2, IL-4, IL-6, IL-10, TNF-α and INF-γ. On day 2, wells were aspirated and washed with wash buffer made up of 0.05% Tween® 20 (VWR™ Life sciences, Pennsylvania, USA) in phosphate buffered saline. Nonspecific binding was minimized by blocking wells with 1x assay diluent (kit supplied) for one hour at room temperature. Seven 2-fold serial dilutions of standards (provided with the kits) were performed while samples were diluted 1:2 in assay diluents and assayed in duplicate. Following the blocking step, samples and standards were added to wells and after one hour of incubation at room temperature, wells were washed and reacted with the specific detection antibody. Assay diluent was added to specific wells and this served as the background control. After washing, avidin-horse radish peroxidase was added to wells and incubated for 30 minutes at room temperature. Subsequently, 3,3',5,5'-tetramethylbenzidine (TMB) substrate was added to wells and after a 15-minute incubation, the reactions were stopped by adding 50µl of 2N H₂SO₄ to each well. Colour development was measured at 450nm using the Sunrise™ absorbance reader (Tecan, Salzburg, Austria). The average absorbance of standards was calculated and standard curves were generated for each plate by plotting the mean absorbance values against the corresponding concentration of the standard cytokine. The resultant equation from each plate was used to determine concentrations of cytokines.

4.3.4 Determination of humoral immune responses

CCHFV specific immunoglobulin G (IgG) production after immunizing mice with candidate vaccines was analyzed using an indirect immunofluorescent assay in which slides contain BIOCHIPs coated with CCHFV transfected and control transfected cells (EUROIMMUN AG, Lubeck, Germany). The cells were transfected with plasmids encoding the CCHFV glycoprotein precursor protein and the nucleoprotein. Frozen mice serum samples were thawed and diluted 1:8 using sample dilution buffer (kit supplied). The samples were then reacted with BIOCHIP slides for 30 minutes at room temperature. Afterward, slides were washed and reacted with fluorescein labeled goat anti-mouse immunoglobulin G, diluted 1:20 in 0.1% filter sterilized Evans blue, for a further 30 minutes at room temperature. Unbound secondary antibody was washed off with PBS-Tween (pH 7.2) and slides visualized with the Nikon ECLIPSE Ni-U fluorescence microscope (Melville, New York, USA). Positive samples were serially diluted starting 1:8 and total IgG endpoint antibody titers were determined in an IFA. Positive samples were also isotyped in order to categorize the antibody response into either Th1 type or Th2 type response. Serial dilution of positive reactants was performed and immunofluorescent assays were repeated as above. However, fluorescein-conjugated rat anti-mouse IgG1, IgG2a and IgG2b were used as detection antibodies (Biolegend, San Diego, USA). Detection antibodies were diluted 1:50 in 0.1% filter sterilized Evans blue. Slides were visualized with the Nikon ECLIPSE Ni-U fluorescence microscope.

4.3.5 Statistical analysis

Pairwise comparisons between groups were assessed with the Kruskal-Wallis test. Statistical significance was set at $p < 0.05$. Analysis were performed with the SAS software Version 9.3.

4.4 Results

4.4.1 Humoral immune responses

To establish if vaccination can induce humoral immune responses, 6-8 weeks old NIH mice (n=3/group) were immunized three times intramuscularly with Sindbis based replicons encoding CCHFV nucleoproteins and glycoprotein precursor genes. Animals in the control group were immunized with a Sindbis replicon encoding the green fluorescence protein. One mouse from the group immunized with pSinCCHF-52S and poly (I:C) was euthanized before the study ended thus humoral and cellular immune responses could not be investigated. Two weeks after receiving the last dose mice were sacrificed and the serum samples were screened for CCHFV specific IgG antibodies. Mice responded with the production of CCHFV nucleoprotein specific antibodies as shown in Tables 4.4 and 4.5. Antibodies specific to the CCHFV nucleoprotein were elicited in mice immunized with pSinCCHF-52S independently or were co-immunized with pSinCCHF-52M. However, CCHFV nucleoprotein specific antibodies were not detected in one mouse which was co-inoculated with pSinCCHF-52S and pSinCCHF-52M in the presence of poly (I:C) and all the mice immunized with pSinCCHF-31S. Immunization with pSinCCHF-52M did not elicit CCHFV glycoprotein-specific antibodies. Tables 4.4 and 4.5 summarize the results.

Total endpoint IgG antibody titers were determined in positive samples and these are shown in Figure 4.3. Mice co-immunized with pSinCCHF-52M and pSinCCHF-52S generated antibody titers ranging from 1024 to 2048 (mean titer 1706) while co-immunization of the two vaccine constructs with poly (I:C) induced the same range of antibody titers (1024 to 2048). All three mice immunized with pSinCCHF-52S had an endpoint antibody titer of 1024. Antibody responses were further characterized into CCHFV NP-specific IgG subtypes, i.e. IgG1, IgG2a and IgG2b. Endpoint titers for each subtype were determined and are shown in Figure 4.4. Although immune responses were of mixed IgG subtypes, calculated IgG2a/IgG1 ratios in responders ranged from 8-64 and these results suggest a predominant Th1 type antibody response in immunized mice.

Table 4. 4: Analysis of CCHFV IgG antibody in mice serum after immunization with Sindbis replicons expressing CCHFV glycoprotein and nucleoprotein using an indirect immunofluorescent assay

Vaccine construct	Mice	CCHFV antibody result	
		NP-specific antibody	GP specific antibody
PSinGFP	Mouse 1	Negative	Negative
	Mouse 2	Negative	Negative
	Mouse 3	Negative	Negative
pSinCCHF-31S	Mouse 1	Negative	_____
	Mouse 2	Negative	_____
	Mouse 3	Negative	_____
pSinCCHF-52S	Mouse 1	Positive	_____
	Mouse 2	Positive	_____
	Mouse 3	Positive	_____
pSinCCHF-52M	Mouse 1	_____	Negative
	Mouse 2	_____	Negative
	Mouse 3	_____	Negative

Table 4. 5: Analysis of CCHFV IgG antibody in mice serum after immunization with Sindbis replicons expressing CCHFV glycoprotein and nucleoprotein using an indirect immunofluorescent assay

Vaccine construct	Mice	CCHFV antibody result	
		NP-specific antibody	GP-specific antibody
pSinGFP + poly (I:C)	Mouse 1	Negative	Negative
	Mouse 2	Negative	Negative
	Mouse 3	Negative	Negative
pSinCCHF-52S + poly (I:C)	Mouse 1	Positive	_____
	Mouse 2	Positive	_____
pSinCCHF-52M	Mouse 1	_____	Negative
	Mouse 2	_____	Negative
	Mouse 3	_____	Negative
pSinCCHF-52M + poly (I:C)	Mouse 1	_____	Negative
	Mouse 2	_____	Negative
	Mouse 3	_____	Negative
pSinCCHF-52MS	Mouse 1	Positive	Negative
	Mouse 2	Positive	Negative
	Mouse 3	Positive	Negative
pSinCCHF-52MS + poly (I:C)	Mouse 1	Negative	Negative
	Mouse 2	Positive	Negative
	Mouse 3	Positive	Negative

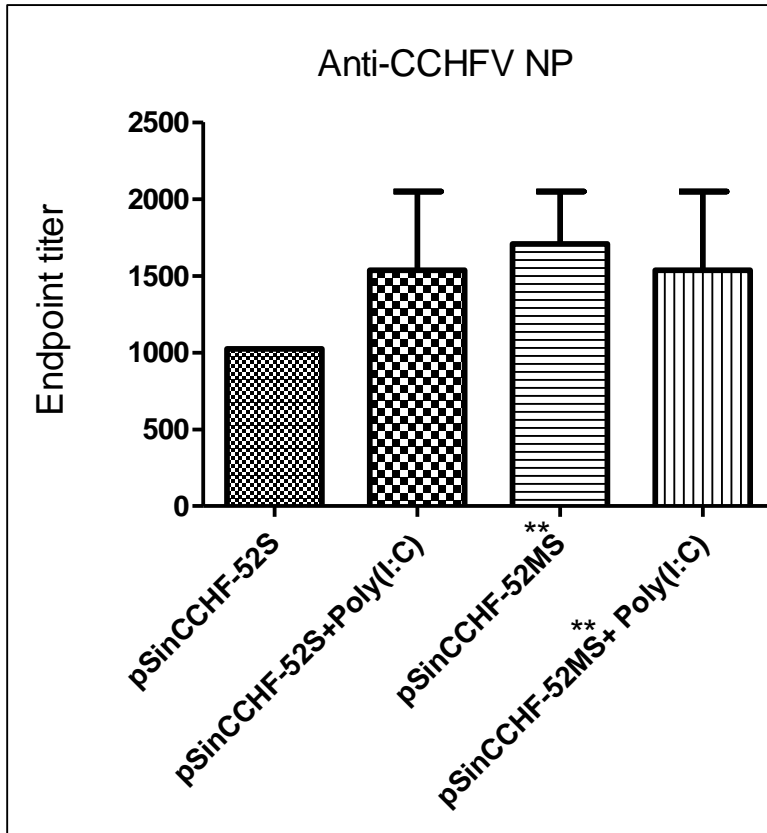


Figure 4. 3: Anti-CCHFV NP IgG total endpoint antibody titer. Mice (NIH; N=3/group) were immunized three times intramuscularly with prepared vaccine constructs expressing CCHFV glycoprotein and nucleoprotein. Serum total endpoint anti-CCHFV NP IgG were analyzed using an indirect immunofluorescent assay. Data is expressed as the mean for three mice and the standard error of the mean. **pSinCCHF-52S + pSinCCHF-52M

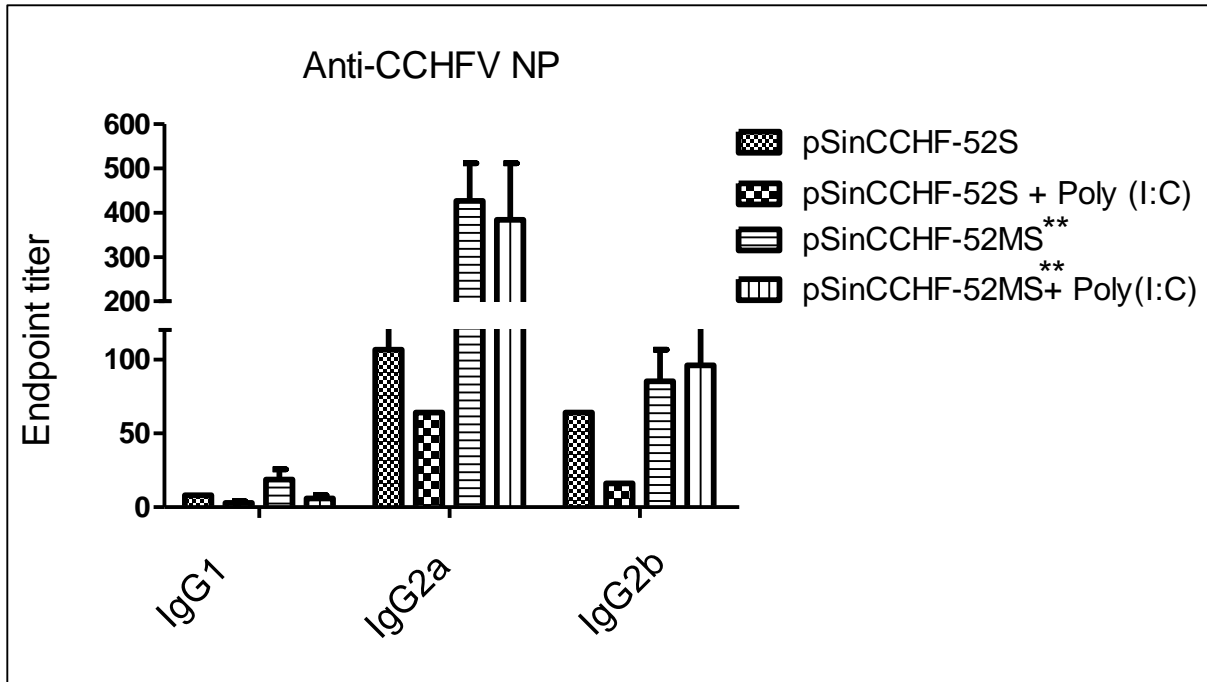
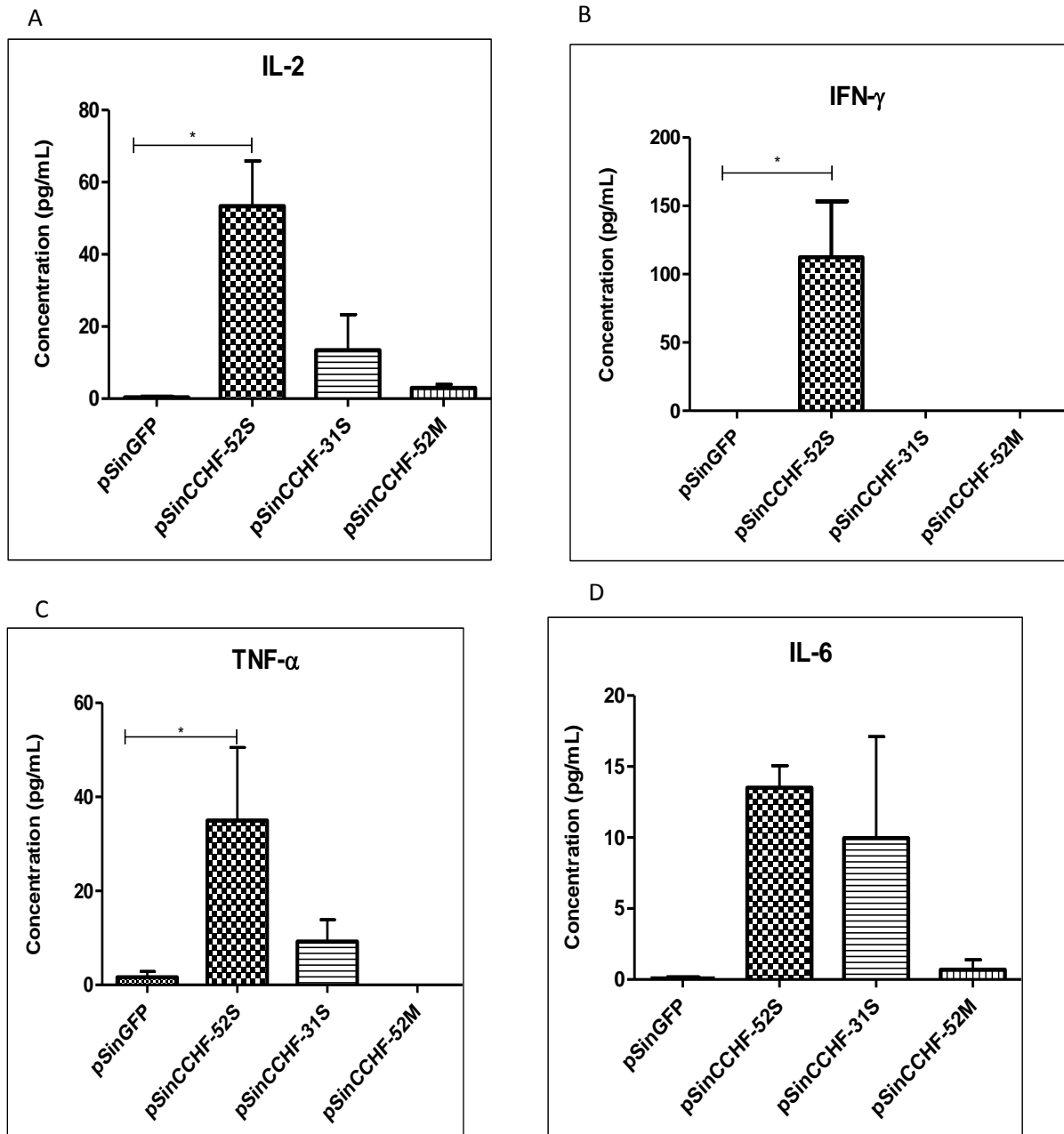


Figure 4. 4: Anti-CCHFV NP IgG isotypes endpoint titer. Mice (NIH; N=3/group) were immunized three times intramuscularly with prepared vaccine constructs expressing CCHFV glycoprotein and nucleoprotein. Serum anti-CCHFV NP IgG subtypes were analyzed using an indirect immunofluorescent assay. Data is expressed as the mean for three mice and the standard error of the mean. **pSinCCHF-52S + pSinCCHF-52M

4.4.2 Cellular immune responses

To characterize cellular immune responses elicited by vaccine constructs and control construct, splenocytes from immunized mice were stimulated *in vitro* with CCHFV specific antigen for 48 hours at 37°C. Afterward cell supernatant was analyzed by ELISA for secretion of IL-2, IL-4, IL-6, TNF- α and IFN- γ cytokines. Splenocyte viability and capacity to secrete the above cytokines was confirmed by stimulating cells with mitogen concanavalin A. Release of cytokines in unstimulated cells was established by stimulating splenocytes with sterile PBS. Cytokine levels secreted from stimulated splenocytes are shown in Figure 4.5. Splenocytes from mice immunized with pSinCCHF-52S consistently resulted in higher levels of Th1-type cytokines; IL-2 ($p = 0.0495$), IFN- γ ($p = 0.0369$) and TNF- α ($p = 0.0495$) compared to the mock vaccine while there was no significant difference in cytokine secretion by cells from mice vaccinated with pSinCCHF-31S. Comparing the two vaccine constructs expressing CCHFV nucleoprotein (pSinCCHF-31S and pSinCCHF-52S), IFN- γ secretion was significantly higher ($p = 0.0369$) by splenocytes from mice immunized with the latter vaccine construct. There was no IL-4 secretion by cells from all groups of mice following stimulation with the CCHFV antigen. Stimulation with concanavalin A though resulted in IL-4

secretion confirming the viability of cells and capability to secrete the cytokine. In addition to IL-4, splenocytes from mice immunized with pSinCCHF-52M could not secrete detectable IFN- γ and TNF- α while splenocyte supernatants from mice immunized with pSinCCHF-31S had undetectable levels of TNF- α . Antigenic stimulation of splenocytes originating from mice which received the construct expressing the CCHFV glycoprotein precursor gene (pSinCCHF-52M) yielded very low Th1 and Th2-type cytokines.



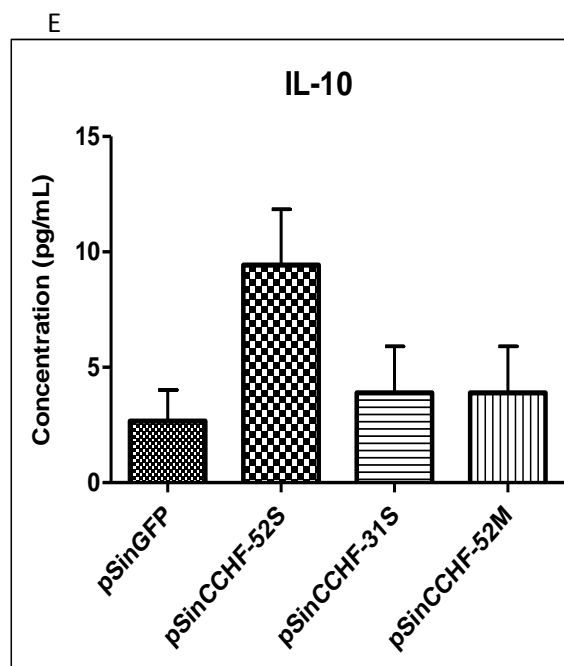
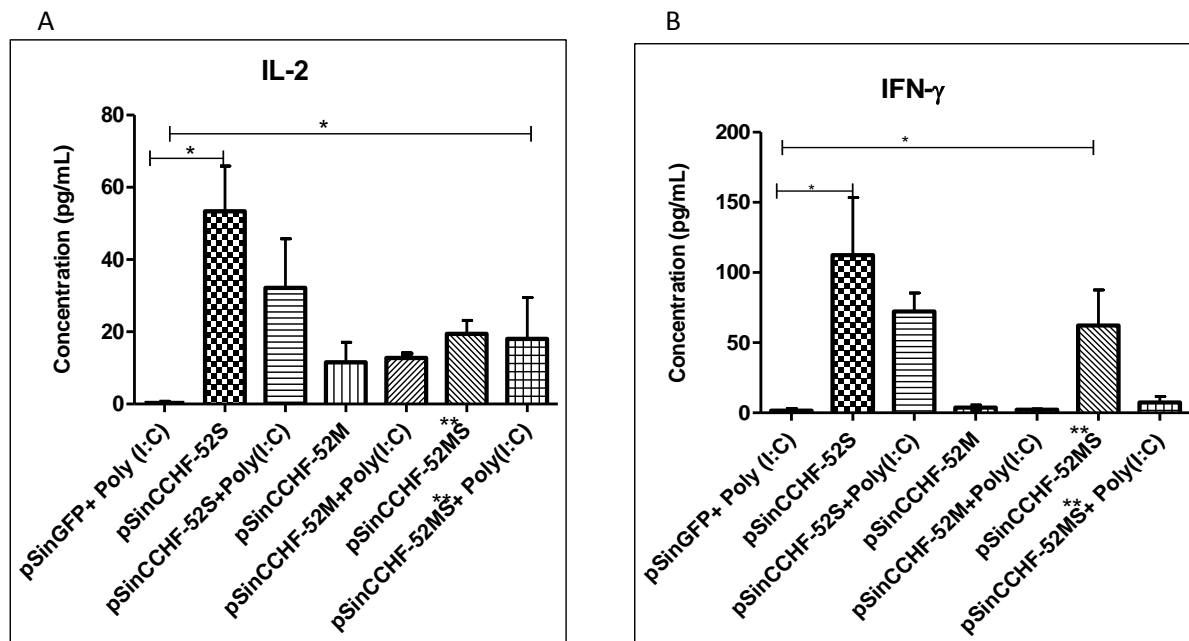


Figure 4. 5: Cytokine secretion levels after splenocyte stimulation with a CCHFV antigen. Mice (NIH; N=3/group) were immunized three times intramuscularly with prepared vaccine constructs expressing CCHFV glycoprotein and nucleoprotein. Harvested splenocytes were stimulated with a CCHF antigen and levels of secreted interleukins in supernatants were analyzed using ELISA. Data is expressed as the mean for three mice and the standard error of the mean. (A) IL-2, (B) IFN- γ , (C) TNF- α , (D) IL-6, (E) IL-10. * $p < 0.05$

To improve the cellular immune responses, constructs pSinCCHF-52M and pSinCCHF-52S were either inoculated independently or were co-inoculated in NIH mice in the presence or absence of adjuvant poly (I:C). Splenocytes from immunized mice were harvested, stimulated *in vitro* and supernatants were assayed for the presence of Th1 and Th2 cytokines. Levels of cytokine secretion after stimulation are shown in Figure 4.6. High levels of IL-2 and IFN- γ were obtained from splenocytes in mice immunized with pSinCCHF-52S both in the presence and absence of adjuvant poly (I:C). Statistical significance was however not achieved for the group vaccinated in the presence of poly (I:C) because of the reduced sample size after a mouse was euthanized before the end of the study. Co-immunisation of pSinCCHF-52S and pSinCCHF-52M did result in enhanced secretion of IFN- γ and IL-2 ($p = 0.0463$) while vaccination with pSinCCHF-52M alone increased secretion of IL-2 ($p = 0.0463$) contrasted to vaccinating with pSinGFP. While co-inoculation of the vaccine constructs improved cytokine secretion when compared to immunization with pSinCCHF-52M alone it was accompanied by reduced cytokine secretion levels when compared to immunization with pSinCCHF-52S by itself. Immunization with the construct expressing the CCHFV glycoprotein precursor (pSinCCHF-52M) whether by itself or in combination with the construct expressing the CCHFV nucleoprotein (pSinCCHF-52S) with or without poly (I:C) did not result in detectable levels of TNF- α in stimulated

cells. Co-immunization of constructs with adjuvant poly (I:C) was intended to improve cytokine secretion, especially Th1 cytokines. However, as shown in Figure 4.6 the adjuvant poly (I:C) did not enhance Th1 cytokine secretion as expected. Splenocytes from mice co-inoculated with pSinCCHF-52S and poly (I:C) secreted lower levels of all the cytokines investigated. Reduced IFN- γ and IL-10 cytokine secretion were also observed in splenocytes from mice which received pSinCCHF-52S and pSinCCHF-52M in the presence of poly (I:C) though comparable IL-2 cytokine levels were obtained.



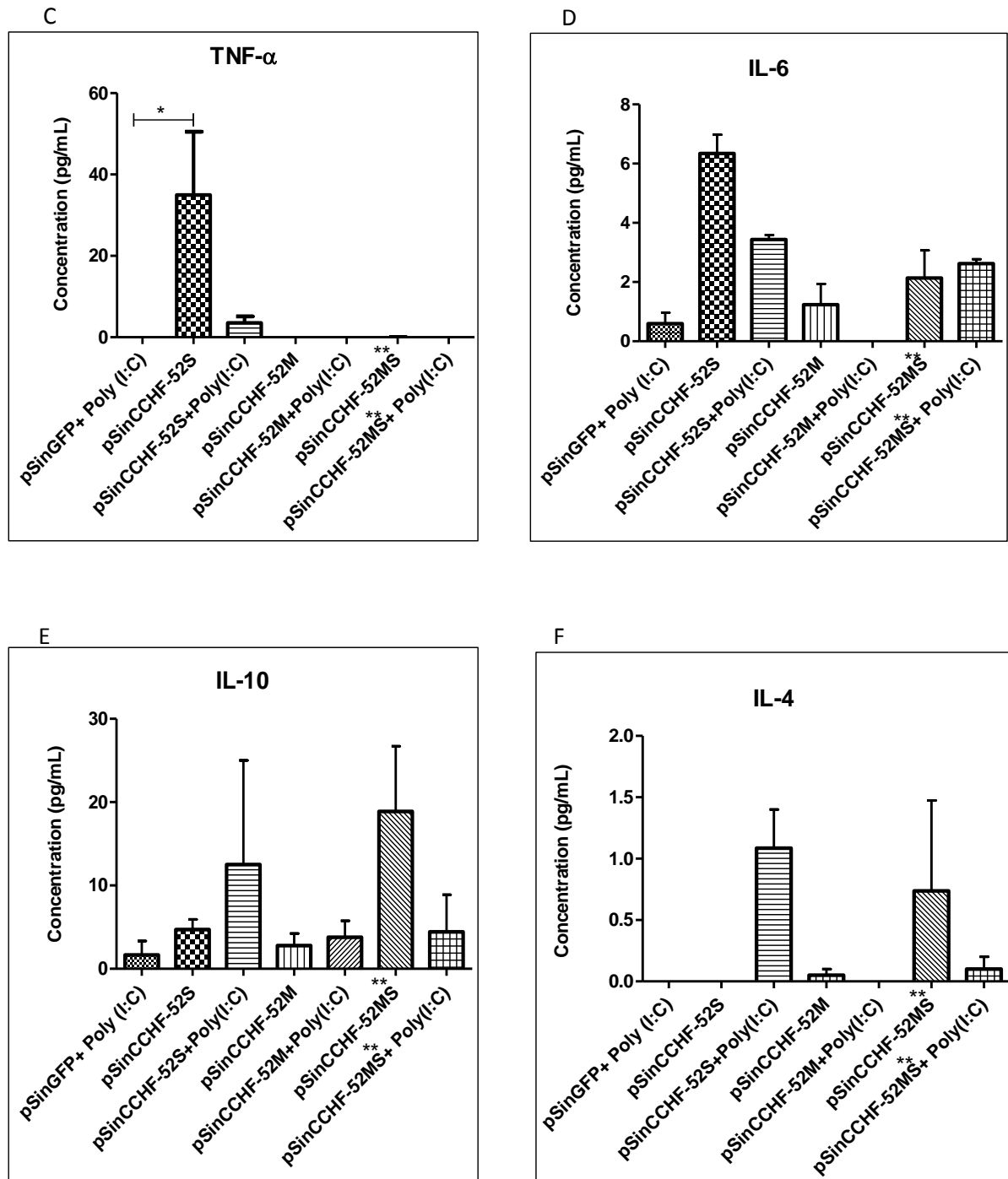


Figure 4. 6: Cytokine profiling by ELISA from splenocytes harvested from NIH mice (N=3/group) after immunization with pSinCCHF-52S and pSinCCHF-52M independently or combined in the presence or absence of adjuvant poly(I:C). (A) IL-2, (B) IFN- γ , (C) TNF- α , (D) IL-6, (E) IL-10, (F) IL-4. Data is expressed as the mean for three mice and the standard error of the mean. **pSinCCHF-52S + pSinCCHF-52M. * $p < 0.05$

4.5 Discussion

In the absence of inanimate systems unto which an immune response can be stimulated and investigated, animal use remains the mainstay of arms of biomedical research such as vaccine development and testing. The welfare of animals in scientific research is guided by principles known as the 3Rs which are replacement, refinement and reduction. These not only prevent or alleviate pain induced in research animals but can also enhance the quality of scientific information obtained. In the previous chapter, the plasmid constructs were characterized *in vitro*. Expression of proteins was characterized in transfected cells. The ability of these constructs to induce a response in an animal model was then investigated. Similar studies described in literature used from 3-18 mice per group and yielded valid data (Buttigieg et al. 2014, Dowall et al. 2016, Hinkula et al. 2017, Zivcec et al. 2018). We decided to investigate immunogenicity of the prepared constructs using three mice per group according to our budgetary allocations.

Cytokines secreted by T lymphocytes can be broadly classified into Th1 (IL-2, IFN and TNF- α) and Th2 (IL-4, IL-5, IL-9, IL-10, and IL-13) (Spellberg and Edwards 2001). These cytokines differ in their effector functions with Th1 cytokines being inflammatory and providing immunity against intracellular pathogens whereas Th2 cytokines are anti-inflammatory, triggering immune responses against extracellular pathogens. Murine IgG subclasses include IgG1, IgG2a, IgG2b, and IgG3 (Grey et al. 1971). Numerous factors including the predominant cytokine regulate expression of these IgG subclasses (Rostamian et al. 2017). Th1 cytokines drive expression of IgG2a and IgG2b while Th2 cytokines promote expression of IgG1 (Abbas et al. 1996). In instances where immune responses are suboptimal, adjuvants are co-delivered with the vaccine to enhance immune responses. Adjuvants can promote either Th1 or Th2 immune responses as per the immune correlates of protection. The aim of this study was to characterize immune responses generated by mice immunized with Sindbis replicons encoding CCHFV glycoprotein precursor and nucleoprotein genes. NIH mice 6-8 weeks old were randomly assigned to groups. Mice were inoculated three times intramuscularly with the prepared Sindbis replicons, three weeks apart. A construct expressing the green fluorescence protein served as a mock vaccine. Adjuvant poly (I:C) was co-inoculated with the vaccine constructs to enhance Th1 cytokine responses. Two weeks after receiving the third dose, mice were sacrificed and blood was collected for determination of antibody responses. IgG antibody isotyping was performed in positive reactants in order to classify the antibody response into either Th1 or Th2. IgG2a/IgG1 > 1 signify a Th1 antibody response while IgG2a/IgG1 < 1 suggest a Th2 antibody response.

Cytokine secretion by cells of the immune system is indicative of a cellular immune response. Splenocytes are white blood cells situated in the spleen comprising of T lymphocytes (CD4+ and CD8+ T cells), B lymphocytes, macrophages and dendritic cells performing distinct functions (Bronte and Pittet 2013). Memory splenocytes generated after the initial encounter with an antigen secrete cytokines upon re-exposure to the same antigen. Splenocytes were harvested from sacrificed mice. A single cell suspension of the harvested splenocytes was

prepared and stimulated with CCHFV antigen. Concanavalin A, a T cell mitogen (Weiss et al. 1987) was used as a positive control. Supernatants were harvested after 48 hours of stimulation at 37°C and these were assayed for Th1 and Th2 cytokines.

CCHFV NP-specific antibodies were induced in animals immunized with vaccine construct pSinCCHF-52S but not in animals which received pSinCCHF-31S. Calculated CCHFV NP IgG2a/IgG1 ratios were greater than 8 and these results suggest a predominant Th1 antibody response. CCHFV GP specific antibodies were not elicited in animals immunized with pSinCCHF-52M. The absence of GP specific antibodies could have been due to the low expression rates by the vaccine construct pSinCCHF-52M. However, failure by vaccine construct pSinCCHF-31S to induce CCHFV NP-specific antibodies was not expected since the construct demonstrated higher replicative kinetics compared to pSinCCHF-52S in transfected cells. Reasons for the absence of antigen antibodies in sera from animals immunized with pSinCCHF-31S are not entirely clear. Factors such as the smaller number of animals used in the study or the lower rates of apoptosis induction by construct pSinCCHF-31S compared to pSinCCHF-52S could be some of the reasons. In light of the antibody responses obtained, vaccine construct pSinCCHF-52S was therefore selected and an animal experiment performed in which the adjuvant poly (I:C) was co-administered to investigate whether immunogenicity of vaccine construct could be enhanced. The nature of the immune response generated by combining the GP and NP was also investigated by co-inoculating pSinCCHF-52S and pSinCCHF-52M. While, co-immunization of GP and NP has been investigated before (Hinkula et al. 2017), the researchers used the mature CCHFV glycoproteins Gn and Gc as opposed to the full-length GP. In our opinion, the non-structural proteins encoded by the full-length GP could play a role in immune induction hence we used the full-length GP open reading frame in our study. Immunizing animals with pSinCCHF-52S alone or combined with pSinCCHF-52M induced high titers of CCHFV NP-specific antibodies.

Levels of Th1 cytokines (IFN- γ , IL-2 and TNF- α) secretion in stimulated splenocytes were higher than Th2 cytokines (IL-4, IL-6 and IL-10) after immunization with pSinCCHF-52S independently and co-immunization with pSinCCHF-52S and pSinCCHF-52M. Taken together, immunization with the prepared vaccine construct pSinCCHF-52S expressing the CCHFV nucleoprotein induced type 1 immunity. Splenocytes from animals immunized with vaccine constructs pSinCCHF-31S and pSinCCHF-52M were poor at secreting the investigated cytokines. Co-immunization with adjuvant poly (I:C) did not enhance Th1 cytokine secretion. Co-inoculation with plasmids expressing the CCHFV nucleoprotein and glycoprotein improved cytokine secretion compared to immunization with the glycoprotein by itself but reduced secretion of cytokines contrasted with immunization with the construct expressing the nucleoprotein although statistical significance was not achieved in both cases. Further studies are warranted with other CCHFV strains to ascertain whether the full-length GP does suppress cytokine induction when co-administered with the NP.

CHAPTER 5

Further Discussion and concluding remarks

Considering the extensive geographic distribution of CCHFV which is likely to keep on expanding in the wake of climate change, severe human disease course with fatalities up to 30%, human to human spread especially in nosocomial environments, the absence of internationally recognized therapies/vaccines, the virus then poses a significant public health threat. Concerned with the future epidemic threat of CCHFV, the World health organization (WHO) has added the virus to the list of priority infectious microorganisms. Development of treatment/prophylactic agents is therefore vital. *In vitro* studies in vaccine development are essential due to factors such as high cost of *in vivo* studies and limited access to Biosafety Level 4 (BSL-4) facilities for lethal viral challenge hence the need to make sure that the candidate vaccine is worthwhile. Animal models for CCHFV predominantly in the form of knockout mice and the *Cynomolgus macaque* are available. However, the transgenic mice do not accurately depict disease outcome in human beings as viral challenge results in a 100% death rate. CCHFV infection in human beings results in a range of disease states which are not seen in the available mice models. Infection in *macaques* nonetheless resembles the disease spectrum in human beings (Haddock et al. 2018). The challenge though is the cost of the animals and their size meaning few animals can be used in an experiment. These animal models are not available in South Africa and it is not only expensive to import them but requires a process that takes a long period. For immunogenicity purposes, these models are not necessary and in our study, we used the NIH mice which were available at the Animal Unit, University of the Free State. One form of vaccination being investigated is genetic vaccination. DNA vaccines have emerged as an appealing vaccination method. However, low immunogenicity in higher mammals has been their Achilles heel. Several strategies are being investigated to improve immune responses by DNA vaccines. One such strategy is the use of replicon viral vectors. Among the RNA viruses that are being investigated as vaccine vectors are the Alphaviruses. While they have been used to express some viral and bacterial genes, their utility in expression or as vaccine vectors for CCHFV genes has been sparsely investigated. Sindbis replicons expressing full-length open reading frames of the CCHFV glycoprotein precursor (GP) and nucleoprotein (NP) from South African strains were prepared and used as vaccine candidates in this study.

Although the immune correlates of protection are not known, the two major structural proteins, envelope glycoproteins and nucleoprotein, are prime candidates for vaccine development. The NP has advantages in the sense that it is the most abundant virion protein with most of the immune response produced in an infection directed against it. Besides that, its amino acid sequence shows the least variation (Hewson et al. 2004b). The immune response produced against the NP is therefore expected to offer cross-protection against various global strains. On the other hand, the mature glycoproteins are located on the viral membrane unlike the NP which is intracellular. Their location makes them suitable vaccine targets thus most of the subunit vaccine work has focused on the mature

glycoproteins. However, the glycoprotein has a high amino acid sequence diversity. It remains to be established though if this will impact negatively on its choice as a vaccine target. CCHFV specific immune responses directed against the nucleoprotein and envelope glycoproteins have been reported in immunogenicity studies (Buttigieg et al. 2014, Hinkula et al. 2017, Dowall et al. 2016). However, complete protection after the lethal viral challenge has so far been reported in studies investigating either a Modified Vaccinia virus Ankara (MVA) vector expressing the full-length CCHFV GP or a DNA plasmid vector expressing the mature envelope glycoproteins (Gn and Gc) and the nucleoprotein. The reports so far seem to suggest that the immune responses generated against the NP on their own cannot offer full protection. The NP is not associated with neutralizing antibodies whereas the GP is likely to induce neutralizing antibodies.

Genes encoding the full-length open reading frame of CCHFV GP and NP were amplified by PCR and cloned into a Sindbis based expression vector. Correct gene sequence during PCR amplification is a prerequisite for protein expression. As such some strategies to ensure correct gene sequences were employed. These included the use of a high fidelity polymerase enzyme, annealing primers at a temperature of 68°C and setting the maximum number of PCR cycles at 25. High fidelity enzymes combine low nucleotide base misincorporation with the 3'-5' exonuclease activity to minimize mutations (Joyce and Benkovic 2004). Primer annealing at a temperature of 68°C which is close to the optimal polymerase enzyme extension temperature of 72°C reduces non-specific binding and template extension which may take place at lower temperatures albeit at a slower rate but with high error rates. Although polymerase enzymes are thermostable, they do lose their activity (Lawyer et al. 1993) with an increase in PCR cycles. Reducing the number of PCR cycles, therefore, prevents the accumulation of mutations. These strategies were relatively successful compared to our previous experiments where the approaches were not employed. Initially, GP genes were amplified using Expand™ long template PCR system (Roche, Basel, Switzerland) but after identifying nonsynonymous nucleotide changes the constructs were abandoned and the genes were amplified using Phusion® High fidelity DNA polymerase enzyme (New England Biolabs). There were fewer nucleotide base changes which did not result in amino changes after sequence translation except for one nucleotide change in the CCHF-52M sequence. A nucleotide base deletion, however, occurred during amplification of CCHF-31M introducing a frameshift and the construct was thus not useful.

Expression of CCHFV nucleoproteins and glycoproteins in both BHK-21 and HEK-293 cells was demonstrated by using antibodies directed against the polyhistidine tag fused to the proteins. Confirmation was also performed using serum from CCHF survivors. Transfection of BHK-21 and HEK-293 cells was optimized using the Lipofectamine 3000 reagent and the electroporation technique. Transfection with electroporation resulted in superior protein expression rates compared to transfection with the Lipofectamine 3000 reagent. However, the former resulted in reduced cell viability. These results are expected since electroporation is known to be more efficient than reagent based methods

such as the Lipofectamine 3000 reagent. Cell death with electroporation is attributed to electric impulses which cause irreversible pores on cell membranes. Studies have also demonstrated an inverse relationship between cell viability and plasmid size (Lesueur et al. 2016, Ribeiro et al. 2012). Large DNA molecules are associated with increased cell membrane permeability as a consequence of more pores created as DNA molecules transverse the membrane (Sukharev et al. 1992). This has the effect of uncontrolled movement of molecules into the cells resulting in cell swelling and ultimately bursting. Results obtained in this study corroborated these findings. The largest replicon expressing the CCHFV glycoprotein (15901 base pairs) resulted in lower cell viability (by observation) compared to the smaller replicons expressing the CCHFV NP (12287 base pairs) when the same amount of plasmid DNA was used in electroporation experiments.

Protein expression was superior with replicons expressing the nucleoprotein compared to the replicon expressing the glycoprotein precursor. The differences in expression rates may be explained by the plasmid size differences as reported by other researchers (Lesueur et al. 2016, Ribeiro et al. 2012). Moreover, investigators have reported reduced protein expression levels by DNA replicons which are considerably bigger than conventional expression plasmids (Leitner et al. 2006). The DNA plasmid construct expressing the CCHFV glycoprotein being the largest had the lowest transfection efficiency. Small vectors can transverse the cytoplasm with less resistance than bigger vectors which are more prone to shear factors. Moreover, small vectors are more likely to reach the cell nucleus because of higher motility rates in the cytoplasm (Lesueur et al. 2016). The glycoprotein expression rates were still lower in equimolar experiments thus ruling out a fewer number of plasmid molecules as the cause of reduced gene expression. One way of increasing transfection efficiencies and ultimately gene expression with large plasmids is to increase the amount of DNA plasmid required for transfection. While this improves transfection efficiencies, large amounts of plasmid DNA gets to a stage where the high DNA concentration becomes toxic to the cells. This was observed with the plasmids expressing glycoprotein. Electroporating with DNA plasmid concentrations greater than 15µg was accompanied with improved transfection efficiencies but reduced viability rates. That cell death was observed within a few hours after electroporation (as evidenced by the many floating cells) may mean that cell death with the plasmid expressing CCHFV glycoprotein was not due to protein expression since protein expression takes several hours (Lesueur et al. 2016) but irreversible damage to the cell membrane upon contact with plasmids during electroporation. Contrasted with the plasmids expressing the CCHFV nucleoprotein, there were fewer floating cells and many cells were attached at the same stage. Cell death could have reduced glycoprotein expression since the majority of cells which took up the plasmids could not attach and grow. Our challenges in expressing the CCHFV glycoprotein are not surprising since other groups have reported lower expression rates (Meyers et al. 2006, Garrison et al. 2017). Besides that, our CCHFV genes were not codon optimized for expression in mammalian cells, and this could have contributed to low protein expression rates especially with the glycoproteins. Gene codon optimization of the complete open reading frame of the glycoprotein precursor was reported to improve expression of CCHFV Gn

and Gc (Garrison et al. 2017). Recombinant protein expression rates can also be protein dependent, with some proteins expressing better than others. Cellular immune responses produced against CCHFV proteins particularly glycoproteins could have also contributed to low expression rates.

In this study, prepared Sindbis based vaccine constructs induced apoptosis in transfected BHK-21 cells, a feature which has been reported with alphavirus replicons (Leitner et al. 2006, Ljungberg et al. 2007). Apoptosis rather than an increase in protein expression is understood to be one of the mechanisms by which immunogenicity is enhanced by alphavirus replicons. Dendritic cells which lie at the nexus of innate and adaptive immunity engulf apoptotic cells promoting their maturation (Cella et al. 1999) and facilitating antigen presentation on the major histocompatibility complex class 1 (Albert et al. 1998). Moreover, their role in adaptive immune responses is either to stimulate naïve T cells or suppress activated T cells (Mellman and Steinman 2001). Demonstration of apoptosis induction in our study was therefore vital. Besides enhancing immune responses, apoptosis lowers the risks of plasmid DNA integrating with host DNA thus complementing the safety of the Sindbis based replicon vaccines. Apart from that, transient protein expression as a consequence of apoptosis limits the chances of antigen tolerance (Leitner et al. 2004).

To rule out the electroporation procedure as the driver of apoptosis, cells electroporated in the absence of plasmid DNA served as the electroporation control. Enrichment of nucleosomes in the cytoplasm was the lowest with the electroporation control during critical periods of apoptosis. The enrichment factors only became comparable to those from cells electroporated in the presence of plasmids late into the experiment when high cell death was expected. Decreasing enrichment factors over time observed in this study are expected since DNA fragmentation precedes cell membrane disintegration thus over time nucleosomes escape from the cytoplasm into culture media. *In vivo*, apoptotic cells do not remain in circulation for extended periods of time but are removed by phagocytes before membrane breakdown (van Nieuwenhuijze et al. 2003). Cells transfected with pSinGFP replicon, encoding the green fluorescence protein (GFP) exhibited higher apoptotic rates compared to constructs expressing the CCHFV nucleoprotein which was not expected. However, the GFP is known to induce apoptosis in transfected BHK-21 cells (Liu et al. 1999). Apoptosis induction by viral infections and after transfections with alphaviral replicons has been reported to limit viral replication (Terenzi et al. 1999). In line with these findings, there was an inverse correlation between replicative capacity and apoptosis by the vaccine constructs as shown by results obtained in chapter 3. Vaccine construct pSinCCHF-52M which induced the highest apoptotic rate had the least replicative capacity. Meanwhile, pSinCCHF-31S which expressed the highest replicative rate generated the lowest apoptotic rate. However, other factors such as poor transfection efficiency could have also contributed to the low replicative rate by vaccine construct pSinCCHF-52M.

Self-amplification of vaccine constructs by transcription of CCHFV RNA was demonstrated in BHK-21 cells. The use of the qRT-PCR technique for quantitating self-replication rates of vaccine constructs was employed. Standard

curves were generated based on PCR amplicons and were subjected to requirements for validating RT-qPCR. Demonstration of replicon activity is important because it proves the functional activity of the viral replicase in transcribing Sindbis virus RNA and CCHFV RNA thus the prepared replicons were capable of expressing CCHFV proteins. After transcription CCHFV RNA is translated into specific proteins which are internalized, processed and presented by antigen presenting cells to T cells stimulating an immune response. Viral replicase activity in alphavirus replicons also results in the production of dsRNA intermediates which are believed to activate antiviral pathways and initiate apoptosis potentiating immune responses (Leitner et al. 2000). Sindbis replicon activity described in this study was therefore important.

The ultimate goal in this study was to demonstrate the expression of CCHFV proteins by Sindbis replicons which serve as immunogens *in vivo*. CCHFV RNA transcription by the vaccine constructs is one of the many steps in protein synthesis. Studies have shown that there is a poor correlation between gene transcript and protein levels (Edfors et al. 2016, Silva and Vogel 2016) thus CCHFV RNA levels obtained in self-replication experiments cannot be used to estimate protein expression levels by vaccine constructs. Our Western blot results with regard to pSinCCHF-52S and pSinCCHF-31S attest to these findings. Although not accurately quantitative, the visualization of expressed proteins on a Western blot does give an indication of the yield of protein when using the same experimental conditions. The NP-specific band from cells transfected with pSinCCHF-52S was more pronounced (see Chapter 2, Figure 2.18) contrasted to the NP band from pSinCCHF-31S which was faint yet the vaccine construct generated higher CCHFV NP RNA copies. Assaying both the gene transcription and the protein expression levels would be desirable. CCHFV RNA levels obtained in this study are however subject to other factors such as plasmid transfection and RNA extraction efficiencies. Nonetheless, these differences in protein expression by pSinCCHF-31S and pSinCCHF-52S could have also contributed to higher immunogenicity by the latter.

According to our knowledge, this is the first study to investigate immune responses elicited by Sindbis replicons expressing CCHFV NP and GP from South African strains known to have caused disease in the past. Majority of studies described in literature made use of the GP and NP from the IbAr 10200 CCHF strain. This is significant because there are amino acid differences between the GP and NP of South African strains and those from the IbAr 10200 CCHF strain which should influence the immune system differently. Besides that, the IbAr 10200 CCHF strain was isolated from a tick (Causey et al. 1970) and there is no record of human infections whereas strains used in our study were isolated from individuals with disease. Of the three vaccine constructs investigated in this study, the construct expressing the CCHFV nucleoprotein (pSinCCHF-52S) elicited high antibody titers and higher levels of Th1 type cytokines compared to Th2 type cytokines. IgG antibody isotyping revealed higher IgG2a levels compared to IgG1. These results are indicative of Type 1 immunity and are in agreement with similar studies described in the literature (Garrison et al. 2017, Hinkula et al 2017). In this study, the CCHFV genes were expressed by the same

vector and animals received similar doses of the vaccine constructs. Clearly the glycoprotein is larger than the nucleoprotein, but further increase in the amount of plasmid DNA did not result in increased protein expression with the construct. Our optimization results demonstrated an increase in protein expression with increase in the amount of DNA although plasmid amounts more than 4 µg did not improve transfection efficiencies with the Lipofectamine reagent. Differences in immune responses observed could, therefore, be antigen-dependent. Superior specific cellular immune responses by the constructs expressing the nucleoprotein compared to the construct expressing the glycoprotein are not surprising since the nucleoprotein is the most immunodominant protein. However, the low immunogenicity of pSinCCHF-31S compared to pSinCCHF-52S was not anticipated since the two full-length nucleoproteins had only one amino acid difference and the percentage of pSinCCHF-31S transfected cells expressing NP when visualized by IFA was almost similar to pSinCCHF-52S transfected cells. The NPs and GPs included in the study were either from one of the two CCHFV strains and the two strains were chosen based on the presence or absence of reassortment in GP sequences.

One mouse from the group co-immunised with pSinCCHF-52S and pSinCCHF-52M in the presence of poly (I:C) did not respond to immunization with antibody production. There are inter and intra species differences with regard to the induction of immune responses following vaccination (Playfair 1968). These differences may account for the absence of CCHFV NP-specific antibodies from the mouse serum. Non-responders to immunization have been reported in other studies (Buttigieg et al. 2014, Ljungberg et al. 2007).

Factors causing poor immune responses by the construct expressing CCHFV glycoprotein can be multifactorial. Protein expression by the vaccine construct pSinCCHF-52M was the least of the prepared vaccine constructs. There are three instances described in literature where the full-length CCHFV GP open reading frame was used as an immunogen (Sahib 2010, Buttigieg et al. 2014, Garrison et al. 2017) and there are differences with our study. All three instances reported superior humoral and/or cellular immune responses compared to our study. While they all went on to do a lethal viral challenge which we could not do in our study, viral challenge protected all the animals in one study (Buttigieg et al. 2014). In the other two studies, there was no protection (Sahib 2010) and a 60% survival rate (Garrison et al. 2017). They all used the entire CCHFV GP open reading frame from the CCHF IbAr 10200 strain which was codon optimized for human usage in two of the studies (Garrison et al. 2017, Sahib 2010). Different animal models, IFNAR^{-/-} or C57BL/6 (Garrison et al. 2017), A129 mice (Buttigieg et al. 2014), STAT-1 mice (Sahib 2010) were used. In two of the studies, the GP sequences were cloned in viral vectors (Buttigieg et al. 2014, Sahib 2010) while in the study by Garrison et al. the GP sequence was expressed by a plasmid DNA vector. Mice in all the three studies were immunised intramuscularly, receiving 25µg of plasmid DNA (Garrison et al. 2017), 1 x 10⁷ plaque forming units of recombinant MVA expressing CCHFV GP (Buttigieg et al. 2014) and 1 x 10¹⁰ total particles of recombinant adenovirus expressing CCHFV GP (Sahib 2010) per immunisation. In this study, the entire coding open

reading frame of a South African strain SPU 187/90 was cloned into a Sindbis virus expression vector. The above distinctions can be the source of the differences in immune responses between our study and similar studies described in the literature.

The low immunogenicity observed with pSinCCHF-52M could also have been due to the intrinsic properties of the glycoprotein gene. In a separate study by a colleague in our department, the gene encoding NSm protein from the same glycoprotein sequence downregulated expression of numerous innate immune response markers in transfected HEK-293 cells (Viljoen N, unpublished Ph.D.). The genes encoding retinoic acid-inducible gene-I (RIG-1), interferon beta (IFN- β), IFN-receptor and signal transducer and activator of transcription (STAT-1) were downregulated. RIG-1 recognizes CCHFV RNA in the cytoplasm stimulating type 1 interferon response (Spengler et al. 2015). Activation of STAT-1 guides innate and adaptive immune responses (Stockinger and Decker 2009) and interferons besides possessing antiviral properties are a vital cog between the innate and humoral immunity activating dendritic, CD4⁺ and CD8⁺ T cells (Hervas-Stubbs et al. 2011). Successful activation of the innate immune response is critical for the induction of robust adaptive immune responses. Innate immune marker downregulation may explain the observed reduction in cytokine secretion by cells from mice co-immunized with pSinCCHF-52S and pSinCCHF-52M compared to immunization with pSinCCHF-52S by itself. However, it remains to be demonstrated if downregulation of these innate immune markers occurs *in vivo*.

Current understanding informed by successful efficacy studies seems to suggest that mice protection following lethal CCHFV challenge is mediated by immune markers directed against the GP. This makes the GP an antigen of choice. On the other hand efficacy studies employing the NP have been few despite the antigen being recognized as highly immunogenic. A vaccine candidate by Dowal et al did not confer protection though it elicited humoral and cellular immune responses in immunized animals. Zivcec et al reported a 33% survival rate after lethal viral challenge. Both studies used the NP from the IbAr 10200 CCHF strain and the antigens were viral vectored. The latest study by Zivcec et al, however, suggests that NP-specific immune responses may play a role in conferring protection from lethal viral challenge. While in this study we could not do challenge studies, the NP from a CCHFV South African strain expressed by Sindbis DNA replicon induced high titers of CCHFV NP-specific antibodies and Th type 1 cytokines in mice following immunization. Neutralizing antibodies are likely to be induced by the GP not NP even though immune correlates of protection are not yet described. Fatal cases are characterized by the absence of humoral immune responses. It is not yet established if it is a case of dying before antibody induction or death is a consequence of no antibody response. Although we could not assay for neutralizing antibodies as it requires BSL-4 facilities to grow the virus it will be interesting to investigate how our vaccine candidate will fare in lethal viral challenge studies.

The intramuscular delivery is a popular route of DNA vaccine administration after studies in rodents had demonstrated that the muscle presents the best transfection efficiencies (Fynan et al. 1993). As such our vaccine constructs were delivered via the intramuscular route. This route of vaccine delivery requires more plasmid DNA when compared to gene gun delivery approaches. Nonetheless, a range of DNA vaccine dosages have been administered through the intramuscular route with success. Some researchers have used 100 µg per immunization (Ljungberg et al. 2007) while others have used as low as 0.08 µg per dosage (Knudsen et al. 2012). In our study, we used 100µg per immunization. In some studies, researchers have compared a range of doses which we could not do because of the costs associated. Ljungberg et al compared the immunogenicity of 100 µg, 10 µg and 1 µg of a VEE based replicon encoding human immunodeficiency virus type 1 gp160 while Leitner et al assessed the immunogenicity of a Sindbis based replicon encoding β-gal in mice after immunization with three doses (10 µg, 1 µg and 0.1 µg). Though lower doses seemed to induce higher cellular and humoral immune responses, there was no statistical difference between the groups. These results perhaps mean high doses are not necessary or that more studies are needed.

The role of polyinosinic-polycytidylic acid (poly (I:C)) as an adjuvant was investigated. Poly(I:C) exerts its adjuvant effects by activating pathogen recognition receptors promoting induction of type 1 interferons and Th 1 cellular immunity (Coffman et al. 2010). Type 1 immunity has been reported in successful efficacy studies thus cell-mediated immune enhancing effects of poly (I:C) were investigated in our study. However, poly (I:C) did not result in enhanced cellular immune responses as anticipated. This is in contrast to a study by Ma et al who reported enhanced cellular and humoral immune responses after co-administration of poly (I:C) and a plasmid DNA vaccine expressing eastern equine encephalitis virus (EEEV) genes *C*, *E3*, *E2*, *6K* and *E1*. Although the same immunization schedule was used to inoculate similar amounts of poly (I:C) and plasmid DNA per mouse (50µg and 100µg respectively) and there are differences with this present study. In our study, we used NIH mice to evaluate the immunogenicity of CCHFV nucleoprotein and glycoproteins expressed by the Sindbis virus replicon while Ma et al used BALB/c mice to evaluate the immunogenicity of EEEV genes (*C*, *E3*, *E2*, *6K* and *E1*) expressed by the pcDNA3.1 vector. These differences make comparisons of the results obtained in the two studies difficult.

Besides that, the poly (I:C) used in our study is subject to rapid degradation by cellular nucleases upon injection into cells despite reported success in some studies (Pulko et al. 2009, Currie et al. 2008, Salem et al. 2005). To prevent degradation by cellular nucleases poly (I:C) is stabilized carboxymethylcellulose and poly-L-lysine (poly ICLC) (Longhi et al. 2009). Poly (I:C) and its nuclease resistant analog poly ICLC are being investigated for cancer immunotherapy but immune responses have been variable (Caskey et al. 2011). One proposed role of adjuvants is that they act as a depot for the antigen thus allowing slow release of antigen resulting in continual stimulation of the immune system (Awate et al. 2013). This is efficiently achieved when the adjuvant complexes with the antigen. This

is not the case with Poly (I:C) and plasmid DNA both of which are negatively charged. Protein expression by DNA vectors takes several hours and without the two interacting, the protein may start accumulating when the poly (I:C) has been degraded. Moreover, poly (I:C) has been shown to induce apoptosis in several mammalian cells when it engages TLR3 (Paone et al. 2008, Sun et al. 2011, Weber et al. 2010). Given the possibility that poly (I:C) is likely to exert its effects first (if it is not degraded) before the transfected cells fully express the protein, apoptosis may further limit protein expression especially that the replicons themselves also induce apoptosis. The amount of antigen produced after DNA vaccination is already limited because of inefficient transfection of host cells (Bins et al. 2013). The other scenario is that by signaling type 1 interferons production, poly (I:C) produces an antiviral state in cells hinders viral replicase activity. On the other hand, TLR3 signaling possesses an extra advantage in that it promotes antigen cross-presentation (Steinhagen et al. 2011). This is key in DNA vaccination in which somatic cells at the injection site are most likely to be transfected after vaccine delivery at the expense of antigen presenting cells which are pivotal in immune induction. Cross-priming of antigen-presenting cells by somatic cells ensues resulting in priming of CD8⁺ T cells (Ulmer and Otten 2000). Promoting cross-priming is therefore vital and is believed to improve the immunogenicity of DNA vaccines. Besides TLR3, poly (I:C) activates other pathogen recognition receptors such as MDA-5 thus its adjuvanticity is not restricted to TLR3 signaling (Steinhagen et al. 2011).

Although already existing immunity against alphaviruses may interfere with vaccinations, the threat is not as notable as with adenovirus vectors. Sindbis virus like most other alphaviruses (except Chikungunya virus) is endemic in limited regions of the world. Human Sindbis outbreaks seldom occur thus it is only a small proportion of the human population with immunity against Sindbis virus. That said, the presence of antibodies in horses produced in response to infection with one alphavirus strain has been shown to impede productive infections with other alphaviruses (Calisher et al. 1973). What this means is that immunization with one replicon has the potential to hinder follow up vaccinations be it by replicons from the same viral strain or a different strain. Evidence substantiating this notion has been demonstrated in humans (McClain et al. 1998). In light of these findings, the effect of the international chikungunya virus outbreaks on alphavirus immunity particularly the use of alphavirus replicon vectors in vaccine development, therefore, needs investigation.

In summary, the study presented the preparation of Sindbis replicons expressing the nucleoprotein and the glycoprotein precursor of South African CCHFV strains, characterization of mammalian cells transfected with the prepared replicons and immunogenicity evaluation of the prepared replicons in an animal model. The CCHFV glycoprotein and nucleoprotein genes were amplified by RT-PCR and their nucleotide base sequences were confirmed by Sanger and next-generation sequencing. The functionality of prepared constructs was confirmed by performing protein expression in BHK-21 and HEK-293 cells. The ability of the constructs to transcribe CCHFV RNA was confirmed by assaying CCHFV gene-specific RNA. Induction of apoptosis by replicons was demonstrated by

analyzing the enrichment of nucleosomes in the cytoplasm of transfected BHK-21 cells. The replicon expressing the glycoprotein was poorly immunogenic failing to induce CCHFV glycoprotein-specific antibodies in vaccinated mice. However, mice immunization with pSinCCHF-52S generated high titers of CCHFV NP IgG antibodies and higher levels of Th1 type contrasted with Th2 type cytokines. IgG subtyping revealed higher levels of IgG2a compared to IgG1 confirming a predominant type 1 immune response. Induction of IgG2a and IgG1 in immunized mice may indicate the ability of the vaccine constructs to stimulate both arms of the immune system. Neutralizing antibodies against CCHFV are expected to bind to the mature glycoproteins on the viral surface thus antibodies against the GP are believed to confer protection. Nonetheless, in the absence of known correlates of protection, further studies in virus susceptible animals are necessary to determine whether the induced NP immune responses are protective. Our study shows the utility of Sindbis replicons in vaccine development against CCHFV.

References

- Abbas AK, Murphy KM, Sher A. Functional diversity of helper T lymphocytes. *Nature* 1996; 383(6603):787-93.
- Abdelmotelb AM, Rose-Zerilli MJ, Barton SJ, Holgate ST, et al. Alpha-tryptase gene variation is associated with levels of circulating IgE and lung function in asthma. *Clin Exp Allergy* 2013; 44(6):822–830.
- Adams MJ, Lefkowitz EJ, King AMQ, Harrach B, et al. Changes to taxonomy and the International Code of Virus Classification and Nomenclature ratified by the International Committee on Taxonomy of Viruses (2017). *Arch Virol* 2017; 162(8):2505-2538.
- Appel RD, Bairoch A, Hochstrasser DF. A new generation of information retrieval tools for biologists: the example of the ExPASy WWW server. *Trends Biochem Sci* 1994; 19 (6):258-60.
- Ahmed AA, McFalls JM, Hoffmann C, Filone CM, et al. Presence of broadly reactive and group-specific neutralizing epitopes on newly described isolates of Crimean-Congo hemorrhagic fever virus. *J Gen Virol* 2005; 86:3327–36.
- Akinci E, Bodur H, Leblebicioglu H. Pathogenesis of Crimean-Congo Hemorrhagic Fever. *Vector-Borne and Zoonotic Dis* 2013; 13(7):429-437.
- Albert ML, Pearce SF, Francisco LM, Sauter B, et al. Immature dendritic cells phagocytose apoptotic cells via alpha v beta 5 and CD36, and cross-present antigens to cytotoxic T lymphocytes. *J Exp Med* 1998; 188:1359-1368.
- Anagnostou V, Papa A. Evolution of Crimean-Congo Hemorrhagic Fever virus. *Infect Genet Evol* 2009; 9(5):948-54.
- Appannanavar SB, Mishra B. An Update on Crimean Congo Hemorrhagic Fever. *J Glob Infect Dis* 2011; 3(3):285–292.
- Atanasiu P, Orth G, Rebiere JP, Boiron M, et al. Production of tumors in the hamster by inoculation of deoxyribonucleic acid extracted from tissue cultures infected with polyoma virus. *C R Hebd Seances Acad Sci* 1962; 254:4228–30.
- Atkinson B, Chamberlain J, Logue CH, Cook N, et al. Development of a real-time RT-PCR assay for the detection of Crimean-Congo hemorrhagic fever virus. *Vector Borne Zoonotic Dis* 2012; 12(9):786-93.
- Aradaib IE, Erickson BR, Karsany MS, Khristova ML, et al. Multiple Crimean- Congo hemorrhagic fever virus strains are associated with disease outbreaks in Sudan, 2008–2009. *PLoS Negl Trop Dis* 2011; 5:e1159.
- Aradaib IE, Erickson BR, Mustafa ME, Khristova ML, et al. Nosocomial Outbreak of Crimean-Congo Hemorrhagic Fever, Sudan. *Emerg Infect Dis* 2010; 16(5):837–839.
- Arslan S, Engin A, Özbilüm N, Bakır M. Toll-like receptor 7 Gln11Leu, c.4-151A/G, and +1817G/T polymorphisms in Crimean Congo hemorrhagic fever. *J Med Virol* 2015; 87(7):1090–5.

Arslan S, Engin A. Relationship between NF- κ B1 and NF- κ BIA genetic polymorphisms and Crimean-Congo hemorrhagic fever. *Scand J Infect Dis* 2012; 44(2):138–43.

Awate S, Babiuk LA, Mutwiri G. Mechanisms of Action of Adjuvants. *Front Immunol* 2013; 4:114.

Ayad LAK, Pissis SP. MARS: improving multiple circular sequence alignment using refined sequences. *BMC Genomics* 2017; 18:86.

Azevedo V, Levitus G, Miyoshi A, Cândido AL, et al. Main features of DNA-based immunization vectors. *Braz J Med Biol Res* 1999; 32(2):147- 153.

Bajpai S, Nadkar MY. Crimean Congo hemorrhagic fever: requires vigilance and not panic. *J Assoc Physicians India* 2011; 59:164-7.

Banfalvi G. Methods to detect apoptotic cell death. *Apoptosis* 2017; 22(2):306-323.

Bankevich A, Nurk S, Antipov D, Gurevich AA, et al. SPAdes: A New Genome Assembly Algorithm and Its Applications to Single-Cell Sequencing. *J Comput Biol* 2012; 19(5):455–477.

Barnwal B, Karlberg H, Mirazimi A, Tan YJ. The Non-structural Protein of Crimean-Congo Hemorrhagic Fever Virus Disrupts the Mitochondrial Membrane Potential and Induces Apoptosis. *J Biol Chem* 2016; 291(2):582-92.

Benmaamar R, Astray RM, Wagner R, Pereira CA. High-level expression of rabies virus glycoprotein with the RNA-based Semliki Forest Virus expression vector. *J Biotechnol* 2009 23; 139(4):283-90.

Bente DA, Forrester NL, Watts DM, McAuley AJ, et al. Crimean-Congo hemorrhagic fever: History, epidemiology, pathogenesis, clinical syndrome and genetic diversity. *Antivir Res* 2013; 100:159–189.

Bente DA, Alimonti JB, Shieh WJ, Camus G, et al. Pathogenesis and immune response of Crimean-Congo hemorrhagic fever virus in a STAT-1 knockout mouse model. *J Virol* 2010; 84:11089–11100.

Berezky S, Lindegren G, Karlberg H, Akerström S, et al. Crimean-Congo hemorrhagic fever virus infection is lethal for adult type I interferon receptor-knockout mice. *J Gen Virol* 2010; 91(6):1473-7.

Bergeron E, Albariño CG, Khristova ML, Nichol ST. Crimean-Congo hemorrhagic fever virus-encoded ovarian tumor protease activity is dispensable for virus RNA polymerase function. *J Virol* 2010; 84:216–226.

Bertolotti-Ciarlet A, Smith J, Strecker K, Paragas J, et al. Cellular localization and antigenic characterization of Crimean-Congo hemorrhagic fever virus glycoproteins. *J Virol* 2005; 79:6152–6161.

Bins AD, van den Berg JH, Oosterhuis K, Haanen JB. Recent advances towards the clinical application of DNA vaccines. *Neth J Med* 2013; 71(3):1-9.

Blackburn NK, Besselaar TG, Shepherd AJ, Swanepoel R. Preparation and use of monoclonal antibodies for identifying Crimean-Congo hemorrhagic fever virus. *Am J Trop Med Hyg* 1987; 37:392–397.

Black WC, Piesman J. Phylogeny of hard- and soft-tick taxa (Acari: Ixodida) based on mitochondrial 16S rDNA sequences. *Proc Natl Acad Sci USA* 1994; 91(21):10034-8.

Bodur H, Akinci E, Ascioglu S, Öngürü P, et al. Subclinical Infections with Crimean-Congo Hemorrhagic Fever Virus, Turkey. *Emerg Infect Dis* 2012; 18(4):640–642.

Bodur H, Erbay A, Akinci E, Öngürü P, et al. Effect of oral ribavirin treatment on the viral load and disease progression in Crimean-Congo hemorrhagic fever. *Int J Infect Dis* 2011; 15:e44–e47.

Bonney LC, Watson RJ, Afrough B, Mullojonova M, et al. A recombinase polymerase amplification assay for rapid detection of Crimean-Congo Haemorrhagic fever Virus infection. *PLoS Negl Trop Dis* 2017; 11(10):e0006013.

Boshra H, Lorenzo G, Rodriguez F, Brun A. A DNA vaccine encoding ubiquitinated Rift Valley fever virus nucleoprotein provides consistent immunity and protects IFNAR^{-/-} mice upon lethal virus challenge. *Vaccine* 2011; 29:4469–75.

Bronte V, Pittet MJ. The spleen in local and systemic regulation of immunity. *Immunity* 2013; 39(5):806–818.

Brulet J-M, Maudoux F, Thomas S, Thielemans K, et al. DNA vaccine encoding endosome-targeted human papillomavirus type 16 E7 protein generates CD4⁺ T cell-dependent protection. *Eur J Immunol* 2007; 37:376-84.

Begum F, Wissernan CL Jr, Casals J. Tick-borne viruses of West Pakistan. IV. Viruses similar to, or identical with, Crimean hemorrhagic fever (Congo- Semunya), Wad Medani and Pak Argas 461 isolated from ticks of the Changa Manga Forest, Lahore District, and Hunza, Gilgit Agency, W. Pakistan. *Am J Epidemiol* 92:197-202.

Bukbuk DN, Dowall SD, Lewandowski K, Bosworth A, et al. Serological and Virological Evidence of Crimean-Congo Haemorrhagic Fever Virus Circulation in the Human Population of Borno State, Northeastern Nigeria. *PLoS Negl Trop Dis* 2016; 10 (12):e0005126.

Burney MI, Ghafoor A, Saleen M, Webb PA, et al. Nosocomial outbreak of viral hemorrhagic fever caused by Crimean Hemorrhagic Fever-Congo virus in Pakistan. *Am J Trop Med Hyg* 1976; 29:941-947.

Burt FJ. Laboratory diagnosis of Crimean–Congo hemorrhagic fever virus infections. *Future Virol* 2011; 6(7):831–841.

Burt FJ, Paweska JT, Ashkettle B, Swanepoel R. Genetic relationship in southern African Crimean–Congo haemorrhagic fever virus isolates: evidence for occurrence of reassortment. *Epidemiol Infect* 2009; 137:1302–1308.

Burt FJ, Paweska JT, Swanepoel R. Crimean-Congo haemorrhagic fever in South Africa. In *Crimean-Congo haemorrhagic fever*. (eds C Whitehouse, O Ergonul) Springer Press. 2007.

Burt FJ, Leman PA, Smith JF, Swanepoel R. The use of a reverse transcription-polymerase chain reaction for the detection of viral nucleic acid in the diagnosis of Crimean-Congo haemorrhagic- fever. *J Virol Methods* 1998; 70:129-37.

Burt FJ, Swanepoel R, Shieh WJ, Smith JF, et al. Immunohistochemical and in situ localization of Crimean-Congo hemorrhagic fever (CCHF) virus in human tissues and implications for CCHF pathogenesis. *Arch Pathol Lab Med* 1997; 121:839-46.

Burt FJ, Spencer DC, Leman PA, Patterson B, et al. Investigation of tick-borne viruses as pathogens of humans in South Africa and evidence of Dugbe virus infection in a patient with prolonged thrombocytopenia. *Epidemiol Infect.* 1996; 116:353–61.

Burt FJ, Leman PA, Abbott JC, Swanepoel R. Serodiagnosis of Crimean–Congo haemorrhagic fever. *Epidemiol Infect* 1994; 113(3):551–562.

Butenko, A.M. et al. (1968) Isolation and investigation of Astrakhan strain (“Drozdo”) of Crimean hemorrhagic fever virus and data on serodiagnosis of this infection. *Mater. 15 Nauchn. Sess. Inst. Polio Virus Entsefalitov (Moscow)* 3, 88–90 (in Russian; in English, NAMRU3-T866). In: Whitehouse, C.A. (2004) Crimean-Congo hemorrhagic fever. *Antivir Res* 145-60.

Buttigieg KR, Dowall SD, Findlay-Wilson S, Miloszewska A, et al. A novel vaccine against Crimean-Congo Haemorrhagic Fever protects 100% of animals against lethal challenge in a mouse model. *PloS One* 2014; 9:e91516.

Casals J, Henderson BE, Hoogstraal H, Johnson KM. et al. A review of Soviet viral hemorrhagic fevers. *J Infect Dis* 1970; 122:437–453.

Casals J. Antigenic similarity between the virus causing Crimean hemorrhagic fever and Congo virus. *Proc Soc Exp Biol Med* 1969; 131:233–236.

Cagatay A, Kapmaz M, Karadeniz A, Basaran S, et al. Haemophagocytosis in a patient with Crimean Congo haemorrhagic fever. *J Med Microbiol* 2007; 56:1126–1128.

Calisher CH, Sasso DR, Sather GE. Possible evidence for interference with Venezuelan equine encephalitis virus vaccination of equines by pre-existing antibody to Eastern or Western Equine encephalitis virus, or both. *Appl Microbiol* 1973; 26(4):485-8.

Canakoglu N, Berber E, Tonbak S, Ertek M, et al. Immunization of Knock-Out α/β Interferon Receptor Mice against High Lethal Dose of Crimean-Congo Hemorrhagic Fever Virus with a Cell Culture Based Vaccine. *PLoS Neglected Trop Dis* 2015; 9:e0003579.

Capodagli GC, Deaton MK, Baker EA, Lumpkin RJ, et al. Diversity of ubiquitin and ISG15 specificity among nairoviruses' viral ovarian tumor domain proteases. *J Virol* 2013; 87(7):3815-27.

Caskey M, Lefebvre F, Filali-Mouhim A, Cameron MJ, et al. Synthetic double-stranded RNA induces innate immune responses similar to a live viral vaccine in humans. *J Exp Med* 2011; 208(12):2357-66.

Causey OR, Kemp GE, Madbouly MH, David-West TS. Congo virus from domestic livestock, African hedgehog, and arthropods in Nigeria. *Am J Trop Med Hyg* 1970; 19:846–850.

- Ceianu CS, Panculescu-Gatej RI, Coudrier D, Bouloy M. First serologic evidence for the circulation of Crimean-Congo hemorrhagic fever virus in Romania. *Vector Borne Zoonotic Dis* 2012; 12(9):718-21.
- Celis E. Toll-like receptor ligands energize peptide vaccines through multiple paths. *Cancer Res* 2007; 67(17):7945-7.
- Cella M, Salio M, Sakakibara Y, Langen H, et al. Maturation, activation, and protection of dendritic cells induced by double-stranded RNA. *J Exp Med* 1999; 189:821-829.
- Cevik MA, Elaldi N, Akinci E, Onguru P, et al. 2008. A preliminary study to evaluate the effect of intravenous ribavirin treatment on survival rates in Crimean-Congo hemorrhagic fever. *J Infect* 2008; 57:350–351.
- Charrel RN, Attoui H, Butenko AM, Clegg JC, et al. Tick-borne virus disease of human interest in Europe. *Clin Microbiol Infect* 2004; 10:1040-1055.
- Chatellard P, Pankiewicz R, Meier E, Durrer L, et al. The IE2 promoter/enhancer region from mouse CMV provides high levels of therapeutic protein expression in mammalian cells. *Biotechnol Bioeng* 2007; 96:106–17.
- Chen JP, Cosgriff TM. Hemorrhagic fever virus-induced changes in hemostasis and vascular biology. *Blood Coagul Fibrinolysis* 2000; 11:461–483.
- Chinikar S, Mazaheri V, Mirahmadi R, Nabeth P, et al. A serological survey in suspected human patients of Crimean-Congo hemorrhagic fever in Iran by determination of IgM-specific ELISA method during 2000 – 2004. *Arch Iranian Med* 2005; 8 (1):52 – 55.
- Chumakov, M.P. (1974) On 30 years of investigation of Crimean hemorrhagic fever. *Tr. Inst. Polio Virusn. Entsefalitov Akad. Med. Nauk SSSR* 22, 5–18 (in Russian; in English, NAMRU3-T950). In: Whitehouse, C.A. (2004) Crimean-Congo hemorrhagic fever. *Antivir Res* 145-60.
- Chumakov MP, Smirnova SE, Tkachenko EA. Relationship between strains of Crimean haemorrhagic fever and Congo viruses. *Acta Virol* 1970; 14:82–85.
- Chumakov, M.P. et al. (1968) New data on the virus causing Crimean hemorrhagic fever (CHF). *Vopr. Virusol.* 13, 377 (in Russian; in English, NAMRU3-T596). In: Whitehouse CA. (2004) Crimean-Congo hemorrhagic fever. *Antivir Res* 145-60.
- Christova I, Kovacheva T, Georgieva D, Ivanova S, et al. Vaccine against Congo-Crimean haemorrhagic fever virus—Bulgarian input in fighting the disease. *Probl Infect Parasit Dis* 2010; 37:7–8.
- Coffman RL, Sher A, Seder RA. Vaccine adjuvants: putting innate immunity to work. *Immunity* 2010; 33(4):492-503.
- Coffman RL, Lebman DA, Rothman P. Mechanism and regulation of immunoglobulin isotype switching. *Adv Immunol* 1993; 54:229-70.
- Colby LA, Quenee LE, Zitzow LA. Considerations for Infectious Disease Research Studies Using Animals. *Comp Med* 2017; 67(3): 222–231.

Connolly-Andersen AM. Pathogenesis of an emerging pathogen-Crimean-Congo hemorrhagic fever. Thesis, Stockholm, 2010.

Currie AJ, van der Most RG, Broomfield SA, Prosser AC, et al. Targeting the effector site with IFN- α inducing TLR ligands reactivates tumor-resident CD8 T cell responses to eradicate established solid tumors. *J Immunol* 2008; 180(3):1535-44.

Covello G, Siva K, Adami V, Denti MA. An electroporation protocol for efficient DNA transfection in PC12 cells. *Cytotechnology* 2014; 66(4):543–553.

Davis ME, Gack MU. Ubiquitination in the antiviral Immune response. *Virology* 2015; 479-480:52-65.

Deyde VM, Khristova ML, Rollin PE, Ksiazek TG, et al. Crimean-Congo hemorrhagic fever virus genomics and global diversity. *J Virol* 2006; 80:8834–8842.

de Groot RJ, Hardy WR, Shrako Y, Strauss J. Cleavage-site preferences of Sindbis virus polyproteins contains the non-structural proteinase. Evidence for temporal regulation of polyprotein processing in vivo. *EMBO J* 1990; 9(8): 2631–2638.

Dickson DL, Turell MJ. Replication and tissue tropisms of Crimean–Congo hemorrhagic fever virus in experimentally infected adult *Hyalomma truncatum* (Acari: Ixodidae). *J Med Entomol* 1992; 29:767–773.

Dowall SD, Carroll MW, Hewson R. Development of vaccines against Crimean-Congo haemorrhagic fever virus. *Vaccine*. 2017; 35(44):6015-6023.

Dowall SD, Buttigieg KR, Findlay-Wilson SJ, Rayner E, et al. A Crimean-Congo hemorrhagic fever (CCHF) viral vaccine expressing nucleoprotein is immunogenic but fails to confer protection against lethal disease. *Hum Vaccines Immunother* 2016; 12:519–27.

Drosten C, Kümmerer BM, Schmitz H, Günther S. Molecular diagnostics of viral hemorrhagic fevers. *Antiviral Res* 2003; 57:61–87.

Drosten C, Götting S, Schilling S, Asper M, et al. Rapid detection and quantification of RNA of Ebola and Marburg viruses, Lassa virus, Crimean-Congo hemorrhagic fever virus, Rift Valley fever virus, dengue virus, and yellow fever virus by real-time reverse transcription-PCR. *J Clin Microbiol* 2002a; 40(7):2323-30.

Drosten C, Minnak D, Emmerich P, Schmitz H. Crimean-Congo Hemorrhagic Fever in Kosovo. *J Clin Microbiol*. 2002b; 40(3):1122–1123.

Dubensky TW Jr, Driver DA, Polo JM, Belli BA, et al. Sindbis virus DNA-based expression vectors: utility for in vitro and in vivo gene transfer. *J Virol* 1996; 70(1):508- 19.

Duh D, Saksida A, Petrovec M, Dedushaj I, et al. Novel one-step real-time RT-PCR assay for rapid and specific diagnosis of Crimean-Congo hemorrhagic fever encountered in the Balkans. *J Virol Methods* 2006; 133(2):175-9.

Dunster L, Dunster M, Ofula V, Beti D, et al. First Documentation of Human Crimean-Congo Hemorrhagic Fever, Kenya. *Emerg Infect Dis* 2002; 8(9):1005–1006.

Durden LA, Logan TM, Wilson ML, Linthicum KJ. Experimental vector incompetence of a soft tick, *Ornithodoros sonrai* (Acari: Argasidae), for Crimean–Congo hemorrhagic fever virus. *J Med Entomol* 1993; 30:493–496.

Eickhoff C, Jose R, Vasconcelos JR, Sullivan NL, et al. Co-administration of a plasmid DNA encoding IL-15 improves long-term protection of a genetic vaccine against *Trypanosoma cruzi*. *PLoS Negl Trop Dis* 2011; 5:e983.

Edfors F, Danielsson F, Hallström BM, Käll L, et al. Gene-specific correlation of RNA and protein levels in human cells and tissues. *Molecular Systems Biology* 2016; 12:883.

Elata AT, Karsany MS, Elageb RM, Hussain MA, et al. A nosocomial transmission of crimean-congo hemorrhagic fever to an attending physician in North Kordufan, Sudan. *Viol J* 2011; 8(1):303.

El Azazy OM, Scrimgeour EM. Crimean-Congo haemorrhagic fever virus infection in the western province of Saudi Arabia. *Trans R Soc Trop Med Hyg* 1997; 91:275-278.

Elliott RM, Schmaljohn CS, Collett MS. Bunyaviridae genome structure and gene expression. *Curr Top Microbiol Immunol* 1991; 169:91–141.

Elmore S. Apoptosis: a review of programmed cell death. *Toxicol Pathol* 2007; 35:495–516.

Engin A, Arslan S, Kizildag S, Oztürk H, et al. Toll-like receptor 8 and 9 polymorphisms in Crimean-Congo hemorrhagic fever. *Microbes Infect* 2010; 12(12–13):1071–8.

Ergonul O. Crimean-Congo hemorrhagic fever virus: new outbreaks, new discoveries. *Curr Op* 2012; 2:215-220.

Ergonul O, Whitehouse CA. Crimean-Congo Hemorrhagic Fever. A Global Perspective. Dordrecht (the Netherlands): Springer 2007:75-88.

Ergonul O, Celikbas A, Baykam N, Eren S, et al. Analysis of risk-factors among patients with Crimean-Congo haemorrhagic fever virus infection: severity criteria revisited. *Clin Microbiol Infect* 2006; 12(6):551-4.

Ergonul O. Crimean-Congo haemorrhagic fever. *Lancet Infect Dis* 2006; 6:203–14.

Ergunay K, Kocak Tufan Z, Bulut C, Kinikli S, et al. Antibody responses and viral load in patients with Crimean-Congo hemorrhagic fever: a comprehensive analysis during the early stages of the infection. *Diagn Microbiol Infect Dis* 2014; 79(1):31-6.

Estrada-Pena A, Palomar AM, Santibanez P, Sanchez N, et al. Crimean-Congo hemorrhagic fever virus in ticks, Southwestern Europe, 2010. *Emerg Infect Dis* 2012; 18(1):179-80.

Fagone P, Shedlock DJ, Bao H, Kawalekar OU, et al. Molecular adjuvant HMGB1 enhances anti-influenza immunity during DNA vaccination. *Gene Ther* 2011; 18:1070-7.

Fenwick N, Griffin G, Gauthier C. The welfare of animals used in science: How the “Three Rs” ethic guides improvements. *Can Vet J* 2009; 50(5):523–530.

Ferraro B, Morrow MP, Hutnick NA, Shin TH, et al. Clinical Applications of DNA Vaccines: Current Progress. *Clin Infect Dis* 2011; 53(3):296–302.

Filipe AR, Calisher CH, Lazuick J. Antibodies to Congo-Crimean haemorrhagic fever, Dhori, Thogoto and Bhanja viruses in southern Portugal. *Acta Virol* 1985; 29(4):324–8.

Flingai S, Czerwonko M, Goodman J, Kudchodkar SB, et al. Synthetic DNA vaccines: improved vaccine potency by electroporation and co-delivered genetic adjuvants. *Front Immunol* 2013; 4(354):1–8.

Foulke RS, Rosato RR, French GR. Structural polypeptides of Hazara virus. *J Gen Virol* 1981; 53:169–172.

Fritzen A, Risinger C, Korukluoglu G, Christova I, et al. Epitope-mapping of the glycoprotein from Crimean-Congo hemorrhagic fever virus using a microarray approach. *PLoS Negl Trop Dis* 2018; 12(7): e0006598.

Frolov I, Hoffman TA, Prágai BM, Dryga SA, et al. Alphavirus-based expression vectors: strategies and applications. *Proc Natl Acad Sci USA* 1996; 93(21):11371–11377.

Frolov I, Schlesinger S. Comparison of the effects of Sindbis virus and Sindbis virus replicons on host cell protein synthesis and cytopathogenicity in BHK cells. *J Virol* 1994; 68(3):1721–1727.

Fynan EF, Webster RG, Fuller DH, Haynes JR et al. DNA vaccines: protective immunizations by parenteral, mucosal, and gene-gun inoculations. *Proc Natl Acad Sci USA* 1993; 90(24):11478–11482.

Garcia Rada A. First outbreak of Crimean-Congo haemorrhagic fever in western Europe kills one man in Spain. *BMJ* 2016; 354:i4891.

Gargili A, Midilli K, Ergonul O, Ergin S, et al. 2011. Crimean–Congo hemorrhagic fever in European part of Turkey: genetic analysis of the virus strains from ticks and a seroepidemiological study in humans. *Vector Borne Zoonotic Dis* 2011; 11:747–752.

Garrison AR, Shoemaker CJ, Golden JW, Fitzpatrick CJ, et al. A DNA vaccine for Crimean-Congo hemorrhagic fever protects against disease and death in two lethal mouse models. *PLoS Negl Trop Dis* 2017; 11(9):e0005908.

Garrison AR, Alakbarova S, Kulesh DA, Shezmukhamedova D, et al. Development of a TaqMan minor groove binding protein assay for the detection and quantification of Crimean-Congo hemorrhagic fever virus. *Am J Trop Med Hyg* 2007; 77(3):514–20.

Gear JH, Thomson PD, Hopp M, Andronikou S, et al. Congo-Crimean haemorrhagic fever in South Africa. Report of a fatal case in the Transvaal. *S Afr Med J* 1982; 62:576–580.

Gerdts V, Wilson HL, Meurens F, van Drunen Littel-van den Hurk S, et al. Large animal models for vaccine development and testing. *ILAR J* 2015; 56(1):53-62.

Ghiasi SM, Salmanian AH, Chinikar S, Zakeri S. Mice orally immunized with a transgenic plant expressing the glycoprotein of Crimean-Congo hemorrhagic fever virus. *Clin Vaccine Immunol* 2011; 18:2031–7.

Gilbert SC. Clinical development of Modified Vaccinia virus Ankara vaccines. *Vaccine* 2013; 31(39):4241-6

Goedhals D, Paweska JT, Burt FJ. Long-lived CD8⁺ T cell responses following Crimean-Congo haemorrhagic fever virus infection. *PLoS Negl Trop Dis* 2017; 11(12):e0006149.

Goedhals D, Bester PA, Paweska JT, Swanepoel R, et al. Next-generation sequencing of southern African Crimean-Congo haemorrhagic fever virus isolates reveals a high frequency of M segment reassortment. *Epidemiol Infect* 2014; 142(9):1952-62.

Gonzalez JP, Wilson ML, Cornet JP, Camicas JL. Host passage- induced phenotypic changes in Crimean–Congo haemorrhagic fever virus. *Res Virol* 1995; 146:131–140.

Gonzalez-Scarano F, Pobjecky N, Nathanson N. La Crosse bunyavirus can mediate pH-dependent fusion from without. *J Virol* 1984; 132(1):222–225.

Gorchakov R, Volkova E, Yun N, Petrakova O, et al. Comparative analysis of the alphavirus-based vectors expressing Rift Valley fever virus glycoproteins. *Virol* 2007; 366:212–225.

Graci JD, Cameron CE. Mechanisms of action of ribavirin against distinct viruses. *Rev Med Virol* 2006; 16:37–48.

Grey HM, Hirst JW, Cohn M. A new mouse immunoglobulin: IgG3. *J Exp Med* 1971; 133(2):289–304.

Haddock E, Feldmann F, Hawman DW, Zivcec M, et al. A cynomolgus macaque model for Crimean–Congo haemorrhagic fever. *Nat Microbiol* 2018; 3(5):556-562.

Hanahan D. Studies on transformation of *Escherichia coli* with plasmids. *J Mol Biol* 1983; 166(4):557-80.

Hariharan MJ, Driver DA, Townsend K, Brumm D, et al. DNA Immunization against Herpes Simplex Virus: Enhanced efficacy using a Sindbis virus-based vector. *J Virol* 1998; 72(2):950–958.

Hatipoglu CA, Bulut C, Yetkin MA, Ertem GT, et al. Evaluation of clinical and laboratory predictors of fatality in patients with Crimean-Congo haemorrhagic fever in a tertiary care hospital in Turkey. *Scand J Infect Dis* 2010; 42(6-7):516-21.

Hemachudha T, Griffin DE, Giffels JJ, Johnson RT, et al. Myelin basic protein as an encephalitogen in encephalomyelitis and polyneuritis following rabies vaccination. *N Engl J Med* 1987; 316:369–374.

Hervas-Stubbs S, Perez-Gracia JL, Rouzaut A, Sanmamed MF, et al. Direct effects of type I interferons on cells of the immune system. *Clin Cancer Res* 2011; 17(9):2619-27.

Herweijer H, Latendresse JS, Williams P, Zhang G, et al. A plasmid-based self-amplifying Sindbis virus vector. *Hum Gene Ther* 1995; 6(9):1161-7.

Hewson R, Gmyl A, Gmyl L, Smirnova SE, et al. Evidence of segment reassortment in Crimean-Congo haemorrhagic fever virus. *J Gen Virol* 2004a; 85(10):3059-70.

Hewson R, Chamberlain J, Mioulet V, Lloyd G, et al. Crimean-Congo haemorrhagic fever virus: sequence analysis of the small RNA segments from a collection of viruses worldwide. *Virus Res* 2004b; 102(2):185-9.

Higuchi R, Dollinger G, Walsh PS, Griffith R. Simultaneous amplification and detection of specific DNA sequences. *Biotechnology (N Y)* 1992; 10(4):413-7.

Hikke MC, Pijlman GP. Veterinary Replicon Vaccines. *Annu Rev Anim Biosci* 2017; 5:89-109.

Hinkula J, Devignot S, Åkerström S, Karlberg H, et al. Immunization with DNA plasmids coding for Crimean-Congo hemorrhagic fever virus capsid and envelope proteins and/or virus-like particles induces protection and survival in challenged mice. *J Virol* 2017; 91(10):e02076-16.

Hoogstraal, H. The epidemiology of tick-borne Crimean-Congo Hemorrhagic Fever Virus in Asia, Europe and Africa. *J Med Entomol* 1979; 15(4):307-417.

Holman DH, Penn-Nicholson A, Wang D, Woraratanadham J, et al. A complex adenovirus- vectored vaccine against Rift Valley fever virus protects mice against lethal infection in the presence of preexisting vector immunity. *Clin Vaccine Immunol* 2009; 16:1624–1632.

Izadi SSM. Evaluation of the efficacy of ribavirin therapy on survival of Crimean-Congo hemorrhagic fever patients: a case–control study. *Jpn J Infect Dis* 2009:11–15.

Jääskeläinen AJ, Kallio-Kokko H, Ozkul A, Bodur H, et al. Development and evaluation of a real-time RT-qPCR for detection of Crimean-Congo hemorrhagic fever virus representing different genotypes. *Vector Borne Zoonotic Dis* 2014; 14(12):870-2.

James TW, Frias-Staheli N, Bacik JP, Livingston Macleod JM, et al. Structural basis for the removal of ubiquitin and interferon-stimulated gene 15 by a viral ovarian tumor domain-containing protease. *Proc Natl Acad Sci USA* 2011; 108(6):2222-7.

Jelinek T. Japanese encephalitis vaccine in travelers. *Expert Rev Vaccines* 2008; 7:689–693.

Joyce CM, Benkovic SJ. DNA polymerase fidelity: kinetics, structure, and checkpoints. *Biochemistry* 2004; 43(45):14317-24.

Kallio K, Hellström K, Jokitalo E, Ahola T. RNA Replication and Membrane Modification Require the Same Functions of Alphavirus Nonstructural Proteins. *J Virol* 2015 18; 90(3):1687-92.

- Kamboj A, Pateriya AK, Mishra A, Ranaware P, et al. Novel molecular beacon probe-based real-time RT-PCR assay for diagnosis of Crimean-Congo hemorrhagic fever encountered in India. *BioMed Res Int* 2014; 2014:496219.
- Kamrud KI, Hooper JW, Elgh F, Schmaljohn CS. Comparison of the protective efficacy of naked DNA, DNA-based Sindbis replicon, and packaged Sindbis replicon vectors expressing Hantavirus structural genes in hamsters. *Virology* 1999; 263:209–219.
- Karti SS, Odabasi Z, Korten V, Yilmaz M, et al. Crimean-Congo hemorrhagic fever in Turkey. *Emerg Infect Dis* 2004; 10:1379-1384.
- Keshtkar-Jahromia M, Kuhn JH, Christova I, Bradfute SB, et al. Crimean-Congo hemorrhagic fever: Current and future prospects of vaccines and therapies. *Antivir Res* 2011; 90:85-92.
- Khan AS, Maupin GO, Rollin PE, Noor AM, et al. Scrimgeour EM. Crimean-Congo haemorrhagic fever in Oman. *Lancet* 1996; 347(9002):692.
- Kindt TJ, Goldsby RA, Osborne BA. *Kuby Immunology*. 6th Edition. New York: W.H Freeman and Co, 2007: 475–92.
- Kim JA, Cho K, Shin MS, Lee WG, et al. A novel electroporation method using a capillary and wire-type electrode. *Biosens Bioelectron* 2008; 15; 23(9):1353-60.
- Kim DY, Atasheva S, McAuley AJ, Plante JA, et al. Enhancement of protein expression by alphavirus replicons by designing self-replicating subgenomic RNAs. *Proc Natl Acad Sci* 2014; 111:10708–10713.
- Kızıldağ S, Arslan S, Özbilüm N, Engin A, et al. Effect of TLR10 (2322A/G, 720A/C, and 992T/A) polymorphisms on the pathogenesis of Crimean Congo hemorrhagic fever disease. *J Med Virol* 2018; 90(1):19–25.
- Ko H-J, Ko S-Y, Kim Y-J, Lee EG, et al. Optimization of Codon Usage Enhances the Immunogenicity of a DNA Vaccine Encoding Mycobacterial Antigen Ag85B. *Infect Immun* 2005; 73:5666-74.
- Knudsen ML, Mbewe-Mvula A, Rosario M, Johansson DX, et al. Superior induction of T cell responses to conserved HIV-1 regions by electroporated alphavirus replicon DNA compared to that with conventional plasmid DNA vaccine. *J Virol* 2012; 86(8):4082-90.
- Kortekaas J, Oreshkova N, Cobos-Jiménez V, Vloet RPM, et al. Creation of a non-spreading Rift Valley fever virus. *J Virol* 2011; 85:12622–12630.
- Kubar A, Hacımeroglu M, Ozkul A, Bagriacik U, et al. Prompt administration of Crimean–Congo hemorrhagic fever (CCHF) virus hyperimmunoglobulin in patients diagnosed with CCHF and viral load monitorization by reverse transcriptase-PCR. *Jpn J Infect Dis* 2011; 64:439-443.
- Kubista M, Andrade JM, Bengtsson M, Forootan A, et al. The real-time polymerase chain reaction. *Mol Aspects Med* 2006; 27(2-3):95-125.
- Kuhn JH, Wiley MR, Rodriguez SE, Bao Y, et al. Genomic characterization of the genus Nairovirus (family Bunyaviridae). *Viruses* 2016; 8(6):164.

- Laakso S, Mäki M. Assessment of a semi-automated protocol for multiplex analysis of sepsis-causing bacteria with spiked whole blood samples. *Microbiologyopen*. 2013; 2(2):284–292.
- Labuda M, Austyn JM, Zuffova E, Kozuch O, et al. Importance of localized skin infection in tick-borne encephalitis virus transmission. *Virology* 1996; 219(2):357-66.
- Lawyer FC, Stoffel S, Saiki RK, Chang SY, et al. High-level expression, purification, and enzymatic characterization of full-length *Thermus aquaticus* DNA polymerase and a truncated form deficient in 5' to 3' exonuclease activity. *PCR Methods Appl* 1993; 2(4):275-87.
- Leblebicioglu H, Ozaras R, Irmak H, Sencan I. Crimean-Congo hemorrhagic fever in Turkey: Current status and future challenges. *Antiviral Res* 2016; 126:21-34.
- Leitner WW, Bergmann-Leitner ES, Hwang LN, and Restifo NP. Type I interferons are essential for the efficacy of replicase-based DNA vaccines. *Vaccine* 2006; 24:5110-5118.
- Leitner WW, Hwang LN, Bergmann-Leitner ES, Finkelstein SE, et al. Apoptosis is essential for the increased efficacy of alphaviral replicase-based DNA vaccines. *Vaccine* 2004; 22(11-12):1537–1544.
- Leitner WW, Hwang LN, de Veer MJ, Zhou A, et al. Alphavirus-based DNA vaccine breaks immunological tolerance by activating innate antiviral pathways. *Nat Med* 2003; 9:33-9.
- Leitner WW, Ying H, Driver DA, Dubensky TW, et al. Enhancement of tumor-specific immune response with plasmid DNA replicon vectors. *Cancer Res* 2000; 60(1):51-5.
- Lesueur LL, Mir LM, Andre FM. Overcoming the specific toxicity of large plasmids electrotransfer in primary cells in vitro. *Mol Ther Nucleic Acids* 2016; 8(5):e291.
- Liu HS, Jan MS, Chou CK, Chen PH, et al. Is green fluorescent protein toxic to the living cells? *Biochem Biophys Res Commun* 1999; 260(3):712-7.
- Ljungberg K, Whitmore AC, Fluet ME, Moran TP, et al. Increased Immunogenicity of a DNA-Launched Venezuelan Equine Encephalitis Virus-Based Replicon DNA Vaccine. *J Virol* 2007; 81(24):13412–13423.
- Longhi MP, Trumpfheller C, Idoyaga J, Caskey M, et al. Dendritic cells require a systemic type I interferon response to mature and induce CD4⁺ Th1 immunity with poly IC as adjuvant. *J Exp Med* 2009; 206(7):1
- Loudon PT, Yager EJ, Lynch DT, Narendran A, et al. GM-CSF increases mucosal and systemic immunogenicity of an H1N1 influenza DNA vaccine administered into the epidermis of non-human primates. *PLoS One* 2010; 5:e11021.
- Ma J, Wang H, Zheng X, Xue X, et al. CpG/Poly (I:C) mixed adjuvant priming enhances the immunogenicity of a DNA vaccine against eastern equine encephalitis virus in mice. *Int Immunopharmacol* 2014; 19(1):74-80.
- Maes P, Clement J, Van Ranst M. Recent approaches in Hantavirus vaccine development. *Expert Rev Vaccines* 2009; 8:67–76.

- Maiga O, Sas MA, Rosenke K, Kamissoko B, et al. Serosurvey of Crimean–Congo Hemorrhagic Fever Virus in Cattle, Mali, West Africa. *Am J Trop Med Hyg.* 2017; 96(6):1341–1345.
- Maltezou HC, Papa A, Tsiodras S, Dalla V, et al. Crimean-Congo hemorrhagic fever in Greece: a public health perspective. *Int J Infect Dis* 2009; 13(6):713-6.
- Marriott AC, Polyzoni T, Antoniadis A, Nuttall PA. Detection of human antibodies to Crimean-Congo haemorrhagic fever virus using expressed viral nucleocapsid protein. *J Gen Virol* 1994; 75 (9):2157-61.
- Mariott AC, Nuttall PA. Comparison of S RNA segment and nucleoprotein sequences of Crimean Congo hemorrhagic fever, Hazara and Dugbe Virus. *Virol* 1992; 189:795-9.
- Mathiot CC, Fontenille D, Georges AJ, Coulanges P. Antibodies to haemorrhagic fever viruses in Madagascar populations. *Trans R Soc Trop Med Hyg* 1989; 83(3):407-9.
- Metanat M, Sharifi-Mood B, Salehi M, Alavi-Naini R. Clinical outcomes in Crimean-Congo hemorrhagic fever: a five-years experience in the treatment of patients in oral ribavirin. *Int J Virol* 2006; 2:21–24.
- McClain DJ, Pittman PR, Ramsburg HH, Nelson GO, et al Immunologic interference from sequential administration of live attenuated alphavirus vaccines. *J Infect Dis* 1998; 177(3):634-41.
- McGinty RK, Tan S. Nucleosome Structure and Function. *Chem Rev* 2015; 115(6):2255–2273.
- McKenna PM, Koser ML, Carlson KR, Montefiori DC, et al. Highly attenuated rabies virus-based vaccine vectors expressing simian-human immunodeficiency virus 89.6P Env and simian immunodeficiency virus mac239 Gag are safe in rhesus macaques and protect from an AIDS-like disease. *J Infect Dis* 2007; 195:980–988.
- Miller A, Center RJ, Stambas J, Deliyannis G, et al. Sindbis virus vectors elicit hemagglutinin-specific humoral and cellular immune responses and offer a dose-sparing strategy for vaccination. *Vaccine* 2008; 26(44):5641-8.
- Meyers AFA. Expression and analysis of Crimean Congo haemorrhagic fever virus nucleoprotein. University of Manitoba. Canada: Winnipeg; 2006.
- Mellman I, Steinman RM. Dendritic cells: specialized and regulated antigen processing machines. *Cell* 2001; 106(3):255-8.
- Mohamed Al Dabal L, Rahimi Shahmirzadi MR, Baderldin S, Abro A, et al. An outbreak of Crimean-Congo hemorrhagic fever in the United Arab Emirates, 1994-1995. *Am J Trop Med Hyg.* 1997; 57(5):519-25.
- Morikawa S, Qing T, Xinqin Z, Saijo M, et al. Genetic diversity of the M RNA segment among Crimean-Congo hemorrhagic virus strains in China. *Virol* 2002; 296:159-164.
- Moming A, Tuoken D, Yue X, Xu W, et al. Mapping of B-cell epitopes on the N- terminal and C-terminal segment of nucleocapsid protein from Crimean-Congo hemorrhagic fever virus. *PLoS One* 2018; 13(9):e0204264.
- Mousavi-Jazi M, Karlberg H, Papa A, Christova I, et al. Healthy individuals' immune response to the Bulgarian Crimean-Congo hemorrhagic fever virus vaccine. *Vaccine* 2012; 30(44):6225-9.

- Msimang V, Weyer J, Leman P, Kemp A, et al. Update: Crimean-Congo haemorrhagic fever in South Africa. *Communicable Diseases Surveillance Bulletin* 11(3): 62-64.
- Nabeth P, Thior M, Faye O, Simon F. Human Crimean-Congo Hemorrhagic Fever, Sénégal. *Emerg Infect Dis* 2004; 10(10):1881–1882.
- Naslund TI, Kostic L, Nordström EK, Chen M, et al. Role of innate signalling pathways in the immunogenicity of alphaviral replicon-based vaccines. *Virol J* 2011; 8:36.
- Nielsen PE, Egholm M, Berg RH, Buchardt O. Sequence-selective recognition of DNA by strand displacement with a thymine-substituted polyamide. *Science* 1991; 254:1497–1500.
- Negredo A, de la Calle-Prieto F, Palencia-Herrejón E, Mora-Rillo M, et al. Crimean Congo Hemorrhagic Fever@Madrid Working Group Autochthonous Crimean-Congo Hemorrhagic Fever in Spain. *N Engl J Med* 2017; 377(2):154-61.
- Németh V, Oldal M, Egyed L, Gyuranecz M, et al. Serologic evidence of Crimean-Congo hemorrhagic fever virus infection in Hungary. *Vector Borne Zoonotic Dis* 2013 ;13(4):270-2.
- Nga TV, Karkey A, Dongol S, Thuy HN, et al. The sensitivity of real-time PCR amplification targeting invasive *Salmonella* serovars in biological specimens. *BMC Infect Dis* 2010; 10:125.
- Nuttall PA, Jones LD, Labuda M, Kaufman WR. Adaptations of arboviruses to ticks. *J Med Entomol* 1994 ; 31(1):1-9.
- Onishchenko GG. Infectious diseases in natural reservoirs: epidemic situation and morbidity in the Russian Federation and prophylactic measures. *Zh Mikrobiol Epidemiol Immunobiol* 2001; (3):22-8.
- Osman HA, Eltom KH, Musa NO, Bilal NM, et al. Development and evaluation of loop-mediated isothermal amplification assay for detection of Crimean Congo hemorrhagic fever virus in Sudan. *J Virol Methods* 2013; 190(1-2):4-10.
- Ozkaya E, Dincer E, Carhan A, Uyar Y, et al. Molecular epidemiology of Crimean- Congo hemorrhagic fever virus in Turkey: occurrence of local topotype. *Virus Res* 2010; 149:64–70.
- Ozturk B, Tutuncu E, Kuscu F, Gurbuz Y, et al. Evaluation of factors predictive of the prognosis in Crimean-Congo hemorrhagic fever: new suggestions. *Int J Infect Dis* 2012; 16(2):e89-93.
- Ozturk B, Kuscu F, Tutuncu E, Sencan I, et al. Evaluation of the association of serum levels of hyaluronic acid, sICAM-1, sVCAM-1, and VEGF-A with mortality and prognosis in patients with Crimean-Congo hemorrhagic fever. *J Clin Virol* 2010; 47:115–119.
- Paone A, Starace D, Galli R, Padula F, et al. Toll-like receptor 3 triggers apoptosis of human prostate cancer cells through a PKC- α -dependent mechanism. *Carcinogenesis* 2008; 29(7):1334-42.
- Papa A, Weber F, Hewson R, Weidmann M, et al. Meeting report: First International Conference on Crimean-Congo hemorrhagic fever. *Antivir Res* 2015; 120:57–65.

- Papa A, Papadimitriou E, Bozovic B, Antoniadis A. Genetic characterization of the M RNA segment of a Balkan Crimean-Congo hemorrhagic virus strain. *J Med Virol* 2005; 75:466-466.
- Papa A, Christova I, Papadimitriou E, Antoniadis A. Crimean-Congo Hemorrhagic Fever in Bulgaria. *Emerg Infect Dis* 2004; 10(8):1465–1467.
- Papa A, Bino S, Llagami A, Brahimaj B, et al. Crimean-Congo hemorrhagic fever in Albania, 2001. *Eur J Clin Microbiol Infect Dis* 2002; 21(8):603-6.
- Pasare C, Medzhitov R. Toll-like receptors: linking innate and adaptive immunity. *Microbes Infect* 2004; 6(15):1382-7.
- Paschkis KE, Cantarow A, Stasney J. Induction of neoplasms by injection of tumor chromatin. *J Natl Cancer Inst* 1955; 15:1525–32.
- Perlman RL. Mouse models of human disease: An evolutionary perspective. *Evol Med Public Health* 2016; 2016(1):170-6.
- Perng YC, Lenschow DJ. ISG15 in antiviral immunity and beyond. *Nat Rev Microbiol* 2018; 16(7):423–39.
- Peters CJ, Zaki SR. Role of the endothelium in viral hemorrhagic fevers. *Crit Care Med* 2002; 30(5): S268–S273.
- Playfair JH. Strain differences in the immune response of mice. I. The neonatal response to sheep red cells. *Immunology* 1968; 15(1):35–50.
- Plyusnin A, Beaty BJ, Elliott RM, Goldbach R, et al. Family Bunyaviridae. In: King A.M.Q., Adams M.J., Carstens E.B., Lefkowitz E.J., editors. *Virus Taxonomy—Ninth Report of the International Committee on Taxonomy of Viruses*. Elsevier/Academic Press; London, UK: 2011:725–741.
- Polo J, Belli BA, Driver DA, Frolov I, et al. Stable alphavirus packaging cell lines for Sindbis virus and Semliki Forest virus-derived vectors. *Proc Natl Acad Sci USA* 1999; 96:4598–4603.
- Pulko V, Liu X, Krco CJ, Harris KJ, et al. TLR3-stimulated dendritic cells up-regulate B7-H1 expression and influence the magnitude of CD8 T cell responses to tumor vaccination. *J Immunol* 2009; 183(6):3634-41.
- Pushko P, Parker M, Ludwig GV, Davis NL, et al. Replicon-helper systems from attenuated Venezuelan equine encephalitis virus: Expression of heterologous genes in vitro and immunization against heterologous pathogens in vivo. *Virol* 1997; 239:389–401.
- Redding L, Werner DB. DNA vaccines in veterinary use. *Expert Rev Vaccines* 2009; 8(9):1251–1276.
- Rennick D, Davidson N, Berg D. Interleukin-10 gene knock-out mice: a model of chronic inflammation. *Clin Immunol Immunopathol* 1995; 76:S174-8.
- Restifo NP. Building better vaccines: how apoptotic cell death can induce inflammation and activate innate and adaptive immunity. *Curr Opin Immunol* 2000; 12(5):597–603.

- Ribeiro S, Mairhofer J, Madeira C, Diogo MM, et al. Plasmid DNA size does affect nonviral gene delivery efficiency in stem cells. *Cell Reprogram* 2012; 14:130–137.
- Richards GA, Weyer J, Blumberg LH. Viral haemorrhagic fevers in South Africa. *S Afr Med J* 2015; 14; 105(9):748-51.
- Richards GA. Nosocomial transmission of viral haemorrhagic fever in South Africa. *S Afr Med J* 2015; 105 (9):709-712.
- Rodriguez LL, Maupin GO, Ksiazek TG, Rollin PE, et al. Molecular investigation of a multisource outbreak of Crimean–Congo hemorrhagic fever in the United Arab Emirates. *Am J Trop Med Hyg* 1997; 57(5):512–518.
- Rostamian M, Sohrabi S, Kavosifard H, Niknam HM. Lower levels of IgG1 in comparison with IgG2a are associated with protective immunity against *Leishmania tropica* infection in BALB/c mice. *J Microbiol Immunol Infect* 2017; 50(2):160-166.
- Russell WMS, Burch RL. *The Principles of Humane Experimental Technique*. London, UK: Universities Federation for Animal Welfare; 1959.
- Ryder AB, Nachbagauer R, Buonocore L, Palese P, et al. Vaccination with Vesicular Stomatitis Virus-Vectored Chimeric Hemagglutinins Protects Mice against Divergent Influenza Virus Challenge Strains. *J Virol* 2015; 90(5):2544-50.
- Sadeuh-Mba SA, Yonga Wansi GM, Demanou M, Gessain A, et al. Serological evidence of rift valley fever Phlebovirus and Crimean-Congo hemorrhagic fever orthonairovirus infections among pygmies in the east region of Cameroon. *Virol J* 2018; 15 (1):63.
- Saijo M, Tang Q, Shimayi B, Han L, et al. Antigen-capture enzyme-linked immunosorbent assay for the diagnosis of Crimean–Congo hemorrhagic fever using a novel monoclonal antibody. *J Med Virol* 2005; 77(1):83–88.
- Salgame P, Varadhachary AS, Primiano LL, Fincke JE, et al. An ELISA for detection of apoptosis. *Nucleic Acids Res* 1997; 25(3):680–681.
- Salem ML, Kadima AN, Cole DJ, Gillanders WE. Defining the antigen-specific T-cell response to vaccination and poly(I:C)/TLR3 signaling: evidence of enhanced primary and memory CD8 T-cell responses and antitumor immunity. *J Immunother* 2005; 28(3):220-8.
- Saluzzo JF, Aubry P, McCormick J, Digoutte JP. Haemorrhagic fever caused by Crimean Congo haemorrhagic fever virus in Mauritania. *Trans R Soc Trop Med Hyg* 1985; 79(2):268.
- Sanjuan R, Moya A, Elena SF. The contribution of epistaxis to the architecture of fitness an RNA virus. *Proc Natl Acad Sci USA* 2004; 101(43):15376-15379.
- Sahib MM. Rapid development of optimized recombinant adenoviral vaccines biosafety level 4 viruses: University of Manitoba. Canada: Winnipeg; 2010. (Thesis)

Sasaki S, Amara RR, Oran AE, Smith JM, et al. Apoptosis-mediated enhancement of DNA-raised immune responses by mutant caspases. *Nat Biotechnol* 2001; 19(6):543–7.

Saxenaa S, Dahiya SS, Sonwane AA, Patel CL, et al. A sindbis virus replicon-based DNA vaccine encoding the rabies virus glycoprotein elicits immune responses and complete protection in mice from lethal challenge. *Vaccine* 2008; 26(51):6592–6601.

Schmieder R, Edwards R. Quality control and preprocessing of metagenomic datasets. *Bioinformatics* 2011; 27(6):863–4.

Schnittler HJ, Feldmann H. Viral hemorrhagic fever—a vascular disease? *Thromb Haemost* 2003; 89:967–972.

Scholtz FEM, Zivcec M, Dzimiński JV, Deaton MK, et al. Crimean-Congo hemorrhagic fever virus suppresses innate immune responses via a ubiquitin and ISG15 specific protease. *Cell Rep* 2017; 20(10):2396–2407.

Schuster I, Mertens M, Köllner B, Korytář T, et al. A competitive ELISA for species-independent detection of Crimean-Congo hemorrhagic fever virus specific antibodies. *Antiviral Res* 2016; 134:161–166.

Schwarz TF, Nsanze H, Longson M, Nitschko H, et al. Polymerase Chain Reaction for diagnosis and identification of distinct variants of Crimean-Congo hemorrhagic fever virus in United Arab Emirates. *Am J Trop Med Hyg* 1996; 55:190–196.

Schwarz TF, Nitschko H, Jager G, Nsanze H, et al. Crimean–Congo haemorrhagic fever in Oman. *Lancet* 1995; 346(8984):1230.

Shayan S, Bokaeian M, Shahrivar MR, Chinikar S. Crimean-Congo Hemorrhagic Fever. *Laboratory Medicine* 2015; 46(3):180–189.

Shepherd AJ, Swanepoel R, Leman PA. Antibody response in Crimean–Congo hemorrhagic fever. *Rev Infect Dis* 1989; 11(4):S801–S806.

Shepherd AJ, Swanepoel R, Gill DE. Evaluation of enzyme-linked immunosorbent assay and reversed passive hemagglutination for detection of Crimean–Congo hemorrhagic fever virus antigen. *J Clin Microbiol* 1988; 26(2):347–353.

Shi J, Hu Z, Deng F, Shen S. Tick-Borne Viruses. *Virol Sin.* 2018; 33(1):21–43.

Shepherd AJ, Swanepoel R, Shepherd SP, McGillivray GM. Antibody to Crimean-Congo hemorrhagic fever virus in wild mammals from southern Africa. *Am J Trop Med Hyg* 1987; 36:133–142.

Shirako Y, Strauss J. Regulation of Sindbis virus RNA replication: uncleaved P123 and nsP4 function in minus strand RNA synthesis, whereas cleaved products from P123 are required for efficient plus-strand RNA synthesis. *J Virol* 1994; 68 (3):1874–1885.

Sievers F, Wilm A, Dineen D, Gibson TJ, et al. Fast, scalable generation of high-quality protein multiple sequence alignments using Clustal Omega. *Mol Syst Biol* 2011; 7:539.

Simon M, Johansson C, Mirazimi A. Crimean–Congo hemorrhagic fever virus entry and replication is clathrin-, pH- and cholesterol-dependent. *J Gen Virol* 2009; 90(1):210–215.

Simon M, Johansson C, Lundkvist A, Mirazimi A. Microtubule-dependent and microtubule-independent steps in Crimean–Congo hemorrhagic fever virus replication cycle. *Virology* 2009; 385(2):313–322.

Simpson DI, Knight EM, Courtois G, Williams MC, et al. (1967) Congo Virus: a hitherto undescribed occurring in Africa. I. Human isolations--clinical notes. *East Afr Med J* 1967; 44(2):86-92.

Silva GM, Vogel C. Quantifying gene expression: the importance of being subtle. *Molecular Systems Biology* 2016; 12:885.

Singh M, Cattaneo R, Billeter MA. A recombinant measles virus expressing hepatitis B virus surface antigen induces humoral immune responses in genetically modified mice. *J Virol* 1999; 73(6):4823-8.

Singh SK, Koshkin A, Wengel J, Nielsen P. LNA (Locked Nucleic Acids): Synthesis and High-Affinity Nucleic Acid Recognition. *Chem Commun* 1998; 29(4):455-456.

Spellberg B, Edwards JE Jr. Type 1/Type 2 immunity in infectious diseases. *Clin Infect Dis* 2001; 32(1):76-102.

Spengler JR, Kelly Keating M, McElroy AK, Zivcec M, Coleman-McCray JD et al. Crimean-Congo hemorrhagic fever in humanized mice reveals glial cells as primary targets of neurological infection. *J Infect Dis* 2017; 216(11):1386-1397.

Spengler JR, Bergeron É, Rollin PE. Seroepidemiological Studies of Crimean-Congo Hemorrhagic Fever Virus in Domestic and Wild Animals. *PLoS Negl Trop Dis* 2016; 10(1):e0004210.

Spengler JR, Patel JR, Chakrabarti AK, Zivcec M et al. RIG-I Mediates an Antiviral Response to Crimean-Congo Hemorrhagic Fever Virus. *J Virol* 2015; 89(20):10219–10229.

Spik K, Shurtleff A, McElroy AK, Guttieri MC, et al. Immunogenicity of combination DNA vaccines for Rift valley virus, tick-borne encephalitis virus, Hantaan virus, and Crimean Congo hemorrhagic fever virus. *Vaccine* 2006; 24(21):4657–4666.

Steinhagen F, Kinjo T, Bode C, Klinman DM. TLR-Based Immune Adjuvants. *Vaccine* 2011; 29(17):3341–3355.

Strauss JH, Strauss EG. The alphaviruses: gene expression, replication, and evolution. *Microbiol Rev* 1994; 58(3):491-562.

Strauss EG, Rice CM, Strauss J. Complete nucleotide sequence of the genomic RNA of Sindbis virus. *Virology* 1984; 133(1): 92–110.

Stockinger S, Decker T. STATs and Infection. Austin (TX): Landes Bioscience; 2000-2013.

Sukharev SI, Klenchin VA, Serov SM, Chernomordik LV, et al. Electroporation and electrophoretic DNA transfer into cells. The effect of DNA interaction with electropores. *Biophys J* 1992; 63(5):1320–1327.

Sun R, Zhang Y, Lv Q, Liu B, et al. Toll-like receptor 3 (TLR3) induces apoptosis via death receptors and mitochondria by up-regulating the transactivating p63 isoform alpha (TAP63alpha). *J Biol Chem* 2011; 286(18):15918-28.

Swanepoel R, Leman PA, Burt FJ, Jardine J, et al. Experimental infection of ostriches with Crimean- Congo haemorrhagic fever virus. *Epidemiol Infect* 1998; 121(2): 427-32.

Swanepoel R, Gill DE, Shepherd AJ, Leman PA, et al. The clinical pathology of Crimean Congo hemorrhagic fever. *Rev Infect Dis* 1989; 11(4):S794-800.

Swanepoel R, Shepherd AJ, Leman PA, Shepherd SP, et al. Epidemiologic and clinical features of Crimean–Congo hemorrhagic fever in southern Africa. *Am J Trop Med Hyg* 1987; 36:120–132.

Swanepoel R, Struthers JK, Shepherd AJ, McGillivray GM, et al. Crimean-congo hemorrhagic fever in South Africa. *Am J Trop Med Hyg* 1983; 32(6):1407-15.

Tantawi HH, Al-Moslih MI, Al-Janabi NY, Al-Bana AS, et al. Crimean-Congo haemorrhagic fever virus in Iraq: isolation, identification and electron microscopy. *Acta Virol* 1980; 24(6):464-7.

Tasdelen Fisgin N, Ergonul O, Doganci L, Tulek N. The role of ribavirin in the therapy of Crimean–Congo hemorrhagic fever: early use is promising. *Eur J Clin Microbiol Infect Dis* 2009; 28:929-933.

Terenzi F, deVeer MJ, Ying H, Restifo NP, et al. The antiviral enzymes PKR and RNase L suppress gene expression from viral and non-viral based vectors. *Nucleic Acids Res* 1999; 27(22):4369-75.

Ulmer JB, Mason PW, Geall A, Mandl CW. RNA-based vaccines. *Vaccine* 2012; 30:4414–4418.

Ulmer JB, Otten GR. Priming of CTL responses by DNA vaccines: direct transfection of antigen presenting cells versus cross-priming. *Dev Biol (Basel)* 2000; 104:9-14.

van Nieuwenhuijze AE, van Lopik T, Smeenk RJ, Aarden LA. Time between onset of apoptosis and release of nucleosomes from apoptotic cells: putative implications for systemic lupus erythematosus. *Ann Rheum Dis* 2003; 62(1):10-4.

Vander Veen RL, Harris H, Kamrud KI. Alphavirus replicon vaccines. *Animal Health Res Rev* 2012; 13(1):1-9.

van de Wal BW, Joubert JR, van Eeden PJ, King JB. A nosocomial outbreak of Crimean-Congo haemorrhagic fever at Tygerberg Hospital. Part IV. Preventative and prophylactic measures. *S Afr Med J* 1985; 68:711-717.

van Eeden PJ, Joubert JR, van de Wal BW. A nosocomial outbreak of Crimean-Congo haemorrhagic fever at Tygerberg Hospital: Part I. Clinical features. *S Afr Med J* 1985a; 68 (10):711-717.

- van Eeden PJ, van Eeden SF, Joubert JR, King JB, et al. A nosocomial outbreak of Crimean–Congo haemorrhagic fever at Tygerberg Hospital. Part II. Management of patients. *S Afr Med J* 1985b; 68:718–721.
- Vincent MJ, Sanchez AJ, Erickson BR, Basak A, et al. Crimean-Congo Hemorrhagic Fever Virus Glycoprotein Proteolytic Processing by Subtilase SKI-1. *J Virol* 2003; 77(16):8640–8649.
- Vorou R, Pierrotsakos IN, Maltezou HC. Crimean-Congo haemorrhagic fever. *Curr Opin Infect Dis* 2007; 20:495-500.
- Wasfi F, Dowall S, Ghabbari T, Bosworth A, et al. Sero-epidemiological survey of Crimean-Congo hemorrhagic fever virus in Tunisia. *Parasite* 2016; 23:10.
- Walker PJ, Widen SG, Firth C, Blasdel KR, et al. Genomic Characterization of Yague, Kasokero, Issyk-Kul, Keterah, Gossas, and Thiafora Viruses: Nairoviruses Naturally Infecting Bats, Shrews, and Ticks. *Am J Trop Med Hyg* 2015; 93(5):1041-51.
- Walter CT, Barr JN. Recent advances in the molecular and cellular biology of bunyaviruses. *J Gen Virol* 2011; 92:2467-2484.
- Watts DM, Ussery MA, Nash D, Peters CJ. Inhibition of Crimean–Congo hemorrhagic fever viral infectivity yields in vitro by ribavirin. *Am J Trop Med Hyg* 1989; 41:581–585.
- Weber A, Kirejczyk Z, Besch R, Potthoff S, et al. Proapoptotic signalling through Toll-like receptor-3 involves TRIF-dependent activation of caspase-8 and is under the control of inhibitor of apoptosis proteins in melanoma cells. *Cell Death Differ* 2010; 17(6):942-51.
- Weber F, Mirazimi A. Interferon and cytokine responses to Crimean-Congo hemorrhagic fever virus; an emerging and neglected viral zoonosis. *Cytokine Growth F R* 2008; 19:395–404.
- Weiss A, Shields R, Newton M, Manger B, et al. Ligand-receptor interactions required for commitment to the activation of the interleukin 2 gene. *J Immunol* 1987; 138(7):2169-76.
- Whitehouse CA. Crimean-Congo hemorrhagic fever. *Antivir Res* 2004; 145-60.
- Wilson CB, Rowell E, Sekimata M. Epigenetic control of T-helper-cell differentiation. *Nat Rev Immunol* 2009; 9:91–105.
- Williams JA. Vector Design for Improved DNA Vaccine Efficacy, Safety and Production. *Vaccines (Basel)* 2013; 1(3): 225–249.
- Wölfel R, Paweska JT, Petersen N, Grobbelaar AA, et al. Low-density microarray for rapid detection and identification of Crimean-Congo hemorrhagic fever virus. *J Clin Microbiol* 2009; 47(4):1025-30.
- Yamaguchi T, Takizawa F, Fischer U, Dijkstra JM. Along the Axis between Type 1 and Type 2 Immunity; Principles Conserved in Evolution from Fish to Mammals. *Biology (Basel)* 2015 ;4(4):814-59.
- Yapar M, Aydogan H, Pahsa A, Besirbellioglu BA, et al. Rapid and quantitative detection of Crimean-Congo hemorrhagic fever virus by one-step real-time reverse transcriptase-PCR. *Jpn J Infect Dis* 2005; 58:358-62.

Yen YC, Kong LX, Lee L, Zhang YQ, et al. Characteristics of Crimean-Congo hemorrhagic fever virus (Xinjiang strain) in China. *Am J Trop Med Hyg* 1985; 34(6):1179-82.

Yenofsky RI, Fine M, Pellow JW. A mutant neomycin phosphotransferase II gene reduces the resistance of transformants to antibiotic selection pressure. *Proc Natl Acad Sci USA* 1990; 87:3435-3439.

Yesilbag K, Aydin L, Dincer E, Alpay G, et al. Tick survey and detection of Crimean–Congo hemorrhagic fever virus in tick species from a non-endemic area, Turkey. *Exp Appl Acarol* 2013; 60:253–261.

Zeller H. Laboratory Diagnosis of Crimean-Congo Hemorrhagic Fever. In: Ergonul O., Whitehouse C.A. (eds) *Crimean-Congo Hemorrhagic Fever*. Springer, Dordrecht, 2007: 233-243.

Zhao D, Huang D, Li Y, Wu M, et al. A Flow-through cell electroporation device for rapidly and efficiently transfecting massive amounts of cells *in vitro* and *ex vivo*. *Sci Rep* 2016; 6:18469.

Zivcec M, Safronetz D, Scott DP, Robertson S, et al. Nucleocapsid protein-based vaccine provides protection in mice against lethal Crimean-Congo hemorrhagic fever virus challenge. *PLoS Negl Trop Dis* 2018; 12(7): e0006628.

Zivcec M, Scholte FE, Spiropoulou CF, Spengler JR, et al. Molecular Insights into Crimean-Congo Hemorrhagic Fever Virus. *Viruses* 2016; 8(4):106.

Zivcec M, Safronetz D, Scott D, Robertson S, et al. Lethal Crimean-Congo hemorrhagic fever virus infection in interferon α/β receptor knockout mice is associated with high viral loads, proinflammatory responses, and coagulopathy. *J Infect Dis* 2013; 207(12):1909-21.

Appendices

Appendix A: Letters of ethics approval Ethical approval for the use of human serum from CCHF survivors in research studies.



IRB nr 00006240
REC Reference nr 230408-011
IORG0005187
FWA00012784

26 February 2016

PROF F BURT
DEPT OF MEDICAL MICROBIOLOGY (VIROLOGY)
FACULTY OF HEALTH SCIENCES
UFS

Dear Prof Burt

ETOVS NR 152/06

PROJECT TITLE: IMMUNE RESPONSES IN SURVIVORS OF CRIMEAN-CONGO HAEMORRHAGIC FEVER
AND EVALUATION OF CANDIDATE VACCINES.

1. You are hereby kindly informed that, at the meeting held on 23 February 2016, the Health Sciences Research Ethics Committee (HSREC) took note with approval of the following:
 - *Request for extension of study period to December 2017*
2. The Committee must be informed of any serious adverse event and/or termination of the study.
3. Any amendment, extension or other modifications to the protocol must be submitted to the HSREC for approval.
4. A progress report should be submitted within one year of approval and annually for long term studies.
5. A final report should be submitted at the completion of the study.
6. Kindly use the ECUFS NR as reference in correspondence to the HSREC Secretariat.
7. The HSREC functions in compliance with, but not limited to, the following documents and guidelines: The SA National Health Act, No. 61 of 2003; Ethics in Health Research: Principles, Structures and Processes (2015); SA GCP(2006); Declaration of Helsinki; The Belmont Report; The US Office of Human Research Protections 45 CFR 461 (for non-exempt research with human participants conducted or supported by the US Department of Health and Human Services- (HHS), 21 CFR 50, 21 CFR 56; CIOMS; ICH-GCP-E6 Sections 1-4; The International Conference on Harmonization and Technical Requirements for Registration of Pharmaceuticals for Human Use (ICH Tripartite), Guidelines of the SA Medicines Control Council as well as Laws and Regulations with regard to the Control of Medicines, Constitution of the HSREC of the Faculty of Health Sciences.

Yours faithfully

DR SM LE GRANGE
CHAIR: HEALTH SCIENCES RESEARCH ETHICS COMMITTEE

Health Sciences Research Ethics Committee
Office of the Dean: Health Sciences
T: +27 (0)51 401 7795/7794 | F: +27 (0)51 444 4359 | E: ethics@ufs.ac.za
Block D, Dean's Division, Room D104 | P.O. Box/Posbus 339 (Internal Post Box G40) | Bloemfontein 9300 | South Africa
www.ufs.ac.za



Appendix B: Laboratory experimental work ethics approval



Research Division
Internal Post Box G40
☎ (051) 401-7795
Fax (051) 4444359

E-mail address: EthicsFHS@ufs.ac.za

Ms M Marais/hv

2015-04-13

REC Reference nr 230408-011
IRB nr 00006240

PROF FJ BURT
DEPARTMENT OF MEDICAL MICROBIOLOGY AND VIROLOGY
NHLS
FACULTY OF HEALTH SCIENCES
UFS

Dear Prof Burt

ECUFS NR 34/2013A

PROF FJ BURT

AND VIROLOGY PROJECT TITLE:

VACCINES FOR MEDICALLY SIGNIFICANT ARBOVIRAL DISEASES.

DEPARTMENT OF MEDICAL MICROBIOLOGY
DEVELOPMENT AND EVALUATION OF NOVEL

1. You are hereby kindly informed that, at the meeting held on 7 April 2015, the Ethics Committee approved the following:
 - *Permission is requested for extension to an existing project*
2. Committee guidance documents: Declaration of Helsinki, ICH, GCP and MRC Guidelines on Bio Medical Research, Clinical Trial Guidelines 2000 Department of Health RSA; Ethics in Health Research: Principles Structure and Processes Department of Health RSA 2004; Guidelines for Good Practice in the Conduct of Clinical Trials with Human Participants in South Africa, Second Edition (2006); the Constitution of the Ethics Committee of the Faculty of Health Sciences and the Guidelines of the SA Medicines Control Council as well as Laws and Regulations with regard to the Control of Medicines.
3. The Committee must be informed of any serious adverse event and/or termination of the study.
4. Any amendment, extension or other modifications to the protocol must be submitted to the Ethics Committee for approval.
5. A progress report should be submitted within one year of approval of long term studies and a final report at completion of both short term and long term studies.
6. Kindly use the ETOVS/ECUFS NR as reference in correspondence to the Ethics Committee Secretariat.

Yours faithfully


DR SM LE GRANGE
CHAIR: ETHICS COMMITTEE





IRB nr 00006240
REC Reference nr 230408-011
IORG0005187
FWA00012784

26 February 2016

PROF FJ BURT
DEPT OF MEDICAL MICROBIOLOGY (VIROLOGY)
FACULTY OF HEALTH SCIENCES
UFS

Dear Prof Burt

ECUFS NR 34/2013A

PROJECT TITLE: DEVELOPMENT AND EVALUATION OF NOVEL VACCINES FOR MEDICALLY SIGNIFICANT ARBOVIRAL DISEASES.

1. You are hereby kindly informed that, at the meeting held on 23 February 2016, the Health Sciences Research Ethics Committee (HSREC) took note with approval of the following:
 - *Request for extension of study period to December 2017*
2. The Committee must be informed of any serious adverse event and/or termination of the study.
3. Any amendment, extension or other modifications to the protocol must be submitted to the HSREC for approval.
4. A progress report should be submitted within one year of approval and annually for long term studies.
5. A final report should be submitted at the completion of the study.
6. Kindly use the ECUFS NR as reference in correspondence to the HSREC Secretariat.
7. The HSREC functions in compliance with, but not limited to, the following documents and guidelines: The SA National Health Act. No. 61 of 2003; Ethics in Health Research: Principles, Structures and Processes (2015); SA GCP(2006); Declaration of Helsinki; The Belmont Report; The US Office of Human Research Protections 45 CFR 461 (for non-exempt research with human participants conducted or supported by the US Department of Health and Human Services- (HHS), 21 CFR 50, 21 CFR 56; CIOMS; ICH-GCP-E6 Sections 1-4; The International Conference on Harmonization and Technical Requirements for Registration of Pharmaceuticals for Human Use (ICH Tripartite), Guidelines of the SA Medicines Control Council as well as Laws and Regulations with regard to the Control of Medicines, Constitution of the HSREC of the Faculty of Health Sciences.

Yours faithfully

DR SM LE GRANGE
CHAIR: HEALTH SCIENCES RESEARCH ETHICS COMMITTEE



Appendix C: Animal Ethics clearance and Section 20 permit



Animal Research Ethics

05-Dec-2017

Dear Prof Felicity Burt

Student Project Number: UFS-AED2017/0066

Project Title: Immunogenicity of Sindbis based replicons for Crimean-Congo hemorrhagic fever virus.


Department: Medical Microbiology (Bloemfontein Campus)

You are hereby kindly informed that, at the meeting held on , the Interfaculty Animal Ethics Committee approved the above project.

Kindly take note of the following:

1.
A progress report with regard to the above study has to be submitted Annually and on completion of the project. Reports are submitted by logging in to RIMS and completing the report as described in SOP AEC007: Submission of Protocols, Modifications, Amendments, Reports and Reporting of Adverse Events which is available on the UFS intranet.
2.
Researchers that plan to make use of the Animal Experimentation Unit must ensure to request and receive a quotation from the Head, Mr. Seb Lamprecht.
3.
Fifty (50%) of the quoted amount is payable when you receive the letter of approval.

Yours Sincerely


Derek Litthauer
2017.12.05
15:40:31
+02'00'

Prof. Derek Litthauer Chair: Animal Research Ethics Committee

Section 20 permit



agriculture, forestry & fisheries

Department:
Agriculture, Forestry and Fisheries
REPUBLIC OF SOUTH AFRICA

Directorate Animal Health, Department of Agriculture, Forestry and Fisheries
Private Bag X138, Pretoria 0001

Enquiries: Mr Herry Gololo • Tel: +27 12 319 7532 • Fax: +27 12 319 7470 • E-mail: HerryG@daff.gov.za
Reference: 12/11/1/4

Professor FJ Burt
Department of Medical Microbiology and Virology
Faculty of Health Sciences
University of the Free State
Tel: (051) 405 3348
E-mail: burtfj@ufs.ac.za

RE: PERMISSION TO DO RESEARCH IN TERMS OF SECTION 20 OF THE ANIMAL DISEASES ACT, 1984 (ACT NO 35 OF 1984)

Dear Prof. Burt,

Your application sent with the email on 23 October 2017 requesting permission under Section 20 of the Animal Disease Act, 1984 (Act No. 35 of 1984) to perform a research project or study, refers.

I am pleased to inform you that permission is hereby granted to perform the following study, with the following conditions:

Conditions:

1. This permission does not relieve the researcher of any responsibility which may be placed on him by any other act of the Republic of South Africa;
2. Written permission from the Director: Animal Health must be obtained prior to any deviation from the conditions approved for this study under this Section 20 permit. Please apply in writing to HerryG@daff.gov.za;
3. All potentially infectious material utilised, collected or generated during the study is to be destroyed at the completion of the study. Records must be kept for five years for auditing purposes. A dispensation application may be considered by the Director Animal Health in the event that any of the above is to be stored or distributed;

4. Ethical approval for the study must be obtained from the relevant authority before the study may start.
5. The study must be conducted in compliance with the Veterinary and Para-Veterinary Professions Act 1982 (Act No. 19 of 82);
6. Subsequent to the completion of the study, all study animals must be euthanized and carcass material collected and disposed of by Compass Medical Waste Services, SA;
7. Work with human embryonic kidney cells may only be performed in the BSL2 laboratory in the Department of Medical Microbiology and Virology;
8. Only previously imported baby hamster kidney cells and human embryonic kidney cells may be used in this study. No samples may be obtained from another supplier or another species without written permission from the Director: Animal Health;
9. Should any additional imported samples be required for the study, importation of the samples will be subject to obtaining a veterinary import permit prior to the importation.
10. Only mice bred by the Animal Unit, University of the Free State, may be used for the study. No outside animals may be sourced without written permission from the Director: Animal Health;
11. This Section 20 approval is valid until 30 November 2018. An application for an extension must be made by the responsible researcher at least one month prior to the expiry of this Section 20 approval.

Title of research/study: Immunogenicity of Sindbis based replicons for Crimean-Congo hemorrhagic fever virus

Researcher: Prof. FJ Burt

Institution: Department of Medical Microbiology and Virology, Faculty of Health Sciences, University of the Free State

Our ref Number: 12/11/1/4

Your ref:

Expiry date: 30 November 2018

Kind regards



DR. MPHOMAJA
DIRECTOR OF ANIMAL HEALTH

Date: 2017 -11- 27

- 2 -

SUBJECT: PERMISSION TO DO RESEARCH IN TERMS OF SECTION 20 OF THE ANIMAL DISEASES ACT, 1984 (ACT NO. 35 OF 1984)



agriculture, forestry & fisheries

Department:
Agriculture, Forestry and Fisheries
REPUBLIC OF SOUTH AFRICA

Directorate Animal Health, Department of Agriculture, Forestry and Fisheries
Private Bag X138, Pretoria 0001

Enquiries: Mr Herry Gololo • Tel: +27 12 319 7532 • Fax: +27 12 319 7470 • E-mail: HerryG@daff.gov.za
Reference: 12/11/1/4

Professor FJ Burt
Department of Medical Microbiology and Virology
Faculty of Health Sciences
University of the Free State
Tel: (051) 405 3348
E-mail: burtfj@ufs.ac.za

RE: DISPENSATION ON SECTION 20 APPROVAL IN TERMS OF THE ANIMAL DISEASES ACT, 1984 (ACT NO 35 OF 1984) FOR: "IMMUNOGENICITY OF SINDBIS BASED REPLICONS FOR CRIMEAN-CONGO HEMORRHAGIC FEVER VIRUS"

A dispensation is hereby granted on Point 3 of the Section 20 approval that was issued for the above mentioned study (attached):

- i) Plasmids expressing recombinant antigens prepared from the study, as well as blood samples and splenocytes from euthanised study mice must be stored in the -80°C freezer at the Department of Medical Microbiology and Virology, Faculty of Health Sciences, University of the Free State.
- ii) Stored samples may not be outsourced without prior written approval from DAFF.
- iii) Should samples be used for further research, written approval from the Director of Animal Health must be obtained prior to start of project

Kind regards,

DR. MPHOMAJA
DIRECTOR: ANIMAL HEALTH

Date: 2017 -11- 27

Appendix D: Next-generation sequencing data

CCHF-31S

ATGGAAAACAAAATTGAGGTGAATA
ACAAAGATGAAATGAACAAGTGGTTTGAAGAGTTCAAAAAAGGAAATGGACTTGTGGACA
CCTTCACAAACTCCTATTCTTTTTGTGAGAGTGTTCAAATTTGGACAAGTTTGTGTTCC
AAATGGCCAGTGCCACCGATGATGCACAAAAGGATTCCATCTACGCGTCTGCTCTGGTGG
AAGCAACAAAATTTTGTGCACCTATATATGAGTGTGCATGGGTTAGCTCCACTGGCATTG
TGAAGAGGGGACTTGAATGGTTCGAAAAAAATGCGGGCACCATTAAAGTCTTGGGATGAAA
GTTTACTGAGCTAAAAGTTGACGTCCCGAAAATAGAACAGCTTGCTAATTACCAACAAG
CTGCCTTGAAATGGAGGAAAGACATAGGTTTCCGTGTCAATGCAAACACAGCGGCTCTGA
GCAACAAAGTCCTCGCAGAGTACAAAGTTCCTGGCGAGATTGTGATGTCTGTCAAAGAGA
TGCTGTCAGACATGATTAGGAGAAGGAACCAGATTCTAAACAGGGGTGGTGATGAGAATC
CACGTGGCCCTGTGAGCCGTGAGCATGTGGACTGGTGCAGGGAGTTTGTCAAAGGCAAAT
ACATCATGGCCTTCAACCCACCATGGGGAGACATCAACAAGTCAGGCCGTTCCGGAATAG
CACTTGTGCGAACAGGCCCTTGCCAAGCTTGCAGAGACTGAAGGAAAGGGAGTATTTGACG
AAGCCAAAAAGACTGTGGAGGCCCTCAATGGGTATCTGGATAAGCACAAGGACGAAGTTG
ACAGAGCGAGTGCTGACAGCATGATAACAAACCTTCTCAAGCACATTGCTAAGGCACAGG
AGCTTTATAAGAATTTCGTCTGCACTCCGTGCACAAGGTGCACAGATTGACACTGCCTTCA
GCTCATACTATTGGCTTTACAAGGCTGGCGTGACCCAGAGACATTCCCGACAGTGTAC
AGTTCTCTTTGAGCTAGGAAAACAGCCAAGAGGTACCAAAAAATGAAGAAGGCTCTGC
TGAGCACCCCAATGAAGTGGGGGAAGAACTTTATGAACTCTTTGCCGACGATTCTTTCC
AGCAGAACAGGATCTACATGCACCTGCTGTGCTTACAGCTGGCAGAATCAGTGAAATGG
GAGTCTGCTTTGGGACAATCCCCGTGGCCAATCCTGATGATGCTGCTCAAGGATCTGGAC
ATACCAAGTCTATTCTCAACCTCCGGACTAACACCGAGACCAACAATCCGTGTGCCAGGA
CCATTGTCAAGCTGTTTGAATTTCAGAAAACAGGGTTCAACATTCAGGACATGGACATAG
TGGCCTCTGAGCACTTGCTGCACCACTCTCTTGTGGTAAGCAATCTCCATTCCAGAACG
CCTACAACGTCAAGGGCAATGCCACCAGTGCTAACATTATCACCACCACCACCACCAC
T
AAA

Histidine tag

CCHF- 52S

ATGGAAAACAAAATTGAGGTGAATA
ACAAAGATGAGATGAACAAGTGGTTTGAAGAGTTCAAAAAAGGAAATGGACTTGTGGACA
CCTTCACAAACTCCTATTCTTTTTGTGAGAGTGTTCAAATTTGGACAAGTTTGTGTTCC
AAATGGCCAGTGCCACCGATGATGCACAAAAGGATTCCATCTACGCATCTGCTCTGGTGG
AGGCAACAAAATTTTGTGCACCTATATATGAGTGTGCATGGGTTAGCTCCACTGGCATTG
TGAAGAGGGGACTTGAATGGTTCGAAAAAAATGCGGGCACCATTAAAGTCTTGGGATGAAA
GTTTACTGAGCTAAAAGTTGACGTCCCGAAAATAGAACAGCTTGCCAATTACCAACAGG
CTGCCTTGAAATGGAGGAAAGACATAGGTTTCCGTGTCAATGCAAACACAGCGGCTCTGA
GCAACAAAGTCCTCGCAGAGTACAAAGTTCCTGGCGAGATTGTGATGTCTGTCAAAGAGA
TGCTGTCAGATGATTAGGAGAAGGAACCAGATTCTAAACAGGGGTGGTGATGAGAATC
CACGTGGCCCTGTGAGCCGTGAGCATGTGGACTGGTGCAGGGAGTTTGTCAAAGGCAAAT
ACATCATGGCCTTCAACCCACCATGGGGGACATCAACAAGTCAGGCCGTTTCAAGGAATAG
CACTTGTGCGAACAGGCCCTTGCCAAGCTTGCAGAGACTGAAGGAAAGGGAGTATTTGACG
AAGCCAAAAAGACTGTGGAGGCCCTCAATGGGTATCTGGACAAGCACAAGGACGAAGTTG
ACAGAGCGAGTGCTGACAGCATGATTACAAACCTTCTCAAGCACATTGCTAAGGCACAGG
AGCTTTATAAGAATTTCGTCTGCACTCCGTGCACAAGGTGCACAGATTGACACTGCCTTCA
GCTCATACTATTGGCTTTACAAGGCTGGCGTGACCCAGAGACATTCCCGACGGTGTAC

AGTTCCTCTTTGAGCTAGGAAAACAGCCAAGAGGTACCAAGAAAATGAAGAAGGCTCTGC
TGAGCACCCCAATGAAGTGGGGGAAGAACTTTATGAAGTCTTCGCCGACGATTCTTTCC
AGCAGAACAGGATCTACATGCACCTGCCGTGCTTACAGCTGGCAGAATCAGTGAAATGG
GAGTCTGCTTTGGGACAATCCCCGTGGCCAATCCTGATGATGCTGCTCAAGGATCTGGAC
ACACCAAGTCTATTCTCAACCTCCAGACTAACACCGAGACCAACAATCCGTGTGCCAGGA
CCATTGTCAAGCTGTTTGAAATTGAGAAAACAGGGTTCAACATTAGGACATGGACATAG
TGGCTCTGAGCACCTGCTGCACCACTCTCTTGTGGCAAGCAATCTCCATTCCAGAACG
CCTACAACGTCAAAGGCAATGCCACCAGTGCCAACATCATCACCACCACCACCACCCT
AAA

Histidine tag

CCHF- 52M

ATGCATATATCATTAATGTATGCAG
TCCTTTGCCTACAGCTGTGTAGTCTGGGAGAACTCATAGATCACACAATGAAATTGGAC
ACAATAAAACAGACGTTATGACAACGCCCGGTGATAACCTGAGCTCTGAACAGCCAGTGA
GCACGGCCTTGTCTATCACACCTGACCCCTCCACTGTTACACCCACAACACCAGCCAGTG
GATCAGAAGGCTCAGGGGAAGTTTACACATCCTCTCCGATCACCACCGAGAGCTTGTCCC
TGCCAGAAACACACCGGAGCTCCCTGCTACAACCTGGTATAGACTCTTCAAGTGCAAGTG
GTGTGATTCTAGTACGCAAGCAGCCGGAGGCACCTCCGCACTAACAGTCCGCACAAGTC
TGCCCAACAGCCCTAGCACACCATCTACACCACAAGACACATAACCATCCTGTGAGAATTC
TACTTTCAGTCACGGGCCCTGGGCCAGAAGAAACATCAACACCTTCGGGATCAGGCAAAG
AGAGCTCAGCAACTAGTAGCCTTCATCCAATCTCCGACAGACTACCAACCCCTCCCGCAA
CAGCTCAGGGACCTACTGAAAATAACAGTCACAACGCCACTGAACACCCCAAGCCCCTGA
CACAGTCAGCAACCCAGGCCTAATGACCTCTCCAACACAGATAGTCCACCCACAAAGTG
CCACCTCCATAAACCGTTCAAGACACATAACCCAGTCCAAAGAACAGGTCTAAAAGAAACC
TTGAGATGGAAATAATCTTGACTTTGTCTCAGGGCTTAAAAAATACTATGGCAAAATAT
TAAGGCTTCTGCGTCTCACCTTAGAGGAGGACACTGAAGGTCTACTGGAATGGTGAAGA
GAAATCTTGGTCTTGATTGTGATGACACTTTCTTTCAAAGAGAAATTGAGGAATCTTCA
TAACTGGTGAGGGCCATTTTAAATGAAGTTCTACAATTTAAACGCCAGGCACGTTGAGTA
CTACAGAGTCAACACCTGCTGAGCTGCCAACAGCTGAACCTTTTAAAGTCTACTTCGCCA
AAGGCTTCCTTTCAATAGATTAGGTTACTATTACGCCAAATGTTACTCAGGAACATCTA
ATTACAGGGCTTCAATTAATTAATATTACCCGACATTCAACTAGAAATAGTTGACACACCTG
GGCCTAAGATCACTAATTTAAAGACCATCAACTGCATAAACTTAAAGGCATCGATCTTCA
AAGAACATAGAGAGGTTGAAATCAATGTGCTTCTCCCTCAAATTGCAGTTAATCTCTCAA
ACTGTCACGTTGTAATCAAAATCACATGTCTGTGACTATTCTTTAGACATTGACGGTACGG
TGAGGCTTCCTCACATTTACCATGAAGGAGTTTTTCATTCCAGGAACCTTACAAAATAGTGA
TAGATAAAAAAATAAGTTGAATGACAGATGCACCTTATTTACCAACTGTGTGATAAAAG
GAAGGGAGGTTTCGTAAGGGTCAGTCAGTTTTGAGGCAGTACAAGACGGAAATCAGGATTG
GCAAAGCATCAACCGCTCTAGAAGACTGCTTTCCGAAGAACCTAGTGATGACTGCATAT
CGAGAACTCAACTATTGAGGACAGAGACTGCAGAGATCCACGGCGACAACCTATGGTGGCC
CGGGTGACAAAATAACCATCTGCAACGGCTCAACTATTGTAGACCAAAGACTGGGCAGTG
AGCTAGGGTGTTACACTATCAATAGAGTGAAGTCATTCAAGCTATGCGAAAATAGTGCCA
CAGGGAAGAGCTGTGAAATAGACAGTGTCCCAGTTAAATGCAGGCAGGGTTATTGCCTAA
GAATCACTCAGGAAGGGAGGGGCCATGTAAAATTATCTAGGGGCTCAGAGGTTGTCTTAG
ATGCATGCGATACAAAGCTGTGAAAATAATGATACCTAAGGGCACTGGTGACATCCTAGTTG
ACTGTTACAGGTGGGCAGCAACATTTTCTAAAGGACAATTTGATAGATCTAGGATGCCCCA
AAATTCCATTATTGGGCAAAATGGCTATTTACATTTGCAGAATGTGGAATCACCACAAA
CAACCATGGCTTTCTTTCTGTTTCAGCTTTGGCTACGTAATAACTTGTATACTTTGCA
AGGCCATCTTTTACTGTGTAATAATTATTGGAACGCTAGGGAAGAGGTTCAAGCAGTATA
GAGAGTTAAACCTCAGACCTGCACCATATGTGAGACAACCTCCTGTAAATGCAATAGATG
CTGAGATGCATGACCTCACTGCAGTTACAACATTTGTCCCCTACTGTGCATCTAGACTAA
CCTCAGATGGGCTTGTAGGCATGTGACACAATGCCCTAAGCGGAAGGAGAAAGTGAAG
AACTGAACATACTTGAACCTAGAAAGAATTCTTGGGTTGTAGAAAGCTGTTGCAGG
TATCAGAGTCCACTGGTGTGGCATTGAAAAGAAGCAGCTGGCTGATTGTGCTGCTTGTGC
TGTTACGGTTTTTCATTGTCAACAGTTCAATCAGCACCCATTGGTCACGGGAAGACAATTG
AGGCATACCGGGCCAGGGAGGGATACACAAGTATATGTCTCTTTGTACTAGGAAGTATCC
TATTTGTAGTCTCTTGCCATATGAAAGGGCTGGTTGACAGTGTGGCAACTCCTTCTTCC
CTGGACTGTCCATTTGCAAAACGTGCTCCATAGGCAGCATTAAATGGCTTTGAAAATGAGT

CCCATAAGTGCTATTGCAGCTTATTCTGTTGCCCTTATTGTAGGCACTGCTCTGCTGATA
AAGAAATTTCATAAGCTGCACTTGAGCATCTGCAAAAAAGAAAAACAGGAAGTAATGTCA
TGTTGGCTGTCTGCAAGCGCATGTGTTTCAGGGCCACCATGGAAGTAAGTAACAGAGCCC
TGTTTATCCGTAGCATCATCAACACCACTTTTGTGTTATGTATACTGATACTAGCAGTTT
GTGTTGTTAGTACCTCAGCAGTGGAGATGGAAAACTACCAGCCGGGACCTGGGAAAGAG
AAGAGGACCTAACAAATTTCTGTATCAGGAATGCCAGGTTACAGAGACTGAATGCCTCT
GCCCTTATGAAGCTCTAGTACTCAGAAGGCCTCTATTCTAGATAGTATAGTTAAAGGTA
TGAAAAATCTGCTAAATTCACAAGTTTAGAAACAAGTTTATCAATTGAGGCACCATGGG
GGGCAATAAATGTTTCAGTCAACCTACAAACCAACTGTGTCAACTGCAAAACATAGCACTCA
GTTGGAGCTCTGTGGAACACAGAGGCAATAAGATCTTGGTTTCAGGCAGATCAGAATCAA
TTATGAAGCTGGAAGAAAGGACAGGAATCAGCTGGGACCTCGGCGTGGAAGACGCCCTCTG
AGTCTAAACTGCTTACAGTCTCTGTTCATGGACTTGCTCTCAGATGTACTCTCCTGTCTTCG
AGTACTTATCAGGAGACAGACAGGTGGAAGAGTGGCCCAAGGCAACTTGACAGGTGACT
GCCCAGAAAGATGTGGCTGCACATCATCAACATGTTTACACAAAGAATGGCCCCACTCAA
GAAATTGGAGGTGCATCCCACTTGGTGCTGGGGTG TAGGGACTGGCTGCACCTGTTGTG
GATTAGATGTGAAGGACCTTTTTTACAGATTATATGTTTGTCAAGTGGAAGTTGAATATA
TTAAGACAGAAGCCATAGTGTGTGTAGAACTTACCAGTCAGGAAGGCAGTGTAGCTTGA
TTGAAGCAGGCACAAGGTTCAATTTAGGTCCTGTAACTCATCACTGTGAGAACCACGAA
ACATCCAACAGAAAGCTCCCTCCTGAAATAATCACACTGCATCCCAGGATCGAAGAAGGTT
TTTTTGACCTGATGCATGTACAGAAAGTGTTATCGGCAAGCACAGTGTGTAAGTTGCAGA
GTTGCACACATGGTGTGCCAGGAGACCTACAGGTCTACCACATCGGGAATTTATTAAAAG
GGGATAAGGTGAATGGACATCTAATTCATAAAATTGAGCCACACTTCAACACTTCCTGGA
TGCTCTGGGATGGTTGTGACCTAGACTACTACTGCAACATGGGAGATTGGCCTTCTTGCA
CATACACAGGAGTCACCCAACACAATCATGCTTCATTTGTAAACCTGCTCAACATTGAAA
CTGATTACACAAAAAACTTCCACTTTCACCTCTAAAAGGGTCACTGCACACGGAGACACAC
CACAACCTAGATCTTAAAGCAAGACCAACCTATGGTGCAGGTGAGATCACTGTACTGGTAG
AAGTTGCTGACATGGAGTTACACACAAAGAAGATTGAAATATCAGGCTTAAAATTTGCAA
GCTTGACTTGCACAGGCTGTTATGCTTGTAGCTCTGGCATCTCATGCAAAGTTAGAATTC
ATGTGGATGAACCAGATGAACCTTACAGTACATGTAAAAGTGATGATCCAGATGTAGTTG
CAGCTAGCTCAAGTCTCATGGCAAGAAAGCTTGAATTTGGAACAGACAGTATATTTAAAG
CTTTCTCAGCCATGCCTAAAACCTTCTCTATGTTTCTACATTGTTGAAAGAGAACACTGTA
AGAGCTGCAGCGAAGAAGACACTAAAAAATGTGTTAACACAAAACCTTGAGCAACCACAAA
GCATTTTGATCGAACACAAGGGAACATAATCGGAAAGCAAAACAGCACTTGCACAGCCA
AGACGAGTTGCTGGTTAGAGTCAGTCAAAAGTTTTTTTTTATGGTCTAAAGAACATGCTTA
GTGGCATTGTTTGGAAATGTTTTTATAGGTATTTTCTGTTTCCTTGCCCCCTTCATCCTGT
TAATACTGTTCTTTATGTTTGGGTGGAGGATCCTATTTTGCTTTAAATGTTGCAGAAGAA
CTAGAGGCCTGTTCAAGTATAGACACTTAAAGGACGATGAAGAACTGGTTATAGAAGGA
TTATTGAAAGATTAAACAATAAAAAAGGAAAAACAACTGCTTGATGGTGAAAGACTTG
CTGATAGAAGAATTGCCGAACGTGTTCTCTACAAAAACACATTTGGCACCACCACCACC
ACCACCTAG

Histidine tag

CCHF-31M

ATGCCCGTCAACATCATGTACACAC
CACTATTGTGTGCTATTCTTTGTCTGCAGGTGTGGGGCTTAGAAGGAACTCATGGATTGT
CCAACAAAACCCAACACAATGACACTAGTACCATAAAGGCGCCCGGAGAGAGTCAGAAAA
CTAGTCTGCCTGCGAACACAGTATCGCCACACGTCAGACCCCCCTCCGTCACATTCA
CAGCATCAGCCAGTGAACCAAGGCTCAGGGGTACGAGCACCTCTCCCTCAGTCACCA
CACAAAGCCCGACCTTACCAGAAACCAGCCAGAGCCCTCACACAATTGACATCAATG
AATCAAGCACAGCCATCGCCGACACCAGCACACAAACAGTCAGGGACATCCTCACACCAA
CAACCTACACCAGTTTGCCAGCACTCCCAGCGCGCAACCAAGCCACAGGAAACACGTC
ACACTGCAAGGGGCTACTGTCAAGTCACCAGCACAAAGCCGGGAGAAACACCATCACCAA
CAAACCCAGGAGGAGCGGGCACAGAGGCCAGCAGCCACACCCAACCATCAGCGAGACAC
CATCCCCCCCCCAACAGCCAGGCTCCCACCGGAATCAACAACCCCAACACATCCAAAC
AATCCATGCTCTCAACACACAGCAGCCCCCACTCAGTGACCCCTCAGTACAGCCAA
CCCTCTCTCAGAGTGAAGTTTCCACGGCTGTTCAAGGTATACACCCAGCCCAACAAACA
GATCTAAGAGAAACCTTGAAATGGAGATAATTTTGACTTTATCTCAAGGTTTGAAGAAGT
ACTACGGCAAGATGCTAAAACCTTCTGGATCTTACTTTAGAAGAAGATACTGAAGGCCTGT
TAGAGTGGTGTAAGAGAAATCTTGGTCTGACCTGCGATGACAACCTCTTTTCAGAGAGAA
TAGAAGAGTTTTTTTTAACTGGTGAGGGTCACCTCAATGAAGTGTTCAGTTCAAAACAC
CAAGCACACCAAGCCCTACGAAACACAGCTCATGTGAGTCACCGACAGTAGAACCCCTTA
AATCTTACTTTGCTAAAGGCTTCTCTCAATGGACTCAGGTTACTTCTCTGCCAAGTGTT
ATCCAAAGTCATCAAATTCAGGACTTCAGCTGATCAATATACCCCAACATTCAATTAGAA
TAACAGACACACCAGGGCCCCAAGATCACTAGTCTGAAGACCATCAATTGCATAAACTTGA
AGGCATTAGTCTTCAAAGAGCATAGGGAGATTGAAATCAATGTTCTCCTCCCTCAAGTCG
CGGTCAACCTCTCAAACCTGCCATGTGCTGATCAATCTCATGTTTGTGACTACTCTTTAG
ACATCGACGGGCGGTAAGACTACCCCATATCCACCATGAAGGAACTTTTCATACCAGGAA
CTTACAAAATAGTTATAGACAAAAAGACAAGCAAAACGACAGGTGCATTTTGGTCACTA
ACTGTGTGATAAAAGGTAGGGAAATTCGCAAAGGCCAGTCAGTGTTAAGGCAATACAGAA
CAGAAATTAAGATTGGCAAAGCATCTTCTGGTTCCAGAAGACTATTGTCTGAAGAGTCTA
GTGATGACTGTTTTATCAAGGACTCAGCTATTGAGGACAGAGAATACGGAATTCACAGTG
ACAACATATGGTGGTCCAGGTGACAAGATAACTATCTGCAACGGTTCAACTATTGTAGATC
AGAGACTGGGCAGTGAAGTAGGGTGTACACTATCAATAGAGTGAAATCATTTTAAGCTTT
GCGAGAACAGTGCTACAGGTAATCTTGTGAAATAGATAGCACCCAGTTAGATGTAGGC
AGGGTTTTTGTCTGAAAATCACTCAGGAGGGAAGGGGCCACGTGAAGCTATCAAGAGGCT
CAGAAGTTGTCTTGGACGCTGTGATTCAAGCTGTGAAATAATGATACCAAAGGGCACTG
GGGACATCCTAGTTGACTGTTTCAGGTGGGCAGCAACATTTCTTAAAAGATAACTTGGTTG
ATCTAGGATGCCCCAACATTCCACTATTAGGCAAAATGGCCATCTACATTTGTAGAAATGT
CAAATCATCCCAAGACAACATATGGGTTTTCTTTTTTGGTTTTAGCTTTGGTTATGTGATAA
CCTGTATACTTTGTAAGGTAATCTTCTATCTATTAATAGTTGTAGGGACATTAGGGAAAA
AGTTTAAACAGTACAGAGAGTTGAAACCTCAGACCTGTACCATATGTGAAACGACTCCTG
TTAATGCAATAGATGCTGAGATGACGACCTCAACTGCAAGTTACAATATATATGCTTATT
GTGCATCTAGGTTAACCTCAGATGGTCTTGCCAGACATGTAATGCAATGCCCCAAACGGA
AGGAAAAAATAGAAGAAACCGAATTATATTTAACTTAGAAAGAATCCCCTGGATTGTTA
GGAAATTACTGCAGGTGTGAGAATCCACCGGTGTAGCACTAAAGAGGAGTAGTTGGTTGG
TTGTACTACTTGTGCTACTCACAGTTTCATTGTCAACAGTACAATCAGCACCTATCGGCC
ATGGAAGACAGTCGAAGTGTATCAAACCAGAGAGGGGTACACAAGTATTTGCCTTTTTG
TACTAGGAAGAACCTGTTTGTGTGATCTTGCTGATGAGGGGGTTGGTTGACAGTGTGCG
GCAATAGTTTTTTTCCCTGGCTTATCCATTTGTAAGACATGTTCTATTGGCAGTATAAACG
GCTTTGAAATTGAATCTCACAATGTTACTGTAGCCTATTTTGTGCTGCCCTACTGTAGAC
ACTGCTCTGCCGATATAGAAATACACAAGTTGCACTTGAACATCTGCAAGAAAAGGAAAA
CTGGGAGTAATGTCATGTTAGCCGTCTGTAAGCGCATGTGCTTTAGGGCAACTATGGAAG
TAAGCAGTAAGGC-TTACTTATCCGAAACATCATCAACACTACTTTTGTGTGTGCATAC
TGATATTAGCAGTTTGTGTTGTGTCAGCACATCTGCAGTGGAGATGGAAAGCCTGCCAGCTG
GCACCTGGGAAGAGAGGAAGACCTGACAAACTTCTGTCATCAGGAATGCCAAGTCACTG
AGACTGAATGCCTCTGTCTTATGAAGCTCTTGTGCTCAGGAAACCCCTTATTTTGGACA
GTATTGTTAAAGGCAAGAAGAACTTGCTAAATTCAACAAGCCTAGAAAACAAGCTTATCAA
TTGAGGCACCATGGGGGGCAATAAATGTCCAGTCACTTTCAAACCAACTGTGTGAGCTG
CAAACATAGCACTTAGTTGGAGCTCAGTAGAACATAGAGGTAACAAGATTTTGGTTTCAG
GCAGGTCAGAGTCAATCATGAAATTAGAGGAAAGGACAGGAATTAGCTGGGATCTGGGTG
TGGAAGACGCCTCTGAATCCAAATTGCTCACTGTCTCTGTTATGGACTTGTACAGATGT
ATTCCTCTGTCTTTGAATACCTATCAGGTGATAGACAAGTGAGGAATGGCCCAAGGCAA

CCTGCACAGGAGATTGCCAGAAAGATGTGGCTGTACGTCGTCAACCTGCCTACACAAGG
AATGGCCCCATTCAAGAACTGGAGATGCAACCTACTTGGTGTGGGGAGTCGGCACTG
GATGCACCTGTTGTGGGCTGGATGTGAAAGACCTCTTTACAGATTACATGTTTGTCAAGT
GGAAAGTTGACTACATTAACAGAAAGCTATAGTATGTGTTGAGCTTACTAGCCAGGAAA
GACAATGTAGCTTGATTGAGGCAGGCACAAGATTCAACTTGGGTCTGTGACTATCACAT
TGTGACAGCCAAGAAACATTGAGCAAAAGCTCCCTCCAGAAATAGTCACATTGCATCCTA
GGATTGAAGAAGGCTTCTTTGACTTAATGCATGTACAAAAAGTGTATCAGCAAGTACAG
TGTGCAAGCTACAAAGTTGTACACATGGTGTGCCAGGAGACCTACAGATTTACCACATTG
GAACTTGTGTTAAAAGGAGACAAGGTGAATGGGCACCTGATTACACAAGATTGAACCACACT
TCAACACTTCCTGGATGTCTTGGGACGGCTGTGACCTAGACTACTACTGTAATATGGGGG
ATTGGCCATCTTGCTCATACACTGGCGTAACCCAAACACAATCATGCTGCATTTGTAAACA
TGCTCAACATCGAACTGATTATACAAAAAACTTCCACTTTCACTCTAAGAGAGTTACAG
CACATGGAGACACACCACAATTAGATTTAAAAGCCAGACCAACTTATGGTGCAGGTGAAA
TCACTGTGCTGGTGGAGGTTGCTGACATGGAGTGCATACAAAGAAAATTGAGATATCAG
GTTTGAAGTTTGCAAGCTTAACCTGCACAGGCTGTTATGCTTGTAGTTCTGGTATCTCCT
GTAAGGTTAGAATCCATGTGGATGAACCAGATGAGCTCACAGTACATGTGAAGAGTGAGG
ATCCAGACATAGTTGCTGCTAGCTCAAGTCTCATGGCTAGGAAGCTTGAATTTGGGACAG
ATAGCACATTTAAAGCCTTTTCAGCCATGCCAAAACCTCCTTATGCTTTTACATTGTGG
AGAGGGAATACTGCAAAAGCTGCAGTAAAGAAGACACAAAAATGTGTCAACACAAAGC
TTGAGCAACCACAAAGCATTTTAATCGAGCACAAAGGGACGATAATTGGGAAGCAGAACG
ACACTTGTACAGCCAAAGCAAGTTGCTGGCTAGAGTCAGTCAAGAGTTTTTTTTATGGAC
TAAAGAATATGCTTAGTGGCATTTTTGGCAATGTTTTCATAGGGATTCTCTTATCCTCG
CTCCTTTTATCATGCTAATACTTTTCTTCATGTTTGGATGGAGGATCCTGTTCTGCTTTA
AGTGTGTCAGAAGAACTAGAGGCCATTTAAGTATAGACACCTCAAAGACGATGAAGAAA
TCGGTTACAGGAAAAATCATTGAGAGGCTAAACAACAAAAAAGGGAAAAACAACTGCTTG
ACGGTGAAAGGCTAGCTGATAGGAAAATCGCTGAGCTGTTCTCCACAAAAACACACATTG
GC **CACCACCACCACCACCAC**TAA

Histidine tag

Appendix E: Apoptosis ELISA raw data post electroporation

24hrs

<>	1	2	3
A	0.0760	0.1410	0.1930
B	0.0730	0.1330	0.2070
C	0.0610	0.1230	0.0000
D	0.0630	0.1210	0.0000
E	2.2770	0.1140	0.0000
F	2.2500	0.1140	0.0000
G	0.0890	0.1300	0.0000
H	0.0830	0.1200	0.0000

36hrs

<>	1	2	3
A	0.0720	0.3120	0.3540
B	0.0710	0.4060	0.4730
C	0.0420	0.2120	0.0000
D	0.0440	0.2250	0.0000
E	2.0410	0.3070	0.0000
F	2.1200	0.2940	0.0000
G	0.0910	0.2570	0.0000
H	0.1050	0.2220	0.0000

48hrs

<>	1	2	3
A	0.0660	0.2640	0.4110
B	0.0620	0.2710	0.4360
C	0.0415	0.2430	0.0000
D	0.0405	0.2440	0.0000
E	2.0540	0.2980	0.0000
F	2.0130	0.2750	0.0000
G	0.1270	0.3760	0.0000
H	0.1290	0.3630	0.0000

60hrs

<>	1	2	3
A	0.1020	0.4450	0.3000
B	0.1030	0.3330	0.2610
C	0.0400	0.3830	0.0000
D	0.0380	0.3440	0.0000
E	2.0670	0.4310	0.0000
F	2.0240	0.3420	0.0000
G	0.1610	0.4470	0.0000
H	0.1450	0.4960	0.0000

72hrs

<>	1	2	3
A	0.1350	0.2190	0.2200
B	0.1210	0.1980	0.2140
C	0.0355	0.1220	0.0000
D	0.0345	0.1160	0.0000
E	2.3290	0.1340	0.0000
F	2.2560	0.1420	0.0000
G	0.1650	0.1790	0.0000
H	0.1450	0.1920	0.0000

Appendix F: ELISA raw data mouse experiment 1

Cytokine responses

IFN- γ

Plate 1

<>	1	2	3	4	5	6	7	8	9	10	11	12
A	1.7320	1.8240	1.7540	0.1080	0.0210	2.4700	0.1620	0.0530	2.3290	0.2320	0.0240	2.6320
B	1.1190	1.1060	1.0990	0.1080	0.0220	2.5210	0.1800	0.0510	2.4380	0.2400	0.0260	2.6280
C	0.5770	0.5970	0.5670	0.0270	0.0240	1.6430	0.0530	0.0770	2.6770	0.0440	0.0240	2.5300
D	0.3130	0.3030	0.2950	0.0240	0.0240	1.6450	0.0600	0.0660	2.7950	0.0430	0.0260	2.7140
E	0.1740	0.1570	0.1660	0.0550	0.0240	2.3720	0.0470	0.0350	1.3850	0.0440	0.0240	1.7680
F	0.0990	0.0970	0.0980	0.0560	0.0220	2.3030	0.0510	0.0370	1.4590	0.0450	0.0300	1.8000
G	0.0590	0.0600	0.0570	0.0150	0.0220	0.0200	0.0190	0.0060	0.0000	-0.0040	0.0000	0.0010
H	0.0250	0.0240	0.0230	0.0010	0.0010	0.0010	0.0020	0.0000	0.0010	0.0010	0.0000	0.0000

Plate 2

<>	1	2	3	4	5	6	7	8	9	10	11	12
A	1.3270	1.3030	1.1730	0.0760	0.0820	2.9690	0.0010	0.0010	0.0010	0.0050	0.0000	0.0000
B	0.8190	0.7440	0.7320	0.0710	0.0680	1.4290	0.0010	0.0010	0.0010	0.0010	0.0010	-0.0020
C	0.4550	0.3950	0.4410	0.0830	0.0800	2.7900	0.0000	0.0020	0.0000	0.0010	0.0010	0.0010
D	0.3200	0.2960	0.2880	0.0020	0.0000	0.0000	-0.0030	-0.0010	0.0020	0.0020	0.0050	0.0010
E	0.2240	0.2060	0.2010	0.0010	0.0010	0.0010	0.0010	0.0000	0.0010	0.0020	0.0020	0.0000
F	0.2000	0.1720	0.1600	0.0010	0.0010	0.0010	-0.0010	0.0010	0.0000	-0.0010	-0.0010	0.0000
G	0.1660	0.1440	0.1560	0.0000	0.0020	0.0000	0.0020	0.0030	0.0010	0.0020	0.0010	0.0000
H	0.1300	0.1330	0.1310	0.0000	-0.0010	-0.0010	-0.0020	0.0000	0.0010	0.0010	0.0030	-0.0010

IL-2

Plate 1

<>	1	2	3	4	5	6	7	8	9	10	11	12
A	2.0410	2.0520	2.0880	0.5680	0.2560	3.4030	1.3900	0.9800	3.0070	1.0400	0.4040	3.1740
B	1.2390	1.1630	1.1760	0.3770	0.1070	3.7900	1.4900	0.5280	3.0240	1.0750	0.3670	3.1660
C	0.7100	0.6560	0.6610	0.1610	0.2170	3.5720	0.9130	0.5880	3.0720	0.5820	0.5200	2.5190
D	0.3440	0.3480	0.3640	0.1830	0.1320	3.5580	0.9010	0.5540	3.3310	0.6140	0.5170	2.4820
E	0.1940	0.1870	0.1840	0.2680	0.2500	3.6010	0.0920	0.0430	3.0590	0.1460	0.1030	3.3150
F	0.1110	0.1140	0.0920	0.2550	0.1850	3.5510	0.0750	0.0410	2.8680	0.1340	0.1010	3.8000
G	0.0630	0.0660	0.0690	-0.0020	0.0000	0.0000	0.0020	0.0000	0.0010	0.0010	0.0000	0.0010
H	0.0250	0.0280	0.0290	0.0040	0.0130	0.0140	0.0000	0.0010	0.0020	0.0000	0.0050	0.0090

Plate 2

<>	1	2	3	4	5	6	7	8	9	10	11	12
A	2.1580	2.1230	2.1770	0.4440	0.3930	3.4610	0.0000	0.0000	0.0010	0.0010	0.0010	0.0000
B	1.2600	1.1690	1.1830	0.0820	0.0720	2.2350	0.0010	0.0000	-0.0010	0.0010	-0.0010	-0.0040
C	0.7140	0.6610	0.6650	0.1300	0.0530	1.3010	0.0000	0.0000	0.0000	0.0000	0.0000	0.0010
D	0.3460	0.3510	0.3660	0.0010	0.0010	0.0000	0.0000	0.0010	0.0000	0.0020	-0.0010	0.0000
E	0.1970	0.1900	0.1860	-0.0010	0.0010	0.0010	-0.0010	-0.0040	0.0020	0.0010	0.0010	-0.0030
F	0.1110	0.1160	0.0920	0.0010	0.0000	0.0010	-0.0010	0.0000	0.0000	0.0000	0.0000	0.0010
G	0.0670	0.0660	0.0690	0.0010	0.0020	-0.0020	0.0010	0.0010	0.0000	0.0010	0.0000	-0.0010
H	0.0380	0.0410	0.0400	0.0000	0.0020	-0.0010	0.0010	0.0000	0.0010	0.0000	0.0000	0.0000

TNF- α

Plate 1

<>	1	2	3	4	5	6	7	8	9	10	11	12
A	2.2710	2.0150	1.9350	0.0700	0.0450	1.0180	0.1240	0.0590	1.2520	0.0830	0.0400	1.1990
B	1.1420	1.0620	1.0150	0.0610	0.0430	0.9310	0.1220	0.0580	1.1900	0.0820	0.0410	1.1690
C	0.6180	0.5580	0.5670	0.0380	0.0380	0.7630	0.0810	0.0700	1.6890	0.0720	0.0520	1.1420
D	0.3530	0.3220	0.3230	0.0370	0.0360	0.7230	0.0780	0.0630	1.7240	0.0650	0.0540	1.0990
E	0.2210	0.2180	0.1820	0.0500	0.0350	1.3600	0.0320	0.0410	0.9170	0.0410	0.0370	0.8520
F	0.1130	0.0910	0.1020	0.0510	0.0360	1.5070	0.0330	0.0380	0.9390	0.0400	0.0370	0.8690
G	0.0640	0.0540	0.0610	0.0010	0.0010	0.0010	0.0000	-0.0010	0.0010	0.0050	0.0020	-0.0030
H	0.0340	0.0300	0.0290	0.0020	0.0020	0.0010	-0.0010	0.0020	0.0050	0.0000	0.0010	-0.0020

Plate 2

<>	1	2	3	4	5	6	7	8	9	10	11	12
A	2.8560	2.8910	2.9080	0.1310	0.1170	0.8040	0.1200	0.1250	0.2430	0.1040	0.0620	0.4040
B	1.6160	1.5500	1.5620	0.1250	0.1150	0.7680	0.1190	0.1190	0.2430	0.1000	0.0210	0.4130
C	0.8210	0.7210	0.8110	0.0020	0.0020	0.0000	-0.0040	0.0070	-0.0030	0.0040	0.0030	0.0030
D	0.3300	0.3330	0.3390	0.0010	0.0010	0.0020	0.0020	0.0020	0.0010	0.0010	0.0020	0.0030
E	0.1910	0.1920	0.1990	0.0020	0.0020	0.0000	-0.0040	0.0070	-0.0030	0.0040	0.0030	0.0030
F	0.1230	0.1300	0.1350	0.0010	0.0010	0.0020	0.0020	0.0020	0.0010	0.0010	0.0020	0.0030
G	0.0740	0.0840	0.0660	0.0010	0.0020	0.0020	0.0010	0.0010	0.0020	0.0010	0.0030	0.0020
H	0.0360	0.0350	0.0370	0.0020	0.0020	0.0010	0.0020	0.0010	0.0020	0.0020	0.0030	0.0030

IL-6

Plate 1

<>	1	2	3	4	5	6	7	8	9	10	11	12
A	1.8860	1.8660	1.8840	0.0740	0.0350	0.4820	0.0710	0.0380	0.5510	0.0630	0.0300	0.6470
B	1.0650	1.0100	1.0440	0.0690	0.0350	0.4830	0.0700	0.0410	0.6410	0.0620	0.0310	0.6440
C	0.5250	0.5100	0.5020	0.0430	0.0310	0.3110	0.1010	0.0590	1.2290	0.0550	0.0420	0.6360
D	0.2880	0.2770	0.2710	0.0410	0.0280	0.3120	0.1060	0.0600	1.2380	0.0540	0.0390	0.6900
E	0.1490	0.1460	0.1400	0.0440	0.0400	0.7450	0.0420	0.0350	0.4480	0.0450	0.0400	0.4240
F	0.0910	0.0970	0.0850	0.0410	0.0388	0.7890	0.0360	0.0360	0.4950	0.0490	0.0390	0.4280
G	0.0570	0.0720	0.0610	0.0040	0.0050	0.0050	0.0030	0.0040	0.0030	0.0050	0.0060	0.0100
H	0.0380	0.0430	0.0420	0.0070	0.0030	0.0070	0.0040	0.0060	0.0050	0.0040	0.0060	0.0100

Plate 2

<>	1	2	3	4	5	6	7	8	9	10	11	12
A	1.9060	1.8790	1.8970	0.0880	0.1070	2.0550	0.0000	0.0020	0.0010	0.0010	0.0010	0.0010
B	1.0660	1.0150	1.0460	0.1920	0.1150	1.1830	-0.0040	0.0000	-0.0010	0.0010	0.0020	0.0040
C	0.5300	0.5150	0.5050	0.1190	0.1300	2.3800	-0.0040	0.0060	0.0020	-0.0010	0.0060	0.0090
D	0.2900	0.2790	0.2710	0.0020	0.0030	0.0020	0.0030	0.0020	2.2320	0.0050	-0.0010	0.0050
E	0.1510	0.1480	0.1420	-0.0010	0.0050	-0.0040	0.0030	0.0010	0.0020	0.0020	0.0030	0.0090
F	0.0920	0.0990	0.0860	0.0000	0.0020	0.0010	0.0020	0.0030	0.0020	0.0030	0.0020	0.0040
G	0.0560	0.0710	0.0610	-0.0040	0.0000	-0.0010	-0.0040	-0.0010	0.0010	-0.0040	-0.0010	0.0010
H	0.0380	0.0410	0.0410	-0.0040	0.0060	0.0020	0.0060	0.0040	0.0020	-0.0010	0.0000	-0.0020

IL-4

Plate 1

<>	1	2	3	4	5	6	7	8	9	10	11	12
A	2.3060	2.1050	2.0280	0.0260	0.0280	0.9440	0.0360	0.0230	0.5300	0.0230	0.0270	1.0840
B	1.2490	1.1470	1.1610	0.0190	0.0230	0.9810	0.0350	0.0220	0.5580	0.0210	0.0240	1.3390
C	0.6840	0.6540	0.6290	0.0220	0.0230	0.9280	0.0290	0.0250	0.2230	0.0210	0.0230	0.4370
D	0.3530	0.3260	0.3350	0.0210	0.0190	1.0750	0.0420	0.0260	0.2340	0.0250	0.0260	0.4160
E	0.1940	0.1830	0.1730	0.0370	0.0190	1.4940	0.0210	0.0180	1.1690	0.0190	0.0200	1.0190
F	0.1010	0.0950	0.1050	0.0230	0.0220	1.4560	0.0200	0.0190	1.1710	0.0160	0.0230	1.0200
G	0.0620	0.0610	0.0600	0.0030	0.0020	0.0010	0.0010	-0.0050	0.0020	0.0020	0.0030	0.0030
H	0.0210	0.0220	0.0230	0.0030	0.0020	0.0020	0.0020	0.0010	0.0020	0.0020	0.0030	0.0010

Plate 2

<>	1	2	3	4	5	6	7	8	9	10	11	12
A	2.4430	2.2110	2.2500	0.0230	0.0230	1.1960	0.0010	0.0020	0.0030	0.0030	0.0020	0.0000
B	1.2720	1.2510	1.2690	0.0280	0.0380	0.5060	0.0010	0.0020	0.0020	0.0010	0.0010	0.0000
C	0.6790	0.7100	0.7050	0.0280	0.0410	1.4540	0.0010	0.0020	0.0010	0.0010	0.0010	0.0020
D	0.3820	0.3480	0.3510	0.0020	0.0020	0.0020	0.0080	0.0040	0.0020	0.0020	0.0010	0.0020
E	0.1820	0.1880	0.1870	0.0020	0.0050	0.0050	0.0030	0.0030	0.0010	0.0070	0.0010	0.0030
F	0.1020	0.1080	0.1040	0.0010	0.0020	0.0030	0.0010	0.0020	-0.0010	0.0030	0.0040	0.0030
G	0.0590	0.0660	0.0680	0.0010	0.0020	0.0020	0.0020	0.0000	0.0020	-0.0080	0.0010	0.0020
H	0.0160	0.0230	0.0220	0.0010	0.0020	0.0010	-0.0030	0.0000	0.0010	0.0020	0.0020	0.0010

IL-10

Plate 1

<>	1	2	3	4	5	6	7	8	9	10	11	12
A	1.2620	1.0790	1.2890	0.0300	0.0230	0.1390	0.0260	0.0230	0.3210	0.0240	0.0230	0.2900
B	0.6140	0.6660	0.6380	0.0250	0.0240	0.1400	0.0270	0.0240	0.3230	0.0270	0.0250	0.2980
C	0.3170	0.3170	0.3160	0.0210	0.0220	0.2710	0.0240	0.0220	0.2310	0.0230	0.0220	0.2820
D	0.1490	0.1590	0.1570	0.0210	0.0210	0.2070	0.0210	0.0200	0.2380	0.0230	0.0200	0.2830
E	0.0800	0.0840	0.0840	0.0250	0.0250	0.2330	0.0220	0.0200	0.2710	0.0210	0.0250	0.2680
F	0.0480	0.0550	0.0470	0.0300	0.0260	0.2470	0.0230	0.0220	0.2750	0.0210	0.0260	0.2720
G	0.0310	0.0330	0.0340	0.0020	0.0020	0.0010	0.0000	0.0010	0.0010	0.0020	0.0020	0.0010
H	0.0220	0.0240	0.0250	0.0010	0.0010	0.0000	0.0010	0.0000	0.0010	0.0010	0.0010	0.0000

Plate 2

<>	1	2	3	4	5	6	7	8	9	10	11	12
A	0.9910	1.0470	0.9980	0.0300	0.0330	0.1940	0.0010	0.0010	-0.0030	0.0020	0.0020	0.0000
B	0.5340	0.5500	0.5440	0.0470	0.0360	0.1380	0.0000	0.0010	0.0010	0.0020	0.0010	0.0010
C	0.2720	0.2860	0.2730	0.0400	0.0310	0.1700	0.0020	0.0010	0.0010	0.0010	0.0020	0.0010
D	0.1510	0.1430	0.1520	0.0020	0.0020	0.0000	0.0010	0.0060	0.0060	-0.0010	0.0000	0.0010
E	0.0840	0.0800	0.0770	0.0010	0.0020	-0.0040	0.0030	0.0020	0.0030	0.0020	0.0020	0.0020
F	0.0510	0.0490	0.0450	0.0010	0.0010	-0.0030	0.0010	0.0000	-0.0010	0.0000	0.0050	0.0010
G	0.0360	0.0360	0.0330	0.0000	0.0010	0.0010	0.0010	0.0020	0.0020	0.0000	0.0000	0.0000
H	0.0210	0.0190	0.0170	0.0020	0.0010	0.0010	0.0020	0.0040	0.0030	0.0000	0.0000	0.0000

Standard curves for determination of cytokines

Plate 1

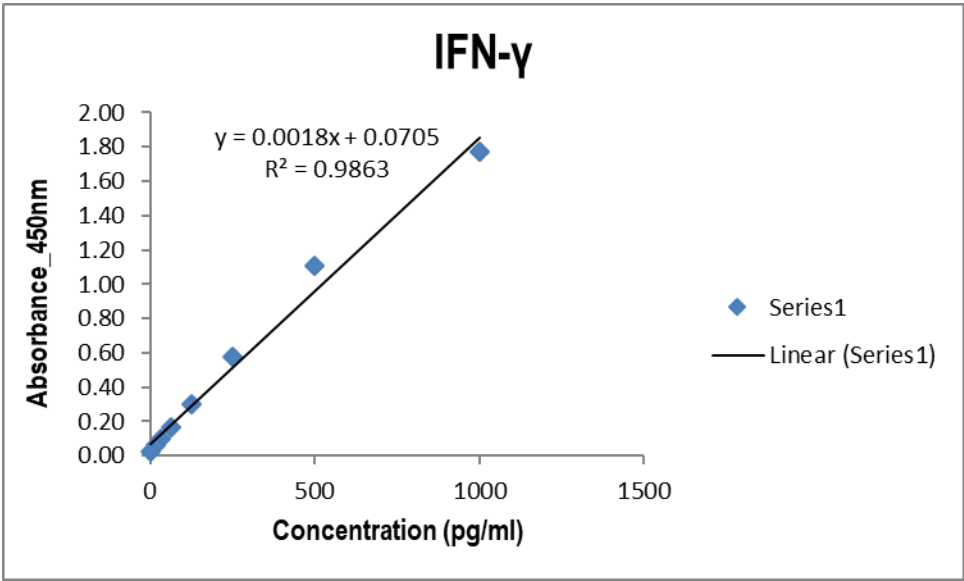


Plate 2

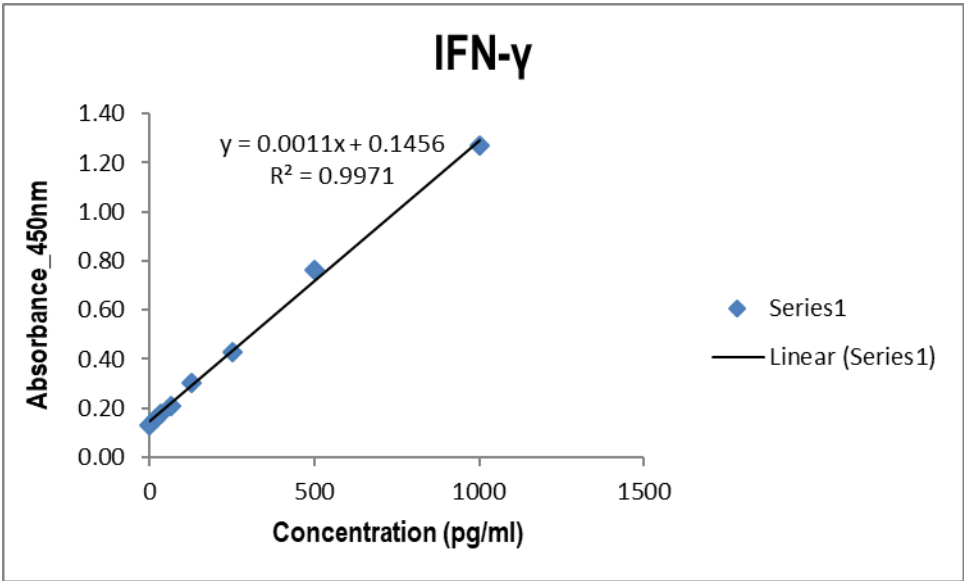


Plate 1

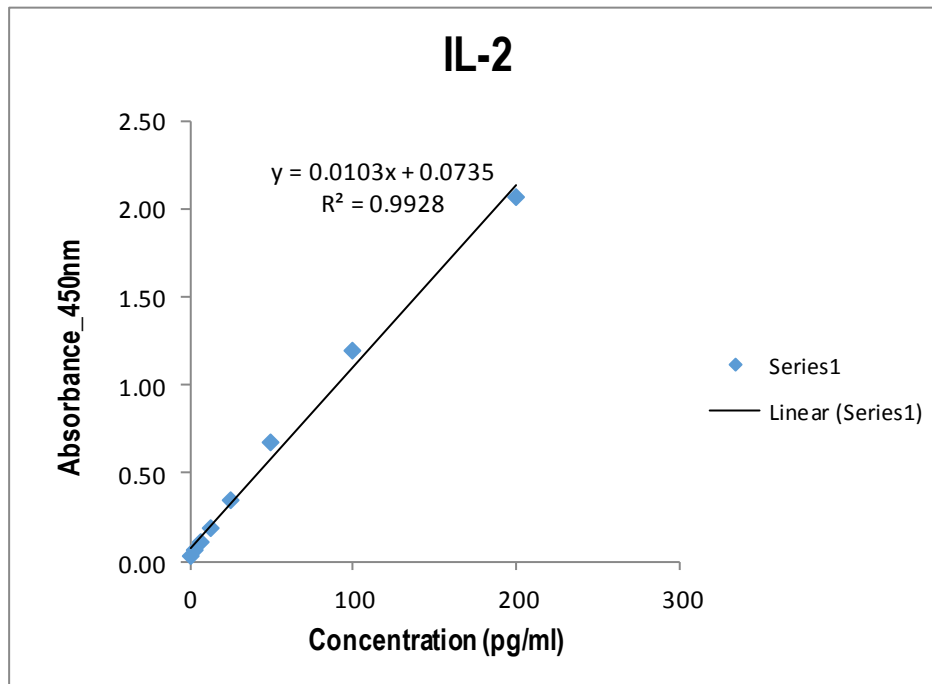


Plate 2

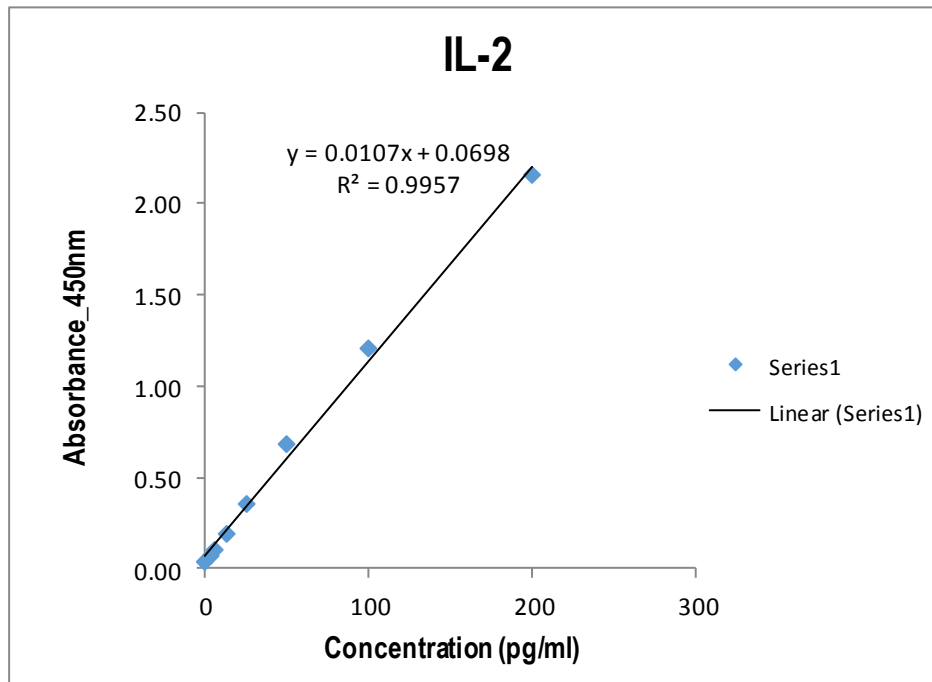


Plate 1

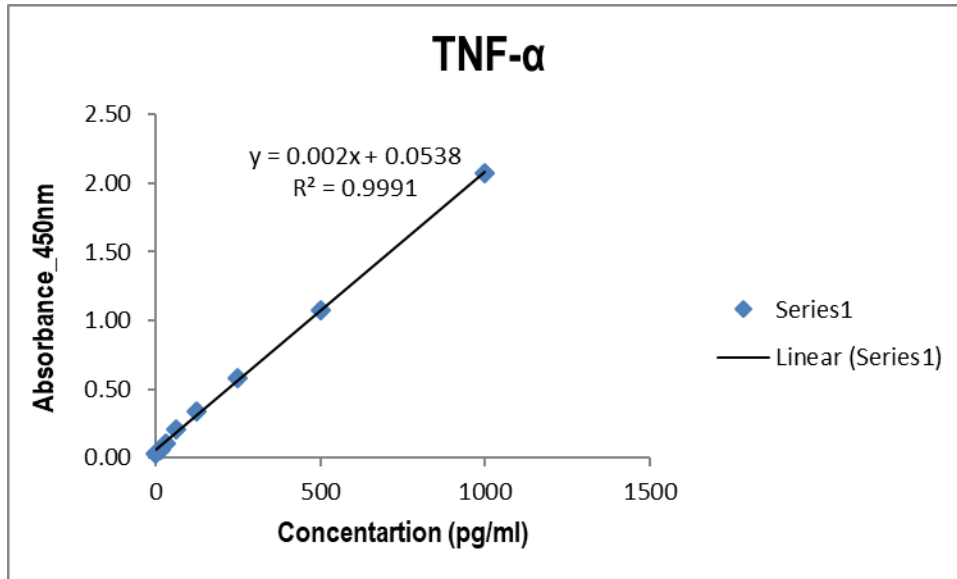


Plate 2

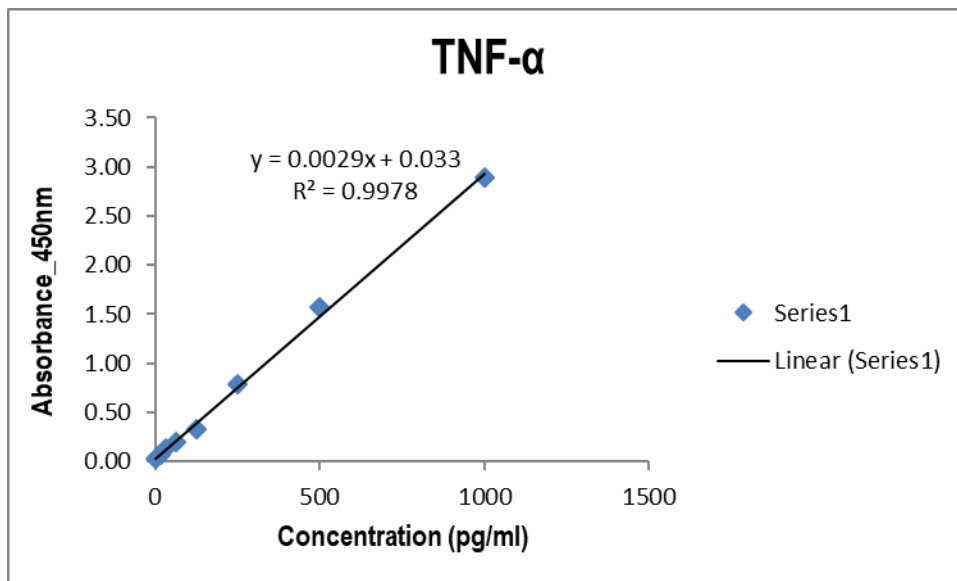


Plate 1

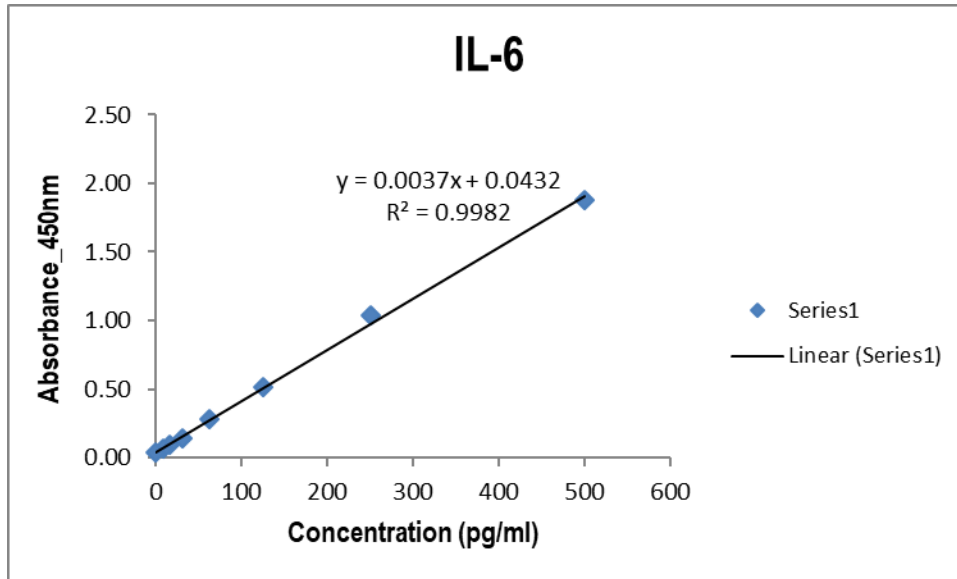


Plate 2

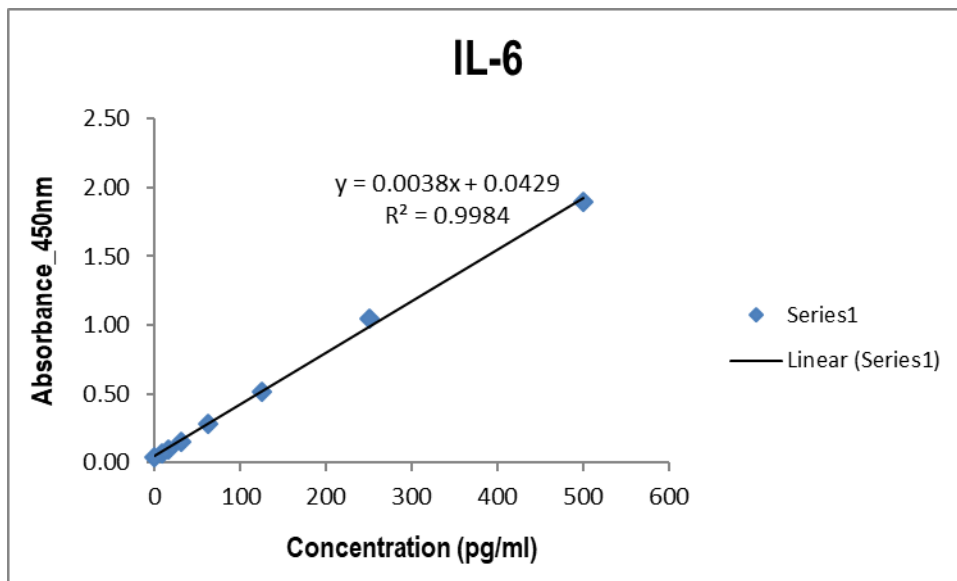


Plate 1

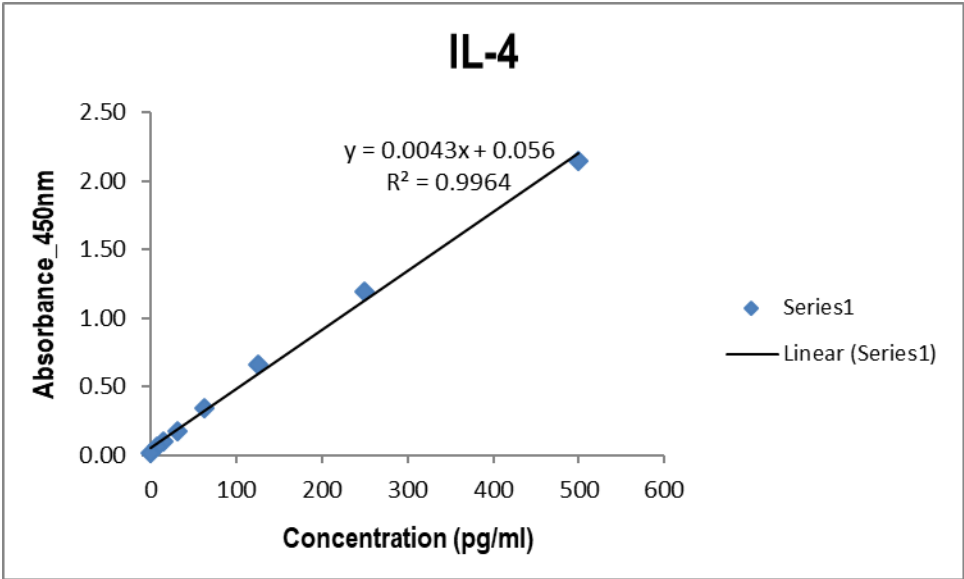


Plate 2

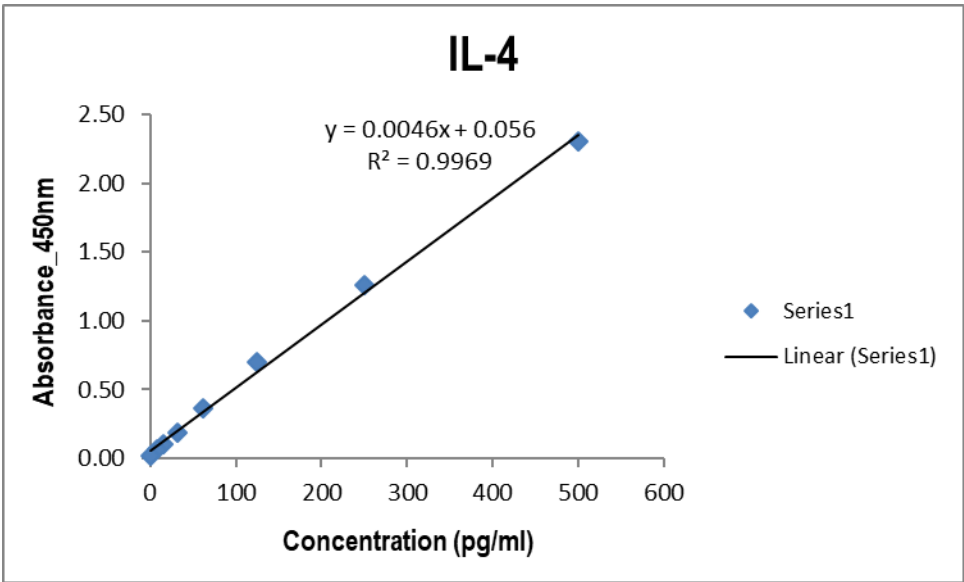


Plate 1

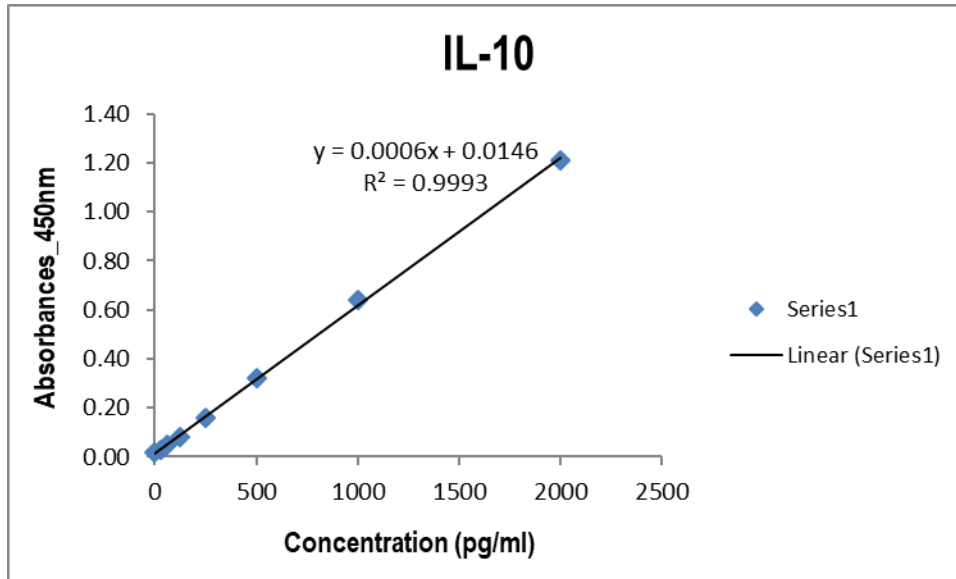
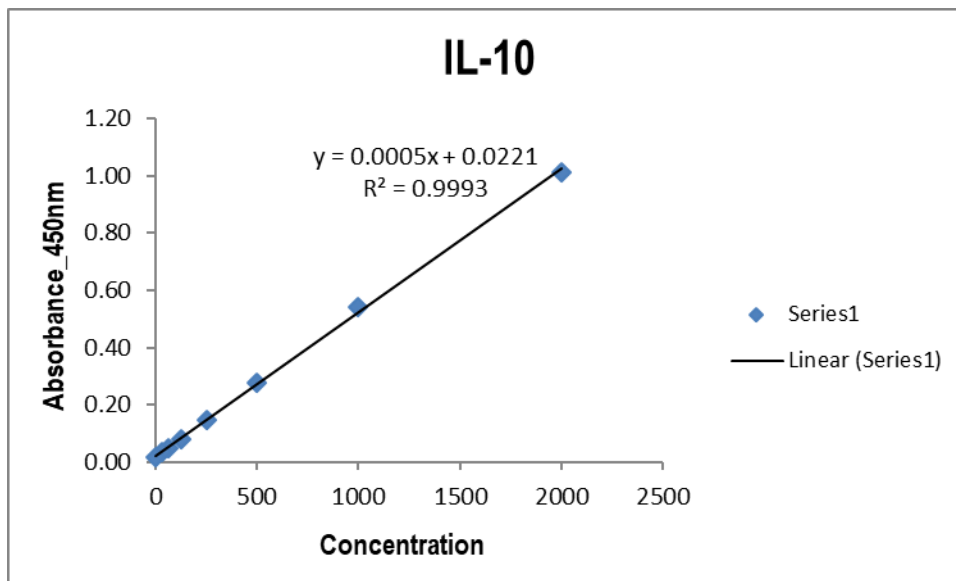


Plate 2



Appendix G: ELISA raw data mouse experiment 2

Cytokine responses part 2

IFN- γ

Plate 1

<>	1	2	3	4	5	6	7	8	9	10	11	12
A	1.2990	1.2620	1.2050	0.0360	0.0470	2.7450	0.0290	0.0230	2.0380	0.0230	0.0310	3.0820
B	0.6760	0.6830	0.6400	0.0320	0.0490	2.8260	0.0300	0.0250	1.9910	0.0240	0.0290	3.0240
C	0.3500	0.3490	0.3240	0.0360	0.0300	2.8520	0.0260	0.0250	2.3170	0.0490	0.0450	2.1970
D	0.1800	0.1690	0.1630	0.0390	0.0250	2.9240	0.0270	0.0260	2.6700	0.0440	0.0400	2.1540
E	0.1010	0.0990	0.0900	0.0290	0.0290	2.3980	0.0260	0.0230	1.3040	0.0280	0.0230	1.1730
F	0.0610	0.0570	0.0560	0.0310	0.0280	2.8830	0.0250	0.0230	1.2520	0.0240	0.0210	0.9670
G	0.0420	0.0400	0.0420	0.0030	0.0020	0.0020	0.0020	0.0010	0.0020	0.0020	0.0020	0.0010
H	0.0270	0.0240	0.0230	0.0220	0.0210	0.0220	0.0230	0.0010	0.0020	0.0010	0.0010	0.0010

Plate 2

<>	1	2	3	4	5	6	7	8	9	10	11	12
A	1.2940	1.2110	1.2350	0.1140	0.0370	3.4190	0.1050	0.0320	3.1930	0.0270	0.0300	0.0310
B	0.6820	0.6630	0.6380	0.1750	0.0470	3.6030	0.1020	0.0330	3.3120	0.0210	0.0290	0.0310
C	0.3490	0.3460	0.3160	0.1590	0.0270	3.1760	0.0700	0.0240	3.1180	0.0660	0.0290	2.7000
D	0.1960	0.1770	0.1690	0.1680	0.0290	3.1140	0.0750	0.0290	3.0470	0.0760	0.0280	2.8120
E	0.1030	0.1000	0.0990	0.0260	0.0240	2.9760	0.0380	0.0310	2.9810	0.0530	0.0320	3.0790
F	0.0640	0.0580	0.0600	0.0250	0.0220	2.9480	0.0380	0.0300	2.9970	0.0450	0.0290	3.0860
G	0.0450	0.0390	0.0410	0.0010	0.0020	0.0020	0.0020	0.0020	0.0030	0.0020	0.0020	0.0020
H	0.0270	0.0220	0.0240	-0.0040	-0.0060	-0.0030	-0.0060	0.0020	0.0020	0.0010	0.0020	0.0010

IL-2

Plate 1

<>	1	2	3	4	5	6	7	8	9	10	11	12
A	1.0470	0.9990	0.9750	0.3450	0.3990	3.6690	0.1840	0.2090	3.7220	0.1580	0.1540	3.7370
B	0.5600	0.5640	0.5450	0.3470	0.3700	3.6670	0.1700	0.2110	3.6890	0.1530	0.1480	3.7240
C	0.3220	0.3520	0.3410	0.3550	0.3300	3.5380	0.4650	0.4410	3.7700	0.4220	0.3130	3.6380
D	0.1620	0.1820	0.1630	0.3650	0.3440	3.6500	0.4990	0.4490	3.7760	0.4240	0.3070	3.5790
E	0.1020	0.1182	0.1030	0.2400	0.1870	3.6030	0.1890	0.1420	3.6350	0.2420	0.1740	3.7070
F	0.0527	0.0636	0.0620	0.2520	0.1970	3.6280	0.2110	0.1350	3.6300	0.2430	0.1600	3.6140
G	0.0262	0.0362	0.0371	0.0050	0.0060	0.0060	0.0050	0.0080	0.0060	0.0010	0.0020	0.0040
H	0.0230	0.0200	0.0220	0.0040	0.0040	0.0060	0.0030	0.0050	0.0040	0.0040	0.0050	0.0050

Plate 2

<>	1	2	3	4	5	6	7	8	9	10	11	12
A	1.0040	1.1070	1.0480	0.7160	0.4700	1.1060	0.5630	0.4750	3.5630	0.0020	0.0020	0.0030
B	0.5440	0.5810	0.5290	0.7130	0.4800	1.1640	0.5820	0.4580	3.6290	0.0040	0.0050	0.0080
C	0.3190	0.3160	0.3040	0.2950	0.2330	3.4120	0.3350	0.2200	3.5070	0.3300	0.2120	3.5360
D	0.2090	0.2078	0.2074	0.3060	0.2380	3.4080	0.3290	0.2300	3.5530	0.3890	0.2450	3.5280
E	0.1030	0.0870	0.0880	0.2690	0.2370	3.3830	0.2910	0.2420	3.5660	0.5960	0.3880	3.4550
F	0.0500	0.0408	0.0469	0.2760	0.2370	3.3910	0.3000	0.2840	3.5170	0.5650	0.3470	3.4910
G	0.0250	0.0218	0.0269	0.0060	0.0050	0.0080	0.0030	0.0030	0.0020	0.0020	0.0020	0.0030
H	0.0210	0.0230	0.0220	0.0050	0.0060	0.0040	0.0050	0.0010	0.0030	0.0040	0.0050	0.0080

TNF- α

Plate 1

<>	1	2	3	4	5	6	7	8	9	10	11	12
A	2.6070	2.4080	2.4620	0.0520	0.0410	0.8640	0.0350	0.0290	0.8350	0.0310	0.0330	1.2200
B	1.4870	1.3890	1.3600	0.0420	0.0440	0.8510	0.0310	0.0270	0.8090	0.0290	0.0290	1.2740
C	0.7630	0.6760	0.7270	0.0370	0.0370	0.8050	0.0430	0.0380	0.9760	0.0270	0.0300	1.1450
D	0.3830	0.3570	0.3650	0.0330	0.0360	0.8810	0.0420	0.0390	1.0130	0.0420	0.0340	1.1440
E	0.2100	0.1840	0.1950	0.0250	0.0230	0.7100	0.0190	0.0200	0.6160	0.0170	0.0190	0.6350
F	0.1250	0.0970	0.1210	0.0330	0.0260	0.6760	0.0360	0.0210	0.6220	0.0200	0.0180	0.5670
G	0.0625	0.0585	0.0610	0.0030	0.0020	0.0030	0.0020	0.0020	0.0020	0.0020	0.0020	0.0010
H	0.0260	0.0240	0.0250	-0.0010	-0.0050	0.0010	0.0030	-0.0020	-0.0030	-0.0040	0.0010	0.0000

Plate 2

<>	1	2	3	4	5	6	7	8	9	10	11	12
A	3.0180	2.8880	2.8870	0.0520	0.0440	0.5650	0.0610	0.0390	0.8890	0.0200	0.0220	0.0260
B	1.7120	1.6760	1.6660	0.1000	0.0420	0.6130	0.0530	0.0280	1.1470	0.0170	0.0190	0.0200
C	0.8800	0.8510	0.8560	0.0470	0.0310	1.1230	0.0440	0.0270	0.8590	0.0290	0.0260	0.8470
D	0.4450	0.4010	0.3980	0.0450	0.0310	1.1960	0.0480	0.0270	0.8430	0.0310	0.0290	0.9260
E	0.2240	0.2070	0.2180	0.0420	0.0350	0.8850	0.0310	0.0220	0.6090	0.0310	0.0280	0.8180
F	0.1190	0.1110	0.1200	0.0360	0.0260	0.8680	0.0240	0.0230	0.5790	0.0250	0.0260	0.7070
G	0.0595	0.0555	0.0610	0.0030	0.0040	0.0030	0.0030	0.0020	0.0020	0.0030	0.0020	0.0020
H	0.0241	0.0320	0.0300	0.0180	0.0240	0.0050	0.0020	0.0000	0.0040	-0.0040	0.0020	0.0020

IL-6

Plate 1

<>	1	2	3	4	5	6	7	8	9	10	11	12
A	1.6950	1.7260	1.7390	0.0430	0.0290	0.5990	0.0410	0.0290	0.6090	0.0240	0.0300	0.3870
B	0.9370	0.9470	0.9240	0.0390	0.0270	0.6220	0.0360	0.0270	0.6390	0.0260	0.0280	0.4240
C	0.5030	0.5030	0.4750	0.0410	0.0320	0.5530	0.0450	0.0330	1.0980	0.0360	0.0330	0.9560
D	0.2670	0.2590	0.2360	0.0410	0.0320	0.5720	0.0450	0.0350	1.1280	0.0380	0.0270	1.0210
E	0.1460	0.1320	0.1290	0.0370	0.0350	0.6170	0.0270	0.0170	0.3530	0.0210	0.0200	0.2390
F	0.0890	0.0790	0.0630	0.0350	0.0420	0.6000	0.0240	0.0170	0.3130	0.0190	0.0180	0.2410
G	0.0590	0.0530	0.0460	0.0020	0.0010	0.0020	0.0020	0.0010	0.0010	0.0030	0.0010	0.0020
H	0.0240	0.0240	0.0160	0.0140	0.0130	0.0010	0.0010	0.0010	0.0020	0.0010	0.0010	0.0010

Plate 2

<>	1	2	3	4	5	6	7	8	9	10	11	12
A	1.6150	1.6420	1.6780	0.0700	0.0590	1.2240	0.0500	0.0390	0.6680	0.0240	0.0260	0.0290
B	0.8690	0.8840	0.8560	0.0730	0.0610	1.2570	0.0470	0.0370	0.6440	0.0220	0.0240	0.0280
C	0.4520	0.4500	0.4490	0.0520	0.0420	0.5710	0.0500	0.0380	0.6750	0.0420	0.0440	0.4390
D	0.2370	0.2380	0.2440	0.0560	0.0440	0.5710	0.0550	0.0500	0.6950	0.0420	0.0380	0.4520
E	0.1420	0.1440	0.1380	0.0520	0.0450	0.7680	0.0490	0.0420	0.8350	0.0480	0.0330	0.8540
F	0.0820	0.0770	0.0790	0.0530	0.0450	0.7620	0.0520	0.0410	0.8320	0.0410	0.0320	0.7750
G	0.0620	0.0530	0.0530	0.0020	0.0020	0.0020	0.0020	0.0020	0.0020	0.0030	0.0020	0.0020
H	0.0280	0.0220	0.0260	0.0810	0.0350	0.0000	0.0020	0.0020	0.0020	0.0030	0.0020	0.0010

IL-4

Plate 1

<>	1	2	3	4	5	6	7	8	9	10	11	12
A	0.7710	0.6870	0.6850	0.0360	0.0460	0.6760	0.0320	0.0390	1.5590	0.0340	0.0500	0.4630
B	0.4040	0.3830	0.3290	0.0310	0.0380	0.8000	0.0400	0.0360	1.5690	0.0300	0.0370	0.5450
C	0.2500	0.2110	0.1970	0.0350	0.0380	0.8540	0.0390	0.0360	0.4020	0.0270	0.0280	3.0800
D	0.1520	0.1240	0.1250	0.0360	0.0420	0.9010	0.0350	0.0370	0.4280	0.0340	0.0320	3.0510
E	0.1060	0.0740	0.0700	0.0330	0.0400	0.4910	0.0350	0.0350	0.4080	0.0260	0.0320	1.3160
F	0.0680	0.0460	0.0440	0.0390	0.0400	0.4660	0.0330	0.0280	0.4150	0.0220	0.0200	1.2890
G	0.0375	0.0351	0.0380	0.0020	0.0020	0.0020	0.0010	0.0010	0.0020	0.0020	0.0010	0.0010
H	0.0251	0.0260	0.0240	0.0140	0.0200	0.0020	0.0020	0.0010	0.0040	0.0010	0.0010	0.0010

Plate 2

<>	1	2	3	4	5	6	7	8	9	10	11	12
A	0.9190	0.8940	0.8880	0.0340	0.0320	0.2070	0.0300	0.0230	0.0970	0.0240	0.0180	0.0300
B	0.4490	0.4330	0.4170	0.0400	0.0300	0.2210	0.0260	0.0220	0.1120	0.0130	0.0140	0.0180
C	0.2530	0.2410	0.2310	0.0390	0.0310	0.6100	0.0320	0.0330	0.1430	0.0250	0.0230	1.1540
D	0.1450	0.1370	0.1250	0.0430	0.0320	0.6210	0.0350	0.0410	0.1420	0.0240	0.0270	1.1290
E	0.0680	0.0910	0.0710	0.0260	0.0280	1.6280	0.0260	0.0240	3.0420	0.0200	0.0200	2.4380
F	0.0570	0.0530	0.0440	0.0260	0.0180	1.5220	0.0220	0.0200	3.0300	0.0160	0.0140	2.4010
G	0.0370	0.0470	0.0330	0.0020	0.0020	0.0030	0.0020	0.0020	0.0020	0.0020	0.0020	0.0010
H	0.0320	0.0400	0.0320	0.0140	0.0110	0.0010	0.0020	0.0020	0.0030	0.0010	0.0020	0.0020

IL-10

Plate 1

<>	1	2	3	4	5	6	7	8	9	10	11	12
A	0.6310	0.5850	0.5920	0.0510	0.0750	0.4310	0.0340	0.0270	0.0790	0.0310	0.0450	0.2810
B	0.3280	0.2970	0.2910	0.0560	0.0680	0.4470	0.0250	0.0230	0.0880	0.0360	0.0430	0.2730
C	0.1690	0.1660	0.1440	0.0320	0.0300	0.2000	0.0320	0.0320	0.2380	0.0230	0.0270	0.1980
D	0.0960	0.0890	0.0860	0.0330	0.0330	0.2160	0.0370	0.0340	0.2580	0.0260	0.0300	0.2030
E	0.0620	0.0540	0.0520	0.0340	0.0330	0.2040	0.0220	0.0180	0.3900	0.0260	0.0280	0.1390
F	0.0390	0.0300	0.0330	0.0310	0.0280	0.2140	0.0170	0.0180	0.3600	0.0230	0.0280	0.1350
G	0.0310	0.0330	0.0280	0.0020	0.0020	0.0010	0.0020	0.0020	0.0030	0.0030	0.0030	0.0010
H	0.0240	0.0190	0.0190	0.0190	0.0160	0.0170	0.0160	-0.0030	-0.0060	0.0010	0.0010	0.0010

Plate 2

<>	1	2	3	4	5	6	7	8	9	10	11	12
A	0.7300	0.6190	0.6470	0.0340	0.0250	0.3000	0.0240	0.0230	0.1460	0.0250	0.0280	0.0670
B	0.3630	0.3090	0.3120	0.0330	0.0270	0.3350	0.0240	0.0250	0.1560	0.0260	0.0300	0.0320
C	0.1700	0.1740	0.1500	0.0390	0.0300	0.2050	0.0270	0.0250	0.1450	0.0460	0.0430	0.0760
D	0.1020	0.0950	0.0940	0.0380	0.0320	0.2320	0.0270	0.0270	0.1670	0.0490	0.0350	0.1250
E	0.0620	0.0560	0.0570	0.0270	0.0230	0.0860	0.0360	0.0360	0.4000	0.0560	0.0580	0.2810
F	0.0360	0.0330	0.0370	0.0220	0.0180	0.0760	0.0340	0.0360	0.4010	0.0610	0.0590	0.3000
G	0.0290	0.0240	0.0340	0.0030	0.0030	0.0020	0.0020	0.0020	0.0020	0.0020	0.0020	0.0020
H	0.0220	0.0160	0.0200	0.0200	0.0170	0.0190	0.0170	-0.0010	-0.0030	0.0020	0.0020	0.0010

Standard curves for determination of cytokines

Plate 1

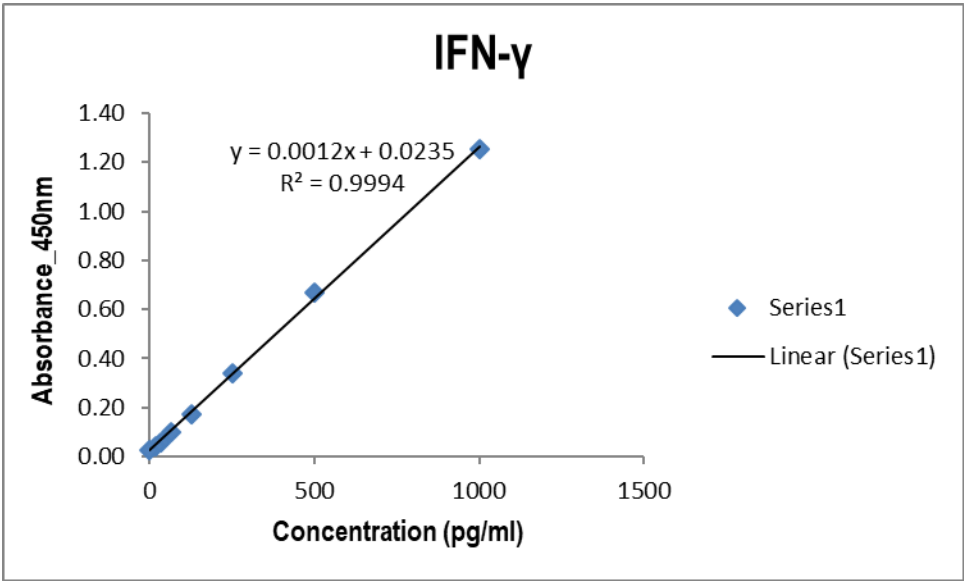


Plate 2

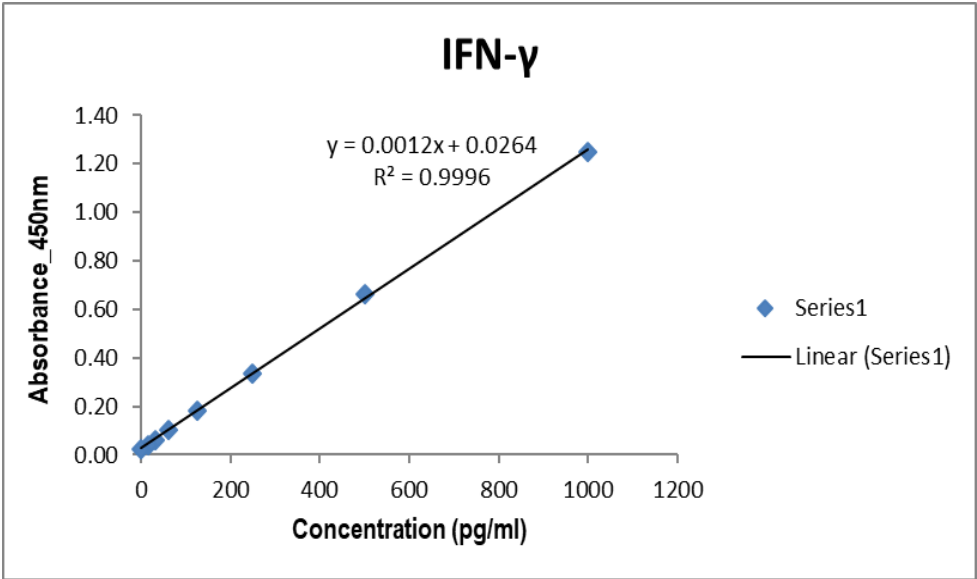


Plate 1

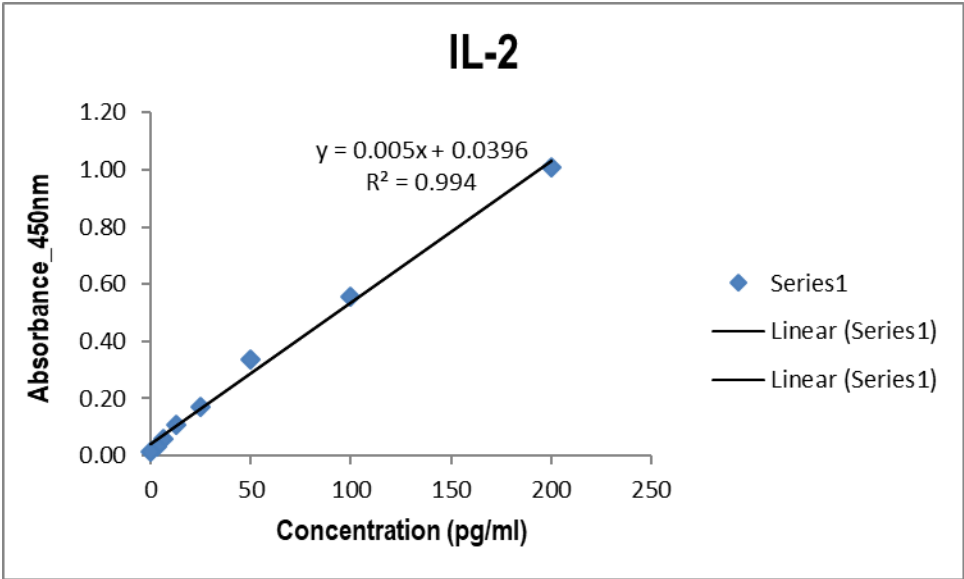


Plate 2

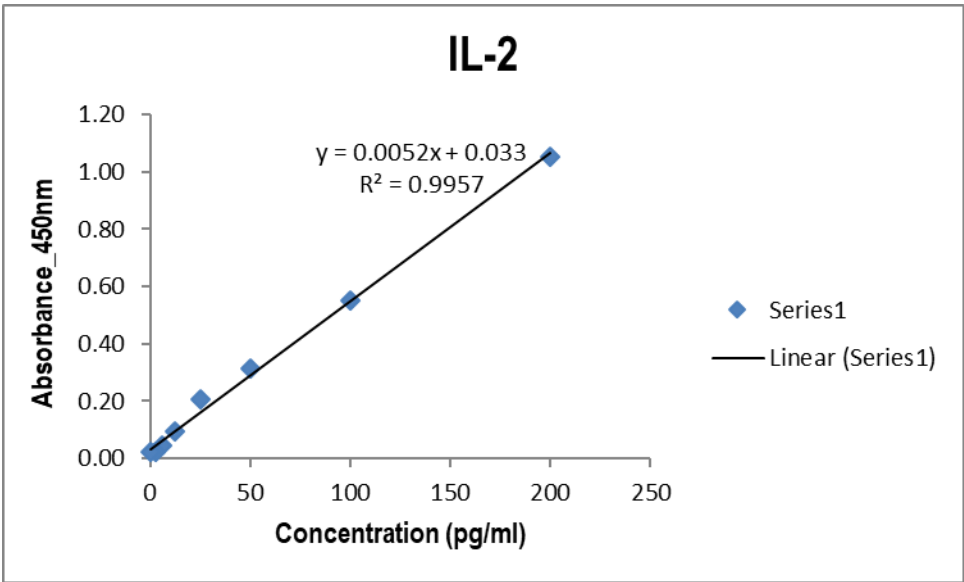


Plate 1

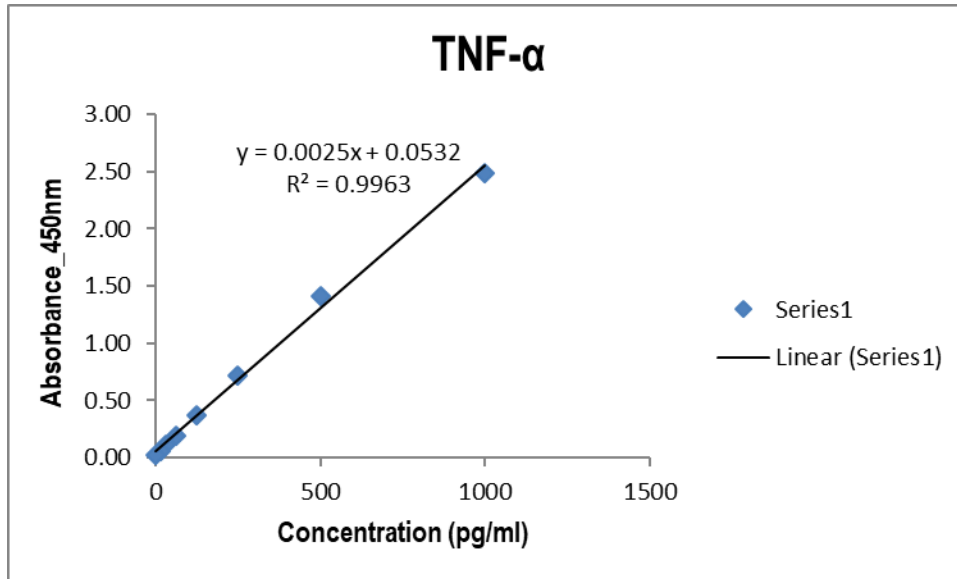


Plate 2

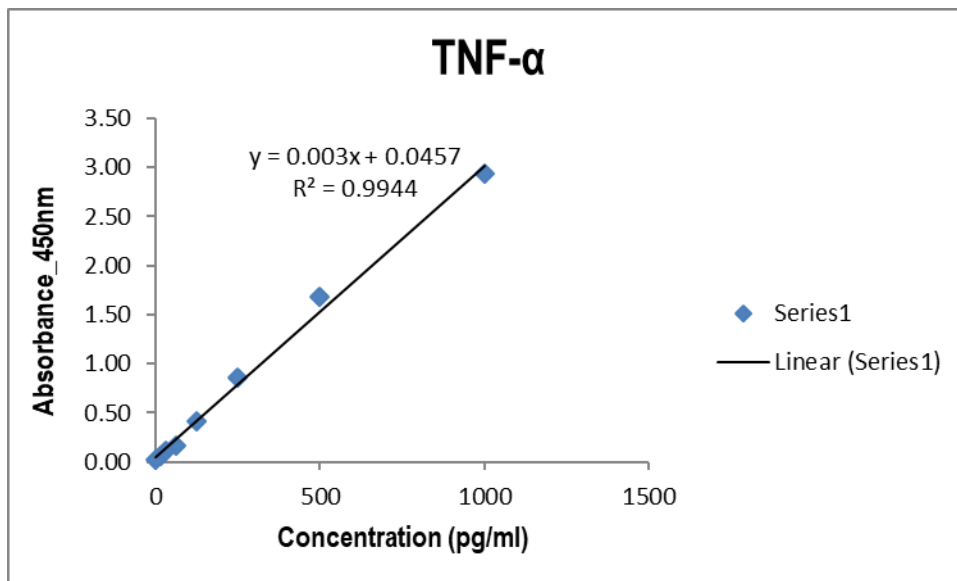


Plate 1

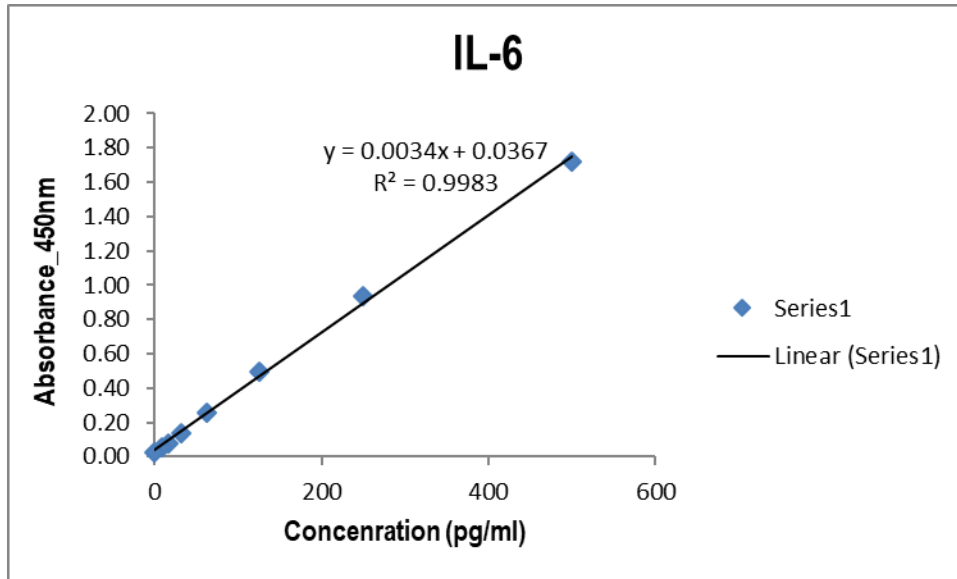


Plate 2

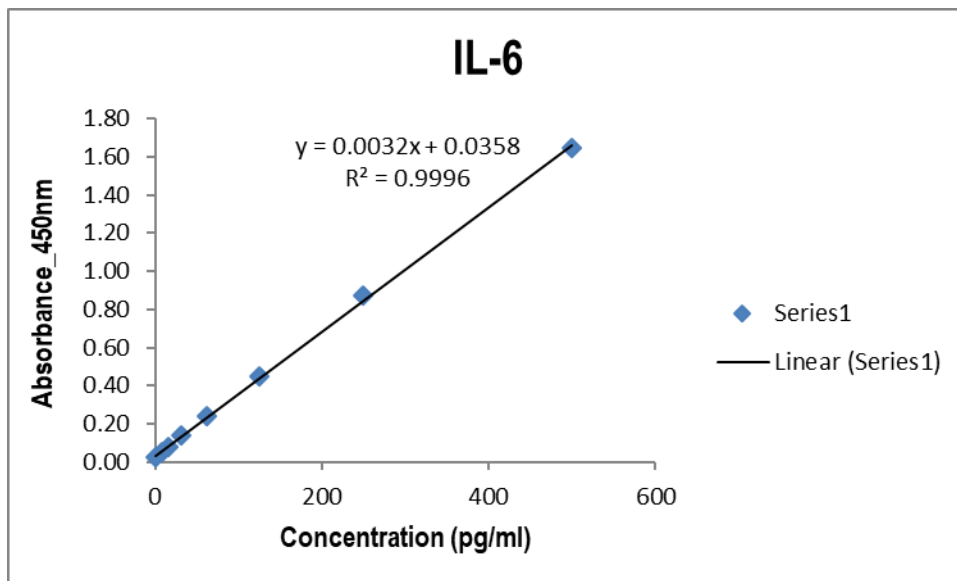


Plate 1

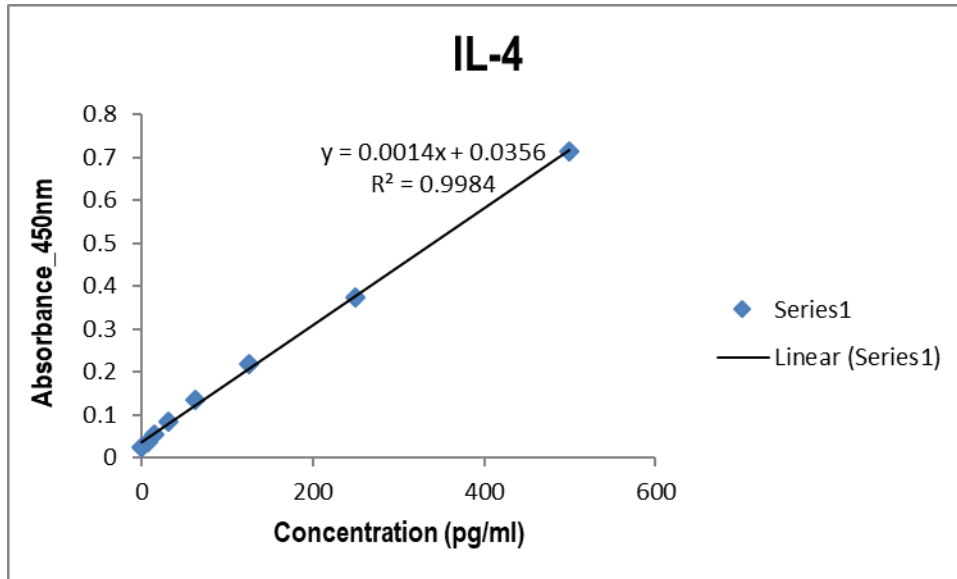


Plate 2

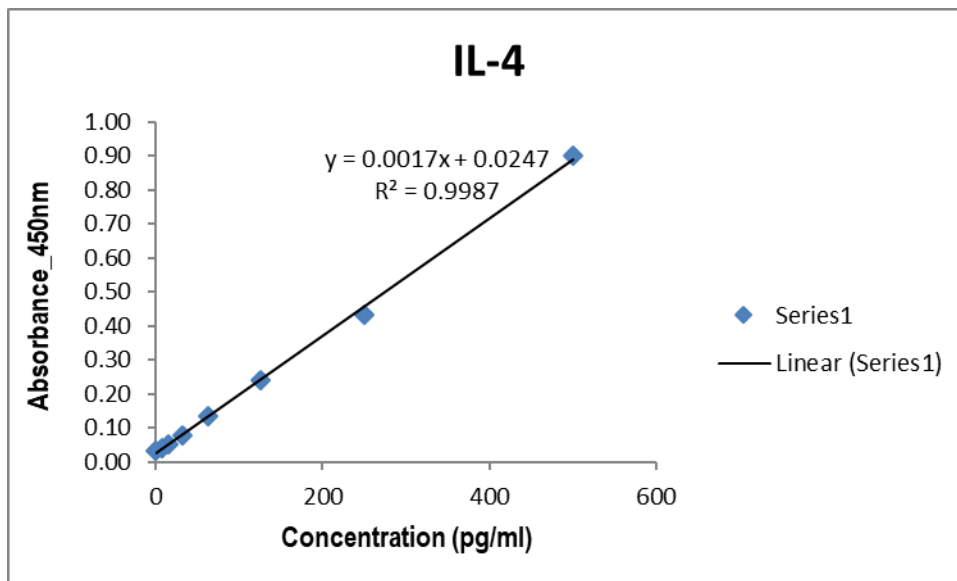


Plate 1

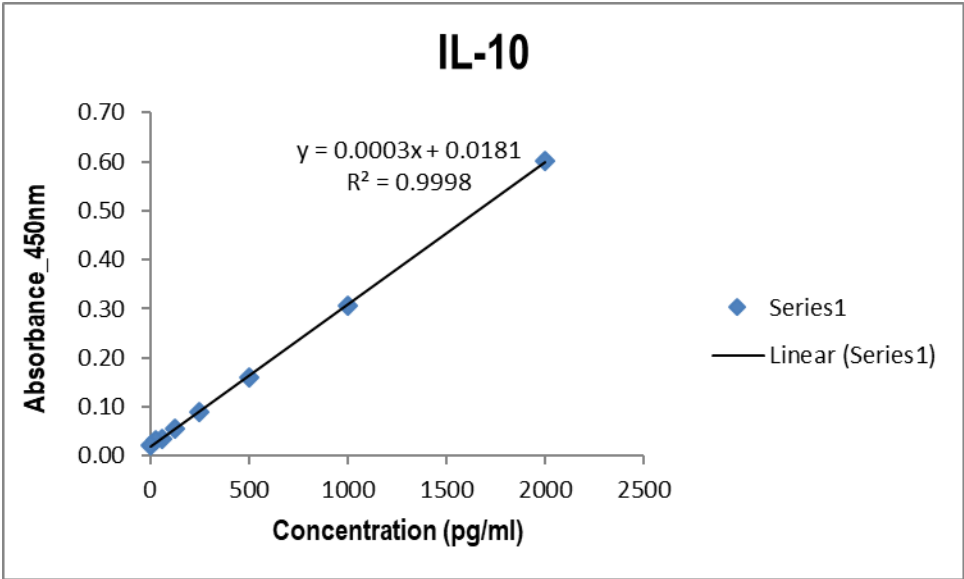
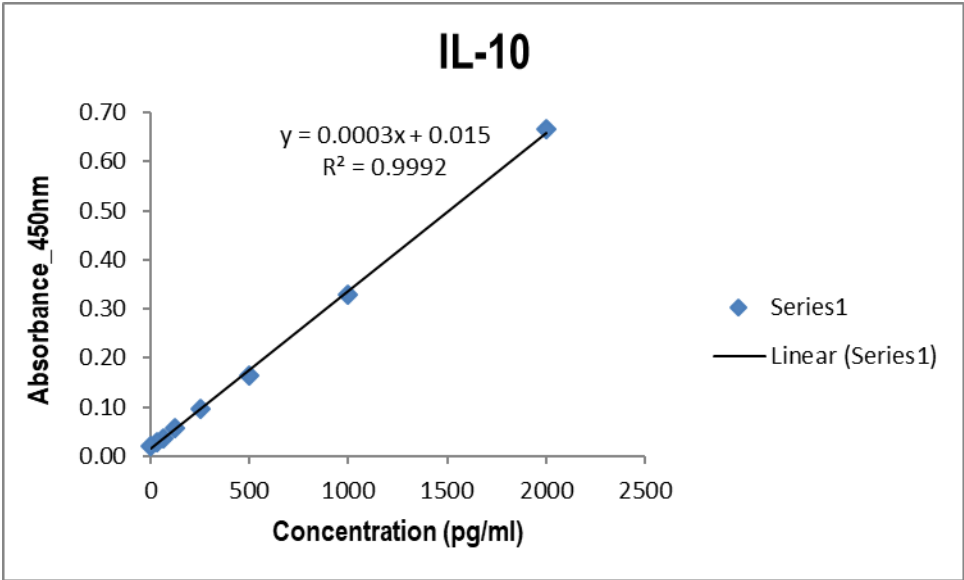


Plate 2



Appendix H: Composition of buffers, media and solutions

Composition of buffers

1. 50X TAE (1 L)

Dissolve 242 g Tris in 500 ml deionized water, add 100 ml 0.5 M EDTA at a pH of 8.0 and 57.1 ml glacial acetic acid. Adjust volume to 1 L using deionized water and store at room temperature. Dilute to 1X working concentration by the addition of 40 ml 50X TAE in a final volume of 2 L deionized water.

2. 10X PBS (1 L)

Dissolve 80 g of NaCl, 2 g of KCl, 17.8 g of $\text{Na}_2\text{HPO}_4 \cdot 2\text{H}_2\text{O}$ and 2.4 g of KH_2PO_4 in 800 ml. Adjust pH to 7.4 using HCl and adjust volume to 1 L using deionized water. Autoclave and store at room temperature. Dilute to 1X working concentration by the addition of 200 ml 10X PBS in a final volume of 2 L deionized water.

3. Transfer buffer (1 L)

Dissolve 2.9 g glycine, 5.8 g Tris and 0.37 g SDS in 200 ml methanol. Adjust volume to 1 L using deionized water and store at 4°C.

4. 1X TBS (1 L)

Dissolve 6.05 g Tris and 8.76 g NaCl in 800 ml deionized water. Adjust pH to 7.5 using 1 M HCl, adjust the volume to 1 L using deionized water and store at 4°C.

5. NET/BSA

Dissolve 4.3g NaCl, 1.04g $\text{Na}_2\text{EDTA} \cdot 2\text{H}_2\text{O}$ and 3.02g tris (hydroxymethyl) aminomethane. Add 2.5ml Nonidet P40 and supplement with 1mg/ml bovine serum albumin before use.

Composition of media

1. SOC media (1 L)

Dissolve 20 g of Bacto-Tryptone, 5 g of Bacto-Yeast Extract, 0.5 g NaCl and 2.5 ml of 1 M KCl in 900 ml deionized water. Adjust the pH to 7.0 using 10 M NaOH and adjust the volume to 970 ml. Add 10 ml 1 M MgCl_2 and 20 ml 1 M glucose before use and store at 4°C.

2. LB media (1 L)

Dissolve 10 g Bacto-tryptone, 5 g Bacto-yeast extract and 10 g NaCl in 800 ml deionized water. Adjust the pH to 7.5 using 1 M NaOH and adjust the volume to 1 L using deionized water. Autoclave, allow to cool and store at 4°C.

3. 2X TY media (1 L)

Dissolve 16 g Bacto-tryptone, 10 g Bacto-yeast extract and 5 g NaCl in 800 ml deionized water. Adjust the volume to 1 L using deionized water. Autoclave, allow to cool and store at 4°C.

Agar plates were prepared by the addition of 15 g Bacto-agar per 1 L of liquid media. After sterilization by autoclaving, media was allowed to cool, was poured in sterile plates and stored in an inverted position at 4°C after solidification.

Composition of solutions

1. 125 mM EDTA

Prepare 0.5 M EDTA by dissolving 186.12 g $\text{Na}_2\text{EDTA}\cdot 2\text{H}_2\text{O}$ in 800 ml deionized water, adjust the pH to 8.0 using NaOH pellets and adjust the volume to 1 L using deionized water. Sterilize by autoclaving and store at room temperature. Dilute to a final concentration of 125 mM in the desired volume using nuclease-free water.